1996

Studies of terminal phosphinidene complexes of zirconium.

Tricia Lynn. Breen
University of Windsor

INFORMATION TO USERS

This manuscript has been reproduced from the microfilm master. UMI films the text directly from the original or copy submitted. Thus, some thesis and dissertation copies are in typewriter face, while others may be from any type of computer printer.

The quality of this reproduction is dependent upon the quality of the copy submitted. Broken or indistinct print, colored or poor quality illustrations and photographs, print bleedthrough, substandard margins, and improper alignment can adversely affect reproduction.

In the unlikely event that the author did not send UMI a complete manuscript and there are missing pages, these will be noted. Also, if unauthorized copyright material had to be removed, a note will indicate the deletion.

Oversize materials (e.g., maps, drawings, charts) are reproduced by sectioning the original, beginning at the upper left-hand corner and continuing from left to right in equal sections with small overlaps. Each original is also photographed in one exposure and is included in reduced form at the back of the book.

Photographs included in the original manuscript have been reproduced xerographically in this copy. Higher quality 6" x 9" black and white photographic prints are available for any photographs or illustrations appearing in this copy for an additional charge. Contact UMI directly to order.

UMI

A Bell & Howell Information Company
300 North Zeeb Road, Ann Arbor MI 48106-1346 USA
313/761-4700 800/521-0600

Studies of Terminal Phosphinidene Complexes of Zirconium

by

Tricia L. Breen

A Dissertation
Submitted to the Faculty of Graduate Studies and Research
through the Department of Chemistry and Biochemistry
in Partial Fulfillment of the Requirements for
the Degree of Doctor of Philosophy at the
University of Windsor

Windsor, Ontario, Canada
June, 1996

Abstract

Synthetic routes to terminal phosphinidene complexes of zirconium have been investigated. The attempted generation of [Cp_2Zr=PR] in the presence of polar organic unsaturates results in insertion of the organic molecule into the Zr-P single bond of the precursor. The stabilization of the Zr=P multiple bond requires a sterically demanding substituent on phosphorus. In the absence of the required steric demands, bimolecular reactions and C-H activation of the cyclopentadienyl rings occur. However, the supermesityl substituent allows for the trimethylphosphine trapping of [Cp_2Zr=PMes*] as the stable eighteen electron adduct. (Cp_2Zr=PMes*)(PMe_3) **84** is the first stable zirconium terminal phosphinidene complex.

Initial reactivity studies of **84** were directed at exploring the nature of the Zr=P multiple bond. Organic reagents, as well as some of their lower congeners, react with **84** which acts as a source of the phosphinidene moiety. This group may be exchanged for an oxo, sulfido or two chloride groups to yield a variety of organophosphorus derivatives and the corresponding zirconocene oxide, sulfide or dichloride. **84** also undergoes 1,2-addition reactions of polar E-H bonds to afford complexes of the form Cp_2Zr(PHMes*)(ER) and Cp_2Zr(PHMes*)(EHR). Variable temperature NMR studies reveal that metal-mediated inversion of the pyramidal phosphide ligands can be stopped upon cooling. Zr-E π-interactions are generally weak, yet they have an influence over both the ^{31}P NMR chemical shift and the inversion barrier of the phosphide ligand.

[2+2] cycloaddition reactions of **84** with alkynes have furnished the first examples of phosphametallacyclobutenes. These complexes readily insert unsaturated polar organic molecules into the Zr-P bond, thus providing a family of four-, five- and six-membered metallacycles. Steric factors exert considerable influence over this entire group of complexes, causing reduced inversion barriers at phosphorus and [4+2] retrocycloadditions.

The aforementioned phosphametallacycles provide a route to novel main group heterocycles via metallacycle transfer reactions with main group dihalides. These complexes offer several advantages as potential synthons for these phosphacycles, such as the possibility of substitution patterns that are not available by conventional syntheses.

The chemistry described herein is distinguished by the reactive nature of Zr-P single and double bonds, a trait which provides intriguing and unparalleled chemistry.

Dedication

This work is dedicated to the memory of my grandfather, Tadeusz Basinski.

"When there was no dream of mine
You dreamed of me"
—Robert Hunter

"The most exciting phrase to hear in science,
the one that heralds new discoveries, is not
'Eureka!' (I've found it!), but 'That's funny...' "
—Isaac Asimov

"Once in a while
you get shown the light
in the strangest of places
if you look at it right"
—Robert Hunter

Acknowledgments

I wish to acknowledge a number of people who have been important to me during the course of my education at the University of Windsor. I would first like to express my sincere gratitude to Dr. Douglas W. Stephan for his support and guidance. I am especially grateful to him for his consistent belief in my capabilities and his talent of inspiring greater efforts while still managing to boost confidence.

My tenure in the Stephan lab has been a very enjoyable experience. I would like to thank the members of our research group for their help, companionship and amicable commiseration over the all-too-frequent frustrations of research. Special thanks are offered to Dr. T. Timothy Nadasdi, whose advice initiated my tenure in the Stephan lab. Dr. Jianwei Ho, Dr. Yujin Huang, Robert Drake, Dr. Richard H. Heyn, Dr. Nola Etkin and Jeff Stewart are all especially acknowledged for their help and friendship over the years. My gratitude is particularly extended to Dr. Hilary A. Jenkins, for a rare and enduring friendship.

I am also grateful to Dr. Stephen J. Loeb and Dr. James R. Green for helpful advice and discussions. Mike Fuerth, Jerry Vriesacker, Terry Edwards, Jim Olsen, Al Ditchburn, Dave Hill and Vivi Lazarescu are thanked for expertise that is essential to the research program in our department.

Finally, words cannot express my appreciation to Steve for being by my side throughout this long, strange trip.

Table of Contents

List of Figures

List of Tables

Abbreviations

Å	Angstrom
Ar	aryl
br	broad
Cp	cyclopentadienyl anion (η^5-C_5H_5)
Cp*	pentamethylcyclopentadienyl anion (η^5-C_5Me_5)
d	doublet
δ	chemical shift
dmpe	1,2-bis(dimethylphosphino)ethane
Et	ethyl (C_2H_5)
eq	equivalent
Fc	calculated structure factor
Fo	observed structure factor
g	grams
h	hour
HOMO	highest occupied molecular orbital
Hz	Hertz
J	coupling constant
LUMO	lowest unoccupied molecular orbital
m	multiplet
Me	methyl (CH_3)
Mes	2,4,6-Me_3-C_6H_2
Mes*	2,4,6-*t*-Bu_3-C_6H_2
MHz	Megahertz
min	minutes
μL	microlitre
mL	millilitre
mmol	millimoles
MS	mass spectrometry
NMR	nuclear magnetic resonance
Np	neopentyl ($(CH_3)_3CCH_2$)

ORTEP	Oak Ridge Thermal Ellipsoid Program
Ph	phenyl (C_6H_5)
ppm	parts per million
pyr	pyridine
q	quartet
R	agreement factor
R_w	weighted agreement factor
s	singlet
s	estimated standard deviation
t	triplet
t-Bu	tertiary butyl ($C(CH_3)_3$)
THF	tetrahydrofuran
Tol	tolyl ($C_6H_4CH_3$)

Chapter One
Introduction

Complexes containing early metal-ligand multiple bonds have been ardently pursued for a number of years, stimulated by fundamental studies of Schrock-type alkylidenes. Early metal-heteroatom multiple bonds are especially alluring due to their potential use in the synthesis of organic compounds containing heteroatoms, as well as fundamental interest in mechanistic issues and the nature of structure and bonding. While the chemistry of early metal imido and chalcogenido species has attracted considerable attention, the highly reactive nature of the early metal-phosphorus multiple bond has delayed the development of this area. As a consequence, this dissertation describes the syntheses of zirconium phosphinidene complexes as well as reactivity studies. A review of early metal-ligand multiply bonded complexes reveals striking similarities in synthesis and reactivity. Since studies of Schrock-type alkylidenes are the foundation for these comparisons, this chapter begins with a description of the bonding and reactivity of this fascinating class of compounds. This is followed by a discussion of early metal-chalcogenido and pnictogenido multiple bonds and their reactivity.

1.1 The Nature of the Metal Alkylidene Bond

Compounds with metal-carbon multiple bonds were discovered in 1964 by E.O. Fischer, with the synthesis of **1**.[1] To date, many examples of Fischer carbenes have been prepared and have found applications in metal-mediated organic syntheses. Fischer carbenes are formally derived from the coordination of a carbene ($:CR_2$) to a low oxidation state metal centre. Less than a decade after Fischer's discovery, interest in metal-ligand multiple bonds was galvanized by Schrock's serendipitous discovery of the first transition metal alkylidene species **2**, which resulted from the attempted synthesis of pentakisneopentyl tantalum (V).[2] Subsequent to this seminal experiment, a

substantial body of work has been developed. The bonding in the Schrock alkylidenes differs considerably from their Fischer carbene counterparts, thus the chemical behaviour of these two classes of compounds is completely different.

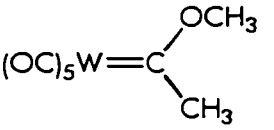

1

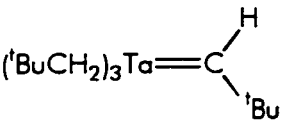

2

Metal-ligand multiple bonds generally consist of a σ bond as well as one or two π bonds. Overlap of the metal *d* orbitals with *p* orbitals on the ligand constitute the π bonding. *Ab initio* calculations have provided important information about the nature of the metal-carbon multiple bond.[3] The $M=CR_2$ double bond can either be covalent, resembling ethylene, or it can be a donor-acceptor bond. The former consists of a triplet metal centre bonding to a triplet carbene fragment (**A** in Fig. 1.1), while in the latter a singlet carbene lone pair is donated into an empty metal orbital and backbonding occurs from a filled metal orbital into the vacant carbene *p*-orbital (**B** in Fig. 1.1).

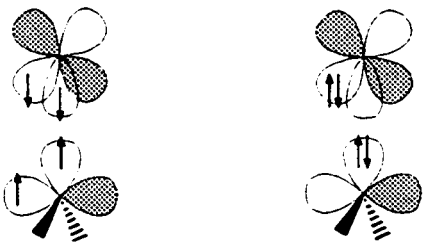

A B

Figure 1.1 Bonding in metal-alkylidenes: ethylene-like covalent bonding (**A**) and donor-acceptor bonding (**B**)

Early transition metals in high oxidation states with few *d* electrons prefer ethylene-like bonding as in **A**, while donor-acceptor bonding (**B**) is commonly favoured by low-valent late metal species. Thus, Schrock-type alkylidenes have ethylene-like covalent bonds as depicted in **A**, while Fischer-type carbene species are characterized by **B**. The nature of the carbene fragment also controls the bonding in alkylidene complexes. Free carbenes with only hydrogen or alkyl substituents have triplet ground states, prefer bonding as

in **A**, and are thus generally found in Schrock-type alkylidene complexes. In contrast, the carbene groups in Fischer carbene species contain substituents with $p\pi$ lone pairs, have singlet ground states and thus prefer bonding as in type **B**. Bonding between the heteroatom lone pair and the carbene carbon both stabilizes the complex and significantly reduces the metal-carbon bond order, as illustrated by the resonance forms in Equation 1.1.

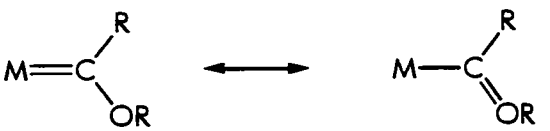

(1.1)

1.2 General Reactions Affording Early Metal-Ligand Multiple Bonds

There are several general routes that have been exploited in the formation of metal-ligand multiple bonds.[3] The following syntheses have been utilized for alkylidene complexes as well as for species containing metal-heteroatom multiple bonds. Therefore, this discussion serves as a guideline for the preparation of early metal multiply bonded complexes with a focus on Schrock-type alkylidenes.

The majority of Schrock alkylidenes have been prepared by routes involving cleavage of hydrogen from the α atom of a precursor compound. This method is generalized in Equation 1.2, in which the equilibrium favouring α-elimination can be manipulated by several factors, such as the use of strongly basic leaving groups (X), the addition of an external base to consume HX, or increasing the steric congestion around the metal.

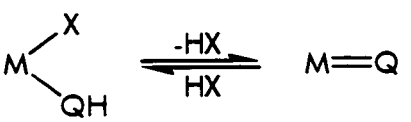

(1.2)

Strongly basic leaving groups, such as σ alkyl substituents or dialkylamido ligands have been used to synthesize alkylidene complexes. However, it is often unclear as to whether the added base is creating the multiple bond by coordination to

the metal followed by proton transfer and elimination, or simply via direct deprotonation without prior coordination. This conundrum is exemplified by Schrock's original synthesis of alkylidene **2**, of which the mechanism is still ambiguous (Fig. 1.2).

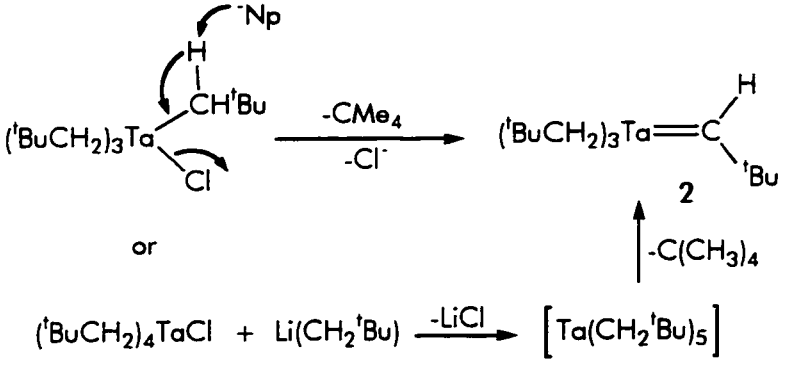

Figure 1.2 Possible mechanisms for the formation of alkylidene **1**.

It has since been demonstrated that both intramolecular and intermolecular deprotonation are viable mechanisms for the formation of metal-ligand multiple bonds. A clear example of the latter is given in Equation 1.3.[4]

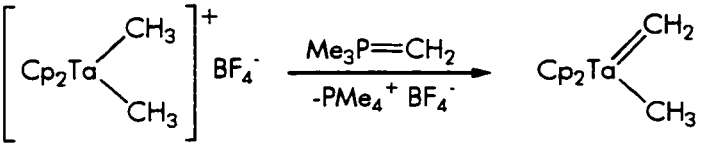

(1.3)

Steric congestion also has a considerable effect on the formation of these species. Complex **3** is stable when R = methyl or benzyl, however bulkier R groups such as neopentyl result in elimination to alkylidene **4**. In a related sense, α elimination can be promoted by the addition of a strongly coordinating species such as trimethylphosphine. The phosphine is thought to increase the steric congestion at the metal through coordination, thus provoking α elimination and formation of the alkylidene (Eq. 1.4).

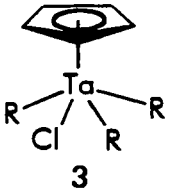

3

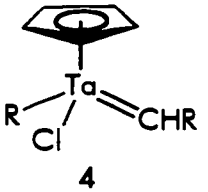

4

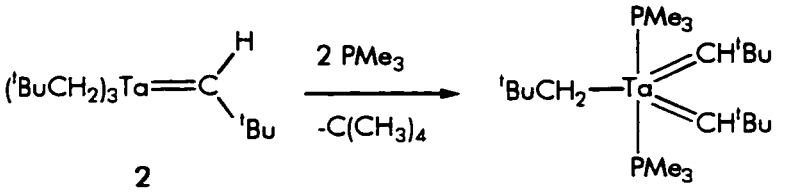

2 (1.4)

Multiple bonds may also be formed through cleavage of carbon from the α atom of the precursor ligand. The driving force for this reaction is the actual multiple bond formation. An example is the extrusion of olefins from metallacyclobutanes to furnish the corresponding alkylidene complex. Although these reactions are generally reversible (Eq. 1.5), they have been used as sources of alkylidene complex.[3]

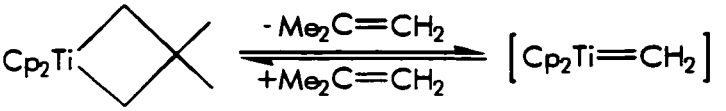

(1.5)

It is noteworthy that the corresponding titanacyclobutenes generally do not revert to the alkylidene and free alkyne. An exception to this is titanacyclobutene **5**, which reversibly loses acetylene at elevated temperatures (Eq. 1.6).[5]

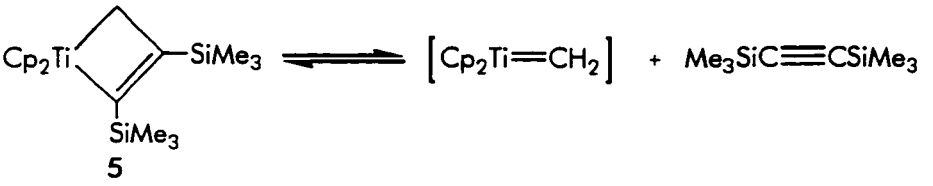

5 (1.6)

Finally, alkylidene complexes have resulted from the transition metal mediated P-C bond cleavage of a Wittig reagent. This strategy has been used to form the first group IV metal alkylidene compound **6**, as depicted in Equation 1.7.[3]

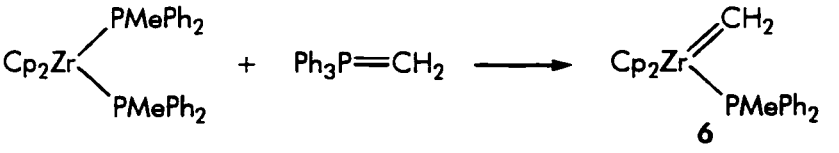

6 (1.7)

1.3 Reactivity of Schrock-Type Alkylidene Complexes

The reactivity of metal-ligand multiple bonds has been interpreted in terms of both frontier orbital control and charge control.[3] Comparisons between *ab initio* and

frontier molecular orbital calculations have revealed that the reactivities of metal-carbon multiple bonds can be understood in terms of frontier orbital theory, whereas a charge controlled mechanism is inadequate. By extension, all π-bonded ligands can be understood in the context of frontier molecular orbital theory.

In a typical Schrock alkylidene, the alkylidene ligand is best described as a closed-shell anion CR_2^{2-} which acts as a π-donor to the metal. The filled ligand π orbitals are lower in energy than the metal *d* orbitals. The π-bonding molecular orbitals most closely resemble ligand orbitals and the π* orbitals are primarily of metal *d* character. Thus the HOMO of the molecule is localized on the alkylidene carbon, which is subject to attack by electrophiles. Conversely, localization of the LUMO on the metal renders it subject to attack and coordination by nucleophiles.

Due to the nucleophilicity of the Schrock-type alkylidene carbon, simple reactions with Lewis Acids result in the formation of adducts. For example, a typical Schrock alkylidene, $Cp_2Ta(CH_2)CH_3$, reacts with $AlMe_3$ to form the adduct $Cp_2Ta(CH_2AlMe_3)(CH_3)$.[3] The classic example of this reaction is the "masking" of the Tebbe-Grubbs reagent by coordination of aluminium alkyls (Eq. 1.8).[6]

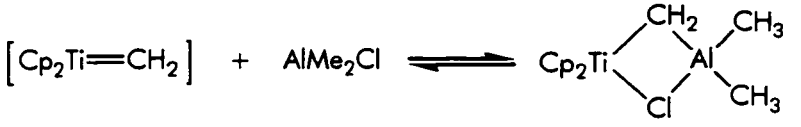

(1.8)

Other organic electrophiles react with Schrock alkylidene complexes through electrophilic attack on the alkylidene ligand. Reactions with organic carbonyl compounds result in the formation of olefins and oxometal species.[3] These reactions are thought to proceed via an electrophilic attack on the alkylidene ligand, involving a [2+2] process directly analogous to that of Wittig phosphorus ylides (R_3P=CR'R").[7] The Schrock alkylidene exhibits enhanced reactivity relative to their isoelectronic Wittig analogues. Aldehydes, ketones, esters, amides and even CO_2 can be converted to olefin

derivatives (Fig. 1.3). The success of these reactions can be attributed in part to the stability of the M=O bond as compared to P=O.

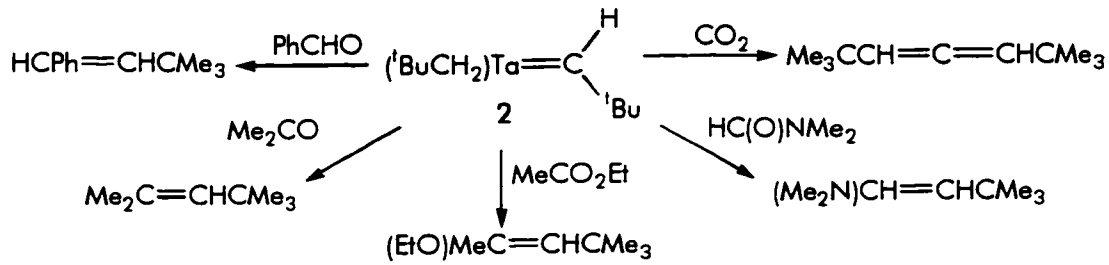

Figure 1.3 Metathetical reactions of Schrock-type alkylidene complexes

A second major class of reactions of alkylidene ligands is metallacycle formation through [2+2] cycloadditions with olefins. As discussed in the previous section, these reactions are generally reversible as illustrated in Equation 1.7. The first example of this reaction was the formation of metallacyclobutane **7** via reaction of a titanium methylidene with neohexene (Eq. 1.9).[8]

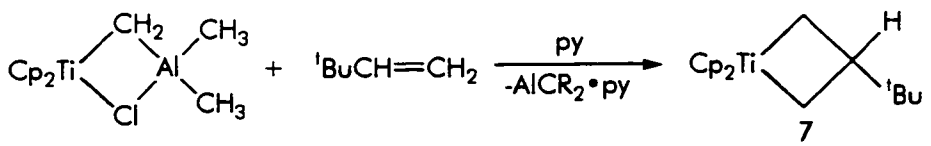

(1.9)

In a similar way, reactions of alkylidenes with alkynes produce metallacyclobutenes. While this mechanism is true of titanium alkylidene complexes, the analogous reaction of tantalum neopentylidene **8** with diphenylacetylene instead yields a rearrangement product. The reaction is thought to proceed through an initial coordination of the alkyne to the tantalum centre, followed by attack by the neopentylidene α-carbon atom to give a metallacyclobutene intermediate which rearranges to give **9** (Eq. 1.10).[9]

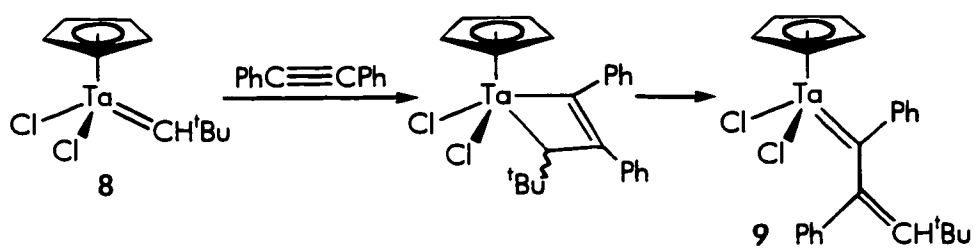

(1.10)

1.4 The Nature of the Metal-Heteroatom Multiple Bond

Bonding in complexes with metal-heteroatom multiple bonds is closely related to the bonding in metal alkylidenes.[3] Due to the high electronegativity of oxygen and nitrogen, the *p* orbitals of oxo and imido ligands are lower in energy than the metal *d* orbitals. Like the alkylidene ligand, these ligands are best described as the closed-shell anions NR^{2-} and O^{2-}, thus high oxidation state metals with empty *d* orbitals form multiple bonds to these ligands. Both NR^{2-} and O^{2-} have one filled orbital of σ symmetry and two filled orbitals of π symmetry, hence both have the potential of forming triple bonds. The bond order in complexes with imido ligands can be approximated by the position of the substituent on nitrogen. Linear M-N-R geometry suggests that the nitrogen is *sp* hybridized and acting as a six-electron donor, implying there is a metal-nitrogen triple bond (**A** in Fig. 1.4). Conversely, deviations from linearity imply a reduced bond order, however this only results when the six-electron linear form would cause the electron count to exceed eighteen (**B** in Fig. 1.4).

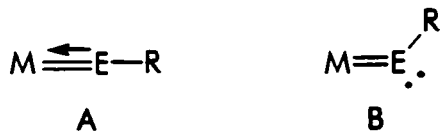

A B

Figure 1.4 Four-electron (**A**) and six-electron (**B**) donation in metal-pnictogenide complexes.

The preceding discussion of bonding in alkylidene, oxo and imido species is important to terminal phosphinidene complexes.[10] Analogous to carbene, the phosphinidene fragment can coordinate to the metal in either a singlet or a triplet state. The singlet phosphinidene coordinates to low-valent transition metals to give electrophilic complexes akin to Fischer carbenes, while the triplet phosphinidene forms Schrock alkylidene-like complexes with high-valent early metal centres. Like the aforementioned imido ligand, triplet phosphinidene coordination results in two potential bonding modes (**A** and **B** in Fig. 1.4).

1.5 Group 4 Terminal Chalcogenido Complexes

Terminal metal oxo species of high-valent group 5-8 metals are well-known, however analogous complexes of the group 4 metals have only appeared in the literature since 1989. An obstacle to the synthesis of these species is the preference the group 4 metals have for structures with bridging ligands over terminal multiple bonds. Several methods have been contrived to successfully combat this tendency.

The first example that demonstrated the reactive nature of the group 4 metal oxo linkage was reported by Bergman and coworkers in 1989.[11a] A transient oxozirconocene [$Cp^*_2Zr{=}O$] was generated through the α elimination of benzene from $Cp^*_2ZrPh(OH)$. The unstable intermediate could not be isolated; however, in the presence of alkyne a [2+2] cycloaddition followed by an *ortho*-metallation gave **10** (Fig. 1.5).

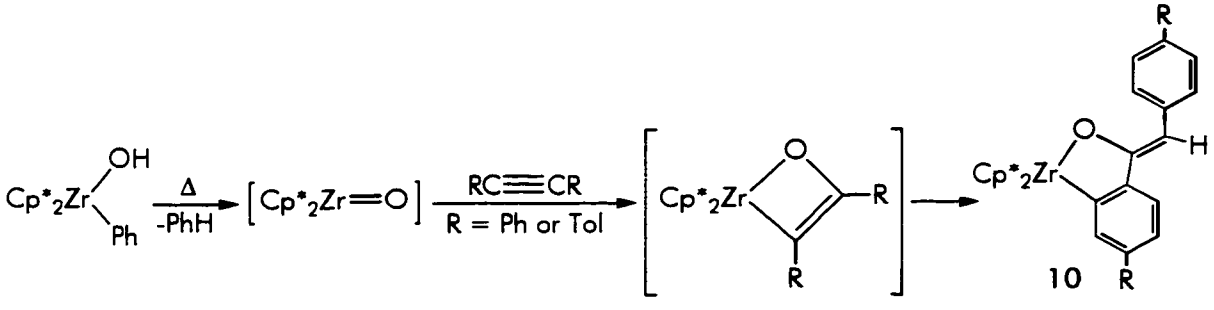

Figure 1.5 Synthesis and trapping of the [$Cp^*_2Zr{=}O$] intermediate.

The C-H bond activation was attributed to the elevated temperatures necessary to effect the α elimination reaction, thus a room temperature route involving the deprotonation of $Cp^*_2Zr(OH)(OSO_2CF_3)$ **11** was devised.[11b] This resulted in the successful generation of [$Cp^*_2Zr{=}O$], which could be trapped by alkynes or nitriles (Fig. 1.6). For example, deprotonation of **11** in the presence of diphenylacetylene resulted in the clean formation of oxametallacyclobutene **12**. Complex **12** has also been prepared by Hillhouse and coworkers through treatment of the zirconocene diphenylacetylene complex $Cp^*_2Zr(PhCCPh)$ with N_2O.[11d] Deprotonation of **11** in the presence of a nitrile afforded **13**, which is derived from the addition of two equivalents of nitrile.

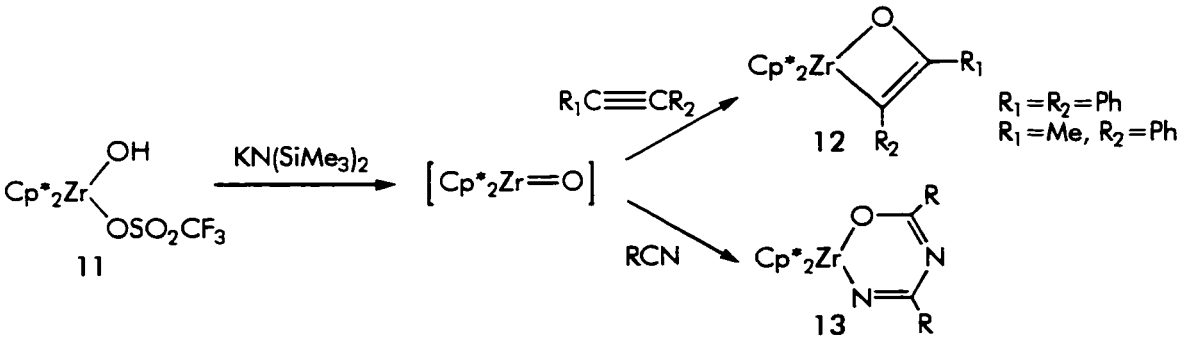

Figure 1.6 Room temperature route to and reactivity of $[Cp^*_2Zr{=}O]$.

Although $[Cp^*_2Zr{=}O]$ was too reactive to be isolated as the adduct of either phosphine or pyridine donors, the isoelectronic $[Cp^*_2Zr{=}S]$ could be trapped in this manner.[11b,c] $[Cp^*_2Zr{=}S]$ was generated via the room temperature dehydrohalogenation of $Cp^*_2Zr(I)(SH)$. Performing this reaction in the presence of a pyridine donor afforded the monomeric terminal sulfido complex **14**, the structure of which confirmed the formation of the first group 4 terminal sulfide (Eq. 1.11).

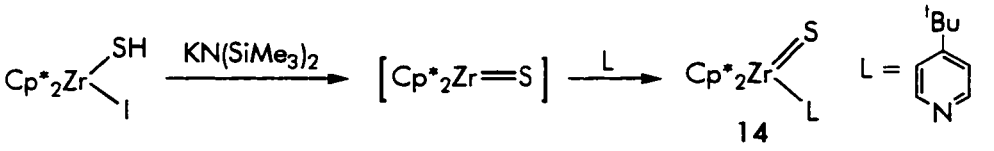

(1.11)

Analogous to the above reactions of $[Cp^*_2Zr{=}O]$, the intermediate $[Cp^*_2Zr{=}S]$ or **14** reacted with alkyne or nitrile to furnish thiametallacyclobutenes and six-membered metallacycles, respectively. A notable trait of both thia- and oxametallacyclobutenes is their reversibility of formation. Both species undergo thermal reversion to $[Cp^*_2Zr{=}X]$ and alkyne, which can be observed by alkyne exchange experiments. Likewise, simply warming thiametallacycle **15** in the presence of 4-tert-butylpyridine resulted in the formation of **14** (Eq. 1.12). The interesting feature of these cycloreversions is that much milder conditions were necessary to induce the cycloreversion of **15**. These reactions illustrate the rather unexpected increased stability of the Zr=S linkage relative to the Zr=O linkage. This phenomenon conflicts with the presumed oxophilicity of early transition metals and poor ability of sulfur to π-bond to these early metals.

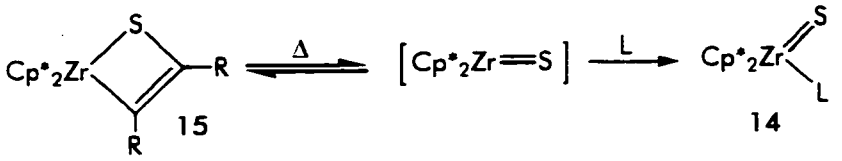

(1.12)

It has long been established that macrocyclic ligands are capable of stabilizing terminal titanium oxo complexes,[3, 12] a characteristic that was also recently demonstrated for zirconium.[13] However, it was not until the 1991 studies by Geoffroy *et al.* that the rich reactivity of these species was unearthed.[14] Ti=O and Ti=S multiple bonds (**16** and **17** in Fig. 1.7) were demonstrated to exhibit a high nucleophilicity. For example, [2+3] cycloadditions of **16** with an electron deficient epoxide yielded metallacycle **18**, while a [2+2] cycloaddition of the Ti=O or Ti=S bond of **16** or **17** with the C=O bond of ketones furnished metallacycles **19** and **20**, respectively. It is noteworthy that these reactions only succeeded with organic molecules possessing strongly electron-withdrawing fluorinated substituents. The reactions with ketones are related to the mechanism of metathetical reactions previously described for Schrock-type alkylidenes; however, with **16** and **17** the reaction terminates at the stable [2+2] cycloaddition product. The absence of the [2+2] retrocycloaddition step may be due to Ti-O and Ti-S bond strengths.

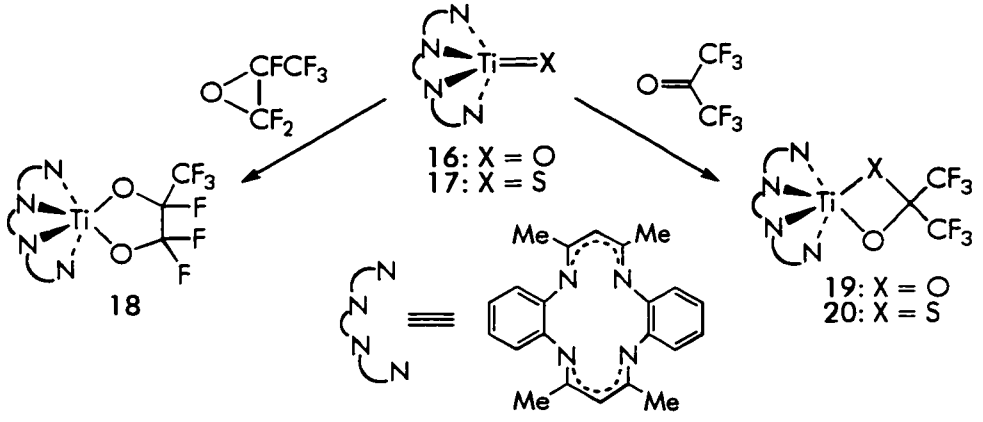

Figure 1.7 Ring-opening and cycloaddition reactions of **16** and **17**.

Recent work has expanded on the reactivity of the Ti=O multiple bond.[15] The terminal oxo species ($Cp^*_2Ti{=}O$)(pyr) **21** was prepared through the reaction of Cp^*_2Ti or $Cp^*_2Ti(C_2H_4)$ with N_2O in the presence of pyridine. Like its oxozirconocene analogues,[11]

this species was found to undergo facile and reversible [2+2] cycloaddition reactions with alkynes to give oxatitanacyclobutenes. A notable point is the tolerance of these systems for terminal alkynes, which give metallacycles **22** resulting from highly regioselective [2+2] cycloaddition reactions. Thermolysis of **22** resulted in conversion to the corresponding hydroxoacetylide complexes **23**, which are the stable thermodynamic products of these reactions (Eq. 1.13).

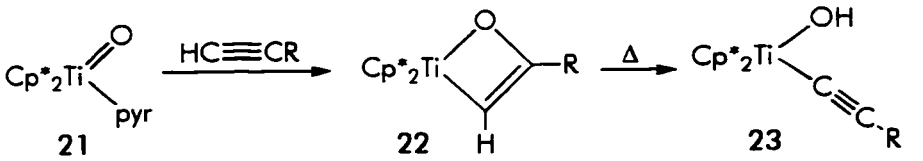

21 22 23 **(1.13)**

Although a number of terminal oxo derivatives of the group 4 metals are known, multiple bonds to the heavier chalcogens selenium and tellurium have proven to be more elusive. In general, metal-ligand multiple bonds to heavier main group elements are considerably more scarce,[16] a trend that is attributed to both decreased $d\pi$-$p\pi$ overlap and the increased tendency of the larger atoms to bridge two or more metal centres. The first terminal tellurido complexes of zirconium and hafnium were reported in 1992 by Christou and Arnold.[17] The synthetic route to these species (Eq. 1.14) is reminiscent of Schrock's use of PMe_3 to promote α elimination in the preparation of alkylidenes.[4] Addition of one equivalent of chelating phosphine dmpe to the homoleptic tellurolates **24** resulted in the formation of adducts **25** and **26**. An additional equivalent of dmpe promoted the elimination of TeR_2 and formation of terminal tellurides **27** and **28**, extremely rare examples of terminal telluride complexes.

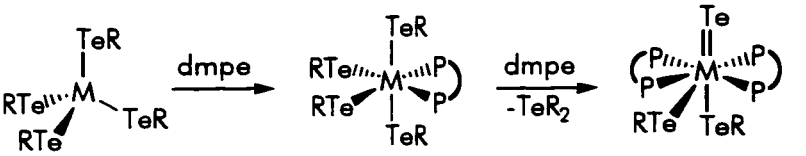

24 **25**: M = Zr; **26**: M = Hf **27**: M = Zr; **28**: M = Hf **(1.14)**

Comparisons between the bonding in terminal chalcogenido Group 4 complexes have been facilitated by the comprehensive research of Parkin and coworkers.[18] The

complete series of terminal chalcogenido complexes $Cp^*_2Zr(X)(pyr)$ (X = O **29**, S **30**, Se **31**, Te **32**) were synthesized through the simple reaction of $Cp_2^*Zr(CO)_2$ with a chalcogen source (N_2O, S_8, Se or Te) in the presence of pyridine. Complexes **29 - 32** were basic enough to react with methyl ketone $PhC(O)CH_3$ to give hydrochalcogenido enolate derivatives of the form $Cp^*_2Zr(XH)\{\eta^1\text{-}OC(Ph)=CH_2\}$ **33**. Similarly, oxo derivative **29** underwent 1,2-additions of both polar and nonpolar substrates to yield complexes such as **34** and **35** (Fig. 1.8).[18a] These reactions are highlighted by the facile reaction with H_2, thus emphasizing the highly reactive nature of the oxo complex. Analogous to Bergman's work,[11] **29** reacted with aldehyde ^{t}BuCHO to give the six-membered metallacycle **36**. While the reactivity studies by Parkin *et al.* are significant, the eminent feature of this work is the crystallographic characterization of the entire series of terminal chalcogenido complexes. A significant point is that both the Zr-O single and Zr=O double bond lengths are anomalously short, reflecting the significant contribution of resonance structure $Zr^+\text{-}E^-$. This ionic contribution is less consequential in the bonding description of the less electronegative heavier chalcogens.

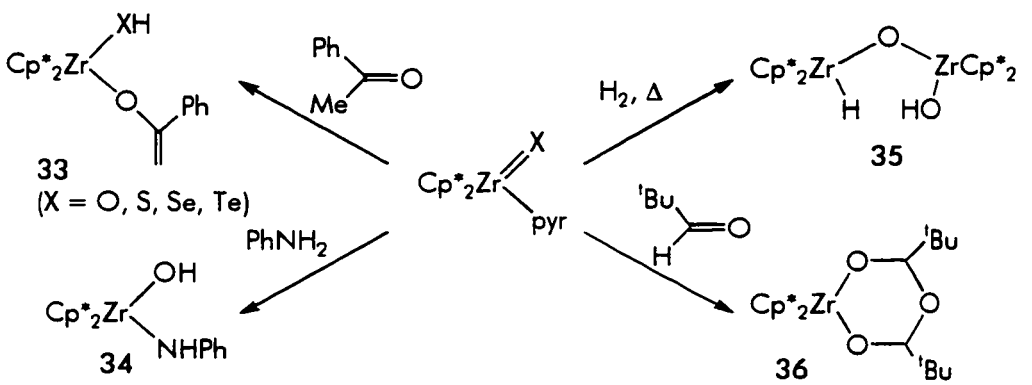

Figure 1.8 Reactions of $Cp^*_2Zr(X)(pyr)$ (E = O **25**, S **26**, Se **27**, Te **28**)

1.6 Group 4 Terminal Pnictogenido Complexes

Group 4 terminal imido complexes were discovered in 1988 by the research groups of Bergman[19] and Wolczanski.[20] These initial forays into the chemistry of the Zr=N multiple bond revealed the intriguing ability of these complexes to induce C-H

bond activations through σ bond metatheses. The syntheses of both Bergman's and Wolczanski's imido complexes were accomplished through both reversible and irreversible α elimination reactions as depicted in Figures 1.9 and 1.10, respectively.

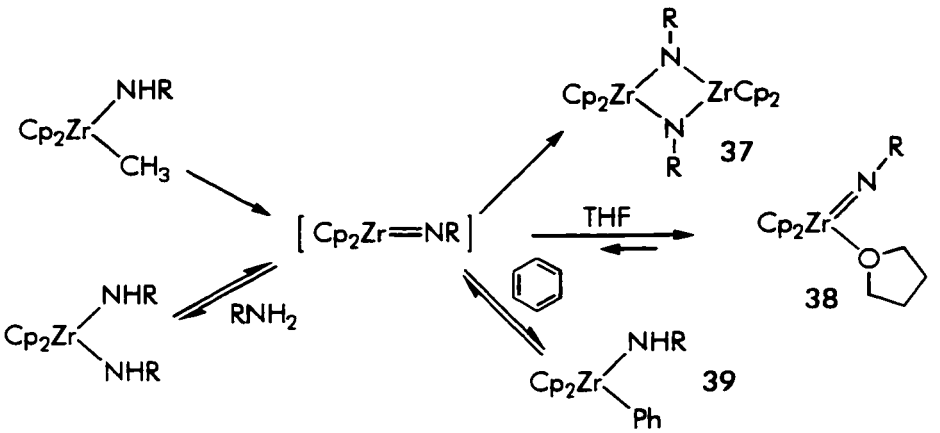

Figure 1.9 Generation, dimerization, THF trapping and C-H activation reactions of $[Cp_2Zr{=}NR]$.

The transient terminal imido intermediates could be trapped by THF. As with almost all terminal imido ligands, there is a linear geometry at nitrogen in imide **38**. When sterically demanding substituents on nitrogen were used to inhibit dimerization, it was found that $[Cp_2Zr{=}NR]$ effected C-H bond cleavage in benzene, leading to phenyl substituted zirconocene amide **39**. Transient imido complex **40** was found to exhibit even higher C-H activation reactivity toward small alkanes. This species was found to induce C-H activation not only in benzene, but also in methane.

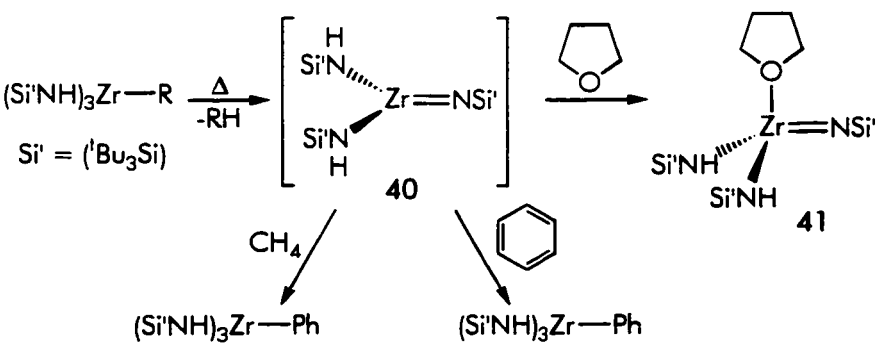

Figure 1.10 Generation, THF trapping and C-H activation reactions of **40**.

The higher reactivity of **40** relative to [Cp_2Zr=NR] can be attributed to the greater degree of coordinative unsaturation in the three-coordinate system.

The first structurally characterized titanium imido complex **42** was reported in 1990 by Roesky *et al.*[20] The coordinative unsaturation in this species was so great that three molecules of pyridine were necessary for its stabilization (Eq. 1.15).

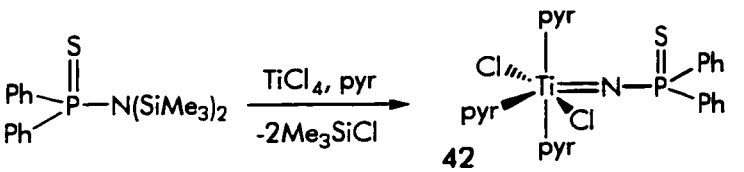

(1.15)

Subsequently, Wolczanski prepared the titanium analogue of **40**,[22a] but later reported that the use of the silox ligand ($^tBu_3SiO$) instigated higher reactivity in the resulting imido species (Eq. 1.16).[22b] Alkylation of (silox)$_2$($^tBu_3$SiNH)TiCl provided **43**, the source of the reactive titanium imido species **44**, which was found to C-H activate a host of alkyl and aryl C-H bonds. An interesting point is that dimerization of **44** is reversible but THF adduct formation is not. This contrasts with studies by Bergman *et al.* in which THF adducts of [Cp_2Zr=NR] are reactive, while bridging imido dimers are not (Fig. 1.14).[23] Presumably the smaller size of titanium, coupled with the steric demands of the ancillary ligands in **44**, markedly decrease the stability of the dimer.

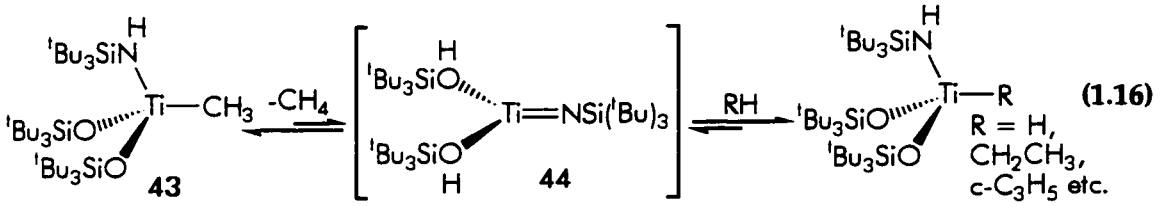

(1.16)

The scope of the reactivity of the Zr=N multiple bond has in every respect been defined by Bergman.[23, 24] As described above, [Cp_2Zr=NR] is available through α eliminations and can be trapped via coordination of THF or other donors. The Zr=N multiple bond undergoes metathetical reactions similar to those of Schrock alkylidenes[3, 4] and Wittig reagents.[7] For example, reaction of **45** with *t*-butylisocyanate resulted in the rapid formation of 1,3-di-*t*-butylcarbodiimide (Eq. 1.17). The reaction is thought to

be initiated by loss of the coordinated labile THF, followed by coordination of the organic carbonyl. Intramolecular attack by the imido group on the η^1-carbonyl gives intermediate **46**, and retrocyclization gives the organic product and zirconium oxides.

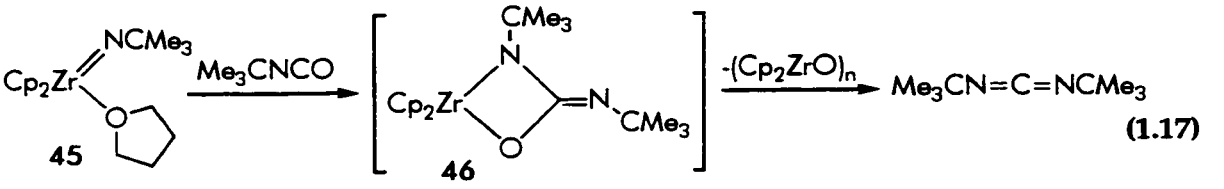

(1.17)

Similar to their oxo and sulfido counterparts,[11] zirconocene imido complexes undergo reversible [2+2] cycloaddition reactions with alkynes.[23, 24] Like titanocene oxo species **21**,[15] the Zr=N multiple bond tolerates terminal alkynes to regioselectively produce azametallacyclobutenes. Azametallacyclobutene complexes have manifested a unique and useful reactivity, such as their role in the catalytic conversion of alkynes to enamines.[24b, c] Reaction of azametallacyclobutene **47** with one equivalent of a primary amine produces enamide amide **48**; addition of a second equivalent proceeds either through direct protonation of the enamide ligand to regenerate the bisamide **49** or through α elimination of the enamine to generate the imido intermediate.

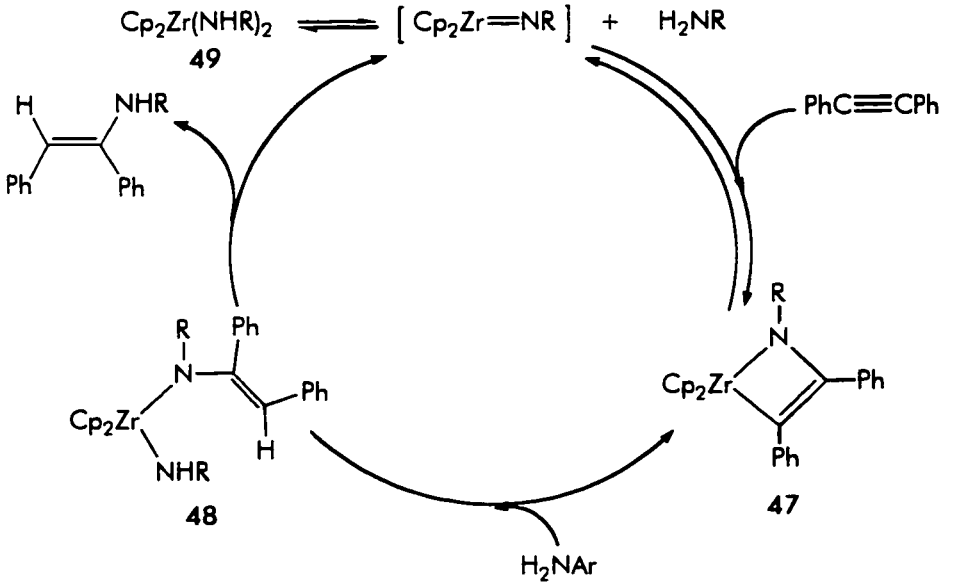

Figure 1.11 Employment of azametallacyclobutenes in the catalytic conversion of alkynes to enamines.

These reactions are thought to be competitive and constitute part of the catalytic cycle that Bergman and coworkers have developed (Fig. 1.11).

Recent work with azametallacyclobutenes has been concerned with insertion reactions.[25] Aldehydes selectively insert into the zirconium-carbon bond of **50** to yield azaoxametallacyclohexenes **51**. Heating **51** induces a [4+2] retrocycloaddition reaction, thus furnishing an α, β-unsaturated imine and a transient [Zr=O] species (Eq 1.18).

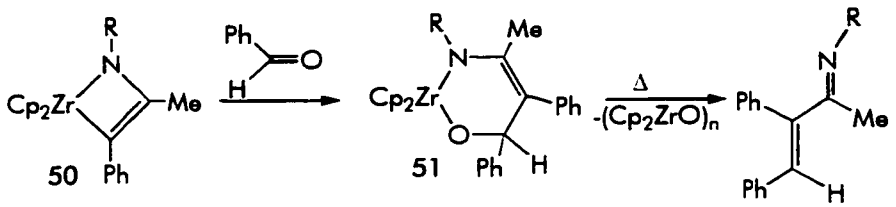

(1.18)

As mentioned in Section 1.2, titanacyclobutanes have been used as sources of the titanium methylidene species.[3] Doxsee and coworkers have cleverly used reactions of **7** with nitriles to yield titanium imido species (Eq. 1.19).[26] The initial [2+2] cycloaddition between the nitrile and the Ti=CH_2 bond, followed by ring-opening and coordination of PMe_3 furnished **52**. In contrast to established reactivity patterns, vinylimido **52** did not undergo metathetical reactions with ketones. In lieu of the [2+2] cycloaddition, a [4+2] cycloaddition between **52** and the ketone yielded the six-membered metallacycle **53**.

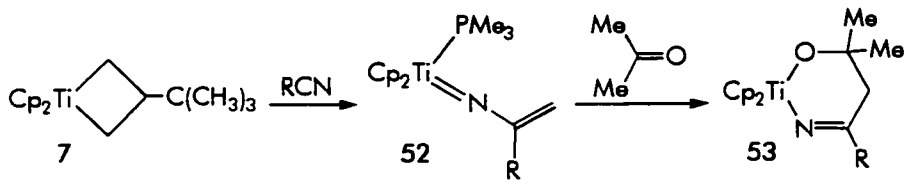

(1.19)

The reactive nature of the group 4 imido functionality has inspired the syntheses of a number of such complexes.[27] An additional synthetic route that has been developed involves the use of low-valent titanium complexes which cleave the N=N bond of azobenzene to afford terminal imido complexes.[27a, d] Despite the attention to syntheses, reactivity studies are limited to those discussed above. In some cases, the explanation for these omissions is the unreactive nature of certain electronically and coordinatively saturated imido species.[27b, f]

Terminal phosphinidene complexes of high-valent early metals have been much slower to develop than their chalcogenido and imido analogues. However, low-valent complexes of phosphinidene in the singlet state have been extensively studied by Mathey and coworkers.[10, 28] Thorough reactivity studies have been performed on the transient species [R-P=M(CO)$_5$] (M = Cr, Mo or W) **54**. These studies have illustrated the rich Fischer carbene-like chemistry of these compounds. The singlet state of the coordinated phosphinidene moiety was indicated via reaction of **54** with water, alcohols and amines (Eq. 1.20). In each case oxidative addition occurred exclusively at the electrophilic phosphorus centre to yield **55**. A number of transformations of **54** have afforded useful organophosphorus derivatives. For example, reactions with alkenes or alkynes result in the insertion of the PR unit into the π bond of the unsaturate, affording phosphiranes and phosphirenes.

$$\underset{\mathbf{54}}{PhP{\rightarrow}M(CO)_5} \xrightarrow[X = OH,\ OR,\ NR_2]{HX} \underset{\mathbf{55}}{Ph(H)(X)P{\rightarrow}M(CO)_5} \qquad \textbf{(1.20)}$$

Terminal phosphinidene complexes of high oxidation state metals were lacking until 1987, when Lappert *et al.* reported the first stable compounds.[29] The molybdenum and tungsten terminal phosphinidene species **56** were synthesized through metathetical reactions (Eq 1.21), and were stabilized by the use of sterically demanding substitiuents on phosphorus. The low field ^{31}P NMR chemical shift of the phosphinidene group in **56** indicates a bent coordination mode of the phosphinidene moiety (**B** in Fig. 1.4). This was confirmed by the crystal structure of the molybdenum complex, which revealed a Mo-P-C angle of 115.8(2)°. These data are consistent with a Mo=P double bond and the presence of a lone pair on phosphorus.

$$1/4\ [\{Cp_2MHLi)\}_4] \xrightarrow{PCl_2R'} \underset{\mathbf{56}}{Cp_2M{=}P(R')} \qquad R' = Ar \text{ or } CH(SiMe_3)_2 \qquad \textbf{(1.21)}$$

Lappert's terminal phosphinidene complexes were the sole specimens until three years later, when Cowley and coworkers accomplished the synthesis of **57** through

cleavage of the phosphaketene ArP=C=O by $WCl_2(PMePh_2)_4$ (Eq. 1.22).[30] The structural parameters of **57** contrasted with those of **56**. The W-P-C angle of 168.2(2)° clearly established **57** as the first linear terminal phosphinidene complex, which is also reflected in the ^{31}P NMR chemical shift of 193.0 ppm. In **57**, the phosphinidene moiety is a six electron donor to the tungsten centre (**A** in Fig. 1.4).

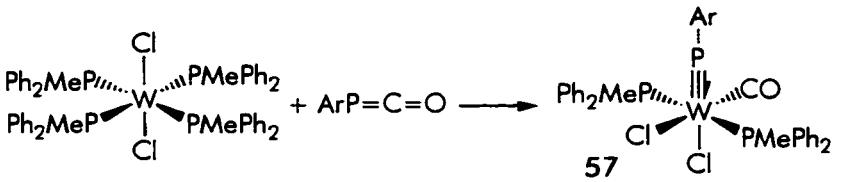

(1.22)

During the course of the research for this thesis, several terminal phosphinidenes of tantalum were reported.[31] The stabilization of these species was effected by highly protective ligands on the metal centre, which also permitted smaller substituents on phosphorus. In this manner, Schrock *et al.* were able to synthesize **59** (Eq. 1.23).[31a] X-ray structures indicated that these complexes are linear terminal phosphinidenes similar to **57**. These species underwent metathetical reactions with small aldehydes to give phosphaalkenes, similar to metathetical reactions of both Schrock alkylidene[3] and zirconocene imido species.[23] Other than the studies presented in this thesis, this brief look at the reactivity of terminal phosphinidene complexes is the only reported data.

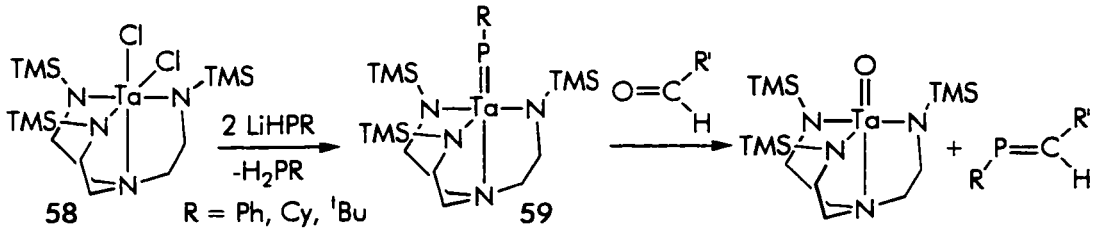

(1.23)

The silox ligand that Wolczanski successfully employed in terminal imido complexes[20b, 22b] was also found to be effective for the stabiiization of tantalum-pnictogen multiple bonds.[31b] The family of compounds consisting of the tantalum imido, phosphinidene and arsinidene complexes **61-63** were all synthesized via oxidative addition of $PhEH_2$ followed by α elimination of hydrogen from the corresponding

$(silox)_3HTaEHPh$ species **60** (Eq. 1.24). The structural characterization of the isomorphous **61** and **62** revealed a bent pnictogenide moiety. These studies not only provide structural information about the still-rare terminal phosphinidene species, they also represent the first characterization of a terminal arsinidene species.

$$(silox)_3Ta + PhEH_2 \longrightarrow \underset{\mathbf{60}}{(silox)_3HTaEHPh} \longrightarrow \underset{E = N\ \mathbf{61},\ P\ \mathbf{62},\ As\ \mathbf{63}}{(silox)_3Ta{=}EPh} + H_2 \qquad \textbf{(1.24)}$$

While not directly related to the present dissertation, the very recent syntheses of the first transition metal-phosphorus triple bonds are worthy of remark. Terminal phosphides had been previously proposed as unstable reaction intermediates.[32] Nonetheless, the research groups of Cummins[33] and Schrock[34] established viable synthetic routes to robust molybdenum and tungsten terminal phosphides, reflecting the tendency of these elements to form triple bonds.[3] Employment of the tungsten analogue of **58** $(N_3N)WCl$ ($N_3N = [Me_3SiNCH_2CH_2)_3N]^{3-}$) in Equation 1.23 yielded $(N_3N)W{\equiv}P$ **64**, while Cummins and coworkers reacted their remarkable three-coordinate molybdenum (III) complex **65** with P_4 to furnish $(NRR')_3Mo{\equiv}P$ **66** (Eq. 1.25). These remarkably stable products are the first and only members of the class of one-coordinate metal phosphides.

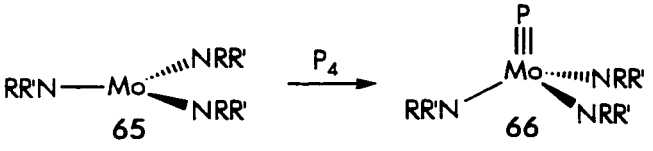

(1.25)

The preceding discussion has shown that although a number of group 4 chalcogenides and imides have been synthesized, the few stable terminal phosphinidene complexes have only incorporated group 5 and 6 metals. Work in our laboratories has focused on ways to remedy this restriction.[35] Studies of zirconium phosphide species have led to the isolation of a number of novel products whose formation can be rationalized by invoking a terminal phosphinidene intermediate. The highly reactive nature of these intermediates accounts for both the observed products as well as the

dearth of stable group 4 terminal phosphinidene complexes. For example, oxidative addition of the P-H bonds of H_2PR was found to occur with transient $Cp_2Zr(II)$.[35a] Intramolecular loss of H_2 yielded the intermediate phosphinidene **67**, which subsequently dimerized and underwent cyclopentadienyl C-H activation and rearrangement to yield **68** (Fig. 1.12). Sterics are critical to these reactions, as the use of a smaller metal centre (titanium) and a more sterically demanding substituent on phosphorus (Mes*) resulted in P-C bond cleavage to give a $[Cp_2Ti{=}PH]$ intermediate.[35b]

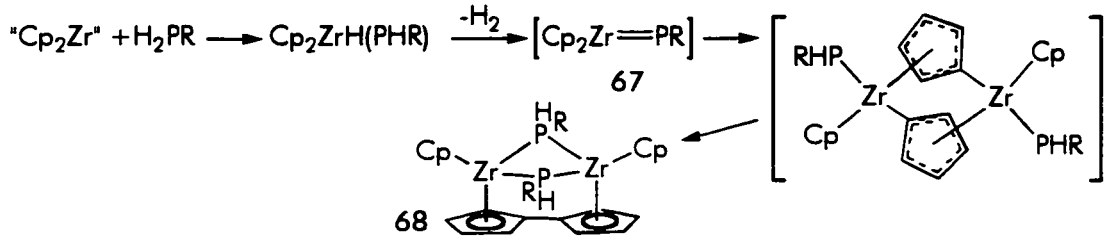

Figure 1.12 Generation of a terminal zirconium phosphinidene intermediate.

Zirconium diphosphides are useful sources of transient terminal phosphinidene species, which are formed through α eliminations of H_2PR. A clear cut case establishing the intermediacy of the terminal phosphinidene required sterically demanding ligands on the metal centre (Fig. 1.13).[35c]

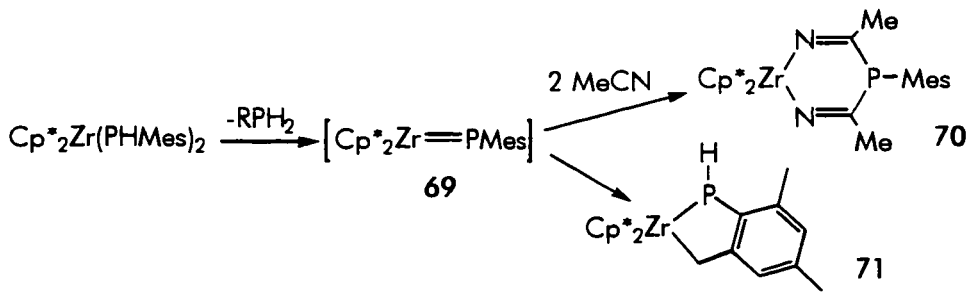

Figure 1.13 Trapping and C-H activation reactions of terminal phosphinidene **69**.

The transient terminal phosphinidene intermediate **69** was trapped with two equivalents of MeCN to give **70**, similar to reactions of $[Cp^*_2Zr{=}O]$ and $[Cp^*_2Zr{=}S]$.[11, 18a] The initial [2+2] cycloaddition was followed by insertion of the second equivalent into

the Zr-P bond, reflecting the reactive nature of the Zr-P bond relative to Zr-O or Zr-S. When nitrile was not present, intramolecular C-H bond activation afforded **71**. Attempts to trap **69** with dative ligands or other reagents unfortunately were unsuccessful.

1.4 Summary and Scope of Thesis

The history of high-valent metal-ligand multiply bonded complexes demonstrates a number of important points. Multiple bonds involving high valent early transition metals are analogous to Schrock-type alkylidenes, and in general are highly reactive complexes. This has indeed been established in many of the studies of zirconium and titanium terminal oxides, sulfides and imides. The above species undergo a variety of reactions, the most significant being [2+2] cycloadditions with organic unsaturates. The outcome of these processes is dependent on the nature of the multiple bond. For example, cycloadditions of organic carbonyl species with Ti=O bonds have been demonstrated to terminate after the initial [2+2] cycloaddition, while analogous reactions employing either Schrock alkylidenes or zirconium imido complexes involves further [2+2] retrocycloadditions to yield the products of metatheses. These metathetical reactions facilitate entry into metal-mediated organic syntheses, while cycloadditions with alkynes furnish synthetically useful metallacyclobutenes.

Application of the above reactions to M=P species has been frustrated by the highly reactive nature of the terminal phosphinidene, a trait which is especially true of the Zr=P bond. Nonetheless, this intense reactivity is a tantalizing goal. Terminal phosphinidenes are expected to undergo not only the cycloadditions established for their chalcogenide and imide counterparts, but as well unique reaction pathways not available for the less reactive bonds. Consequently, a successful terminal phosphinidene requires paradoxical traits: the species must be stable enough to isolate

and use in a controlled reactivity study, yet the compulsory protective ancillary ligands must not hinder potential reactions. The primary goal of this thesis is the synthesis of such a species. As this introduction has illustrated, a wealth of information is available on multiple bonds in general, as well as on the fascinating chemistry of complexes containing zirconium phosphorus bonds. This dissertation will relate how these studies were critical to the development of a synthetic route to the first (and as yet unique) stable group 4 terminal phosphinidene. As a result, the ensuing chapters are predominantly focused on the rich chemistry of the Zr=P multiple bond. Extensive and fruitful reactivity studies that encompass metatheses, 1,2-additions, cycloadditions and metallacycle transfer reactions have provided fundamental information about the nature of the Zr=P multiple bond.

Chapter Two
Synthetic Routes to Terminal Phosphinidene Complexes of Zirconium

2.1 Introduction

The highly reactive nature of the M=P moiety can be implicated in the paucity of stable terminal phosphinidene complexes. Several years ago, a variety of approaches employing P-H bond activation as a means to synthesizing zirconium phosphides and dimeric phosphinidene derivatives were explored in our laboratories.[35] These studies suggested that the stabilization of a terminal zirconium phosphinidene required the presence of a sterically demanding substituent on phosphorus. Studies of related zirconium chalcogenido[11, 15, 17, 18] and imido[19, 20, 23] derivatives have demonstrated that these reactive species can be trapped by donors such as THF or pyridine, isolated as cycloaddition products of organic unsaturates or isolated as the products of C-H activations. Similarly, we have shown that the transient terminal phosphinidene species [Cp^*_2Zr=PMes] can either be trapped via reaction with nitrile to give a six-membered metallacycle or isolated as the product of an intramolecular C-H activation (Fig. 1.13).[35c] These strategies have been employed in the present work. Reactions designed to generate transient terminal phosphinidenes were performed in the presence of organic unsaturates, the use of trapping donors was examined, and the effect of steric demands was investigated.

2.2 Experimental

General Data All preparations were performed under an atmosphere of dry, O_2-free N_2 employing either Schlenk line techniques or a Vacuum Atmospheres inert atmosphere glove box. Solvents were reagent grade, distilled from the appropriate drying agents under N_2 and degassed by the freeze-thaw method at least three times prior to use. Organic reagents were purified by conventional methods. ^1H and $^{13}C\{^1H\}$ NMR spectra

were recorded on a Bruker AC-300 operating at 300 and 75 MHz, respectively. ^{31}P and $^{31}P\{^1H\}$ NMR spectra were recorded on a Bruker AC-200 operating at 81 MHz. Trace amounts of protonated solvents were used as references and chemical shifts are reported relative to $SiMe_4$ and 85% H_3PO_4 respectively. Spectral simulations were performed with the software PANIC. Yields calculated by ^1H NMR were determined in reference to a CH_2Cl_2 internal standard which was introduced by means of an Evans NMR tube. Low and high resolution EI mass spectral data were obtained employing a Kratos Profile mass spectrometer outfitted with a N_2 glove bag enclosure for the inlet port. Combustion analyses were performed by Galbraith Laboratories Inc., Knoxville, TN or Schwarzkopf Laboratories, Woodside, NY. H_2PMes and H_2PMes^* were purchased from the Quantum Design Chemical Co. All other reagents were purchased from the Aldrich Chemical Co. or the Strem Chemical Co. Glass reaction vessels fitted with ground glass joints and Teflon stopcocks are referred to as "bombs". Cp_2ZrMe_2, $Cp_2ZrMeCl$,[36] $(Cp_2ZrCl)_2(\mu\text{-}PMes)$[35a], LiHPMes•2THF, LiHPMes*•3THF[37] were prepared by literature methods. The procedure of Power *et al.* was used for the preparation of Li_2PMes.[38]

Synthesis of $Cp_2ZrMe(PHMes^*)$ 72

To a benzene solution of $Cp_2ZrMeCl$ (272 mg, 1.0 mmol) was added a benzene solution of LiHPMes*•3THF (501 mg, 1.0 mmol). After standing for 10 minutes the LiCl was filtered from the wine-red solution. Yield: 98% (by ^1H NMR). ^1H NMR (25 °C, C_6D_6): δ 7.58 (br s, 2H, Ar-*H*), 6.04 (d, $|J_{P\text{-}H}|$ = 263.9 Hz, 1H, P-*H*), 5.53 (s, 10H, Cp), 1.64 (br s, 18H, *o*-^{t}Bu), 1.33 (s, 9H, *p*-^{t}Bu), -0.14 (d, $|^3J_{P\text{-}H}|$ = 7.1 Hz, 3H, CH_3). $^{13}C\{^1H\}$ NMR (25 °C, C_6D_6): δ 148.0 (s, quat), 139.0 (d, $|J|$ = 7.0 Hz, quat), 121.2 (s, arom. *C*-H), 108.2 (s, Cp), 38.5 (s, *o*-$C(CH_3)_3$), 34.7 (s, *p*-$C(CH_3)_3$), 32.9 (br s, *o*-$C(CH_3)_3$), 31.3 (s, *p*-$C(CH_3)_3$), 24.8 (s, CH_3). ^{31}P NMR (25 °C, C_6D_6): δ 74.1 (d, $|J_{P\text{-}H}|$ = 264.7 Hz).

Synthesis of $Cp_2ZrMe(OCPh_2PHMes^*)$ 73, $Cp_2ZrMe(OC_6H_{10}PHMes^*)$ 74, $Cp_2ZrMe(OC(CH_3)_2PHMes^*)$ 75, $Cp_2ZrMe(NCPhPHMes^*)$ 76 and $Cp_2ZrMe(OC(CH_3)_2PHMes)$ 78

Compounds **73-76** and **78** were prepared through similar routes, thus only one representative procedure is described. To a benzene solution of $Cp_2ZrMeCl$ (136 mg, 0.5 mmol) and benzophenone (91 mg, 0.5 mmol) was added a benzene solution of LiHPMes*•3THF (250 mg, 0.5 mmol). The resulting solution turned orange, then immediately very pale yellow. After standing 2 h, the solvent was removed in vacuo and the product was extracted into pentane. Filtration was followed by a reduction in the volume of the solution under reduced pressure. Colourless crystals formed over 12 h at room temperature and were isolated by filtration. **73**: Yield: 289 mg (83%). ^1H NMR (25 °C, C_6D_6): δ 7.49 (m, 2H, Ph-*H*), 7.33 (m, 1H, Ph-*H*), 7.18 (m, 1H, Ph-*H*), 7.00 (m, 6H, Ph-*H*), 6.72 (m, 2H, Ph-*H*), 5.86 (s, 5H, Cp), 5.71 (s, 5H, Cp), 5.67 (d, $|J_{P-H}|$ = 244.6 Hz, 1H, P-*H*), 1.42 (s, 9H, ^{t}Bu), 1.31 (s, 9H, ^{t}Bu), 1.25 (s, 9H, ^{t}Bu), 0.66 (s, 3H, CH_3). $^{13}C\{^1H\}$ NMR (25 °C, C_6D_6): δ 157.0 (s, quat), 156.6 (d, $|J|$ = 17.1 Hz, quat), 149.4 (s, quat), 147.0 (d, $|J|$ = 21.5 Hz, quat), 143.9 (s, quat), 130.9 (d, $|J|$ = 44.6 Hz, quat), 129.0 (d, $|J|$ = 8.3 Hz, arom. C-H), 127.3 (s, arom. C-H), 126.8 (s, arom. C-H), 126.7 (s, arom. C-H), 126.3 (s, arom. C-H), 125.4 (s, arom. C-H), 122.3 (s, arom. C-H), 111.2 (s, Cp), 110.9 (s, Cp), 94.1 (d, $|J|$ = 18.9 Hz, O-C), 38.6 (s, $C(CH_3)_3$), 37.9 (s, $C(CH_3)_3$), 34.6 (s, $C(CH_3)_3$), 34.3 (d, $|J|$ = 10.7 Hz, $C(CH_3)_3$), 33.8 (s, $C(CH_3)_3$), 31.5 (s, $C(CH_3)_3$), 22.5 (s, CH_3). ^{31}P NMR (25 °C, C_6D_6): δ -8.6 (d, $|J_{P-H}|$ = 244.1 Hz). Anal. Calcd for $C_{42}H_{53}OPZr$: C: 72.47; H: 7.67; Found: C: 72.30; H: 7.45.

74: Yield: 72% (by ^1H NMR). ^1H NMR (25 °C, C_6D_6): δ 7.39 (m, 2H, Ar-*H*), 5.93 (s, 5H, Cp), 5.91 (s, 5H, Cp), 4.79 (d, $|J_{P-H}|$ = 222.5 Hz, 1H, P-*H*), 2.2-1.1 (m, 10H, Cy-*H*), 1.67 (s, 9H, ^{t}Bu), 1.54 (s, 9H, ^{t}Bu), 1.28 (s, 9H, ^{t}Bu), 0.42 (s, 3H, CH_3). $^{13}C\{^1H\}$ NMR (25 °C, C_6D_6): δ 157.2 (br s, quat), 148.6 (s, quat), 132.2 (d, $|J|$ = 38.9 Hz, quat), 122.0 (s, arom. C-H), 110.8 (s, Cp), 110.5 (s, Cp), 87.0 (d, $|J|$ = 9.5 Hz, O-C), 39.6 (d, $|J|$ = 19.0 Hz, CH_2), 38.1

(d, $|J|$ = 26.1 Hz, CH_2), 35.4 (d, $|J|$ = 11.8 Hz, $C(CH_3)_3$), 34.7 (s, $C(CH_3)_3$), 34.3 (s, $C(CH_3)_3$), 31.2 (s, $C(CH_3)_3$), 25.6 (s, CH_2), 22.6 (s, CH_2), 21.9 (d, $|J|$ = 9.7 Hz, CH_2), 20.7 (s, CH_3). ^{31}P NMR (25 °C, C_6D_6): δ -24.9 (d, $|J_{P\text{-}H}|$ = 222.3 Hz). HRMS (EI) *m/e* Calcd for $C_{35}H_{53}OPZr$: 595.2642; *m/e* Found: 595.2630 (M^+ - CH_3).

75: Yield: 73% (by ^1H NMR). ^1H NMR (25 °C, C_6D_6): δ 7.44 (s, 2H, Ar-*H*), 5.87 (s, 5H, Cp), 5.82 (s, 5H, Cp), 5.01 (d, $|J_{P\text{-}H}|$ = 228.7 Hz, 1H, P-*H*), 1.69 (s, 9H, ^{t}Bu), 1.53 (s, 9H, ^{t}Bu), 1.29 (s, 9H, ^{t}Bu), 1.04 (d, $|^3J_{P\text{-}H}|$ = 10.9 Hz, 3H, CH_3), 0.82 (d, $|^3J_{P\text{-}H}|$ = 3.8 Hz, 3H, CH_3), 0.36 (s, 3H, Zr-CH_3). $^{13}C\{^1H\}$ NMR (25 °C, C_6D_6): δ 156.6 (s, quat), 154.3 (s, quat), 148.8 (s, quat), 132.9 (d, $|J|$ = 38.3 Hz, quat), 121.9 (s, arom. *C*-H), 121.8 (s, arom. *C*-H), 110.5 (s, Cp), 110.4 (s, Cp), 84.7 (d, $|J|$ = 12.2 Hz, O-C), 38.2 (s, $C(CH_3)_3$), 38.1 (s, $C(CH_3)_3$), 35.0 (d, $|J|$ = 11.9 Hz, $C(CH_3)_3$), 33.9 (s, $C(CH_3)_3$), 31.3 (s, $C(CH_3)_3$), 19.9 (s, CH_3). ^{31}P NMR (25 °C, C_6D_6): δ -30.1 (d, $|J_{P\text{-}H}|$ = 229.1 Hz). HRMS (EI) *m/e* Calcd for $C_{32}H_{49}OPZr$: 555.2329; *m/e* Found: 555.2334 (M^+ - CH_3).

76: Yield: 56% (by ^1H NMR). ^1H NMR (25 °C, C_6D_6): δ 7.62 (d, $|^4J_{P\text{-}H}|$ = 2.1 Hz, 1H, Ar-*H*), 7.51 (br, 1H, Ar-*H*), 7.17-7.09 (m, 5H, Ph-*H*), 6.17 (d, $|J_{P\text{-}H}|$ = 234.3 Hz, 1H, P-*H*), 5.60 (s, 5H, Cp), 5.58 (s, 5H, Cp), 1.73-1.49 (br, 18H, *o*-^{t}Bu), 1.44 (s, 9H, *p*-^{t}Bu), -0.25 (br s, 3H, CH_3). $^{13}C\{^1H\}$ NMR (25 °C, C_6D_6): δ 177.9 (d, $|J|$ = 30.5 Hz, N=*C*), 150.1 (s, quat), 142.2 (d, $|J|$ = 34.1 Hz, quat), 129.3 (s, arom. *C*-H), 128.1 (s, arom. *C*-H), 125.8 (s, arom. *C*-H), 122.3 (br s, arom. *C*-H), 108.0 (s, Cp), 107.8 (s, Cp), 38.1 (br s, *o*-$C(CH_3)_3$), 35.1 (s, *p*-$C(CH_3)_3$), 33.5 (br s, *o*-$C(CH_3)_3$), 33.4 (br s, *o*-$C(CH_3)_3$), 31.5 (s, p-$C(CH_3)_3$), 17.2 (br s, CH_3). ^{31}P NMR (25 °C, C_6D_6): δ -44.8 (d, $|J_{P\text{-}H}|$ = 233.9 Hz). HRMS (EI) *m/e* Calcd for $C_{36}H_{48}NPZr$: 615.2567; *m/e* Found: 615.2582.

78: Yield: 76% (by ^1H NMR). ^1H NMR (25 °C, C_6D_6): δ 6.80 (s, 2H, Mes-*H*), 5.83 (s, 5H, Cp), 5.82 (s, 5H, Cp), 4.42 (d, $|J_{P\text{-}H}|$ = 216.5 Hz, 1H, P-*H*), 2.50 (s, 6H, *o*-CH_3), 2.07 (s, 3H, *p*-CH_3), 1.29 (d, $|^3J_{P\text{-}H}|$ = 5.5 Hz, 3H, CH_3), 1.24 (d, $|^3J_{P\text{-}H}|$ = 11.8 Hz, 3H, CH_3), 0.38 (s, 3H, Zr-CH_3). $^{13}C\{^1H\}$ NMR (25 °C, C_6D_6): δ 142.4 (d, $|J|$ = 10.4 Hz, quat), 137.8 (s, quat), 130.6 (d, $|J|$ = 24.1 Hz, quat), 129.3 (s, arom. *C*-H),110.5 (s, Cp), 83.2 (d, $|J|$ = 7.6 Hz,

O-C), 33.1 (d, $|J|$ = 4.1 Hz, CH_3), 31.8 (s, CH_3), 24.1 (d, $|J|$ = 11.7 Hz, CH_3), 20.8 (s, CH_3), 19.2 (s, CH_3). ^{31}P NMR (25 °C, C_6D_6): δ -48.9 (d, $|J_{P-H}|$ = 217.7 Hz).

Synthesis of $(Cp_2ZrMe)_2(\mu\text{-PMes})$ 79

To a toluene solution of Cp_2ZrMe_2 (503 mg, 2.0 mmol) was added a toluene solution of H_2PMes (152 mg, 1.0 mmol). The colourless solution was placed in a bomb and heated at 110° for 5 h, during which time it became deep indigo. After cooling to 25 °C, the volume was reduced and the solution allowed to stand for 3 days. Large, extremely air-sensitive dark blue crystals formed and were isolated by filtration. Yield: 511 mg (82%). ^1H NMR (25 °C, C_6D_6): δ 7.08 (s, 2H, Mes-*H*), 5.66 (s, 20H, Cp), 2.35 (s, 6H, *o*-CH_3), 2.27 (s, 3H, *p*-CH_3), 0.24 (d, $|^3J_{P-H}|$ = 3.1 Hz, 6H, Zr-CH_3). $^{13}C\{^1H\}$ NMR (25 °C, C_6D_6): δ 138.1 (s, quat), 134.4 (s, quat), 128.3 (s, arom. C-H), 109.8 (s, Cp), 27.9 (s, CH_3), 26.6 (d, $|J|$ = 9.0 Hz, CH_3), 20.9 (s, CH_3). ^{31}P NMR (25 °C, C_6D_6): δ 303.2 (s). Anal. Calcd for $C_{31}H_{37}PZr$: C: 59.76; H: 5.99; Found: C: 59.67; H: 5.88.

Synthesis of $(Cp_2Zr)(Cp_2ZrPHMes)(\mu\text{-PMes})(\mu\text{-}\eta^1\text{:}\eta^5\text{-}C_5H_4)$ 81

(i) To a toluene solution of Cp_2ZrMe_2 (503 mg, 2.0 mmol) was added a toluene solution of H_2PMes (304 mg, 2.0 mmol). The colourless solution was placed in a bomb and heated at 110° for 5 h, during which time it became dark brown. After cooling to 25 °C, the toluene was removed under reduced pressure and the product was then dissolved in diethyl ether. Upon standing 12 h dark brown crystals formed which were isolated by filtration. Yield: 520 mg (70%). (ii) To a benzene suspension of $(Cp_2ZrCl)_2(\mu\text{-PMes})$ (332 mg, 0.5 mmol) was added excess PMe_3 and a benzene suspension of Li_2PMes (90 mg, 0.55 mmol). The mixture was stirred vigorously for 12h, after which time it was filtered. ^{31}P NMR of the reaction mixture showed the clean formation of $(Cp_2Zr{=}PMes)(PMe_3)$ **83**. After filtration, the solvent was removed in vacuo and the product dissolved in diethyl ether. Upon standing 12 h dark brown crystals formed which were isolated by filtration. Yield 238 mg (64%). ^1H NMR (25 °C, C_6D_6): δ 7.03 (s,

1H, Mes-*H*), 6.95 (s, 1H, Mes-*H*), 6.92 (s, 2H, Mes-*H*), 6.50 (br d, $|^3J_{P\text{-}H}|$ = 7.1 Hz, 1H, C-*H*), 6.29 (s, 5H, Cp), 5.98 (br s, 1H, C-*H*), 5.66 (s, 5H, Cp), 5.25 (s, 5H, Cp), 5.12 (br, 1H, C-*H*), 4.65 (br, 1H, C-*H*), 3.27 (dd, $|^1J_{P\text{-}H}|$ = 203.5 Hz, $|^3J_{P\text{-}H}|$ = 10.8 Hz, 1H, P-*H*), 2.69 (s, 3H, Me), 2.49 (s, 6H, *o*-CH_3), 2.40 (s, 3H, CH_3), 2.25 (s, 3H, CH_3), 2.23 (s, 3H, CH_3). $^{13}C\{^1H\}$ NMR (25 °C, C_6D_6): δ 175.1 (s, quat), 148.1 (d, $|J|$ = 11.9 Hz, quat), 145.3 (d, $|J|$ = 32.4 Hz, quat), 141.1 (d, $|J|$ = 9.2 Hz, quat), 138.5 (d, $|J|$ = 7.8 Hz, quat), 138.0 (s, quat), 135.8 (s, quat), 132.7 (s, quat), 128.8 (s, arom. *C*-H), 128.6 (s, arom. *C*-H), 128.1 (s, arom. *C*-H), 111.2 (s, arom. *C*-H), 110.2 (d, $|J|$ = 4.5 Hz, Cp), 109.8 (s, Cp), 108.8 (s, arom. *C*-H), 106.3 (s, Cp), 106.1 (s, arom. *C*-H), 106.0 (s, arom. *C*-H), 25.2 (s, CH_3), 25.1 (s, CH_3), 24.1 (br s, CH_3), 20.9 (s, CH_3), 20.8 (s, CH_3). ^{31}P NMR (25 °C, C_6D_6): δ 395.4 (d, $|J_{P\text{-}P}|$ = 29.1 Hz), -84.2 (dd, $|^1J_{P\text{-}H}|$ = 203.0 Hz, $|J_{P\text{-}P}|$ = 29.0 Hz). Anal. Calcd for $C_{38}H_{42}P_2Zr_2$: C: 61.42; H: 5.70; Found: C: 61.34; H: 5.67.

Synthesis of (Cp_2Zr=PMes*)(PMe_3) 84

To a benzene solution of $Cp_2ZrMeCl$ (272 mg, 1.0 mmol) and excess PMe_3 was added a benzene solution of LiHPMes*•3THF (501 mg, 1.0 mmol). The reaction mixture stood for 3 days after which time the green-black solution was filtered and the solvent removed in vacuo. The oily residue was taken up in diethyl ether and the solvent was again evaporated in vacuo. This produced a flaky green-black solid. Yield: 545 mg (95%). ^1H NMR (25 °C, C_6D_6): δ 7.68 (s, 2H, Ar-H), 5.49 (s, 5H, Cp), 5.48 (s, 5H, Cp), 1.62 (s, 18H, *o*-^{t}Bu), 1.55 (s, 9H, *p*-^{t}Bu), 0.66 (d, $|^2J_{P\text{-}H}|$ = 6.3 Hz, 9H, P(CH_3)). $^{13}C\{^1H\}$ NMR (25°C, C_6D_6): δ 147.3 (s, quat), 142.7 (d, $|J|$ = 54.5 Hz, quat), 119.7 (s, arom. *C*-H), 104.6 (s, Cp), 38.4 (s, *o*-$C(CH_3)_3$), 34.6 (s, *p*-$C(CH_3)_3$), 32.8 (s, *o*-$C(CH_3)_3$), 31.9 (s, *p*-$C(CH_3)_3$), 17.7 (d, $|J|$ = 18.0 Hz, CH_3). ^{31}P NMR (25 °C, C_6D_6): δ 792.4 (d, $|J_{P\text{-}P}|$ = 23.1 Hz), -12.0 (d, $|J_{P\text{-}P}|$ = 23.4 Hz). Anal. Calcd for $C_{31}H_{48}P_2Zr$: C: 64.88; H: 8.43; Found: C: 64.66; H: 8.28.

General Information on X-Ray Data Collection and Reduction

All X-ray data collection, data reduction, structure solution and refinement performed in this thesis were performed using the same method; thus only one general description is given. Deviations will be noted in appropriate sections of the thesis.

X-ray quality crystals were manipulated and mounted in capillaries in a glove box, thus maintaining a dry, O_2-free environment for each crystal. Diffraction experiments were performed on a Rigaku AFC6 or AFC5R diffractometer equipped with graphite-monochromatized Mo Kα radiation. The initial orientation matrix was obtained from 20 machine-centred reflections selected by an automated peak search routine. These data were used to determine the crystal system. Automated Laue system check routines around each axis were consistent with the crystal system. 25 reflections ($20°<2\theta<25°$) were used to obtain the final lattice parameters and orientation matrix. The observed extinctions were consistent with the space groups given in Table 2.1. The data were collected in three shells ($4.5°<2\theta<50.0°$) and 3 standard reflections were recorded every 197 reflections. Fixed scan rates were employed. Up to 4 repetitive scans of each reflection at the respective scan rates were averaged to insure meaningful statistics. The number of scans of each reflection was determined by the intensity. The intensities of the standards showed no statistically significant change over the duration of data collection. The data were processed using the TEXSAN crystal solution package operating on a SGI Challenger mainframe with remote X-terminals. The reflections with $F_o^2>3\sigma F_o^2$ were used in the refinements.

General Information on Structure Solution and Refinement.

Non-hydrogen atomic scattering factors were taken from the literature tabulations.[39, 40] The heavy atom positions were determined using direct methods. The remaining non-hydrogen atoms were located from successive difference Fourier map calculations. The refinement was carried out by using full-matrix least squares

techniques on F, minimizing the function $\omega(|F_o|-|F_c|)^2$ where the weight ω is defined as $4F_o^2/2\sigma(F_o^2)$ and F_o and F_c are the observed and calculated structure factor amplitudes. In the final cycle of refinement, all heavy atoms were assigned anisotropic temperature factors. The number of carbon atoms assigned anisotropic temperature factors varied and was set to maintain a reasonable data:variable ratio. C-H hydrogen atom positions were calculated and allowed to ride on the carbon to which they are bonded assuming a C-H bond length of 0.95 Å. Hydrogen atom temperature factors were fixed at 1.10 times the isotropic temperature factor of the carbon atom to which they are bonded. The hydrogen atom contributions were calculated, but not refined. An empirical absorption correction was applied to the data sets based on psi-scan data. The locations of the largest peak in the final difference Fourier map calculation as well as the magnitude of the residual electron density were of no chemical significance.

X-Ray Structure Determinations of 73, 79, 81 and 84

The correct enantiomorph of compound **73** was confirmed by inversion and refinement of the model. The hydrogen atom on phosphorus was located and included in the final cycle of refinement. The decay of the crystal of **79** was significant (ca. 20%), but approximately linear during data collection. While a decay correction was applied to the data, inferior data quality is reflected in the poor agreement of chemically similar Zr-C distances of the CH_3 groups and thermal parameters of C(31). Nonetheless, the connectivity of **79** was confirmed. The phosphide hydrogen atom of **81** could not be located. The final values of R, R_w and the maximum Δ/σ on any of the parameters in the final cycle of refinement are given in Table 2.1. ORTEP drawings of **73, 79, 81** and **84** are shown in Figures 2.2, 2.4, 2.5 and 2.8 respectively, with 30% thermal ellipsoids. Selected bond distances and angles are listed in the captions for Figures 2.2, 2.4, 2.5, and 2.8, respectively. Other structural parameters are given in Tables A1.1-A1.12 in Appendix One.

Table 2.1: Crystallographic Parameters for 73, 79, 81 and 84

	73	79	81	84
Formula	$C_{42}H_{53}OPZr$	$C_{31}H_{37}PZr$	$C_{38}H_{42}P_2Zr_2$	$C_{31}H_{48}P_2Zr$
Formula weight	696.07	623.05	743.14	573.88
Cryst Colour, Form	colourless blocks	indigo blocks	brown blocks	dark green blocks
a(Å)	11.062(2)	19.253(6)	13.310(6)	15.011(7)
b(Å)	18.456(2)	7.761(2)	20.958(9)	9.824(5)
c(Å)	18.629(2)	20.197(6)	13.299(3)	21.745(5)
α(deg)				
β(deg)	97.37(1)	107.88(2)	93.22(3)	103.21(3)
γ(deg)				
Crystal System	monoclinic	monoclinic	monoclinic	monoclinic
Space group	Cc	$P2_1/n$	$P2_1/n$	$P2_1/c$
Vol(Å^3)	3771.8(8)	2872(1)	2704(3)	3122(2)
D_{calcd} (gcm^{-3})	1.23	1.44	1.33	1.22
Z	4	4	4	4
Abs coeff, μ, cm^{-1}	3.63	7.98	6.72	4.623
Temp (°C)	24	24	24	24
Scan speed, °/min	8 ($\theta/2\theta$) (1-3 scans)	8 ($\theta/2\theta$) (1-3 scans)	8 ($\theta/2\theta$) (1-3 scans)	16 ($\theta/2\theta$) (1-3 scans)
Scan range (deg)	1.0 above $K\alpha_1$, 1.0 below $K\alpha_2$	1.0 above $K\alpha_1$, 1.0 below $K\alpha_2$	1.0 above $K\alpha_1$, 1.0 below $K\alpha_2$	1.0 above $K\alpha_1$, 1.0 below $K\alpha_2$
Bkgd/scan ratio	0.5	0.5	0.5	0.5
Data collected	3445	5063	6728	6108
2θ range (deg)	4.5-50.0	4.5-50.0	4.5-50.0	4.5-50.0
Index range	$h,k,\pm l$	$h,k,\pm l$	$h,k,\pm l$	$h,k,\pm l$
Data $F_o^2>3\sigma(F_o^2)$	1378	2422	1907	2295
Variables	194	297	289	257
Transmission Factors	0.916-1.030	0.836-1.150	0.765-1.161	0.888-1.000
R (%)[a]	3.5	4.65	8.10	7.26
Rw (%) [a]	5.22	5.63	8.02	7.73
Largest Δ/σ	0.00	0.17	0.03	0.040
Goodness of fit	1.51	1.81	2.04	1.91

[a] $R = \Sigma||F_o|-|F_c|| / \Sigma|F_o|$, $Rw = [\Sigma(|F_o|-|F_c|)^2 / \Sigma|F_o|^2]^{0.5}$

2.3 Results and Discussion

Initial attempts to trap transient terminal phosphinidene species through *in situ* cycloadditions with organic unsaturates instead exposed the reactive nature of the Zr-P single bond. The reaction of $Cp_2ZrMeCl$ with one equivalent of LiHPMes*•3THF rapidly produced Cp_2Zr(PHMes*)Me **72**, as evidenced by the ^{31}P NMR resonance at 74.1 ppm ($|J_{P\text{-}H}|$ = 264.7 Hz), ^{1}H and ^{13}C NMR data. It was anticipated that **72** would be unstable with respect to the intramolecular elimination of methane, thus generating the desired terminal phosphinidene species which could then be trapped by an organic unsaturate. Therefore, **72** was generated in the presence of benzophenone via addition of the phosphide to a solution of $Cp_2ZrMeCl$ and benzophenone. The resulting solution turned orange, presumably a result of the formation of **72**, and then immediately became very pale yellow. After work-up colourless crystals of the product **73** were isolated in 83% yield. The ^{31}P NMR spectrum of **73** showed a single resonance at -8.6 ppm which exhibited a P-H coupling constant of 244.1 Hz, indicative of the phosphide moiety. Due to the large one-bond P-H coupling constant and low-field chemical shift, it was suspected that ketone insertion had occurred before the expected elimination of methane. Indeed, the observation of a ^{1}H NMR singlet at 0.66 ppm suggested the presence of a Zr-Me fragment. Furthermore, two resonances in both the ^{1}H and ^{13}C NMR spectra may be attributed to diastereotopic cyclopentadienyl groups which arise from the presence of the chiral phosphorus centre. These data collectively support the formulation of **73** as $Cp_2ZrMe(OCPh_2PHMes^*)$. In a similar fashion, generation of **72** in the presence of cyclohexanone or acetone afforded the related complexes $Cp_2ZrMe(OC_6H_{10}PHMes^*)$ **74** and $Cp_2ZrMe(OCMe_2PHMes^*)$ **75**, respectively, while the generation of **72** in the presence of benzonitrile yielded the product **76** (Fig. 2.1). The ^{13}C doublet at 177.9 ppm is attributed to the N=C, while the P-C coupling constant of 30.5 Hz confirmed the formation a P-C bond. These data verify the formulation of **76** as

$Cp_2ZrMe(NC(Ph)PHMes^*)$. The use of a less sterically demanding substituent on phosphorus illustrated that the kinetics of the above insertions are unaffected by changing the sterics of the system. The analogous methylzirconocene phosphide complex $Cp_2ZrMe(PHMes)$ **77** was generated from the reaction of $Cp_2ZrMeCl$ with LiPHMes•2THF, as evidenced by the ^{31}P NMR resonance at -6.0 ppm ($|J_{P\text{-}H}| = 228.5$ Hz). Although this species was observed to be quite unstable (*vide infra*), it too underwent rapid insertion of acetone to yield the mesityl analogue of **75** (i.e. $Cp_2ZrMe(OCMe_2PHMes)$ **78**).

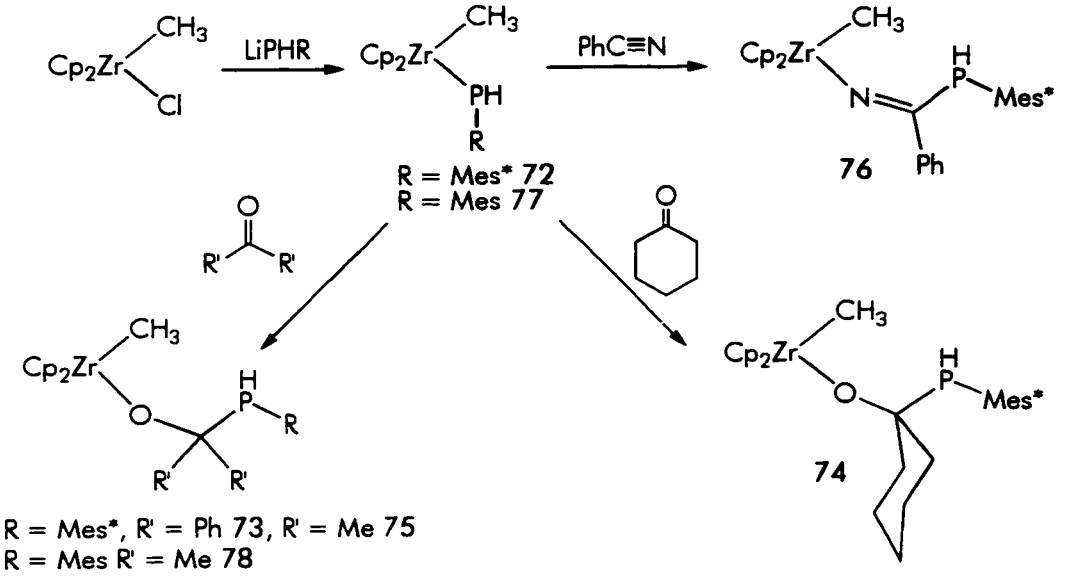

Figure 2.1 Insertions of organic unsaturates into the Zr-P single bond.

The formulation of the above insertion products was confirmed crystallographically for compound **73** (Figure 2.2). The geometry about zirconium is typical of zirconocene derivatives. The Zr-C (methyl group) distance is 2.27(2) Å, while the Zr-O bond is 1.926(9) Å. The O-Zr-C angle of 95.9(5)° is slightly less than the O-Zr-O angle seen in the dialkoxide complex $Cp_2Zr(\mu\text{-}OCH_2CMe_2CH_2O)_2ZrCp_2$.[41] The Zr-O-C angle of 167.7(9)° is similar to that seen in related zirconium alkoxide derivatives, suggesting some degree of Zr-O π-bonding. The structural studies confirm

that insertion of benzophenone into the Zr-P bond generates a secondary phosphorus centre which exhibits typical pseudo-pyramidal geometry.

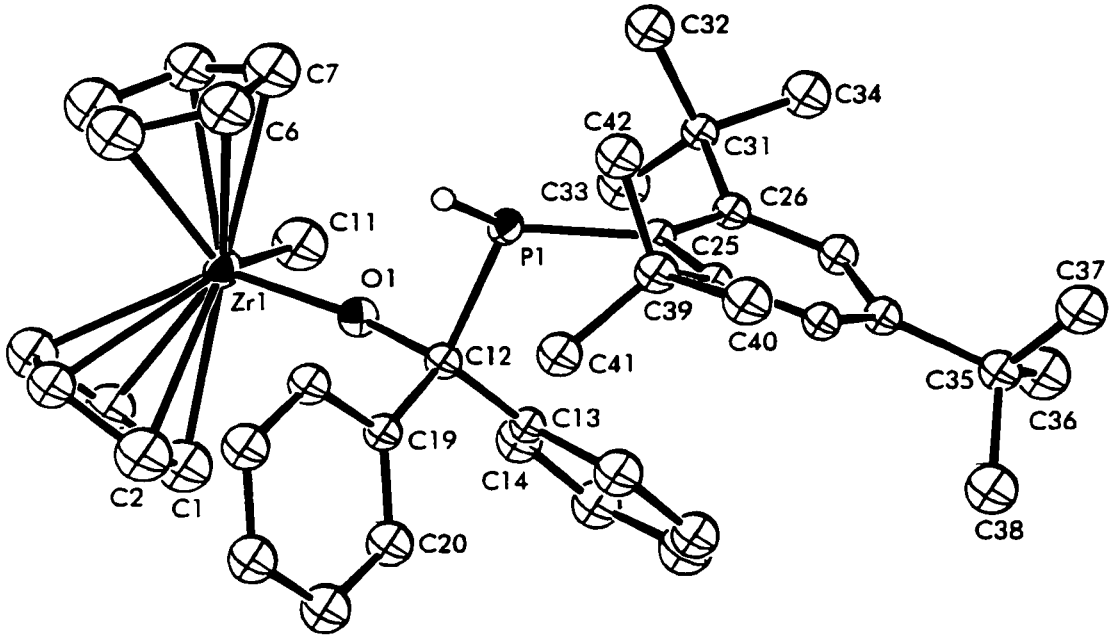

Figure 2.2 ORTEP drawing of **73**; 30% ellipsoids are shown, hydrogen atoms have been omitted for clarity. Selected bond distances and angles: Zr(1)-O(1) 1.926(9) Å; Zr(1)-C(11) 2.27(2) Å; P(1)-C(12) 1.99(1) Å; P(1)-C(25) 1.83(1) Å; O(1)-Zr(1)-C(11) 95.9(5)°; C(12)-P(1)-C(25) 109.7(6)°; Zr(1)-O(1)-C(12) 167.7(9)°.

It is evident that the Zr-P single bond is reactive in its own right. Since it would be difficult (if not impossible) to generate a terminal phosphinidene species without a zirconium phosphide intermediate, trapping with organic unsaturates is not a viable method. Thus, the reaction of $Cp_2ZrMeCl$ with LiPHMes•2THF in the absence of added reagents was monitored by ^{31}P NMR spectroscopy in an attempt to deduce whether methane elimination was indeed occurring to generate a terminal phosphinidene. After 30 minutes at 25 °C the resonance attributable to **77** began to diminish and a singlet at 303 ppm, along with the resonance attributable to the free phosphine H_2PMes, appeared concurrently. No change was observed when this reaction occurred in the presence of PMe_3. These data suggested that rather than an α

elimination of methane, **77** underwent a bimolecular elimination of an equivalent of phosphine to afford a phosphinidene bridged complex (Figure 2.3).

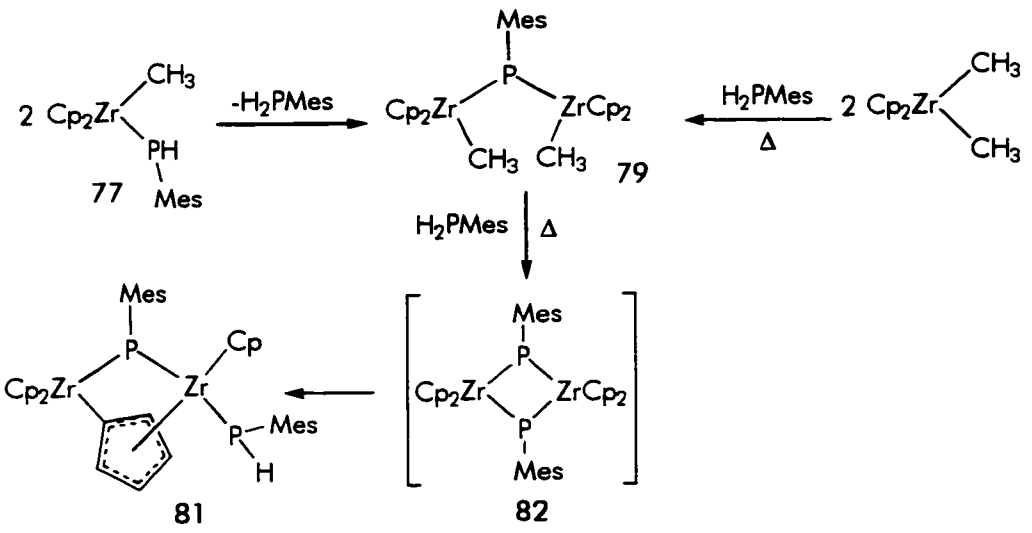

Figure 2.3 Bimolecular reactions of **77** and synthetic routes to **81**.

Attempts to confirm this scenario by the isolation of this new complex were unsuccessful, as NMR data confirmed further reactions had produced a complex mixture of unidentified products. In an effort to pursue this potential bridged phosphinidene dimer, alternative synthetic pathways were sought. Earlier reports by Hey *et al.* described the synthesis of $Cp_2Zr(PPh)_3$ from the reaction of Cp_2ZrMe_2 with H_2PPh (Eq. 2.1).[42]

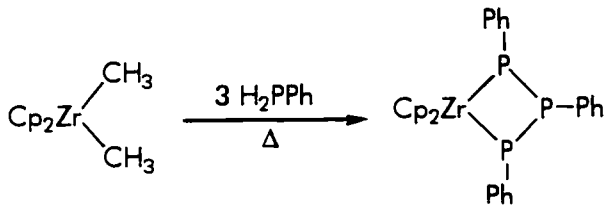

(2.1)

In a similar fashion, heating a colourless mixture of two equivalents of Cp_2ZrMe_2 with H_2PMes at 110 °C for 5 h resulted in a colour change to deep indigo. After cooling and standing for three days, large dark blue crystals of **79** were isolated in 82% yield. The ^{31}P NMR spectrum of **79** consisted of a single resonance at 303 ppm, while ^{1}H and ^{13}C NMR data testified to the presence of two zirconium bound methyl groups. Compound

79 was thus formulated as $(Cp_2ZrMe)_2(\mu\text{-PMes})$. Despite the extreme air-sensitivity of **79**, as well as a problem of crystal decay during data collection, X-ray crystallographic data did confirm the proposed connectivity (Figure 2.4). Two Cp_2ZrMe units are bridged by the mesitylphosphinidene unit with Zr-P distances of 2.606(3) and 2.646(3) Å. The Zr-P-Zr angle is 136.6(1)°, while the sum of the angles about phosphorus indicate a planar geometry similar to that observed for the closely related species $(Cp_2ZrCl)_2(\mu\text{-PMes})$ **80**.[35]

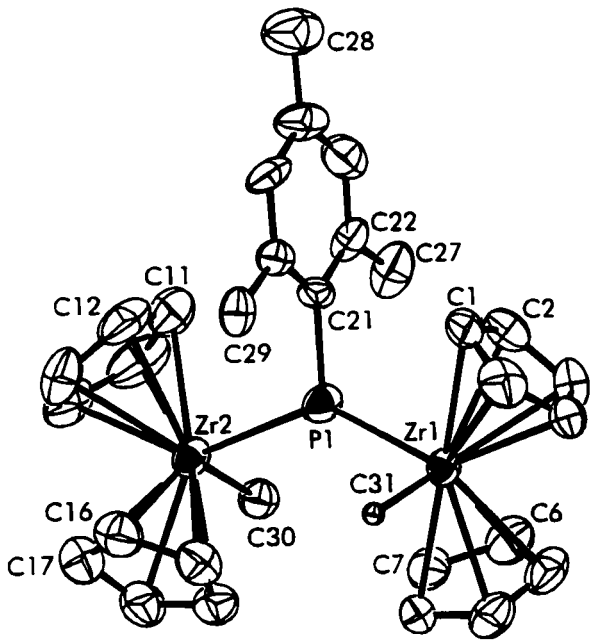

Figure 2.4 ORTEP drawing of **79**; 30% ellipsoids are shown, hydrogen atoms have been omitted for clarity. Selected bond distances and angles: Zr(1)-P(1) 2.606(3) Å; Zr(2)-P(1) 2.646(3) Å; P(1)-C(21) 1.84(1) Å; Zr(1)-P(1)-Zr(2) 136.6(1)°; P(1)-Zr(1)-C(31) 99.4(2)°; P(1)-Zr(2)-C(30) 98.1(3)°.

Further reaction of **79** with an equivalent of H_2PMes at 110° for 5 h resulted in the formation of a dark brown product **81**. A cleaner route to **81** resulted from the thermolysis of Cp_2ZrMe_2 and one equivalent of H_2PMes, which gave **81** in 70% yield. **81** exhibited ^{31}P NMR resonances at 395.4 and -84.2 ppm with a P-P coupling constant of 29.0 Hz. The latter resonance also demonstrated one-bond coupling to proton ($|J_{P\text{-}H}|$ = 203.0 Hz). The ^1H NMR spectrum of **81** showed resonances at 6.29, 5.66 and 5.25 ppm,

attributable to three cyclopentadienyl groups, while resonances at 6.50, 5.98, 5.12 and 4.65 ppm were assigned to an η^1:η^5-C_5H_4 fragment. The ^{13}C NMR data also supported the formulation of **81** as $(Cp_2Zr)(Cp_2ZrPHMes)(\mu\text{-}PMes)(\mu\text{-}\eta^1\text{:}\eta^5\text{-}C_5H_4)$ (Fig. 2.3).

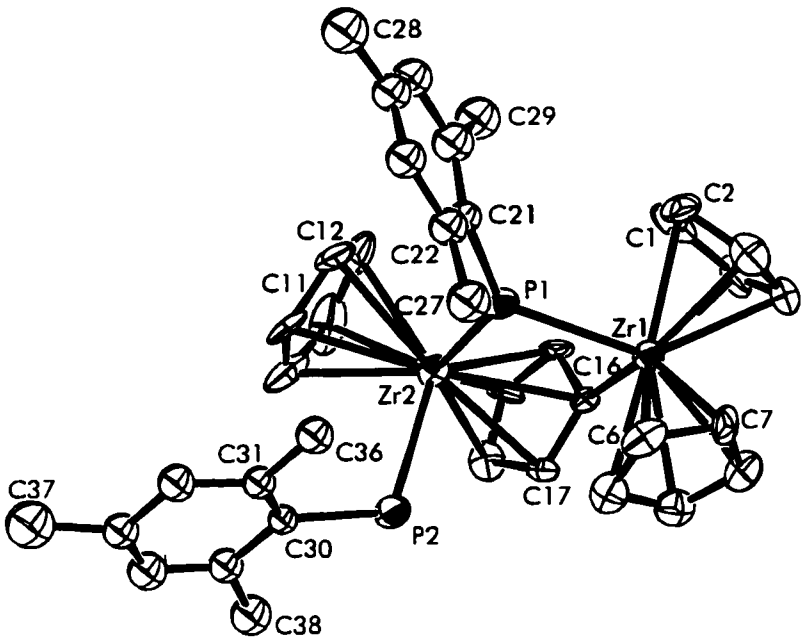

Figure 2.5 ORTEP drawing of **81**; 30% ellipsoids are shown, hydrogen atoms have been omitted for clarity. Selected bond distances and angles: Zr(1)-P(1) 2.586(7) Å; Zr(1)-C(16) 2.49(3) Å; Zr(2)-P(1) 2.576(7) Å; Zr(2)-P(2) 2.718(7) Å; P(1)-Zr(1)-C(16) 88.9(7)°; P(1)-Zr(2)-P(2) 96.5(2)°; Zr(1)-P(1)-Zr(2) 93.3(2)°.

The structure of **81** was confirmed crystallographically (Figure 2.5). The two zirconium centres are bridged by a phosphinidene moiety as well as an η^1:η^5-cyclopentadienyl ring. The bridging Zr-P distances of 2.586(7) and 2.576(7) Å are slightly shorter than those seen in **79** while the Zr-P-Zr angle of 93.3(2)° is significantly smaller than the corresponding angle in **79**, consistent with the presence of the second bridging fragment. The small difference in the bridging Zr-P distances is consistent with a π-component of the Zr(2)-P(1) bond. These parameters compare well with those previously reported for the structurally related species $(Cp_2Zr)(Cp_2ZrCl)(\mu\text{-}PSiPh_3)(\mu\text{-}\eta^1\text{:}\eta^5\text{-}C_5H_4)$ (Zr-P 2.549(6), 2.559(6) Å, Zr-P-Zr 95.2(2)°).[35a]

The terminal phosphide ligand of **81** results in a dramatically longer Zr(2)-P(2) distance of 2.718(7) Å, which compares well with the longer Zr-P distance in $(C_5H_4SiMe_3)_2Zr(PPh_2)_2$ (2.694(3) Å).[43] The P(1)-Zr(2)-P(2) and P(1)-Zr(1)-C(16) angles in **81** of 96.5(2)° and 88.9(7)° respectively, are comparable to the corresponding angles in $(Cp_2Zr)(Cp_2ZrCl)(\mu\text{-}PSiPh_3)(\mu\text{-}\eta^1\text{:}\eta^5\text{-}C_5H_4)$.[35a]

Complex **81** presumably results from the intramolecular C-H activation of one of the cyclopentadienyl rings of the intermediate phosphinidene dimer **82**. Since the preparation of **81** involved prolonged heating, we sought a room temperature route to the phosphinidene dimer in the hopes that C-H activation was only promoted at elevated temperatures. The employment of $(Cp_2ZrCl)_2(\mu\text{-}PMes)$ **80** allowed analogous reactions to be performed via metatheses at room temperature. Although the reaction of **80** with one equivalent of Li_2PMes only gave intractable products, performing the reaction in the presence of PMe_3 resulted in the formation of a species which gave resonances in the ^{31}P NMR spectrum at 780.6 ppm and -8.6 ppm. These signals are due to the terminal phosphinidene species $(Cp_2Zr{=}PMes)(PMe_3)$ **83**, which has also been prepared in our laboratory.[35a] The present synthesis is a significant improvement over the published route in terms of the exclusion of unwanted by-products. The reaction is thought to proceed through initial formation of *bis*-phosphinidene bridged dimer **82** followed by subsequent reaction with PMe_3. Regrettably, compound **83** is not isolable; upon standing overnight at 25 °C or upon removal of the solvent in vacuo **83** degraded to produce free PMe_3 and **81** (Figure 2.6).

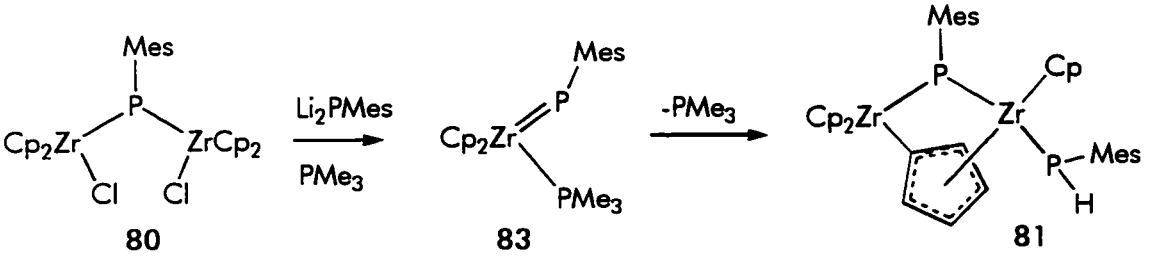

Figure 2.6 Synthesis and decomposition of terminal phosphinidene **83**.

A plausible mechanism involves dissociation of PMe_3 from **83**, dimerization and subsequent irreversible intramolecular cyclopentadienyl C-H bond activation. Thus, while **83** appears to be the kinetic product from this mixture, **81** is the thermodynamic product.

We have previously described a similar intramolecular C-H bond activation in the transient phosphinidene species [Cp^*_2Zr=PMes] to produce $Cp^*_2\overline{ZrPH(C_6H_2\text{-}(2\text{-}CH_2)\text{-}4,6\text{-}Me_2)}$ **71** (Fig. 1.13).[35c] Presumably, the greater steric demands of the permethylcyclopentadienyl ligands prevent dimerization, consequently favouring intramolecular C-H bond activation of the mesityl ligand. The set of reactions employing the mesityl group as the substituent on phosphorus imply that even this sterically demanding group is not bulky enough to stabilize a terminal phosphinidene species. Thus, reactions employing the surpassingly bulky supermesityl phosphine were attempted. The extreme steric bulk of this species is reflected in the inability to successfully dilithiate the phosphine. As described, the reaction of $Cp_2ZrMeCl$ with phosphide rapidly produced Cp_2Zr(PHMes*)Me **72**, which is unstable with respect to α elimination of methane. When this occurred in the presence of PMe_3, forest-green product **84** was obtained cleanly, in nearly quantitative isolated yield. The compound exhibited ^{31}P NMR doublet resonances at 792.4 and -12.0 ppm, neither displaying coupling to protons. These data, along with ^1H and ^{13}C spectra, support the formulation of **84** as the trimethylphosphine adduct of a terminal phosphinidene derivative, (Cp_2Zr=PMes*)(PMe_3) (Fig. 2.7). Both the low field ^{31}P NMR chemical shift and the ^1H NMR observation of separate resonances for the inequivalent cyclopentadienyl ligands indicate that the phosphinidene moiety is of a bent geometry.

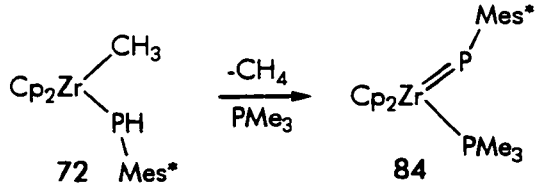

Figure 2.7 Synthesis of terminal phosphinidene **84**.

The structure of **84** was subsequently confirmed crystallographically (Figure 2.8). The formal Zr-P double bond (Zr-P(1)) in **84** is 2.505(4) Å, considerably shorter than either the Zr-P(2) bond in **84** or the single Zr-P bond in $Cp_2ZrCl(PMes^*)(SiMe_3)$.[44] The geometry at P(1) is bent, as indicated by the Zr-P(1)-C(1) angle of 116.1(4)°, consistent with four electron donation from the phosphinidene group and a resulting eighteen electron configuration at zirconium.

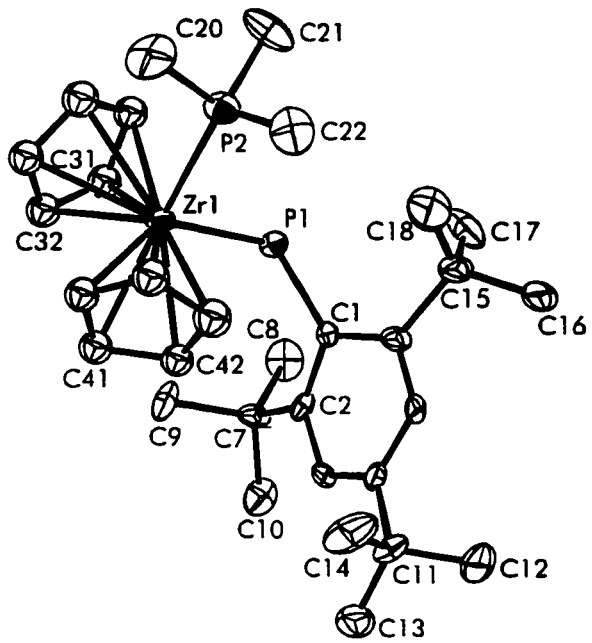

Figure 2.8 ORTEP drawing of **84**; 30% ellipsoids are shown, hydrogen atoms have been omitted for clarity. Selected bond distances and angles: Zr(1)-P(1) 2.505(4) Å; Zr(1)-P(2) 2.741(5) Å; P(1)-Zr(1)-P(2) 101.4(1)°; Zr(1)-P(1)-C(1) 116.1(4)°.

The formation of **84** is thought to proceed via intramolecular loss of methane and subsequent trapping of the terminal phosphinidene intermediate with trimethylphosphine. The stability of **84** can be attributed to the extreme steric bulk of the supermesityl ligand, which prohibits dimerization and subsequent C-H activation. The stabilizing requirement of strong Lewis bases attests to the innate reactivity of the Zr-P double bond. We have determined that the species can be trapped by pyridine[45] as well as trimethylphosphine, however the use of weaker bases such as THF or

triphenylphosphine only lead to products of disproportionation and intractable species. While subsequent work in our laboratories has yielded **84** through alternate synthetic routes,[35a] the original method has nevertheless proven to be superior, providing greater purity and yields. **84** is stable in the solid state under a nitrogen atmosphere for weeks at a time, attesting to the feasibility of a reactivity study.

2.4 Conclusion

In summary, valuable information has been obtained about both the reactive nature of the Zr-P single bond as well as the steric requirements necessary for the stabilization of a terminal zirconium phosphinidene. The chemistry herein demonstrates the ease with which organic unsaturates can insert into the Zr-P single bond of methylzirconocene phosphide complexes. Such insertions occur before intramolecular elimination of methane can transpire, regardless of steric considerations. In the absence of such unsaturates, it has also been demonstrated that steric demands are critical to both the formation and stabilization of terminal phosphinidenes. These species can be observed only when steric demands preclude further reaction, and can only be isolated as eighteen electron adducts of strong Lewis bases. In the absence of the required bulk, dimerization and subsequent intramolecular C-H bond activation have been observed. The successful preparation of terminal phosphinidene **84** motivated investigations directed toward an exploration of its reactivity.

Chapter Three
Reactivity Studies of the Terminal Phosphinidene Complex: $Cp_2Zr(PC_6H_2\text{-}2,4,6\text{-}t\text{-}Bu_3)(PMe_3)$

3.1 Introduction

As described in Chapter One, syntheses and structural studies of terminal phosphinidene complexes of tantalum, tungsten and molybdenum have been described in the literature. These studies are highlights in the area; however it is the reactivity of stable terminal phosphinidene complexes that is expected to be a fertile and intriguing area of research. High-valent transition metal phosphinidenes all contain nucleophilic phosphorus centres, corresponding to Schrock-type alkylidenes. They are distinguished from the transient phosphinidene complexes of low-valent transition metals, which are electrophilic and thus analogous to Fischer carbene complexes.[3, 10] While the reactivity of electrophilic phosphinidenes has been studied,[10, 28] the nucleophilic species have only been examined briefly.[31a] In this chapter, the first detailed reactivity study of an isolated terminal phosphinidene complex (Cp_2Zr=PMes*)(PMe_3) **84** is described. Comparable to Schrock alkylidenes,[3, 4] **84** participates in a number of metathetical reactions with organic and other group 14 reagents. Mechanistic, structural and spectroscopic aspects of this chemistry are discussed.

Similar to (Cp^*_2Zr=O)(pyr) **29**,[18a] **84** undergoes 1,2-additions of polar substrates across the Zr-P double bond. These reactions provide a facile route to complexes of the form Cp_2Zr(PHMes*)(ER) and Cp_2Zr(PHMes*)(EHR). Mixed ligand systems such as these have drawn little attention, due in part to synthetic difficulties associated with their preparation. Numerous studies have invoked arguments based on π-interactions between alkoxide, thiolate, amide and phosphide ligands and early transition metal centres to account for solution behaviour and solid state structures.[46] The convenient synthetic route using **84** has allowed for variable temperature NMR studies of the mixed ligand species. The implications regarding Zr-P and Zr-E π-bonding are discussed.

3.2 Experimental

General Data All preparations, ^{1}H, $^{13}C\{^{1}H\}$, ^{31}P and $^{31}P\{^{1}H\}$ NMR spectroscopy, mass spectrometry and combustion analyses were carried out under conditions similar to those described in Section 2.2.

Synthesis of *trans*-PhCH=PMes* 85, Ph_2C=PMes* 86, 1,3-C_6H_2(HC=PMes*)$_2$ 87 and PhN=C=PMes* 88

The reactions of **84** with several ketones and aldehydes were performed in a similar manner, thus only one representative procedure is described. The reagent employed and the characterization of the products are given. To a benzene solution of **84** (57 mg, 0.1 mmol) was added PhCHO (10.2 μL, 0.1 mmol). The reaction mixture stood overnight after which time the yellow solution was stirred with activated alumina for 1.5 h. The solvent was evaporated under reduced pressure and the product was then extracted into pentane. Filtration and removal of the solvent in vacuo gave the pale yellow oil **85**. **85**: Yield: 80% (by ^{1}H NMR). ^{31}P NMR (25°C, $CDCl_3$): δ 259.2 (d, $|^{2}J_{P\text{-}H}|$ = 24.9 Hz). ^{1}H NMR and $^{13}C\{^{1}H\}$ NMR data were consistent with that reported in the literature.[47]

86: Reagent: Ph_2CO. Yield: 82% (by ^{1}H NMR). ^{31}P NMR (25 °C, C_6D_6): δ 242.1 (s). ^{1}H NMR and $^{13}C\{^{1}H\}$ NMR data were consistent with that reported in the literature.[48]

87: Reagent: 1,3-$C_6H_2(CHO)_2$. Yield: 86% (by ^{1}H NMR). ^{31}P NMR (25 °C, C_6D_6): δ 259.9 (d, $|^{2}J_{P\text{-}H}|$ = 23.8 Hz). ^{1}H NMR and $^{13}C\{^{1}H\}$ NMR data were consistent with that reported in the literature.[49]

88: Reagent: PhNCS. Yield 81% (by ^{1}H NMR). ^{31}P NMR (25 °C, $CDCl_3$): δ -106.3 ppm. ^{1}H NMR and $^{13}C\{^{1}H\}$ NMR data were consistent with that reported in the literature.[50]

Synthesis of Cp_2Zr(PHMes*)(OC_6H_9) 89

To a benzene solution of **84** (114 mg, 0.2 mmol) was added cyclohexanone (20.8 μL, 0.2 mmol). The reaction mixture stood overnight resulting in the formation of an orange

solution. The solvent was then removed in vacuo and the product dissolved in pentane. Orange crystals formed over 12 h at room temperature and were isolated by filtration. Yield: 73 mg (62%). ^{1}H NMR (25 °C, C_6D_6): δ 7.61 (d, $|^4J_{P\text{-}H}|$ = 1.4 Hz, 2H, Ar-*H*), 5.69 (br s, 10H, Cp), 5.11 (d, $|J_{P\text{-}H}|$ = 216.9 Hz, 1H, P-*H*), 4.53 (t, $|J|$ = 3.7 Hz, 1H, =C*H*), 1.76 (s, 18H, *o*-^{t}Bu), 1.55-1.25 (m, 8H, Cy-*H*), 1.34 (s, 9H, *p*-^{t}Bu). ^{13}C{^{1}H} NMR (25 °C, C_6D_6): δ 160.2 (s, O-C=), 150.1 (s, quat), 145.8 (d, $|J|$ = 36.4 Hz, quat), 145.6 (s, quat), 119.4 (s, arom. C-H), 111.1 (s, Cp), 99.2 (s, =CH), 38.3 (s, *o*-$C(CH_3)_3$), 34.6 (s, *p*-$C(CH_3)_3$), 33.1 (br s, *o*-$C(CH_3)_3$), 31.5 (s, *p*-$C(CH_3)_3$), 30.0 (s, CH_2), 24.2 (s, CH_2), 23.5 (s, CH_2), 23.0 (s, CH_2). ^{31}P NMR (25 °C, C_6D_6): δ -31.1 (d, $|J_{P\text{-}H}|$ = 218.1 Hz). HRMS (EI) *m/e* Calcd for $C_{34}H_{49}OPZr$: 594.2564; *m/e* Found: 594.2539. Anal. Calcd for $C_{34}H_{49}OPZr$: C: 68.52; H: 8.29; Found: C: 68.12; H: 8.14.

Synthesis of CH_2=PMes* 90, CHCl=PMes* 91, $\overline{CH_2CH_2}$PMes* 92, 1,2-$C_6H_4(\overline{CH_2CH_2})$PMes* 93, *cis*-$(CH{=}CH_2)\overline{CHCH_2}$PMes* 94, $(CH_2{=}C{=})\overline{CCH_2}$PMes* 95

The reactions of **84** with several alkylidene dichlorides were performed in a similar manner, thus only one representative procedure is described. To a benzene solution of **84** (57 mg, 0.1 mmol) was added CH_2Cl_2 (6.0 μL, 0.1 mmol). The reaction mixture stood overnight after which time the yellow solution was stirred with activated alumina for 1.5 h. The solvent was evaporated under reduced pressure and the product then extracted into pentane. Filtration and removal of the solvent in vacuo gave the pale yellow oil **90**. **90**: Yield: 86% (by ^{1}H NMR). ^{31}P NMR (25 °C, benzene): δ 289.3 (t, $|^2J_{P\text{-}H}|$ = 30.4 Hz). ^{1}H NMR and ^{13}C{^{1}H} NMR data were consistent with that reported in the literature.[51]

91: Reagent: $CHCl_3$. Yield: 76% (by ^{1}H NMR). ^{31}P NMR (25 °C, C_6D_6): δ 251.0 (d, $|^2J_{P\text{-}H}|$ = 18.5 Hz, E-isomer), 249.5 (d, $|^2J_{P\text{-}H}|$ = 43.2 Hz, Z-isomer). ^{1}H NMR and ^{13}C{^{1}H} NMR data were consistent with that reported in the literature.[51, 52]

92: Reagent: $ClCH_2CH_2Cl$. Yield: 45% (by ^1H NMR). ^{31}P NMR (25 °C, benzene): δ -201.9 (s). ^1H NMR and $^{13}C\{^1H\}$ NMR data were consistent with that reported in the literature.[53]

93: Reagent: 1,2-$C_6H_4(CH_2Cl)_2$. Yield: 53% (by ^1H NMR). ^1H NMR (25 °C, C_6D_6): δ 7.30 (d, $|^4J_{P\text{-}H}|$ = 2.3 Hz, 2H, Ar-*H*), 7.52 and 6.85 (m, 4H, Ph), 3.30 (dd, $|^2J|$ = 11.8 Hz, $|^2J_{P\text{-}H}|$ = 8.9 Hz, 2H, C*H*H), 2.98 (dd, $|^2J|$ = 11.8 Hz, $|^2J_{P\text{-}H}|$ = 3.9 Hz, 2H, CH*H*), 1.50 (s, 18H, *o*-^{t}Bu), 1.26 (s, 9H, *p*-^{t}Bu). $^{13}C\{^1H\}$ NMR (25 °C, C_6D_6): δ 154.7 (s, quat), 146.7 (s, quat), 140.3 (d, $|J|$ = 12.1 Hz, quat), 139.9 (d, $|J|$ = 50.0 Hz, quat), 126.1 (d, $|J|$ = 3.8 Hz, arom. *C*-H), 122.1 (d, $|J|$ = 12.1 Hz, arom. *C*-H), 122.0 (s, arom. C-H), 41.9 (d, $|J_{P\text{-}C}|$ = 15.2 Hz, CH_2), 38.9 (s, *o*-$C(CH_3)_3$), 34.6 (s, *p*-$C(CH_3)_3$), 33.5 (d, $|^4J_{P\text{-}C}|$ = 7.2 Hz, *o*-$C(CH_3)_3$), 31.2 (s, *p*-$C(CH_3)_3$). ^{31}P NMR (25 °C, C_6D_6): δ 12.7 (s). HRMS (EI) *m/e* Calcd for $C_{26}H_{37}P$: 380.2633; *m/e* Found: 380.2627.

94: Reagent: *cis*- $ClCH_2CH{=}CHCH_2Cl$. Yield: 38% (by ^1H NMR). ^1H NMR (25 °C, C_6D_6): δ 7.52 (d, $|^4J_{P\text{-}H}|$ = 1.9 Hz, 2H, Ar-*H*), 4.80 (d, $|^3J|$ = 17.0 Hz, 1H, =C*H*H), 4.58 (dd, $|^3J|$ = 10.1 Hz, $|^4J_{P\text{-}H}|$ = 1.8 Hz, 1H, CH*H*), 3.99 (dddd, $|^3J|$ = 17.0 Hz, $|^3J|$ = 10.1 Hz, $|^3J|$ = 9.9 Hz, $|^3J_{P\text{-}H}|$ = 2.7 Hz, 1H, =C*H*), 1.51 (s, 18H, *o*-^{t}Bu), 1.24 (s, 9H, *p*-^{t}Bu). $^{13}C\{^1H\}$ NMR (25 °C, C_6D_6): δ 154.8 (s, quat), 150.2 (s, quat), 143.1 (d, $|J|$ = 52.6 Hz, quat), 139.1 (s, =CH), 120.3 (s, arom. *C*-H), 113.2 (s, $=CH_2$), 38.3 (s, *o*-$C(CH_3)_3$), 34.8 (s, *p*-$C(CH_3)_3$), 33.6 (d, $|^4J_{P\text{-}C}|$ = 9.1 Hz, *o*-$C(CH_3)_3$), 32.5 (d, $|J_{P\text{-}C}|$ = 43.8 Hz, ring CH), 31.1 (s, *p*-$C(CH_3)_3$), 21.4 (d, $|J_{P\text{-}C}|$ = 41.4 Hz, ring CH_2). ^{31}P NMR (25 °C, C_6D_6): δ -174.2 (s). HRMS (EI) *m/e* Calcd for $C_{22}H_{35}P$: 330.2476; *m/e* Found: 330.2462.

95: Reagent: $ClCH_2C{\equiv}CCH_2Cl$. Yield: 53% (by ^1H NMR). ^1H NMR (25 °C, C_6D_6): δ 7.38 (d, $|^4J_{P\text{-}H}|$ = 2.0 Hz, 2H, Ar-*H*), 3.56 (*AB* q, $|J|$ = 2.7 Hz, 2H, $=CH_2$), 1.60 (s, 18H, *o*-^{t}Bu), 1.28 (s, 9H, *p*-^{t}Bu). $^{13}C\{^1H\}$ NMR (25 °C, C_6D_6): δ 200.5 (d, $|^2J_{P\text{-}C}|$ = 10.1 Hz, =C=), 155.1 (s, quat), 149.8 (s, quat), 134.6 (d, $|J|$ = 65.5 Hz, quat), 122.4 (s, arom. *C*-H), 84.4 (d, $|J_{P\text{-}C}|$ = 46.5 Hz, ring C=), 76.6 (s, $=CH_2$), 38.4 (s, *o*-$C(CH_3)_3$), 34.9 (s, *p*-$C(CH_3)_3$), 33.6 (d, $|^3J_{P\text{-}C}|$ = 7.4 Hz, *o*-$C(CH_3)_3$), 31.2 (s, *p*-$C(CH_3)_3$), 22.2 (d, $|J_{P\text{-}C}|$ = 48.9 Hz, ring CH_2). ^{31}P

NMR (25 °C, C_6D_6): δ -149.6 (s). HRMS (EI) *m/e* Calcd for $C_{22}H_{33}P$: 328.2320; *m/e* Found: 328.2309.

Synthesis of PhCHCH(Ph)PMes* 97, *trans*-(PhCHCH$_2$PMes*) 98 and Cp$_2$Zr(PHMes*)(OCH$_2$CH=CH$_2$) 99

The reactions of **84** with three epoxides were performed in a similar manner, thus only one representative procedure is described. To a benzene solution of **84** (57 mg, 0.1 mmol) was added *trans*-stilbene oxide (20 mg, 0.1 mmol). The reaction mixture stood overnight, after which time the solvent was removed in vacuo. Extraction into pentane followed by filtration and solvent removal in vacuo gave the yellow product. **97**: Yield: 53% (by ^{1}H NMR). ^{1}H NMR (25 °C, C_6D_6): δ 7.49 (d, $|{}^4J_{P\text{-}H}|$ = 1.9 Hz, 2H, Ar-*H*), 7.3-6.8 (m, 10H, Ph-*H*), 1.66 (s, 18H, *o*-^{t}Bu), 1.32 (s, 9H, *p*-^{t}Bu), 1.6-1.1 (m, 2H, C*H*). ^{13}C{^{1}H} NMR (25 °C, C_6D_6): δ 156.4 (s, quat), 150.1 (s, quat), 137.6 (s, quat), 137.4 (d, $|J|$ = 53.3 Hz, quat), 137.2 (d, $|J|$ = 12.1 Hz, quat), 130.1 (s, arom. *C*-H), 129.9 (s, arom. *C*-H), 128.5 (s, arom. *C*-H), 126.7(s, arom. *C*-H), 125.8 (s, arom. *C*-H), 121.9 (s, arom. *C*-H), 119.4 (s, arom. *C*-H), 42.5 (d, $|J_{P\text{-}C}|$ = 37.4 Hz, ring CH), 39.2 (s, *o*-C(CH$_3$)), 34.9 (s, *p*-C(CH$_3$)), 33.9 (d, $|{}^4J_{P\text{-}C}|$ = 8.6 Hz, *o*-C(CH$_3$)), 31.5 (s, *p*-C(CH$_3$)). ^{31}P NMR (25 °C, C_6D_6): δ -166.8 (s). HRMS (EI) *m/e* Calcd for $C_{32}H_{41}P$: 456.2946; *m/e* Found: 456.2928.

98: Reagent: PhC(H)CH$_2$O. Yield: 92% (by ^{1}H NMR). ^{31}P NMR (25 °C, C_6D_6): δ -174.8 (d, $|J|$ = 20.4 Hz). ^{1}H NMR and ^{13}C{^{1}H} NMR data were consistent with that reported in the literature.[54]

99: Reagent: MeC(H)CH$_2$O. Yield: 89% (by ^{1}H NMR). ^{1}H NMR (25 °C, C_6D_6): δ 7.60 (d, $|{}^4J_{P\text{-}H}|$ = 1.7 Hz, 2H, Ar-*H*), 5.63 (s, 10H, Cp), 5.00 (m, 3H, C*H*=C*H*$_2$), 4.95 (d, $|J_{P\text{-}H}|$ = 213.9 Hz, 1H, P-*H*), 4.17 (m, 2H, O-C*H*$_2$), 1.76 (s, 18H, *o*-^{t}Bu), 1.37 (s, 9H, *p*-^{t}Bu). ^{13}C{^{1}H} NMR (25 °C, C_6D_6): δ 151.9 (s, quat), 146.3 (d, $|J|$ = 44.3 Hz, quat), 145.2 (s, quat), 139.0 (s, =CH), 120.8 (s, arom. *C*-H), 113.1 (s, =CH$_2$), 111.0 (s, Cp), 74.9 (s, O-CH$_2$), 38.4 (s, *o*-C(CH$_3$)$_3$), 34.5 (s, *p*-C(CH$_3$)$_3$), 33.0 (d, $|{}^4J_{P\text{-}C}|$ = 6.1 Hz, *o*-C(CH$_3$)$_3$), 31.4 (s, *p*-C(CH$_3$)$_3$). ^{31}P

NMR (25 °C, C_6D_6): δ -43.5 (d, $|J_{P-H}|$ = 217.2 Hz). HRMS (EI) *m/e* Calcd for $C_{31}H_{45}OPZr$: 554.2251; *m/e* Found: 554.2274.

Synthesis of $Cp_2Zr(PMes^*(SiMe_2Cl))Cl$ 100

To a benzene solution of **84** (114 mg, 0.2 mmol) was added dichlorodimethylsilane (24.2 μL, 0.2 mmol). The reaction mixture stood for 3 h, during which time the solution became deep red. The solvent was removed in vacuo and the product dissolved in pentane. A red microcrystalline solid precipitated over 12 h at room temperature and was isolated by filtration. Yield: 95 mg (71%). ^{1}H NMR (25 °C, C_6D_6): δ 7.68 (d, $|^4J_{P-H}|$ = 2.2 Hz, 2H, Ar-*H*), 5.89 (br s, 10H, Cp), 1.69 (s, 18H, *o*-^{t}Bu), 1.28 (d, $|^4J_{P-H}|$ = 2.9 Hz, 6H, Me), 1.27 (s, 9H, *p*-^{t}Bu). $^{13}C\{^1H\}$ NMR (25 °C, C_6D_6): δ 155.2 (s, quat), 147.3 (s, quat), 133.9 (s, quat), 123.9 (s, arom. *C*-H), 111.2 (s, Cp), 39.8 (s, *o*-$C(CH_3)_3$), 34.8 (s, *p*-$C(CH_3)_3$), 34.5 (s, *o*-$C(CH_3)_3$), 31.2 (d, $|^2J_{P-C}|$ = 5.0 Hz, Me), 31.0 (s, *p*-$(C(CH_3)_3)$. ^{31}P NMR (25 °C, C_6D_6): δ 117.9 (s). HRMS (EI) *m/e* Calcd for $C_{30}H_{45}Cl_2PSiZr$: 624.1448; *m/e* Found: 624.1471. Anal. Calcd for $C_{30}H_{45}Cl_2PSiZr$: C: 57.48; H: 7.24; Found: C: 57.94; H: 6.91.

Synthesis of $PMes^*(SiMe_2Cl)_2$ 101, $(Me_2GeCl)_2PMes^*$ 102 and $(Me_2GePMes^*)_2$ 103

The reactions of **84** with two equivalents of Me_2SiCl_2 or one and two equivalents of Me_2GeCl_2 were performed in a similar manner, thus only one representative procedure is described. To a benzene solution of **84** (57 mg, 0.1 mmol) was added two equivalents of Me_2SiCl_2 (24.2 μL, 0.2 mmol). The reaction mixture stood overnight after which time the solvent was removed in vacuo. Extraction into pentane followed by filtration and solvent removal in vacuo gave the yellow product. **101**: Yield: 92% (by ^{1}H NMR). ^{1}H NMR (25 °C, C_6D_6): δ 7.48 (d, $|^4J_{P-H}|$ = 3.3 Hz, 2H, Ar-*H*), 1.68 (s, 18H, *o*-^{t}Bu), 1.23 (s, 9H, *p*-^{t}Bu), 0.53 (d, $|^3J_{P-H}|$ = 5.6 Hz, 12H, CH_3). $^{13}C\{^1H\}$ NMR (25 °C, C_6D_6): δ 159.3 (s, quat), 150.8 (s, quat), 122.3 (s, arom. *C*-H), 38.6 (s, *o*-$C(CH_3)_3$), 34.7 (s, *p*-$C(CH_3)_3$), 33.7 (s, *o*-$C(CH_3)_3$), 31.0 (s, *p*-$(C(CH_3)_3)$, 5.6 (d, $|^2J_{P-H}|$ = 17.1 Hz, CH_3). ^{31}P NMR (25 °C, C_6D_6): δ -121.9 (s). HRMS (EI) *m/e* Calcd for $C_{22}H_{41}Cl_2PSi_2$: 462.1862; *m/e* Found: 462.1848.

102: Reagent: Me_2GeCl_2 (two equivalents). Yield: 62% (by ^1H NMR). ^1H NMR (25 °C, C_6D_6): δ 7.46 (d, $|^4J_{P\text{-}H}|$ = 3.1 Hz, 2H, Ar-*H*), 1.62 (s, 18H, *o*-^{t}Bu), 1.22 (s, 9H, *p*-^{t}Bu), 0.77 (d, $|^3J_{P\text{-}H}|$ = 4.1 Hz, 12H, CH_3). $^{13}C\{^1H\}$ NMR (25 °C, C_6D_6): δ 159.1 (s, quat), 155.2 (s, quat), 122.4 (s, arom. *C*-H), 38.6 (s, *o*-$C(CH_3)_3$), 34.7 (s, *p*-$C(CH_3)_3$), 33.7 (d, $|^4J_{P\text{-}C}|$ = 6.4 Hz, *o*-$C(CH_3)_3$), 31.2 (s, *p*-$(C(CH_3)_3)$, 8.6 (d, $|^2J_{P\text{-}C}|$ = 9.8 Hz, CH_3). ^{31}P NMR (25 °C, C_6D_6): δ -79.9 (s). HRMS (EI) *m/e* Calcd for $C_{22}H_{41}Cl_2Ge_2P$: 552.0759; *m/e* Found: 552.0864.

103: Reagent: Me_2GeCl_2 (one equivalent). Yield: 39% (by ^1H NMR). ^1H NMR (25 °C, C_6D_6): δ 7.37 (s, 2H, Ar-*H*), 1.66 (s, 18H, *o*-^{t}Bu), 1.28 (s, 9H, *p*-^{t}Bu), 0.66 (t, $|^3J_{P\text{-}H}|$ = 4.4 Hz, 6H, CH_3). $^{13}C\{^1H\}$ NMR (25 °C, C_6D_6): δ 159.3 (s, quat), 155.1 (s, quat), 122.3 (s, arom. *C*-H), 37.9 (s, *o*-$C(CH_3)_3$), 34.2 (s, *p*-$C(CH_3)_3$), 33.3 (d, $|^4J_{P\text{-}C}|$ = 6.5 Hz, *o*-$C(CH_3)_3$), 31.0 (s, *p*-$(C(CH_3)_3)$, 8.7 (t, $|^2J_{P\text{-}C}|$ = 11.6 Hz, CH_3). ^{31}P NMR (25 °C, C_6D_6): δ -52.7 (s). HRMS (EI) *m/e* Calcd for $C_{40}H_{70}Ge_2P_2$: 758.3389; *m/e* Found: 758.3517.

Synthesis of (^{t}Bu$_2$SnPMes*)$_2$ 104

To a benzene solution of **84** (114 mg, 0.2 mmol) was added a benzene solution of di-*t*-butyltindichloride (61 mg, 0.2 mmol). The reaction mixture stood overnight, after which time the solvent was removed in vacuo. The product was extracted into pentane and this solution was filtered. Large orange crystals formed over three days at room temperature and were isolated by filtration. Yield: 61 mg (30%). ^1H NMR (25 °C, C_6D_6): δ 7.35 (s, 4H, Ar-*H*), 1.83 (s, 36H, ^{t}Bu), 1.46 (s, 36H, ^{t}Bu), 1.30 (s, 18H, ^{t}Bu). $^{13}C\{^1H\}$ NMR (25 °C, C_6D_6): δ 156.5 (s, quat), 147.8 (s, quat), 121.5 (s, arom. *C*-H), 44.3 (s, $C(CH_3)_3$), 39.3 (s, $C(CH_3)_3$), 34.6 (s, $C(CH_3)_3$, 34.3 (s, $C(CH_3)_3$), 32.4 (s, $C(CH_3)_3$), 31.2 (s, $(C(CH_3)_3)$. ^{31}P NMR (25 °C, C_6D_6): δ -84.8 (s) $|^1J(^{117}Sn\text{-}P)|$ = 686.7 Hz, $|^1J(^{119}Sn\text{-}P)|$ = 717.4 Hz. Anal. Calcd for $C_{52}H_{94}Sn_2P_2$: C: 61.31; H: 9.30; Found: C: 60.88; H: 9.01.

Synthesis of (Me$_2$SnPMes*)$_2$ 105

To a benzene solution of **84** (57 mg, 0.1 mmol) was added a benzene solution of dimethyltin sulfide (18 mg, 0.1 mmol). The reaction mixture stood overnight, after

which time the solvent was removed under reduced pressure and the product extracted into pentane. Filtration followed by evaporation of the solvent in vacuo gave **105** as a red solid. Note: attempts to recrystallize this compound from pentane only resulted in the decomposition of **105**. Yield: 46% (by ^{1}H NMR). ^{1}H NMR (25 °C, C_6D_6): δ 7.46 (s, 2H, Ar-*H*), 1.76 (s, 18H, *o*-^{t}Bu), 1.28 (s, 9H, *p*-^{t}Bu), 0.65 (br s, 6H, CH_3). ^{13}C{^{1}H} NMR (25 °C, C_6D_6): δ 157.6 (s, quat), 149.1 (s, quat), 121.5 (s, arom. *C*-H), 38.7 (s, *o*-$C(CH_3)_3$), 34.6 (s, *p*-$C(CH_3)_3$), 33.7 (s, *o*-$C(CH_3)_3$), 31.1 (s, *p*-$(C(CH_3)_3$), 2.3 (br s, CH_3). ^{31}P NMR (25 °C, C_6D_6): δ -108.9 (s) $|\,^1J(^{117}Sn\text{-}P)| = 485.0$ Hz, $|\,^1J(^{119}Sn\text{-}P)| = 504.7$ Hz. HRMS (EI) *m/e* Calcd for $C_{40}H_{70}Sn_2P_2$: 852.2997; *m/e* Found: 852.3044.

Synthesis of (Cp_2Zr=NC(Ph)PMes*)(PMe_3) 107a, 107b

To a benzene solution of **84** (57 mg, 0.1 mmol) was added benzonitrile (10.2 μL, 0.1 mmol). The reaction mixture stood for 2 h after which time the solvent was removed in vacuo and the red product extracted into pentane. This solution was allowed to stand for 2 weeks, after this time two or three thin red crystals of **107b** were obtained. Repeated attempts to isolate larger quantities were unsuccessful. ^{1}H NMR gave an estimated 50% combined yield of **107a** and **107b**. ^{1}H NMR (25 °C, C_6D_6, mixture of **107a** and **107b**): δ 7.71-6.89 (m, 14H, Ph-*H* and Ar-*H*), 5.76 (s, 5H, Cp), 5.75 (s, 5H, Cp), 5.52 (s, 5H, Cp), 5.51 (s, 5H, Cp), 2.05 (s, 18H, *o*-^{t}Bu), 1.92 (s, 18H, *o*-^{t}Bu), 1.48 (s, 9H, *p*-^{t}Bu), 1.39 (s, 9H, *p*-^{t}Bu), 0.36 (d, $|\,^2J_{P\text{-}H}| = 7.10$ Hz, 9H, CH_3), 0.95 (d, $|\,^2J_{P\text{-}H}| = 7.37$ Hz, 9H, CH_3). **107a**: ^{31}P NMR (25 °C, C_6D_6): δ 83.9 (s), -14.7 (s). **107b**: ^{31}P NMR (25 °C, C_6D_6): δ 92.1 (s), -15.2 (s).

Synthesis of $Cp_2Zr(N(Cy))_2C$=PMes* 108

To a benzene solution of **84** (114 mg, 0.2 mmol) was added dicyclohexylcarbodiimide (42 mg, 0.2 mmol). The reaction mixture stood overnight after which time the solvent was evaporated in vacuo and the brown solid dissolved in pentane. Dark brown crystals formed over 12 h at room temperature and were isolated by filtration. Yield: 64 mg

(46%). ^{1}H NMR (25 °C, C_6D_6): δ 7.57 (d, $|^4J_{P\text{-}H}|$ = 1.5 Hz, 2H, Ar-*H*), 5.99 (s, 10H, Cp), 4.56 (m, 1H, C-*H*), 2.86 (m, 1H, C-*H*), 2.65 - 0.60 (m, 20H, CH_2), 2.00 (s, 18H, *o*-^{t}Bu), 1.44 (s, 9H, *p*-^{t}Bu). ^{13}C{^{1}H} NMR (25 °C, C_6D_6): δ 164.3 (d, $|J|$ = 121.6 Hz, C=P), 157.1 (d, $|J|$ = 5.4 Hz, quat), 147.5 (s, quat), 138.7 (d, $|J|$ = 72.3 Hz, quat), 121.2 (s, arom. C-H), 113.8 (s, Cp), 57.8 (d, $|^3J_{P\text{-}C}|$ = 37.9 Hz, C-H), 57.0 (s, C-H), 39.4 (s, *o*-$C(CH_3)_3$), 37.1 (s, CH_2), 35.8 (d, $|J|$ = 3.5 Hz, CH_2), 34.9 (s, *p*-$C(CH_3)_3$), 33.5 (d, $|^4J_{P\text{-}C}|$ = 9.6 Hz, *o*-$C(CH_3)_3$), 31.5 (s, *p*-$(C(CH_3)_3)$, 26.7 (s, CH_2), 25.9 (s, CH_2), 25.8 (s, CH_2), 25.5 (s, CH_2). ^{31}P NMR (25 °C, C_6D_6): δ -9.7 (s). Anal. Calcd for $C_{41}H_{61}N_2PZr$: C: 69.94; H: 8.73; Found: C: 70.38; H: 8.44.

Low Temperature NMR Data for $Cp_2ZrMe(PHMes^*)$ 72

^{1}H NMR (-80 °C, $CD_3C_6D_5$, 200 MHz): δ 7.74 (br s, 1H, Ar-*H*), 7.66 (br s, 1H, Ar-*H*), 5.57 (s, 5H, Cp), 5.30 (s, 5H, Cp), 1.86 (br s, 9H, *o*-^{t}Bu), 1.58 (br s, 9H, *o*-^{t}Bu), 1.33 (s, 9H, *p*-^{t}Bu), -0.07 (br s, 3H, Me). ^{31}P NMR (-80 °C, $CD_3C_6D_5$): δ 67.7 (d, $|J_{P\text{-}H}|$ = 261.5 Hz).

Synthesis of $Cp_2Zr(PHMes^*)(OPh)$ 110, $Cp_2Zr(PHMes^*)(NHPh)$ 112 and $Cp_2Zr(PHMes^*)(PPh_2)$ 115

These compounds were prepared in a similar manner, thus only one representative preparation is described. To a benzene solution of **84** (114 mg, 0.2 mmol) was added phenol (18 mg, 0.2 mmol). The reaction mixture stood 1 h, after which time the solvent was removed in vacuo and the product dissolved in pentane. Yellow-brown crystals of **110** formed after this solution was allowed to stand for 12 h, and were isolated by filtration. **110**: Yield: 62 mg (52%). ^{1}H NMR (25 °C, C_6D_6): δ 7.60 (d, $|^4J_{P\text{-}H}|$ = 1.8 Hz, 2H, Ar-*H*), 7.20 (m, 2H, Ph-*H*), 6.85 (m, 1H, Ph-*H*), 6.61 (m, 2H, Ph-*H*), 5.66 (br s, 10, Cp), 5.29 (d, $|J_{P\text{-}H}|$ = 221.2 Hz, 1H, P-*H*), 1.74 (br s, 18H, *o*-^{t}Bu), 1.35 (s, 9H, *p*-^{t}Bu). ^{13}C{^{1}H} NMR (25 °C, C_6D_6): δ 165.3 (s, quat), 146.0 (s, quat), 145.0 (d, $|J|$ = 36.8 Hz, quat), 129.3 (s, arom. C-H), 121.0 (br s, arom. C-H), 119.6 (s, arom. C-H), 118.0 (s, arom. C-H), 111.3 (s, Cp), 38.3 (br s, *o*-$C(CH_3)$), 34.6 (s, *p*-$C(CH_3)$), 33.1 (br s, *o*-$C(CH_3)$), 31.3 (s, *p*-$C(CH_3)$). ^{31}P NMR (25 °C, C_6D_6): δ -20.0 (d, $|J_{P\text{-}H}|$ = 220.6 Hz). ^{1}H NMR (-70 °C, $CD_3C_6D_5$, 200

MHz): δ 7.63 (br, 2H, Ar-*H*), 7.22-6.89 (m, 3H, Ph-*H*), 6.52 (m, 2H, Ph-*H*), 5.61 (s, 5H, Cp), 5.40 (s, 5H, Cp), 1.89 (s, 9H, *o*-^{t}Bu), 1.68 (s, 9H, *o*-^{t}Bu), 1.36 (s, 9H, *p*-^{t}Bu). ^{31}P NMR (-70 °C, $CD_3C_6D_5$): δ -22.4 (d, $|J_{P\text{-}H}|$ = 222.8 Hz). Anal. Calcd for $C_{34}H_{45}OPZr$: C: 68.99; H: 7.66; Found: C: 68.63; H: 7.38.

112: Yield: 92 mg (78%). ^{1}H NMR (25 °C, C_6D_6): δ 7.60 (d, $|^4J_{P\text{-}H}|$ = 1.7 Hz, 2H, Ar-*H*), 7.25-6.85 (m, 5H, Ph-*H*), 6.59 (s, 1H, N-*H*), 5.51 (br s, 10H, Cp), 5.22 (d, $|J_{P\text{-}H}|$ = 223.2 Hz, 1H, P-*H*), 1.68 (s, 18H, *o*-^{t}Bu), 1.36 (s, 9H, *p*-^{t}Bu). ^{13}C{^{1}H} NMR (25 °C, C_6D_6): δ 156.1 (s, quat), 155.8 (s, quat), 145.8 (s, quat), 144.6 (d, $|J|$ = 36.5 Hz, quat), 120.9 (s, arom. *C*-H), 120.6 (s, arom. *C*-H), 120.5 (s, arom. *C*-H), 119.4 (s, arom. *C*-H), 109.7 (s, Cp), 38.2 (s, *o*-$C(CH_3)_3$), 34.6 (s, *p*-$C(CH_3)_3$), 32.7 (s, *o*-$C(CH_3)_3$), 31.3 (s, *p*-$C(CH_3)_3$). ^{31}P NMR (25 °C, C_6D_6): δ -11.1 (d, $|J_{P\text{-}H}|$ = 223.4 Hz). ^{1}H NMR (-60 °C, $CD_3C_6D_5$): δ 7.72 (br s, 1H, Ar-*H*), 7.67 (br s, 1H, Ar-*H*), 7.37-6.75 (m, 5H, Ph-*H*), 6.60 (br s, 1H, N-*H*), 5.63 (s, 5H, Cp), 5.28 (d, $|J_{P\text{-}H}|$ = 223.0 Hz, 1H, P-*H*), 5.22 (s, 5H, Cp), 1.79 (br s, 9H, *o*-^{t}Bu), 1.70 (br s, 9H, *o*-^{t}Bu), 1.41 (s, 9H, *p*-^{t}Bu). ^{31}P NMR (-60 °C, $CD_3C_6D_5$): δ -13.6 (d, $|J_{P\text{-}H}|$ = 222.3 Hz). Anal. Calcd for $C_{34}H_{46}NPZr$: C: 69.11; H: 7.85; Found: C: 69.47; H: 7.62.

115: Yield: 116 mg (85%). ^{1}H NMR (25 °C, C_6D_6): δ 7.64-6.98 (m, 12H, Ar-*H* and Ph-*H*), 6.67 (d, $|J_{P\text{-}H}|$ = 276.3 Hz, 1H, P-*H*), 5.50 (s, 10H, Cp), 1.70 (br s, 18H, *o*-^{t}Bu), 1.36 (s, 9H, *p*-^{t}Bu). ^{13}C{^{1}H} NMR (25 °C, C_6D_6): δ 149.9 (s, quat), 148.8 (d, $|J|$ = 28.3 Hz, quat), 135.1 (d, $|J|$ = 8.0 Hz, quat), 134.0 (d, $|J|$ = 15.2 Hz, arom. *C*-H), 134.0 (d, $|J|$ = 16.9 Hz, arom. *C*-H), 124.9 (s, arom. *C*-H), 121.7 (br s, arom. *C*-H), 106.9 (s, Cp), 38.8 (s, *o*-$C(CH_3)_3$), 34.8 (s, *p*-$C(CH_3)_3$), 32.9 (s, *o*-$C(CH_3)_3$), 31.2 (s, *p*-$C(CH_3)_3$). ^{31}P NMR (25 °C, C_6D_6): δ 153.2 (dd, $|^2J_{P\text{-}P}|$ = 21.9 Hz, $|J_{P\text{-}H}|$ = 278.9 Hz), 17.4 (d, $|^2J_{P\text{-}P}|$ = 21.9 Hz). ^{1}H NMR (-70 °C, $CD_3C_6D_5$, 200 MHz): δ 7.75-7.00 (m, 12H, Ar-*H* and Ph-*H*), 5.54 (s, 5H, Cp), 5.40 (s, 5H, Cp), 2.00 (br s, 9H, *o*-^{t}Bu), 1.47 (br s, 9H, *o*-^{t}Bu), 1.32 (s, 9H, *p*-^{t}Bu). ^{31}P NMR (-70 °C, $CD_3C_6D_5$): δ 164.6 (br d, $|J_{P\text{-}H}|$ = 292.4 Hz), 5.0 (d, $|^2J_{P\text{-}P}|$ = 20.7 Hz). Anal. Calcd for $C_{40}H_{50}P_2Zr$: C: 70.24; H: 7.37; Found: C: 69.85; H: 7.08.

Generation of $Cp_2Zr(PHMes^*)(SPh)$ 111, $Cp_2Zr(PHMes^*)(PHPh)$ 113 and $Cp_2Zr(PHMes^*)(PHMes)$ 114

These compounds were generated in a similar manner, thus only one representative preparation is described. To a benzene solution of **84** (114 mg, 0.2 mmol) was added thiophenol (20.4 μL, 0.2 mmol). The reaction mixture stood 10 min., after which time the solvent was removed in vacuo. The wine-red residue was characterized by NMR, although the unstable product degraded after 24 h in solution. **111**: Yield: 76% (by ^{1}H NMR). ^{1}H NMR (25 °C, C_6D_6): δ 7.84-6.98 (m, 7H, Ph-*H* and Ar-*H*), 5.96 (d, $|J_{P\text{-}H}|$ = 259.3 Hz, 1H, P-*H*), 5.56 (s, 10, Cp), 1.70 (br s, 18H, *o*-^{t}Bu), 1.32 (s, 9H, *p*-^{t}Bu). $^{13}C\{^1H\}$ NMR (25 °C, C_6D_6): δ 154.2 (d, $|J|$ = 7.5 Hz, quat), 148.1 (s, quat), 147.4 (s, quat), 139.5 (d, $|J|$ = 12.1 Hz, quat), 133.8 (s, arom. *C*-H), 124.3 (s, arom. *C*-H), 122.0 (s, arom. *C*-H), 121.4 (br s, arom. *C*-H), 109.2 (s, Cp), 38.6 (br s, *o*-*C*(CH_3)), 34.7 (s, *p*-*C*(CH_3)), 32.9 (br s, *o*-C(*C*H_3)), 31.3 (s, *p*-C(*C*H_3)). ^{31}P NMR (25 °C, C_6D_6): δ 64.4 (d, $|J_{P\text{-}H}|$ = 259.3 Hz). ^{1}H NMR (-50 °C, $CD_3C_6D_5$, 200 MHz): δ 7.93-7.07 (m, 7H, Ph-*H* and Ar-*H*), 5.54 (s, 5H, Cp), 5.45 (s, 5H, Cp), 1.99 (br s, 9H, *o*-^{t}Bu), 1.53 (br s, 9H, *o*-^{t}Bu), 1.32 (s, 9H, *p*-^{t}Bu). ^{31}P NMR (-70 °C, $CD_3C_6D_5$): δ 63.9 (d, $|J_{P\text{-}H}|$ = 259.3 Hz).

113: Yield: 92% (by ^{1}H NMR). ^{1}H NMR (25 °C, C_6D_6): δ 7.67-6.98 (m, 7H, Ar-*H* and Ph-*H*), 6.60 (d, $|J_{P\text{-}H}|$ = 291.4 Hz, 1H, P-*H*), 5.43 (s, 10, Cp), 3.36 (dd, $|J_{P\text{-}H}|$ = 188.0 Hz, $|^3J_{P\text{-}H}|$ = 15.4 Hz, 1H, P-*H*), 1.65 (br s, 18H, *o*-^{t}Bu), 1.28 (s, 9H, *p*-^{t}Bu). $^{13}C\{^1H\}$ NMR (25 °C, C_6D_6): δ 150.3 (s, quat), 149.9 (s, quat), 133.2 (d, $|J|$ = 12.7 Hz, arom. *C*-H), 128.4 (s, arom. *C*-H), 123.7 (s, arom. *C*-H), 121.7 (s, arom. *C*-H), 107.1 (s, Cp), 38.7 (br s, *o*-*C*(CH_3)), 34.8 (s, *p*-*C*(CH_3)), 32.8 (br s, *o*-C(*C*H_3)), 31.2 (s, *p*-C(*C*H_3)). ^{31}P NMR (25 °C, C_6D_6): δ 151.9 (d, $|J_{P\text{-}H}|$ = 291.2 Hz), -43.6 (d, $|J_{P\text{-}H}|$ = 187.7 Hz). ^{1}H NMR (-80 °C, $CD_3C_6D_5$, 200 MHz): δ 7.73-6.96 (m, 7H, Ar-*H* and Ph-*H*), 6.38 (d, $|J_{P\text{-}H}|$ = 291.6 Hz, 1H, P-*H*), 5.38 (s, 5H, Cp), 5.23 (s, 5H, Cp), 3.20 (br dd, $|J_{P\text{-}H}|$ = 180 Hz, $|^3J_{P\text{-}H}|$ = 16 Hz, 1H, P-*H*), 1.77 (br s, 9H, *o*-^{t}Bu), 1.45 (br s, 9H, *o*-^{t}Bu), 1.31 (s, 9H, *p*-^{t}Bu). ^{31}P NMR (-80 °C, $CD_3C_6D_5$): δ 155.1 (d, $|J_{P\text{-}H}|$ = 294.9 Hz), -46.6 (d, $|J_{P\text{-}H}|$ = 183.1 Hz).

114: Yield: 94% (by ^{1}H NMR). ^{1}H NMR (25 °C, C_6D_6): δ 7.63 (s, 2H, Ar-*H*), 7.01 (s, 2H, Ar-*H*), 6.38 (d, $|J_{P\text{-}H}|$ = 283.0 Hz, 1H, P-*H*), 5.36 (s, 10H, Cp), 3.53 (dd, $|J_{P\text{-}H}|$ = 205.7 Hz, $|^3J_{P\text{-}H}|$ = 12.8 Hz, 1H, P-*H*), 2.51 (s, 6H, *o*-Me), 2.30 (s, 3H, *p*-Me), 1.66 (br s, 18H, *o*-^{t}Bu), 1.35 (s, 9H, *p*-^{t}Bu). ^{13}C{^{1}H} NMR (25 °C, C_6D_6): δ 149.4 (s, quat), 144.7 (s, quat), 138.4 (d, $|J|$ = 9.9 Hz, quat), 133.4 (s, quat), 121.6 (br s, arom. C-H), 119.7 (s, arom. C-H), 107.2 (s, Cp), 38.6 (br s, *o*-$C(CH_3)$), 34.8 (s, *p*-$C(CH_3)$), 32.8 (br s, *o*-$C(CH_3)$), 31.2 (s, *p*-$C(CH_3)$), 24.8 (d, $|^3J_{P\text{-}C}|$ = 9.4 Hz, *o*-Me), 20.9 (s, *p*-Me). ^{31}P NMR (25 °C, C_6D_6): δ 130.6 (ddd, $|J_{P\text{-}H}|$ = 282.5 Hz, $|^2J_{P\text{-}P}|$ = 36.6 Hz, $|^3J_{P\text{-}H}|$ = 14.3 Hz), -60.4 (d, $|J_{P\text{-}H}|$ = 206.1 Hz, $|^2J_{P\text{-}P}|$ = 36.6 Hz). ^{1}H NMR (-70 °C, $CD_3C_6D_5$, 200 MHz): δ 7.78 (br s, 2H, Ar-*H*), 7.69 (br s, 2H, Ar-*H*), 5.96 (d, $|J_{P\text{-}H}|$ = 286.1 Hz, 1H, P-*H*), 5.29 (s, 5H, Cp), 5.23 (s, 5H, Cp), 3.42 (br dd, $|J_{P\text{-}H}|$ = 204.2 Hz, $|^3J_{P\text{-}H}|$ = 15 Hz, 1H, P-*H*), 2.55 (br s, 6H, *o*-Me), 2.40 (s, 3H, *p*-Me), 1.92 (br s, 9H, *o*-^{t}Bu), 1.54 (br s, 9H, *o*-^{t}Bu), 1.34 (s, 9H, *p*-^{t}Bu). ^{31}P NMR (-70 °C, $CD_3C_6D_5$): δ 142.2 (br d, $|J_{P\text{-}H}|$ = 286.8 Hz), -69.7 (dd, $|J_{P\text{-}H}|$ = 204.1 Hz, $|^2J_{P\text{-}P}|$ = 24.4 Hz).

X-Ray Structure Determinations of 104, 107b, 108 and 112

The cyclopentadienyl and phenyl rings in **107b** and **108** as well as the t-butyl groups in **107b** were refined with a constrained geometry in order to maintain a statistically meaningful data:variable ratio. The correct enantiomorph of **108** was confirmed by inversion and refinement of the model. The N-H and P-H hydrogen atoms of **112** were located in a difference Fourier map, and their contributions included but not refined in subsequent least squares calculations. The final values of R, R_w and the maximum Δ/σ on any of the parameters in the final cycle of refinement are given in Table 3.1. ORTEP drawings of **104**, **107b**, **108** and **112** are shown in Figures 3.6, 3.8, 3.10 and 3.12, respectively, with 30% thermal ellipsoids. Selected bond distances and angles are listed in the captions for Figures 3.6, 3.8, 3.10 and 3.12. Other structural parameters are given in Tables A2.1-A2.12 in Appendix Two.

Table 3.1: Crystallographic Parameters for 104, 107b, 108 and 112

	104	107b	108	112
Formula	$C_{52}H_{94}P_2Sn_2$	$C_{38}H_{53}NP_2Zr$	$C_{41}H_{61}N_2PZr$	$C_{34}H_{46}NPZr$
Formula weight	1018.64	768.23	704.14	590.94
Cryst Colour, Form	orange blocks	red plates	brown blocks	orange blocks
a(Å)	12.062(7)	12.918(3)	14.353(6)	9.627(4)
b(Å)	23.090(3)	14.879(4)	13.513(4)	21.063(7)
c(Å)	10.543(3)	19.751(4)	21.101(5)	16.227(4)
α(deg)	101.67(1)			
β(deg)	99.77(3)	98.57(2)	106.78(3)	106.30(3)
γ(deg)	78.99(2)			
Crystal System	triclinic	monoclinic	monoclinic	monoclinic
Space group	$P\bar{1}$	$P2_1/c$	Cc	$P2_1/n$
Vol(Å^3)	2796(2)	3754(1)	3918(2)	3158(2)
D_{calcd} (gcm^{-3})	1.21	1.36	1.19	1.24
Z	2	4	4	4
Abs coeff, μ, cm^{-1}	9.79	6.66	3.50	4.20
Temp (°C)	24	24	24	24
Scan speed, °/min	16 ($\theta/2\theta$) (1-3 scans)	8 ($\theta/2\theta$) (1-3 scans)	8 ($\theta/2\theta$) (1-3 scans)	16 ($\theta/2\theta$) (1-3 scans)
Scan range (deg)	1.0 above $K\alpha_1$, 1.0 below $K\alpha_2$	1.0 above $K\alpha_1$, 1.0 below $K\alpha_2$	1.0 above $K\alpha_1$, 1.0 below $K\alpha_2$	1.0 above $K\alpha_1$, 1.0 below $K\alpha_2$
Bkgd/scan ratio	0.5	0.5	0.5	0.5
Data collected	9862	3701	3616	5747
2θ range (deg)	4.5-50.0	4.5-50.0	4.5-50.0	4.5-50.0
Index range	$\pm h, \pm k, l$	$\pm h, k, l$	$\pm h, k, l$	$\pm h, k, l$
Data $F_o^2 > 3\sigma(F_o^2)$	5988	834	1188	2075
Variables	506	97	146	284
Transmission factors	0.749-1.612	0.737-1.459	0.577-1.058	0.818-0.996
R (%)[a]	4.6	9.0	7.8	7.3
Rw (%) [a]	5.9	9.2	6.2	5.5
Largest Δ/σ	0.00	0.00	0.03	0.00
Goodness of fit	2.76	2.38	1.76	2.76

[a] $R = \Sigma | |F_o| - |F_c| | / \Sigma |F_o|$, $Rw = [\Sigma(|F_o| - |F_c|)^2 | / \Sigma |F_o|^2]^{0.5}$

3.3 Results and Discussion

Reactions of 84 with Ketones and Aldehydes

Compound **84** reacted with benzaldehyde to give an insoluble white precipitate (presumably polymeric zirconocene oxides), free PMe_3, and the E-isomer of the known phosphaalkene Mes*P=CHPh **85**.[47] An analogous synthetic procedure using benzophenone provided an 82% yield of the known phosphaalkene Mes*P=CPh_2 **86**,[48] while in the same manner the use of two equivalents of **84** with isophthalaldehyde furnished benzodiphosphaalkene C_6H_2(1,3-HC=PMes*)$_2$ **87**[49] (Fig. 3.1). In contrast to the published synthetic route the present procedure resulted in the exclusive formation of the EE isomer of **87** in 86% yield. The related reaction of **84** with phenylisothiocyanate gave the heteroallene *trans*-PhN=C=PMes* **88** in 81% yield,[50] along with the crystalline blue by-product $[Cp_2ZrS]_2$.[55]

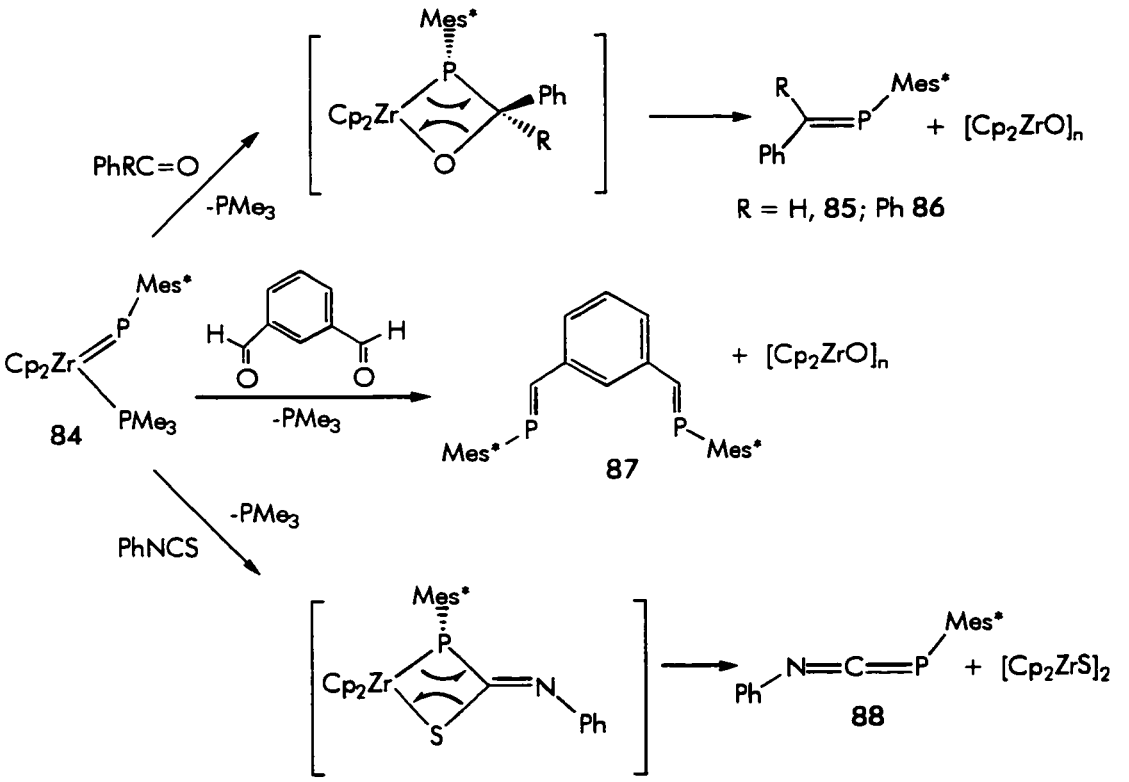

Figure 3.1 Metathetical reactions of **84** with organic carbonyl compounds.

The above reactions are analogous to metathetical reactions of Wittig phosphorus ylides[7] and Schrock alkylidenes.[3,4] They are thought to proceed through initial coordination of the carbonyl species followed by intramolecular attack of the carbon atom by phosphorus to give a cyclic intermediate (Fig. 3.1). Subsequent retrocyclization gives the C=P product and oligomerized Zr=E. The selective regiochemistry resulting in the formation of only the E isomers of the phosphaalkenes corresponds to a minimization of steric crowding in the metallacyclic intermediates. These transformations have been established for Bergman's zirconocene imido complexes,[23] and Schrock has also briefly described the similar use of $((Me_3SiNCH_2CH_2)_3N)Ta{=}PR$ as a phospha-Wittig reagent.[31a]

In contrast to the above reactions, **84** reacted with cyclohexanone to give the enolate derivative $Cp_2Zr(PHMes^*)(OC_6H_9)$ **89**. The formation of **89** is consistent with the basicity of the phosphinidene group of **84** and the presence of acidic, enolizable protons of cyclohexanone.

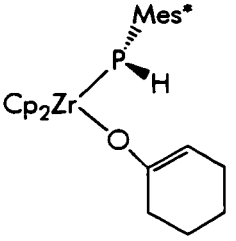

89

Reactions of 84 with Organic Dichlorides

Gem-dichlorides also reacted with **84** to give phosphaalkenes, along with by-products Cp_2ZrCl_2 and PMe_3. For example, $Mes^*P{=}CH_2$ **90**[51] was formed in 86% yield via reaction of **84** with CH_2Cl_2 and the analogous reaction with $CHCl_3$ gave a 1:2 ratio of the *cis* and *trans* isomers of $Mes^*P{=}CHCl$ **91**,[51,52] in an overall yield of 76% (Fig. 3.2). Organophosphacycles were accessible by altering the choice of organic dihalide. For instance, the known phosphirane $\overline{CH_2CH_2}PMes^*$ **92**[53] was prepared in 45% yield by

reaction of **84** with 1,2-dichloroethane, and the use of *ortho*-dichloroxylene produced the new phospholane 1,2-$C_6H_4(\overline{CH_2CH_2})PMes^*$ **93** in 53% yield.

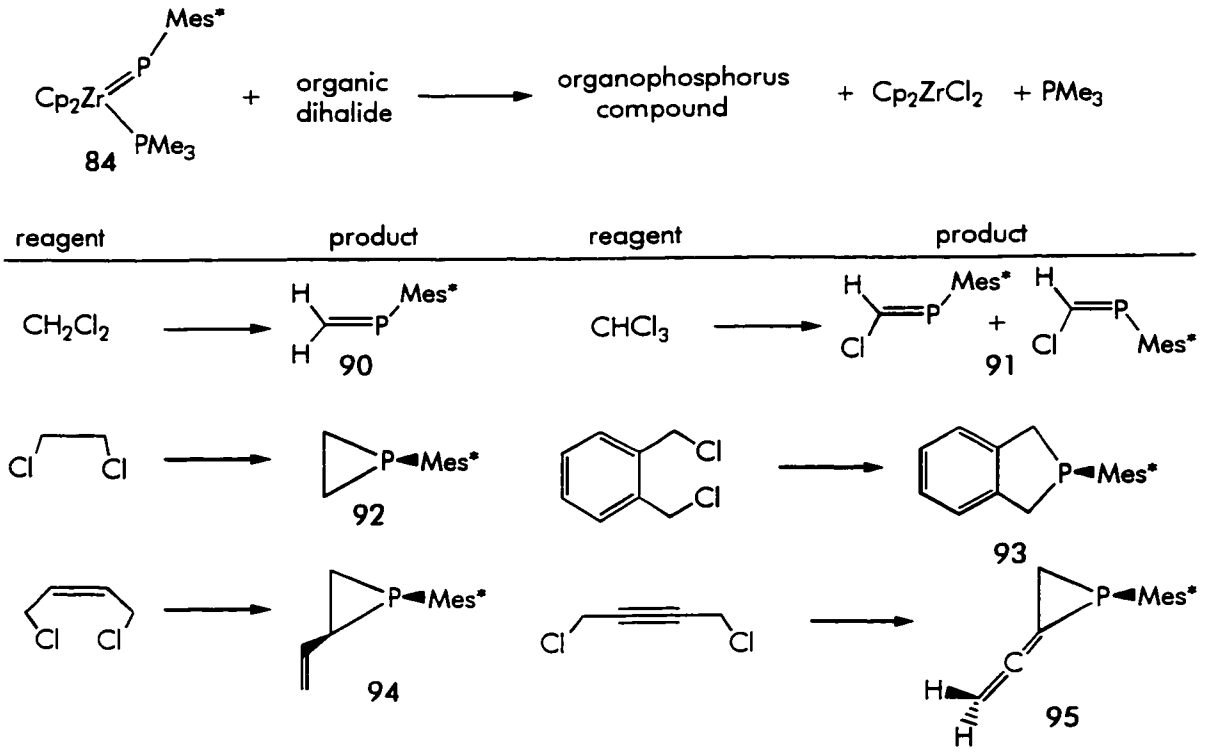

Figure 3.2 Reactions of **84** with organic dichlorides.

In contrast to these results the reaction of **84** with *cis*-1,4-dichloro-2-butene did not produce the anticipated five membered ring, but rather the *cis* isomer of the vinyl substituted phosphirane $(CH_2{=}CH)\overline{CHCH_2}PMes^*$ **94** in 38% yield. Likewise, reaction of **84** with 1,4-dichloro-2-butyne produced the species $(CH_2{=}C{=})\overline{CCH_2}PMes^*$ **95** in 53% yield (Fig. 3.2). Both **94** and **95** exhibited the high field ^{31}P NMR chemical shifts typical of three membered rings.[56] The existence of the vinyl group in **94** was confirmed by ^{13}C and DEPT NMR experiments. Simulations of the ^{1}H NMR vinyl region showed very small coupling of the vinyl protons to phosphorus, suggesting a *cis* orientation of the supermesityl and vinyl groups. This geometry is consistent with the absence of coupling between phosphorus and the vinyl carbon atoms and is also in accordance with ^{13}C NMR data for related vinyl phosphiranes.[57] The presence of the allene

fragment in **95** was verified by ^{13}C NMR spectroscopy. The central carbon of this moiety resonates at 220.5 ppm while signals at 76.6 and 84.4 ($|J_{P\text{-}C}|$ = 46.5 Hz) ppm were confirmed by DEPT experiments to be the exocyclic methylene and the substituted ring carbons, respectively.

The reactions with alkyl halides are thought to involve phosphide-halide intermediates of the form $Cp_2Zr(PMes^*R)Cl$. Structurally related compounds such as $Cp_2Zr(PMes^*H)Cl$,[35a] and $Cp_2Zr(PMes^*SiMe_3)Cl$[44] have been previously characterized. This view is compatible with observations of transient ^{31}P NMR resonances at 165.6, 180.8 and 173.8 ppm in the formations of **93**, **94** and **95** respectively. Although the unusual reactions of **84** with *cis*-1,4-dichloro-2-butene and 1,4-dichloro-2-butyne were observed to progress through these intermediates, the completion of the reaction must proceed via an alternate pathway (Fig. 3.3).

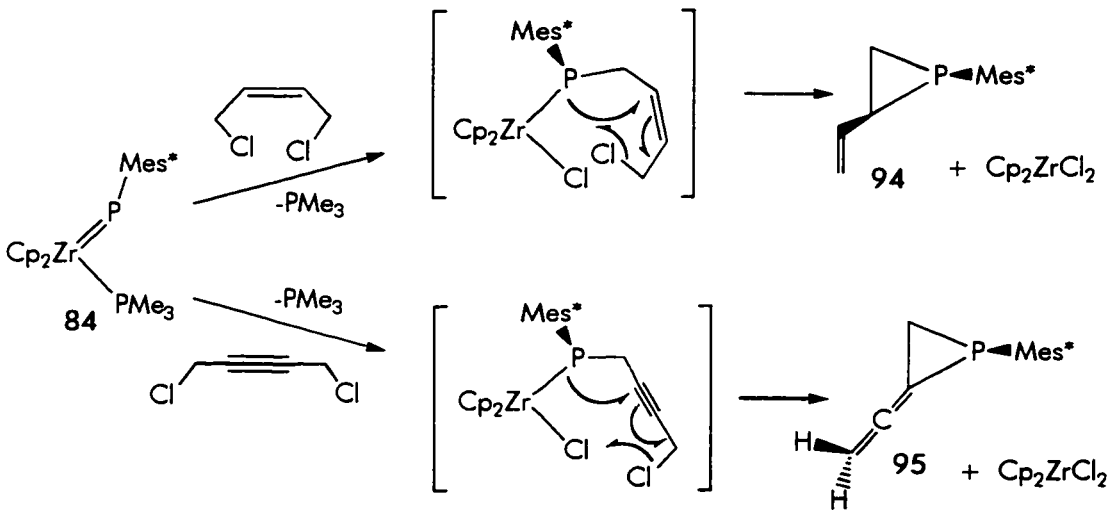

Figure 3.3 Proposed mechanism for the formation of **94** and **95**.

Reactions of 84 with Epoxides

Phosphiranes PhCHCH(Ph)PMes* **97** and *trans*-(PhCHCH$_2$PMes*) **98** were derived from reactions of **84** with *trans*-stilbene oxide and styrene oxide, respectively. The ^{31}P NMR spectrum of the reaction of **84** with *trans*-stilbene oxide revealed the initial appearance of a resonance at 136.4 ppm attributable to an intermediate of the form **96**

(Fig. 3.4). This signal gradually receded and was replaced by the resonance due to **97**. The ^{13}C NMR spectrum of **97** revealed the inequivalence of the two phenyl substituents, indicative of a relative *trans* orientation. A similar reaction between **84** and styrene oxide yielded one pair of enantiomers of the known[54] phosphirane **98**, in which the phenyl and Mes* groups are of a *trans* disposition.

In the related reaction of **84** with propylene oxide the derived product $Cp_2Zr(PMes^*H)(OCH_2CHCH_2)$ **99** was formed through proton abstraction. The reaction probably progresses through coordination of the epoxide to the zirconium centre followed by abstraction of a methyl proton and ring-opening to give **99**. Similar ring-opening of isobutylene oxide has been observed by Bergman *et al.* with zirconocene imido species $Cp_2Zr(NR)(THF)$.[23] In contrast, the aforementioned use of epoxides without methyl substituents results in intramolecular nucleophilic attack of the coordinated epoxide by phosphorus to afford the ring-opened intermediate **96**.

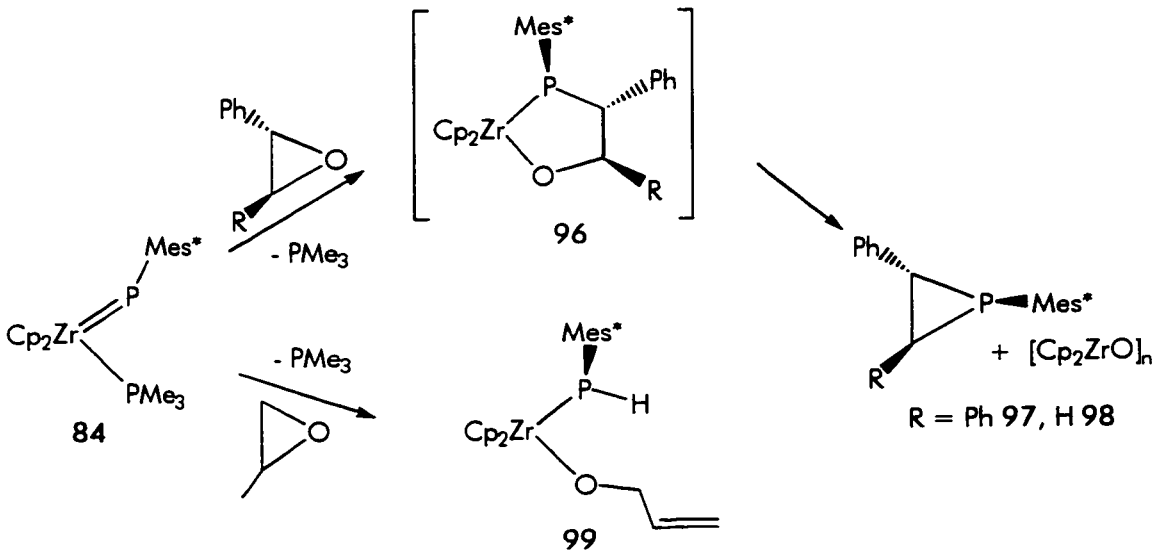

Figure 3.4 Reactions of **84** with epoxides.

Reactions of 84 with Silicon, Germanium, and Tin Dichlorides and Tin Sulfides

Interest in phosphinidenes of the heavier main group elements has intensified in recent years.[58] The observed reactivity of **84** suggests the accessibility of main group

phosphinidenes through reactions of **84** with main group dihalides or chalcogenides. Hence, the use of Me_2SiCl_2 furnished a 71% of $Cp_2Zr(PMes^*(SiMe_2Cl))Cl$ **100**, which appears to be related to the proposed intermediates in reactions of **84** with organic dihalides. However, upon standing in solution **100** did not liberate Cp_2ZrCl_2 and the phosphasilene, a fact which may be ascribed to the inherent strength of the Si-Cl bond. Nonetheless, reaction of **100** with two equivalents of Me_2SiCl_2 furnished Cp_2ZrCl_2 and a 92% yield of the disilylphosphine $PMes^*(SiMe_2Cl)_2$ **101**.

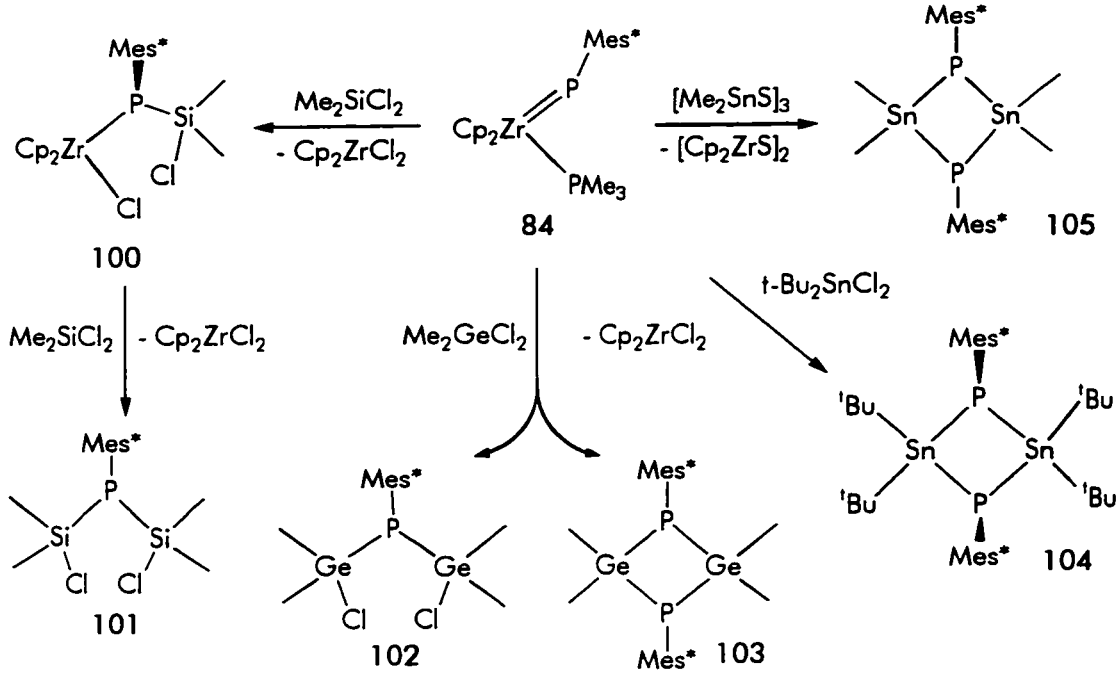

Figure 3.5 Reactions of **84** with silicon, germanium and tin reagents.

The corresponding reaction of **84** with one equivalent of Me_2GeCl_2 resulted in the total consumption of **84** and the formation of two products, **102** and **103**, in a 55:45 ratio. The phosphorus coupled doublet observed for the methyl protons of **102** supported its formulation as $(Me_2GeCl)_2PMes^*$, whereas the similar triplet observed for **103** pointed to a cyclic oligomer of the form $(Me_2GePMes^*)_n$. High resolution mass spectrometry confirmed the formulations of **102** and **103** as $(Me_2GeCl)_2PMes^*$ and $(Me_2GePMes^*)_2$, respectively. Phosphinidene transfer followed by dimerization of a highly unstable

germanium phosphinidene intermediate is a possible mechanism for the formation of **103**, although reaction of **84** with **102** cannot be ruled out. The use of two equivalents of Me_2GeCl_2 greatly improved the yield of **102** to 62% and gave a **102**:**103** ratio of 87:13.

Phosphinidene transfer to a tin centre was observed in the reaction of **84** with *t*-Bu_2SnCl_2. The product **104** was isolated in 30% yield as large orange crystals which exhibited a ^{31}P NMR resonance at -84.8 ppm. ^{1}H and ^{13}C NMR data as well as elemental analysis were consistent with an empirical formulation of (*t*-$Bu_2SnPMes^*$); the dimeric nature of **104** was subsequently verified by X-ray crystallography. Although cyclic Sn-P compounds akin to **104** have been synthesized through standard organic preparations, structural data have not been reported.[59] The crystal structure of **104** represents the first crystallographic data to be described for a tin phosphinidene species (Fig. 3.6).

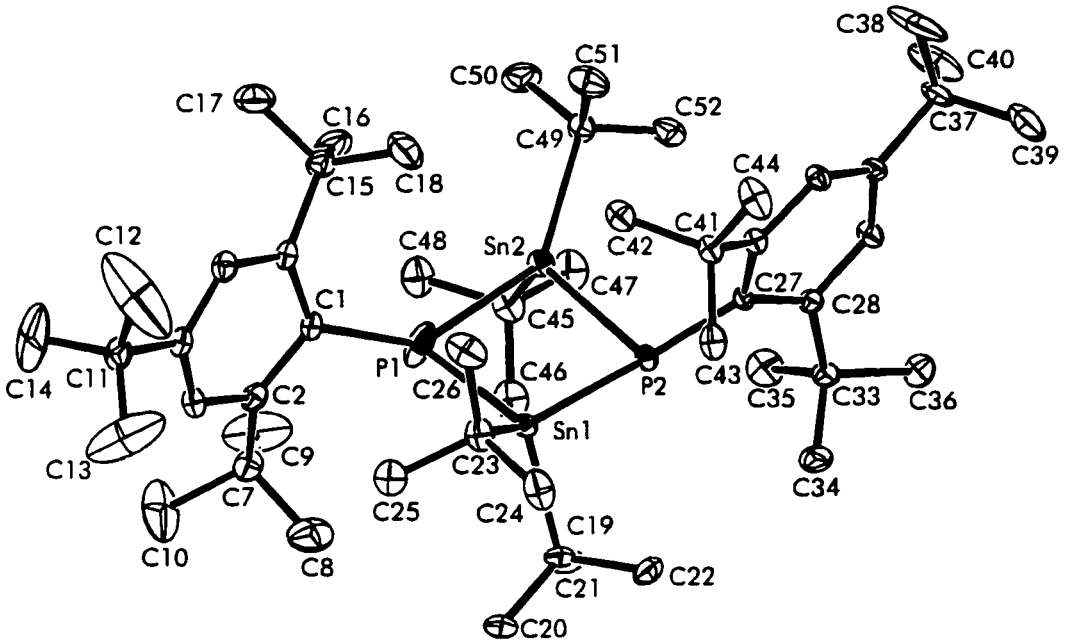

Figure 3.6 ORTEP drawing of **104**; 30% ellipsoids are shown, hydrogen atoms have been omitted for clarity. Selected bond distances and angles: Sn(1)-P(1) 2.524(3) Å; Sn(1)-P(2) 2.614(2) Å; Sn(2)-P(1) 2.556(3) Å; Sn(2)-P(2) 2.557(2) Å; P(1)-Sn(1)-P(2) 87.30(9)°; P(1)-Sn(2)- P(2) 87.87(9)°; Sn(1)-P(1)-Sn(2) 93.0(1)°; Sn(1)-P(2)-Sn(2) 90.92(7)°.

The Sn_2P_2 four-membered ring of **104** is slightly puckered as reflected in the dihedral angle of 170.2(1)° between the two SnP_2 planes. The supermesityl groups adopt a *cisoid* disposition with respect to the Sn_2P_2 core. The P-Sn-P angles average 87.58(9)° while the Sn-P-Sn angles are 93.0(1)° and 90.92(7)°. The Sn(2)-P distances of 2.556(3) and 2.557(2) Å and the Sn(1)-P distances of 2.524(3) and 2.614(2) Å agree well with the Sn-P distances in $Me_2Sn(PMes^*H)_2$.[60] The sum of the angles about P(2) is 335.2°, indicating the approximately pyramidal geometry; however, a distortion at P(1) towards trigonal planarity is evidenced in the sum of the angles of 348.0°. These metric parameters suggest that inversion at phosphorus may be facile in this strained four-membered ring system. This is consistent with the symmetry in solution implied by the ^1H and ^{13}C NMR spectra, though attempts to stop such inversion processes by cooling to -80 °C merely resulted in the observation of spectral broadening.

The ready availability of organotin chalcogenides also provided a route to dimerized tin phosphinidenes. **84** reacted with $(Me_2SnS)_3$[61] to give $[Cp_2ZrS]_2$, PMe_3, and a product of empirical formulation ($Me_2SnPMes^*$). The dimeric character of **105** was subsequently confirmed by high resolution mass spectrometric data. The mechanism of this reaction is thought to proceed in a manner similar to that proposed for reactions of **84** with ketones and aldehydes. Since an intermediate to support this claim could not be detected, a comparable reaction was studied. The reaction between **84** and $(Ph_2SnS)_3$[61] progressed slowly; ^{31}P NMR spectroscopy showed the conversion of the starting material to a resonance at 93.4 ppm with $|\,^1J(^{119}Sn\text{-}P)|$ and $|\,^1J(^{117}Sn\text{-}P)|$ values of 881 and 925 Hz respectively. This signal is tentatively assigned to the intermediate $Cp_2Zr(PMes^*SnPh_2S)$ **106**.

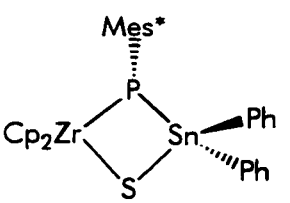

106

Continued surveillance by ^{31}P NMR spectroscopy showed the slow disappearance of the resonance due to **106** and its replacement by a resonance at -174.3 ppm. By comparison to **104** and **105** this peak is attributed to $(Mes^*PSnPh_2)_2$, the isolation of which was precluded by its thermal instability.

By analogy to phosphaalkene formation transient terminal germyl- and stannyl-phosphinidenes are possible intermediates to the dimers **103**, **104** and **105**, although these intermediates could not be detected even by monitoring the reaction mixtures at -80 °C. Monomeric Ge and Sn phosphinidenes are known to be stabilized by bulkier substituents as in $(i\text{-}Pr_3C_6H_2)_2SnPMes^*$,[58a] for example. However, the increased steric demands of the substituents in $(Mes)_2SnCl_2$ inhibited reaction with **84**, and no phosphinidene transfer was observed.

Reactions of 84 with Benzonitrile and Dicyclohexylcarbodiimide

Addition of one equivalent of benzonitrile to a benzene solution of **84** resulted in a rapid colour change to deep red. After one hour the ^{31}P NMR spectrum showed several by-products, a major set of resonances at 83.8 and -14.7 ppm (attributable to **107a**), and an absence of free PMe_3.

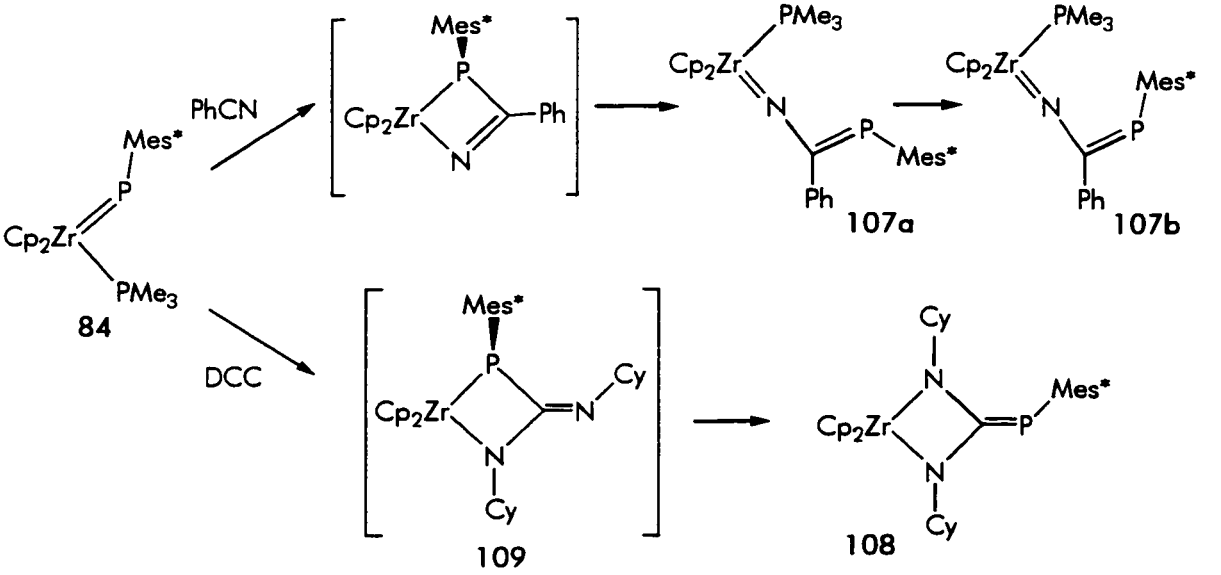

Figure 3.7 Metathetical reactions of **84** with benzonitrile and DCC.

After 24 hours the ^{31}P NMR spectrum revealed the appearance of a new pair of resonances at 92.1 and -15.2 ppm, which can be attributed to the product of isomerization **107b** (Fig. 3.7). ^{1}H NMR data indicated that two closely related species were present in a 55:45 ratio. Prolonged standing in pentane afforded a few thin red crystals, and a subsequent X-ray crystallographic study established the connectivity of **107b** as (Cp_2Zr=NC(Ph)=PMes*)(PMe_3) (Fig. 3.8).

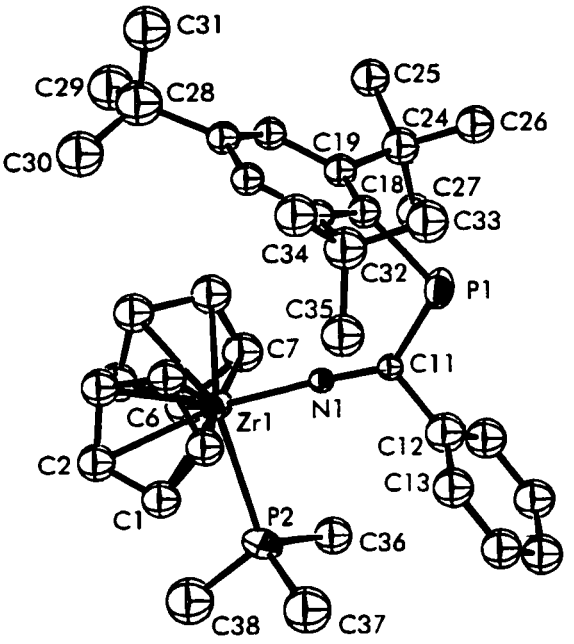

Figure 3.8 ORTEP drawing of **107b**; 30% ellipsoids are shown, hydrogen atoms have been omitted for clarity. Selected bond distances and angles: Zr(1)-N(1) 1.93(2) Å; Zr(1)-P(2) 2.74(1) Å; N(1)-C(11) 1.29(3) Å; P(1)-C(11) 1.81(3) Å; Zr(1)-N(1)-C(11) 176(3)°.

The Zr(1)-N(1)-C(11) vector is approximately linear, similar to the imido complex Cp_2Zr=NR(THF) reported by Bergman *et al.*[19,23] There is a *trans* arrangement of the phenyl and supermesityl groups about the C-P bond of the phosphaalkene moiety (Fig. 3.7). The extremely short N-C distance of 1.29(3) Å and the relatively long C-P bond distance of 1.81(3) Å suggests the resonance form depicted in Figures 3.7 and 3.9c. The participation of such resonance forms (Fig. 3.9) in solution implies that the conversion of **107a** to **107b** is a result of rotation about the P-C bond. In the proposed reaction

mechanism (Fig. 3.7) the *cis* isomer **107a** is formed first, and steric congestion provokes isomerization to the less hindered **107b**. While the ^{31}P NMR shifts could be assigned to the two isomers in this way, correlation of the ^{1}H NMR data was precluded by our inability to separate bulk quantities of the unstable species **107a** and **107b**.

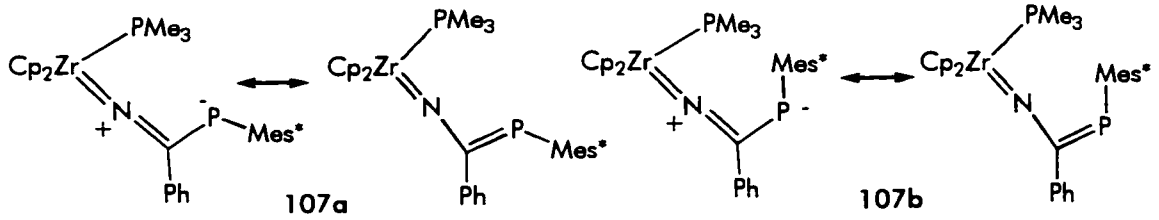

Figure 3.9 Resonance forms of **107a** and **107b**.

The reaction of **84** with dicyclohexylcarbodiimide (DCC) afforded a 46% yield of $Cp_2Zr(N(Cy))_2C{=}PMes^*$ **108**, the structure of which was confirmed by X-ray crystallography (Figure 3.10).

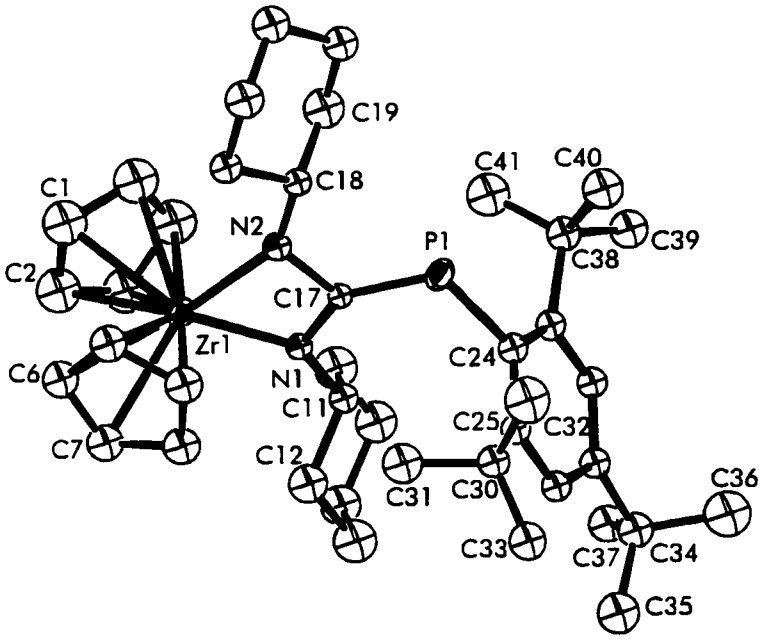

Figure 3.10 ORTEP drawing of **108**; 30% ellipsoids are shown, hydrogen atoms have been omitted for clarity. Selected bond distances and angles: Zr(1)-N(1) 2.11(2) Å; Zr(1)-N(2) 2.08(2) Å; N(1)-C(17) 1.44(3) Å; N(2)-C(17) 1.43(3) Å; P(1)-C(17) 1.74(3) Å; N(1)-Zr(1)-N(2) 66.3(8)°.

The Zr-N bond lengths in **108** of 2.08(2) and 2.11(2) Å are comparable to the terminal amido Zr-N bond distance in $[(Me_2N)_2ZrNCMe_3]_2$ of 2.065(1) Å.[62] The P-C bond length of 1.74(3) Å, much shorter than the analogous P-C distance in **107b**, substantiates the exocyclic phosphaalkene moiety in **108**.

The reactions of **84** with benzonitrile and DCC are comparable to established reactions of tantalum alkylidenes with nitriles.[9] These transformations are also closely related to the synthesis of vinylimido complexes of titanocene through reaction of the titanocene methylidene complex with nitrile in the presence of trapping ligands, as described by Doxsee *et al.* (Eq. 1.19).[26] The present reactions are thought to proceed through cycloaddition intermediates as depicted in Figure 3.9; mechanistic evidence was acquired by monitoring the reaction mixture of **108** by ^{31}P NMR spectroscopy. A signal at 47.3 ppm, attributable to the intermediate **109**, was observed initially and was subsequently replaced by the product resonance. Rearrangement of the intermediates in both reactions results in the rupture of Zr-P bonds and the formation of P-C double bonds. Coordination of PMe_3 traps the imido compound **107**, which would be expected to be extremely reactive in the absence of PMe_3. This may account for some of the unidentified by-products and the instability of **107**. In comparison, an intramolecular rearrangement process to give the exocyclic phosphaalkene moiety occurs in the formation of **108**.

1,2-Addition Reactions of 84 with E-H Bonds

Protic reagents such as phenol, aniline, thiophenol, and primary or secondary phosphines reacted rapidly with **84** to yield a series of compounds of the form $Cp_2Zr(PHMes^*)(ER)$ (ER = OPh **110**, SPh **111**, NHPh **112**, PHPh **113**, PHMes **114**, PPh_2 **115**) (Fig. 3.11). In each case, ^{31}P NMR spectra were consistent with a 1,2-addition of E-H across the Zr=P double bond, evidenced by the P-H coupling in the resulting supermesityl phosphide ligands as well as the P-P coupling in **114** and **115**. ^1H NMR data also supported the formulations above. Although these compounds could be

generated and characterized spectroscopically, they proved difficult to isolate due to their extreme solubility in organic solvents. In addition, the thermal instability of compounds **72** and **113-115** resulted in either disproportionation or elimination of phosphine over a 24 h period at 25 °C. The latter degradation pathway is consistent with established reactivity of zirconocene diphosphides.[35c]

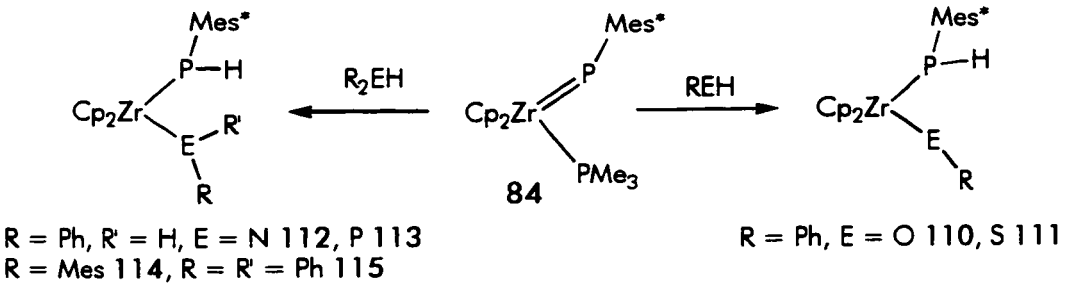

Figure 3.11 1,2-Addition reactions of **84**.

The formulation of **112** was verified via a single crystal diffraction study (Figure 3.12). As expected, the geometry about the zirconium atom of **112** is pseudo-tetrahedral, with two η^5-cyclopentadienyl ligands, a supermesityl phosphide and a phenylamido ligand completing the coordination sphere. The location of both the amido and phosphido hydrogen atoms confirmed a pseudo-trigonal planar geometry at nitrogen and a pseudo-tetrahedral geometry at phosphorus. The Zr-P distance of 2.707(4) Å in **112** is considerably longer than the Zr-P bonds in $Cp_2Zr(PHMes^*)Cl$ (2.558(7) Å),[35a] $(MeCp)_2Zr(PH(2,4,6\text{-}i\text{-}Pr_3C_6H_2)Cl$ (2.6381(8) Å)[63] and $Cp_2Zr(PHMes^*)_2$ (2.681(5), 2.682(5) Å).[64] Moreover, the Zr-N bond length of 2.09(1) Å is shorter than the Zr-N bonds in $Cp_2Zr(NC_4H_4)_2$ (2.171(2), 2.167(2) Å).[65] The P-Zr-N angle of 99.0(3)° in **112** compares with the Cl-Zr-P angles of 97.1(2)° and 93.55(2)° in $Cp_2Zr(PHMes^*)Cl$[35a] and $(MeCp)_2Zr(PH(2,4,6\text{-}i\text{-}Pr_3C_6H_2)Cl$,[63] respectively. The larger angle in **112** may be credited to the greater steric demands of the substituents on the two ancillary ligands. These data are consistent with a formal single Zr-P bond and strong π-character in the Zr-N bond.

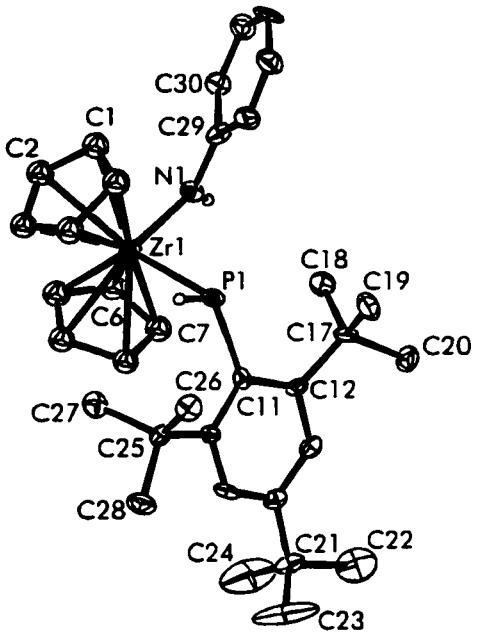

Figure 3.12 ORTEP drawing of **112**; 30% ellipsoids are shown, hydrogen atoms have been omitted for clarity. Selected bond distances and angles: Zr(1)-P(1) 2.707(4) Å; Zr(1)-N(1) 2.09(1) Å; P(1)-C(11) 1.86(1) Å; N(1)-C(29) 1.38(1) Å; P(1)-Zr(1)-N(1) 99.0(3)°.

Temperature Dependent NMR Data

^{1}H and ^{31}P NMR spectra for compounds **72** and **110-115** all showed marked temperature dependences over a temperature range of 30 °C to -80 °C. In each of these compounds, the resonances attributable to the *ortho-t*-butyl groups of the supermesityl substituents were broad at 25 °C, and split into two resonances upon cooling. This temperature dependence arises from sterically inhibited rotation about the P-C bond, a feature common to systems with bulky substituents.[64] In addition, a second dynamic process could be discerned for these compounds. As the temperature was lowered, the broad resonance due to the cyclopentadienyl rings split and eventually sharpened into two lines (Figure 3.13). $\Delta G_c^{\ddagger}$ values pertaining to this process were determined to be 11.8, 13.1, 13.1, 13.4, 12.5, 12.4 and 12.4 kcal mol^{-1} for compounds **72** and **110-115**.

Inequivalent cyclopentadienyl groups in these complexes arise as a result of the incorporation of a PHMes* ligand which provides a chiral phosphorus centre and consequently diastereotopic cyclopentadienyl ligands.

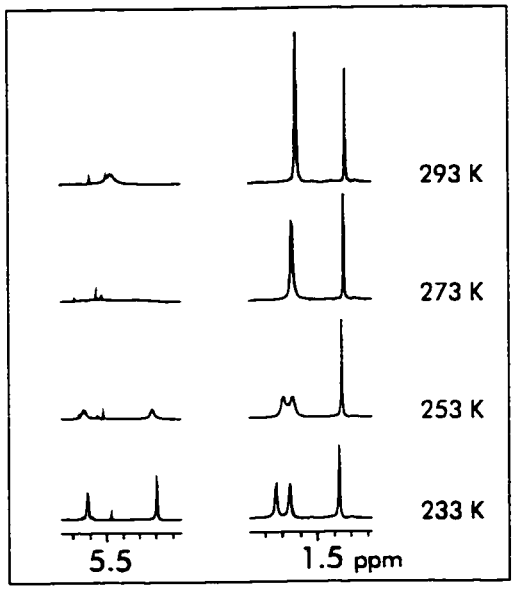

Figure 3.13 Variable temperature ^{1}H NMR spectrum for **112**.

The dynamic process which results in a single cyclopentadienyl ring environment at room temperature must therefore involve facile inversion at phosphorus in addition to rapid rotation about the Zr-E bond (Eq. 3.1).

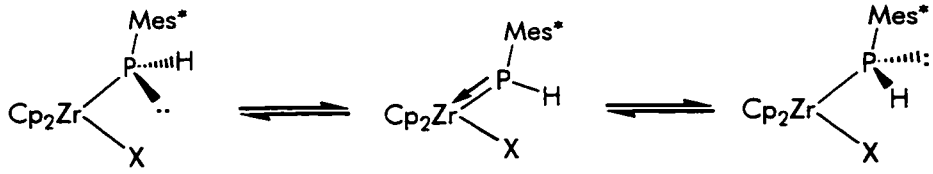

(3.1)

Related metal mediated epimerization of transition metal phosphide complexes,[66-72] as well as rotational barriers about early metal π-bonds to amide,[73,74] alkoxide[75] and thiolate[46b] ligands, have been studied both experimentally and via computational studies. The barriers for the dynamic processes observed herein are consistent with those previously reported for transition metal mediated phosphorus inversion. They are significantly lower than the barrier to inversion for organophosphines.[76] Zr-P π-bonding accounts for this reduction in the energy barrier and is accomplished by alignment of the phosphorus *p* orbital with the LUMO or $1a_1$ orbital of the Cp_2M fragment.[77] This orbital is oriented in the plane which lies between the cyclopentadienyl ligands, hence in the plane of the ancillary donor atoms (Fig. 3.14).

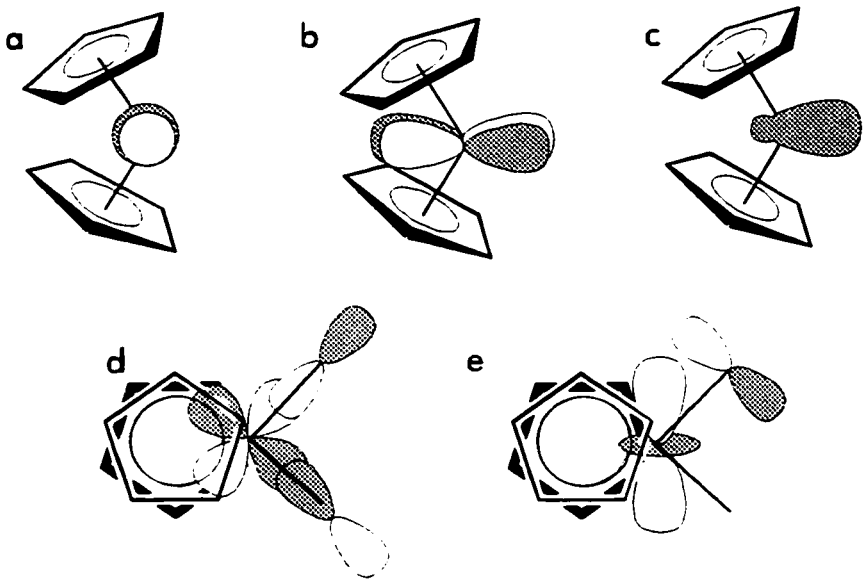

Figure 3.14 Schematic depiction of the (a) $1a_1$ (b) b_2 and (c) $2a_1$ orbitals of the Cp_2M fragment. (d) σ-interaction of the ligand σ orbitals with the b_2 orbital (e) π-interaction of the ligand π orbital with the $1a_1$ orbital.

A degree of M-E π-bonding is a feature common to early metal complexes of the form Cp_2MX_2 (M = Ti, Zr, Hf; X = OR, SR, NHR, PHR).[46] Perhaps one of the most striking examples of such π-bonding is the structural study of $Cp_2Hf(PEt_2)_2$ **116** by Baker *et al.*[66] This species contains both pyramidal and planar phosphorus atoms consistent with the attainment of an eighteen electron configuration at hafnium through a Hf-P π-bond. The diphosphide complexes **113-115** are comparable to **116** as the disparate

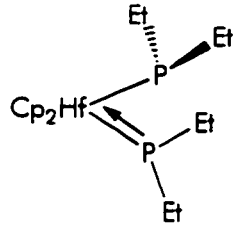

116

nature of the ^{31}P NMR resonances reflects the pyramidal and planar geometries at the phosphorus atoms in these species. This observation at room temperature as well as low temperatures is credited to the steric demands of **113-115**. In contrast, the reduced steric demands of $Cp_2Zr(PEt_2)_2$ or $Cp_2Zr(PCy_2)_2$ do not allow for the observation of the

limiting spectrum, even at low temperatures. The presence of the dative Zr-P bond in **113-115** reflects the Lewis acidity of the zirconium centre, which achieves a formal eighteen electron count. The P-H coupling of 292 Hz associated with the low field resonance in compound **115** indicates that it is the supermesityl phosphide ligand that participates in π-bonding. However, NOE experiments designed to probe this question for **113** and **114** were inconclusive.

As mentioned above, the ^{31}P NMR shift of the phosphide ligand can be used as an indicator of its geometry, thus reflecting the π-donor ability of the other ancillary ligand, E. Better π-donors increase the pyramidalization of the phosphide ligand due to competition for the $1a_1$ orbital of the Cp_2M fragment. Consequently, increased *s* character in the hybridization of phosphorus results in a shielding effect; the reverse is true at the E ligand. Diphosphide complexes such as **116** and **113-115** allow for the observation of both influences via ^{31}P NMR spectroscopy. The NMR data for mixed ligand systems **72** and **110-112** suggest the presence of pyramidal phosphide ligands in which the amount of *s* character can be correlated to the π-donor ability of E. Compound **112** exhibits a relatively high field ^{31}P NMR resonance, and Zr-N π-bonding is confirmed by the crystallographic data (*vide supra*). Similarly, the ^{31}P NMR data for **110** also implies a pyramidal geometry for the phosphide ligand. Although unconfirmed, Zr-O π-bonding is believed to occur in **110**, as supported by structural studies of complexes of the form $Cp_2Zr(OR)_2$.[46] In contrast, the inability of the methyl group in **72** to compete for the $1a_1$ orbital results in a considerably more deshielded phosphorus centre. **111** is an unusual compound in which E (sulfur) has the capability to compete for the $1a_1$ orbital; however the poorer π-donor ability of sulfur relative to oxygen or nitrogen allow the phosphorus lone pair to be a contender for the orbital. The result is far less pyramidalization of the phosphorus centre, thus the ^{31}P NMR signal appears at 64.4 ppm. Although a number of factors (such as sterics) have an effect on the chemical shift, the above argument is reasonable in terms of accounting for

the disparity between the chemical shifts of **72** and **111** as compared to those of **110** and **112-115**.

The $\Delta G_c^{\ddagger}$ values obtained through variable temperature NMR studies are all within the accepted range for metal-assisted inversion at phosphorus. Since the π-donor ability of E affects the ^{31}P NMR chemical shift, this property must also influence the $\Delta G_c^{\ddagger}$ value for inversion at the phosphide ligand. The trend is demonstrated by the higher inversion barriers for **110** and **112**, lower barriers for diphosphides **113-115**, and finally the lowest barrier that is realized for **72**. In the preceding discussion, it was maintained that the thiolate ligand in **111** is a poor π-donor relative to nitrogen or oxygen. While this may be true, the higher barrier to phosphorus inversion for this complex implies that other factors are significant in their influence over the $\Delta G_c^{\ddagger}$ values. In all cases, a steric element substantially affects both chemical shift and inversion barrier. Most likely this is due to the exceptionally bulky supermesityl group that is present in each of these compounds. In comparison, the steric inhibition in $Cp_2Hf(PCy_2)_2$[66] and $Cp^*_2HfH(NHR)$[73] is substantially reduced, and the barriers to inversion and rotation about the Hf-P and Hf-N bonds are diminished to 6 and 10 kcal mol^{-1} respectively.

3.4 Conclusion

The terminal phosphinidene species **84** has proven to be considerably reactive. A variety of organic reagents, as well as some of their lower congeners, participate in reactions with **84**, which acts as a source of the phosphinidene moiety. This group may be exchanged for an oxo, sulfido or two chloride groups, resulting in the formation of an assortment of organophosphorus derivatives and the corresponding zirconocene oxide, sulfide or dichloride. Similar reactions of **84** with C-N multiple bonds effect phosphinidene transfer to carbon. The Zr-P double bond of **84** also readily undergoes 1,2-addition reactions of polar E-H bonds to afford the facile synthesis of complexes of

the form $Cp_2Zr(PHMes^*)(ER)$ and $Cp_2Zr(PHMes^*)(EHR)$. Variable temperature NMR studies reveal that although metal-mediated inversion of pyramidal phosphide ligands occurs rapidly at room temperature, this process can be stopped upon cooling. Zr-E π-interactions are generally weak, yet they have an influence over both the ^{31}P NMR chemical shift and the inversion barrier of the phosphide ligand.

Chapter Four
Synthesis and Reactivity of Phosphametallacyclobutenes: Sterically Induced Epimerizations and Retrocycloadditions

4.1 Introduction

The [2+2] cycloaddition reaction with alkynes is one of the established reactivity patterns within the realm of metal-ligand multiple bonds.[3] This transformation has frequently occurred with Fischer carbenes;[3,78] however, relatively few examples are known for Schrock alkylidenes[3,5,9] and their multiply bonded heteroatomic counterparts.[11,15,19,23,24] Nonetheless, this reaction has been applied to group 4 metal alkylidenes, imides, oxides and sulfides alike to yield metallacyclobutenes. Conspicuous in its absence is the phosphametallacyclobutene, which has been neglected simply due to the lack of terminal phosphinidenes.

The Zr=P multiple bond of **84** or of the transient intermediate [Cp_2Zr=PMes*] has been used in [2+2] cycloaddition reactions with alkynes to produce the first phosphametallacyclobutenes. Reactivity studies reflect the inherently reactive nature of the Zr-P single bond, a trait which is epitomized by the studies described in Chapter Two, as well as previous studies of zirconium phosphides in our laboratories.[35] Various insertion reactions of the phosphametallacyclobutenes have extended the family of metallacycles to include five-, six- and seven-membered rings. Steric factors exercise enormous influence over these complexes, such that they induce both epimerization at the phosphorus centre as well as [4+2] retrocycloadditions. This chapter relates the synthesis, reactivity studies and dynamic behaviour of these intriguing species.

4.2 Experimental

General Data All preparations, ^{1}H, $^{13}C\{^{1}H\}$, ^{31}P and $^{31}P\{^{1}H\}$ NMR spectroscopy, mass spectrometry and combustion analyses were carried out under conditions similar to those described in Section 2.2.

Synthesis of $Cp_2\overline{Zr(P(Mes^*)C(Ph)=CPh)}$ 117 and $Cp_2\overline{Zr(P(Mes^*)C(Me)=CPh)}$ 118 The preparations of **117** and **118** were performed in a similar manner, thus only one procedure is described in detail. To a benzene solution of $Cp_2ZrMeCl$ (272 mg, 1.0 mmol) and diphenylacetylene (178 mg, 1.0 mmol) was added a benzene solution of LiHPMes*•3THF (501 mg, 1.0 mmol). The reaction mixture stood for 3 days after which time the dark red-brown solution was filtered and the solvent removed in vacuo. The oily residue was dissolved in diethyl ether and the solvent was again evaporated under reduced pressure to yield a flaky red-gold solid. **117**: Yield: 588 mg (87%). ^{1}H NMR (25 °C, C_6D_6): δ 7.64 (d, $|J|$ = 7.2 Hz, 2H, Ar-*H*), 7.51 (d, $|J|$ = 2.3 Hz, 2H, Ph-*H*), 7.08-6.57 (m, 8H, Ph-*H*), 5.74 (s, 10H, Cp), 1.54 (s, 18H, *o*-^{t}Bu), 1.40 (s, 9H, *p*-^{t}Bu). $^{13}C\{^{1}H\}$ NMR (25 °C, C_6D_6): δ 210.6 (d, $|J|$ = 15.1 Hz, quat), 152.3 (s, quat), 151.4 (d, $|J|$ = 7.1 Hz, quat), 150.9 (s, quat), 149.2 (s, quat), 143.7 (s, quat), 141.1 (d, $|J|$ = 43.8 Hz, quat), 131.0 (s, arom. *C*-H), 128.1 (s, arom. *C*-H), 127.4 (s, arom. *C*-H), 125.6 (s, arom. *C*-H), 125.5 (s, arom. *C*-H), 123.8 (s, arom. *C*-H), 120.9 (s, arom. *C*-H), 112.4 (s, Cp), 38.0 (s, *o*-$C(CH_3)_3$), 34.7 (s, *p*-$C(CH_3)_3$), 33.4 (d, $|^{4}J_{PC}|$ = 7.9 Hz, *o*-$C(CH_3)_3$), 31.3 (s, *p*-$C(CH_3)_3$). ^{31}P NMR (25 °C, C_6D_6): δ 55.3 (s). HRMS (EI) *m/e* Calcd for $C_{42}H_{49}PZr$: 674.2615; *m/e* Found: 674.2605. **118:** Yield: 418 mg 68%. ^{1}H NMR (25 °C, C_6D_6): δ 7.52 (s, 2H, Ar-*H*), 7.28 - 6.94 (m, 5H, Ph-*H*), 5.73 (s, 10H, Cp), 2.17 (d, $|^{3}J_{PH}|$ = 5.6 Hz, 3H, CH_3), 1.67 (s, 18H, *o*-^{t}Bu), 1.36 (s, 9H, *p*-^{t}Bu). $^{13}C\{^{1}H\}$ NMR (25 °C, C_6D_6): δ 207.0 (d, $|J|$ = 14.5 Hz, quat), 152.5 (d, $|J|$ = 6.8 Hz, quat), 148.9 (s, quat), 148.0 (s, quat), 145.3 (s, quat), 128.3 (s, arom. *C*-H), 125.3 (s, arom. *C*-H), 124.1 (s, arom. *C*-H), 121.0 (s, arom. *C*-H), 111.3 (s, Cp), 38.3 (s, *o*-$C(CH_3)_3$), 34.4 (s, *p*-$C(CH_3)_3$), 33.2 (d, $|^{4}J_{PC}|$ = 8.5 Hz, *o*-$C(CH_3)_3$), 31.3 (s, *p*-$C(CH_3)_3$), 22.4 (d, $|^{2}J_{PC}|$

= 16.9 Hz, CH_3). ^{31}P NMR (25 °C, C_6D_6): δ 70.1 (s). HRMS (EI) *m/e* Calcd for $C_{37}H_{47}PZr$: 612.2458; *m/e* Found: 612.2450.

Synthesis of $Cp_2\overline{Zr(P(Mes^*)C(H)=CPh)}$ 119

To a benzene solution of **84** (115 mg, 0.2 mmol) was added a benzene solution of phenylacetylene (22.0 μL, 0.2 mmol). The reaction mixture stood for 3 hours after which time the dark brown solution was filtered and the solvent removed in vacuo. The oily residue was dissolved in pentane and the volume was reduced under vacuum. Small red-brown crystals precipitated upon standing overnight, and were isolated by filtration. Yield: 107 mg (89%). ^1H NMR (25 °C, C_6D_6): δ 7.61 (d, $|^2J_{P\text{-}H}|$ = 5.4 Hz, 1H, =C-*H*), 7.39 (d, $|^2J_{P\text{-}H}|$ = 2.2 Hz, 2H, Ar-*H*), 7.35-7.27 (m, 5H, Ph-*H*), 5.60 (s, 10H, Cp), 1.71 (s, 18H, *o*-^{t}Bu), 1.31 (s, 9H, *p*-^{t}Bu). $^{13}C\{^1H\}$ NMR (25 °C, C_6D_6): δ 215.0 (d, $|J|$ = 11.6 Hz, quat), 150.9 (d, $|J|$ = 6.2 Hz, quat), 147.6 (s, quat), 146.5 (s, quat), 144.2 (d, $|J|$ = 20.0 Hz, quat), 128.6 (s, arom. *C*-H), 127.9 (s, arom. *C*-H), 127.2 (s, arom. *C*-H), 120.8 (s, arom. C-H), 110.0 (s, Cp), 104.5 (d, $|J|$ = 74.5 Hz, P-CH), 38.1 (s, *o*-$C(CH_3)_3$), 34.2 (s, *p*-$C(CH_3)_3$), 33.1 (d, $|^4J_{PC}|$ = 8.5 Hz, *o*-$C(CH_3)_3$), 31.2 (s, *p*-$C(CH_3)_3$). ^{31}P NMR (25 °C, C_6D_6): δ 85.0 (s).

Synthesis of $Cp_2Zr(C{\equiv}CPh)(C(Ph){=}C(Ph)PHMes^*)$ 120

To a benzene solution of **117** (135 mg, 0.2 mmol) was added phenylacetylene (22.0 μL, 0.2 mmol). The reaction mixture stood for 30 min., after which time the solvent was removed in vacuo and the product dissolved in hexane. Upon standing 12 h a brown microcrystalline solid precipitated which was isolated by filtration. Yield: 134 mg (86%). ^1H NMR (25 °C, C_6D_6): δ 7.50-7.43 (m, 3H, Ph-*H*), 7.10-6.48 (m, 14H, Ph-*H*), 6.78 (d, $|J_{P\text{-}H}|$ = 301.6 Hz, 1H, P-*H*), 6.22 (s, 5H, Cp), 5.90 (s, 5H, Cp), 1.68 (s, 9H, *o*-^{t}Bu), 1.62 (s, 9H, *o*-^{t}Bu), 1.19 (s, 9H, *p*-^{t}Bu). $^{13}C\{^1H\}$ NMR (25 °C, C_6D_6): δ 203.4 (s, quat), 202.9 (s, quat), 157.9 (s, quat), 156.0 (d, $|J|$ = 9.4 Hz, quat), 152.1 (s, quat), 151.5 (s, quat), 150.6 (s, quat), 149.8 (s, quat), 149.5 (s, quat), 138.7 (s, quat), 134.1 (d, $|J|$ = 21.6 Hz, quat), 130.8 (d, $|J|$

= 21.6 Hz, quat), 128.5 (s, arom. *C*-H), 128.0 (s, arom. *C*-H), 127.8 (s, arom. *C*-H), 127.0 (s, arom. *C*-H), 125.6 (s, arom. *C*-H), 125.4 (s, arom. *C*-H), 125.0 (s, arom. *C*-H), 123.9 (s, arom. *C*-H), 122.4 (br s, arom. *C*-H), 122.3 (br s, arom. *C*-H), 108.6 (s, Cp), 108.5 (s, Cp), 38.2 (s, *o*-$C(CH_3)_3$), 37.9 (s, *o*-$C(CH_3)_3$), 34.5 (s, *p*-$C(CH_3)_3$), 33.9 (s, *o*-$C(CH_3)_3$), 33.1 (d, $|J|$ = 4.1 Hz, *o*-$C(CH_3)_3$), 31.2 (s, *p*-$C(CH_3)_3$). ^{31}P NMR (25 °C, C_6D_6): δ -84.3 (d, $|J_{P-H}|$ = 300.9 Hz).

Synthesis of $Cp_2\overline{Zr(P(Mes)P(Mes)C(Ph)=CPh)}$ 122

To a benzene solution of $Cp_2ZrMeCl$ (272 mg, 1.0 mmol) and diphenylacetylene (178 mg, 1.0 mmol) was added a benzene solution of LiHPMes•2THF (302 mg, 1.0 mmol). The reaction mixture stood for 2 days after which time the deep blue-green solution was filtered and the volume of the solution was reduced under vacuum. Hexamethyldisiloxane (ca. 6 mL) was added and the solution was allowed to stand for one week. Dark wine-red crystals were isolated by filtration and washed on the frit with hexane. Yield: 133 mg (19%). ^1H NMR (25 °C, C_6D_6): δ 7.47 (br d, $|J|$ = 1.8 Hz, 2H, Ph-*H*), 7.08-7.03 (m, 4H, Ph-*H*), 6.92-6.86 (m, 3H, Ph-*H*), 6.80-6.75 (m, 1H, Ph-*H*), 6.62-6.58 (m, 4H, Ph-*H*), 5.75 (v br s, 10H, Cp), 2.73 (s, 6H, *o*-Me), 2.68 (br s, 6H, *o*-Me), 2.22 (s, 3H, *p*-Me), 1.91 (s, 3H, *p*-Me). $^{13}C\{^1H\}$ NMR (25 °C, C_6D_6): δ 199.3 (dd, $|J|$ = 28.5 Hz, $|J|$ = 4.1 Hz, quat), 152.9 (d, $|J|$ = 7.3 Hz, quat), 149.5 (s, quat), 143.5 (s, quat), 143.0 (s, quat), 141.8 (dd, $|J|$ = 13.3 Hz, $|J|$ = 7.2 Hz, quat), 141.5 (dd, $|J|$ = 42.8 Hz, $|J|$ = 19.8 Hz, quat), 138.6 (s, quat), 135.6 (s, quat), 133.8 (dd, $|J|$ = 26.3 Hz, $|J|$ = 14.5 Hz, quat), 130.8 (d, $|J|$ = 12.8 Hz, arom. *C*-H), 129.7 (br d, $|J|$ = 12.0 Hz, arom. *C*-H), 128.1 (s, arom. *C*-H), 127.7 (s, arom. *C*-H), 127.4 (s, arom. *C*-H), 126.9 (br s, arom. *C*-H), 126.2 (s, arom. *C*-H), 123.2 (s, arom. *C*-H), 110.5 (br s, Cp), 24.4 (d, $|J|$ = 9.7 Hz, *o*-Me), 24.1 (d, $|J|$ = 9.5 Hz, *o*-Me), 20.8 (s, *p*-Me), 20.5 (s, *p*-Me). ^{31}P NMR (25 °C, C_6D_6): δ 60.4 (d, $|J_{P-P}|$ = 349.8 Hz), -96.2 (d, $|J_{P-P}|$ = 349.8 Hz). ^1H NMR (-80 °C, $CD_3C_6D_5$): δ 7.20-6.49 (m, 14H, Mes-*H* and Ph-*H*), 5.88 (s, 5H, Cp), 5.29 (s, 5H, Cp), 2.86 (s, 3H, Me), 2.80 (s, 3H, Me),

2.58 (s, 3H, Me), 2.23 (s, 3H, Me), 2.11 (s, 3H, Me), 1.95 (s, 3H, Me). ^{31}P NMR (-80 °C, $CD_3C_6D_5$): δ 54.1 (d, $|J_{P\text{-}P}|$ = 348.9 Hz), -101.2 (d, $|J_{P\text{-}P}|$ = 348.9 Hz). Anal. Calcd for $C_{42}H_{42}P_2Zr$: C: 72.07; H: 6.05; Found: C: 72.33; H: 5.82.

Synthesis of $Cp_2\overline{Zr(P(Mes)C(Ph)=CPh)}$ 123

To a benzene suspension of $(Cp_2ZrCl)_2(\mu\text{-PMes})$ **80** (199 mg, 0.3 mmol) was added a benzene solution of diphenylacetylene (107 mg, 0.6 mmol) and a benzene suspension of Li_2PMes (54 mg, 0.33 mmol). The mixture was stirred vigorously for 2 days, after which time it was filtered. The solvent was removed in vacuo and the forest-green product dissolved in diethyl ether. Reduction of the volume resulted in the precipitation of a deep green microcrystalline solid which was isolated by filtration. Yield 267 mg (81%). ^{1}H NMR (25 °C, C_6D_6): δ 7.66 (d, $|J|$ = 8.0 H, 2H, Ph-*H*), 7.13-6.69 (m, 10H, Ph-*H*), 5.83 (s, 10H, Cp), 2.28 (s, 6H, *o*-Me), 2.19 (s, 3H, *p*-Me). $^{13}C\{^1H\}$ NMR (25 °C, C_6D_6): δ 206.2 (d, $|J|$ = 17.0 Hz, quat), 148.9 (d, $|J|$ = 4.9 Hz, quat), 140.4 (d, $|J|$ = 12.1 Hz, quat), 137.9 (d, $|J|$ = 12.2 Hz, quat), 135.5 (s, quat), 131.4 (d, $|J|$ = 50.9 Hz, quat), 131.3 (d, $|J|$ = 8.9 Hz, arom. *C*-H), 129.4 (s, arom. *C*-H), 128.1 (s, arom. *C*-H), 127.7 (s, arom. *C*-H), 126.0 (s, arom. *C*-H), 125.6 (s, arom. *C*-H), 123.7 (s, arom. *C*-H), 113.0 (s, Cp), 24.2 (s, Me), 23.9 (s, Me), 20.5 (s, Me). ^{31}P NMR (25 °C, C_6D_6): δ 31.4 (s).

Synthesis of $Cp_2\overline{Zr(C(=N\text{-}t\text{-}Bu)P(Mes^*)C(Ph)=CPh)}$ 126, $Cp_2\overline{Zr(OCMe_2P(Mes^*)C(Ph)=CPh)}$ 127, $Cp_2\overline{Zr(O(c\text{-}C_6H_{11})P(Mes^*)C(Ph)=CPh)}$ 128, $Cp_2\overline{Zr(N=C(Ph)P(Mes^*)C(Ph)=CPh)}$ 129, $Cp_2\overline{Zr(OCHPhP(Mes^*)C(Ph)=CPh)}$ 130 and $Cp_2\overline{Zr(OCH_2CHPhP(Mes^*)C(Ph)=CPh)}$ 131

The reactions of **117** with *t*-butylisocyanide, acetone, cyclohexanone, benzonitrile, benzaldehyde and styrene oxide were all performed in a similar manner, thus only one preparation is described in detail. To a benzene solution of **117** (135 mg, 0.2 mmol) was added *t*-butylisocyanide (22.6 μL, 0.2 mmol). The reaction mixture stood for 30 min., after which time the solvent was removed in vacuo and the product dissolved in

pentane. Large yellow crystals formed over a 12 h period at room temperature and were isolated by filtration. **126**: Yield: 138 mg (91%). ^{1}H NMR (25 °C, C_6D_6): δ 7.52 (d, $|^{4}J_{P\text{-}H}|$ = 2.1 Hz, 2H, Ar-*H*), 7.14 - 6.68 (m, 10H, Ph-*H*), 5.65 (s, 10H, Cp), 1.64 (s, 18H, *o*-^{t}Bu), 1.23 (s, 9H, ^{t}Bu), 1.08 (s, 9H, ^{t}Bu). ^{13}C{^{1}H} NMR (25 °C, C_6D_6): δ 223.3 (d, $|J|$ = 43.6 Hz, quat), 198.5 (d, $|J|$ = 38.9 Hz, quat), 156.5 (s, quat), 156.3 (d, $|J|$ = 10.9 Hz, quat), 153.2 (d, $|J|$ = 50.5 Hz, quat), 151.2 (s, quat), 141.7 (d, $|J|$ = 32.0 Hz, quat), 132.2 (d, $|J|$ = 55.6 Hz, quat), 130.9 (s, arom. *C*-H), 127.3 (s, arom. *C*-H), 126.7 (s, arom. *C*-H), 126.5 (s, arom. *C*-H), 124.9 (s, arom. *C*-H) 123.9 (d, $|J|$ = 7.1 Hz, quat), 122.2 (s, arom. *C*-H), 106.3 (s, Cp), 61.5 (s, N-$C(CH_3)_3$), 39.3 (s, *o*-$C(CH_3)_3$), 34.7 (s, *p*-$C(CH_3)_3$), 34.4 (d, $|^{4}J|$ = 4.5 Hz, *o*-$C(CH_3)_3$), 31.0 (s, $C(CH_3)_3$), 29.8 (s, $C(CH_3)_3$). ^{31}P NMR (25 °C, C_6D_6): δ 17.8 (s). Anal. Calcd for $C_{47}H_{58}NPZr$: C: 74.36; H: 7.70; Found: C: 74.78; H: 7.47.

127: Yield: 75 mg (51%). ^{1}H NMR (25 °C, C_6D_6): δ 7.38 (s, 2H, Ar-*H*), 6.96 - 6.74 (m, 10H, Ph-*H*), 5.94 (br s, 10H, Cp), 1.72 (br s, 18H, *o*-^{t}Bu), 1.54 (br s, 3H, Me), 1.50 (br s, 3H, Me), 1.23 (s, 9H, *p*-^{t}Bu). ^{13}C{^{1}H} NMR (25 °C, C_6D_6): δ 191.0 (d, $|J|$ = 31.5 Hz, quat), 154.4 (br s, quat), 152.1 (d, $|J|$ = 7.0 Hz, quat), 150.4 (s, quat), 149.7 (s, quat), 143.0 (d, $|J|$ = 19.8 Hz, quat), 132.9 (d, $|J|$ = 65.4 Hz, quat), 131.7 (s, arom. *C*-H), 127.1 (s, arom. *C*-H), 126.0 (s, arom. *C*-H), 124.5 (s, arom. *C*-H), 122.4 (br s, arom. *C*-H) 121.4 (s, arom. *C*-H), 110.8 (br s, Cp), 88.4 (d, $|J|$ = 36.0 Hz, O-*C*), 39.8 (s, *o*-$C(CH_3)_3$), 39.7 (s, *o*-$C(CH_3)_3$), 35.2 (br s, *o*-$C(CH_3)_3$), 34.4 (s, *p*-$C(CH_3)_3$), 33.9 (s, Me), 33.8 (s, Me), 31.1 (s, *p*-$C(CH_3)_3$). ^{31}P NMR (25 °C, C_6D_6): δ 37.6 (s). ^{1}H NMR (-70 °C, $CD_3C_6D_5$, 200 MHz): δ 7.44 (br s, 2H, Ar-H), 7.20 - 6.60 (m, 10H, Ph-*H*), 6.10 (s, 5H, Cp), 5.79 (s, 5H, Cp), 1.86 (br s, 9H, *o*-^{t}Bu), 1.74 (br s, 9H, *o*-^{t}Bu), 1.27 (s, 9H, *p*-^{t}Bu). ^{31}P NMR (-80°C, $CD_3C_6D_5$): δ 36.1 (s). Anal. Calcd for $C_{45}H_{55}OPZr$: C: 73.62; H: 7.55; Found: C: 73.83; H: 7.68.

128: Yield: 90 mg (58%). ^{1}H NMR (25 °C, C_6D_6): δ 7.52 - 6.70 (m, 12H, Ar-*H* and Ph-*H*), 6.11 (br s, 5H, Cp), 5.86 (br s, 5H, Cp), 2.35 - 1.20 (m, 10H, Cy-*H*), 1.69 (br s, 18H, *o*-^{t}Bu), 1.23 (s, 9H, *p*-^{t}Bu). ^{13}C{^{1}H} NMR (25 °C, C_6D_6): δ 189.5 (d, $|J|$ = 29.0 Hz, quat), 152.3 (d, $|J|$ = 8.3 Hz, quat), 150.9 (s, quat), 150.3 (s, quat), 149.6 (s, quat), 143.5 (d, $|J|$ = 19.9 Hz,

quat), 132.0 (d, $|J|$ = 41.2 Hz, quat), 132.8 (s, arom. *C*-H), 126.8 (s, arom. *C*-H), 126.5 (s, arom. *C*-H), 125.2 (s, arom. *C*-H), 122.7 (s, arom. *C*-H), 111.4 (br s, Cp), 89.9 (d, $|J|$ = 31.2 Hz, O-*C*), 40.2 (s, *o*-$C(CH_3)_3$), 35.5 (br s, *o*-$C(CH_3)_3$), 34.5 (s, *p*-$C(CH_3)_3$), 31.1 (s, *p*-$C(CH_3)_3$), 25.6 (s, CH_2), 22.7 (s, CH_2), 22.5(d, $|J|$ = 8.4 Hz, CH_2). ^{31}P NMR (25 °C, C_6D_6): δ 37.4 (s). ^1H NMR (-80 °C, $CD_3C_6D_5$, 200 MHz): δ 7.79 - 6.65 (m, 12H, Ar-H and Ph-H), 6.17 (s, 5H, Cp), 5.67 (s, 5H, Cp), 1.95 and 1.64 (v br, 18H, *o*-^{t}Bu), 1.28 (s, 9H, *p*-^{t}Bu). ^{31}P NMR (-80 °C, $CD_3C_6D_5$): δ 31.6 (s). Anal. Calcd for $C_{48}H_{59}OPZr$: C: 74.47; H: 7.68; Found: C: 74.88; H: 7.41.

129: Yield: 72 mg (46%). ^1H NMR (25 °C, C_6D_6): δ 7.60 (d, $|^4J_{P\text{-}H}|$ = 2.2 Hz, 2H, Ar-*H*), 7.45 - 6.70 (m, 15H, Ph-*H*), 5.89 (br s, 10H, Cp), 1.62 (br s, 18H, *o*-^{t}Bu), 1.24 (s, 9H, *p*-^{t}Bu). $^{13}C\{^1H\}$ NMR (25 °C, C_6D_6): δ 198.3 (d, $|J|$ = 31.2 Hz, quat), 180.3 (d, $|J|$ = 36.4 Hz, quat), 153.6 (d, $|J|$ = 13.3 Hz, quat), 151.7 (s, quat), 145.8 (d, $|J|$ = 6.5 Hz, quat), 142.7 (d, $|J|$ = 22.3 Hz, quat), 138.0 (d, $|J|$ = 42.5 Hz, quat), 131.7 (s, arom. *C*-H), 129.4 (s, arom. *C*-H), 128.6 (s, arom. *C*-H), 126.9 (s, arom. *C*-H), 126.5 (s, arom. *C*-H) 125.2 (s, arom. *C*-H), 122.3 (s, arom. *C*-H), 109.0 (br s, Cp), 40.4 (br s, *o*-$C(CH_3)_3$), 34.8 (s, *p*-$C(CH_3)_3$), 34.4 (br s, *o*-$C(CH_3)_3$), 31.0 (s, *p*-$C(CH_3)_3$). ^{31}P NMR (25 °C, C_6D_6): δ 21.3 (s). ^1H NMR (-60 °C, $CD_3C_6D_5$, 200 MHz): δ 7.36 - 6.66 (m, 17H, Ar-*H* and Ph-*H*), 6.05 (s, 5H, Cp), 5.60 (s, 5H, Cp), 1.64 (br s, 9H, *o*-^{t}Bu), 1.57 (br s, 9H, *o*-^{t}Bu), 1.29 (s, 9H, *p*-^{t}Bu). ^{31}P NMR (-60 °C, $CD_3C_6D_5$): δ 21.5 (s). Anal. Calcd for $C_{49}H_{54}NPZr$: C: 75.53; H: 6.99; Found: C: 75.19; H: 6.75.

130: Yield: 95 mg (61%). ^1H NMR (25 °C, C_6D_6): δ 7.81 (d, $|J|$ = 1.9 Hz, 1H, C-*H*), 7.40 - 6.66 (m, 17H, Ph-*H* and Ar-*H*), 6.45 (s, 5H, Cp), 5.73 (s, 5H, Cp), 2.06 (s, 9H, ^{t}Bu), 1.28 (s, 9H, ^{t}Bu), 1.10 (s, 9H, ^{t}Bu). $^{13}C\{^1H\}$ NMR (25 °C, C_6D_6): δ 188.3 (d, $|J|$ = 33.9 Hz, quat), 160.3 (s, quat), 159.9 (s, quat), 155.6 (d, $|J|$ = 5.3 Hz, quat), 152.3 (d, $|J|$ = 9.6 Hz, quat), 150.5 (d, $|J|$ = 48.2 Hz, quat), 150.4 (s, quat), 144.4 (d, $|J|$ = 24.3 Hz, quat), 143.5 (d, $|J|$ = 14.8 Hz, quat), 132.9 (s, arom. *C*-H), 131.4 (s, arom. *C*-H), 126.3 (s, arom. *C*-H), 125.6 (s, arom. *C*-H), 125.2 (s, arom. *C*-H), 123.0 (s, arom. *C*-H) 122.8 (s, arom. *C*-H), 112.7 (s, Cp),

112.1 (s, Cp), 89.0 (d, $|J_{P\text{-}C}|$ = 16.6 Hz, O-CH), 41.1 (s, *o*-$C(CH_3)_3$), 39.2 (d, $|^3J_{P\text{-}C}|$ = 6.9 Hz, *o*-$C(CH_3)_3$), 36.5 (s, *o*-$C(CH_3)_3$), 34.6 (s, *p*-$C(CH_3)_3$), 33.3 (d, $|^4J_{P\text{-}C}|$ = 18.1 Hz, *o*-$C(CH_3)_3$), 31.1 (s, *p*-$C(CH_3)_3$). ^{31}P NMR (25 °C, C_6D_6): δ 13.9 (s). Anal. Calcd for $C_{49}H_{55}OPZr$: C: 75.24; H: 7.09; Found: C: 75.10; H: 7.14.

131: Yield: 108 mg (68%). ^{1}H NMR (25 °C, C_6D_6): δ 7.56 (dd, $|J|$ = 5.2 Hz, $|J|$ = 1.9 Hz, 1H, C-*H*), 7.33 (d, $|^4J_{P\text{-}H}|$ = 2.0 Hz, 2H, Ar-*H*), 7.11 - 6.53 (m, 15H, Ph-*H*), 6.21 (s, 5H, Cp), 5.85 (s, 5H, Cp), 1.99 (s, 9H, ^{t}Bu), 1.32 (s, 9H, ^{t}Bu), 1.10 (s, 9H, ^{t}Bu). ^{13}C{^{1}H} NMR (25 °C, C_6D_6): δ 192.6 (d, $|J|$ = 53.3 Hz, quat), 157.4 (d, $|J|$ = 35.3 Hz, quat), 156.6 (s, quat), 156.0 (d, $|J|$ = 42.0 Hz, quat), 151.9 (d, $|J|$ = 16.8 Hz, quat), 150.0 (s, quat), 144.5 (d, $|J|$ = 7.8 Hz, quat), 141.4 (s, quat), 131.7 (s, arom. *C*-H), 130.5 (s, arom. *C*-H), 129.9 (d, $|J|$ = 41.4 Hz, quat), 126.6 (s, arom. *C*-H), 125.8 (s, arom. *C*-H), 125.7 (s, arom. *C*-H) 124.2 (s, arom. C-H), 122.7 (d, $|J|$ = 14.3 Hz, arom. *C*-H), 122.4 (s, arom. *C*-H), 112.1 (s, Cp), 112.0 (s, Cp), 80.9 (d, $|^2J_{P\text{-}C}|$ = 24.6 Hz, O-CH_2), 59.6 (d, $|J_{P\text{-}C}|$ = 41.1 Hz, CH), 40.4 (d, $|^3J_{P\text{-}C}|$ = 7.6 Hz, *o*-$C(CH_3)_3$), 40.0 (s, *o*-$C(CH_3)_3$), 34.8 (d, $|^4J_{P\text{-}C}|$ = 18.1 Hz, *o*-$C(CH_3)_3$), 34.6 (s, *p*-$C(CH_3)_3$), 34.4 (s, *o*-$C(CH_3)_3$), 31.1 (s, *p*-$C(CH_3)_3$). ^{31}P NMR (25 °C, C_6D_6): δ -2.4 (d, $|J|$ = 13.9 Hz). Anal. Calcd for $C_{50}H_{57}OPZr$: C: 75.43; H: 7.22; Found: C: 75.86; H: 7.16.

X-Ray Structure Determinations of 122, 126, 127, 128, 130 and 131.

The phenyl rings in **130** were refined with a constrained geometry in order to maintain a statistically meaningful data:variable ratio, and the correct enantiomorph was confirmed by inversion and refinement of the model. The final values of R, R_w and the maximum Δ/σ on any of the parameters in the final cycle of refinement are given in Tables 4.1 and 4.2. ORTEP drawings of **122, 126, 127, 128, 130** and **131** are shown in Figures 4.2, 4.4, and 4.6 - 4.9 respectively, with 30% thermal ellipsoids. Selected bond distances and angles are listed in the captions for Figures 4.2, 4.4, and 4.6 - 4.9. Other structural parameters are given in Tables A3.1-A3.18 in Appendix Three.

Table 4.1: Crystallographic Parameters for 122, 126 and 127

	122	126	127
Formula	$C_{42}H_{42}P_2Zr$	$C_{47}H_{58}NPZr$	$C_{45}H_{55}OPZr$
Formula weight	699.96	759.18	734.12
Cryst Colour, Form	wine-red blocks	yellow blocks	orange blocks
a(Å)	16.61(1)	11.326(4)	13.26(1)
b(Å)	10.018(9)	21.129(6)	15.414(6)
c(Å)	21.215(5)	10.256(4)	11.085(8)
α(deg)		90.08(3)	101.75(5)
β(deg)	93.60(4)	112.37(2)	112.10(5)
γ(deg)		93.70(3)	94.96(5)
Crystal System	monoclinic	triclinic	triclinic
Space group	$P2_1/n$	$P\bar{1}$	$P\bar{1}$
Vol(Å^3)	3522(4)	2263(1)	2021(2)
D_{calcd} (gcm^{-3})	1.32	1.11	1.21
Z	4	2	2
Abs coeff, μ, cm^{-1}	4.31	3.07	3.42
Temp (°C)	24	24	24
Scan speed, °/min	8 ($\theta/2\theta$) (1-3 scans)	16 ($\theta/2\theta$) (1-3 scans)	16 ($\theta/2\theta$) (1-3 scans)
Scan range (deg)	1.0 above $K\alpha_1$, 1.0 below $K\alpha_2$	1.0 above $K\alpha_1$, 1.0 below $K\alpha_2$	1.0 above $K\alpha_1$, 1.0 below $K\alpha_2$
Bkgd/scan ratio	0.5	0.5	0.5
Data collected	6584	7977	7463
2θ range (deg)	4.5-50.0	4.5-50.0	4.5-50.0
Index range	$h,k,\pm l$	$\pm h,\pm k,l$	$\pm h,\pm k,l$
Data $F_o^2 > 3\sigma(F_o^2)$	1015	4051	2495
Variables	196	451	208
Transmission factors	0.936-1.000	0.936-1.000	0.848-1.058
R (%)[a]	7.7	6.3	8.0
Rw (%) [a]	6.4	6.2	6.7
Largest Δ/σ	0.00	0.02	0.00
Goodness of fit	1.72	1.87	1.78

[a] $R = \Sigma \| \|F_o\| - \|F_c\| \| / \Sigma |F_o|$, $Rw = [\Sigma(|F_o| - |F_c|)^2 / \Sigma |F_o|^2]^{0.5}$

Table 4.2: Crystallographic Parameters for 128, 130 and 131

	128	130	131
Formula	$C_{48}H_{59}OPZr$	$C_{49}H_{55}OPZr$	$C_{50}H_{57}OPZr$
Formula weight	774.19	782.17	796.19
Cryst Colour, Form	yellow blocks	yellow blocks	yellow blocks
a(Å)	13.939(2)	31.385(6)	9.944(4)
b(Å)	15.083(2)	16.316(4)	41.12(2)
c(Å)	11.157(3)	16.685(4)	10.974(2)
α(deg)	102.15(2)		
β(deg)	113.25(2)	95.86(2)	106.37(3)
γ(deg)	94.43(1)		
Crystal System	triclinic	monoclinic	monoclinic
Space group	$P\bar{1}$	Cc	$P2_1/c$
Vol(Å^3)	2073.0(9)	8620(2)	4305(2)
D_{calcd} (gcm^{-3})	1.24	1.21	1.23
Z	2	8	4
Abs coeff, μ, cm^{-1}	3.38	3.26	3.27
Temp (°C)	24	24	24
Scan speed, °/min	32 ($\theta/2\theta$) (1-3 scans)	8 ($\theta/2\theta$) (1-3 scans)	8 ($\theta/2\theta$) (1-3 scans)
Scan range (deg)	1.0 above $K\alpha_1$, 1.0 below $K\alpha_2$	1.0 above $K\alpha_1$, 1.0 below $K\alpha_2$	1.0 above $K\alpha_1$, 1.0 below $K\alpha_2$
Bkgd/scan ratio	0.5	0.5	0.5
Data collected	7299	4829	8171
2θ range (deg)	4.5-50.0	4.5-50.0	4.5-50.0
Index range	$\pm h, \pm k, l$	$\pm h, k, l$	$\pm h, k, l$
Data $F_o^2 > 3\sigma(F_o^2)$	3268	1540	2707
Variables	370	248	229
Transmission factors	0.901-1.040	0.955-1.000	0.731-1.000
R (%)[a]	6.3	7.8	9.5
Rw (%) [a]	5.2	6.3	7.6
Largest Δ/σ	0.08	0.00	0.01
Goodness of fit	1.48	1.53	2.34

[a] $R = \Sigma \| \|F_o\| - \|F_c\| \| / \Sigma |F_o|$, $Rw = [\Sigma(|F_o| - |F_c|)^2 | / \Sigma |F_o|^2]^{0.5}$

4.3 Results and Discussion

Synthesis of Phosphametallacycles

The reaction of terminal phosphinidene complex **84** with one equivalent of diphenylacetylene proceeded slowly. As the released trimethylphosphine was successively removed from solution under vacuum, a new singlet at 55.3 ppm was observed in the ^{31}P NMR spectrum. The ^{1}H and $^{13}C\{^{1}H\}$ NMR data supported the formulation of the product as phosphametallacyclobutene $Cp_2\overline{Zr(P(Mes^*)C(Ph)=CPh)}$ **117**, the product of a [2+2] cycloaddition between Zr=PMes* and PhC≡CPh. A more expeditious route to **117** parallels the synthesis of **84**. α elimination of methane from $Cp_2Zr(PMes^*H)Me$ **72** generated the transient terminal phosphinidene intermediate $[Cp_2Zr{=}PMes^*]$. In the presence of one equivalent of diphenylacetylene a [2+2] cycloaddition reaction provided an 87% yield of **117** (Eq. 4.1).

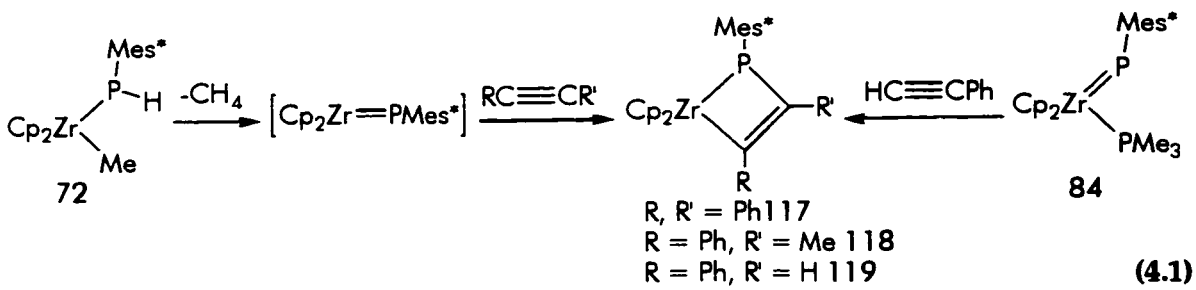

(4.1)

The use of 1-phenylpropyne as a trapping agent gave a 68% yield of $Cp_2\overline{Zr(P(Mes^*)C(Me)=CPh)}$ **118**; however, attempts to use phenylacetylene only resulted in the formation of product mixtures. Presumably, the terminal alkyne introduced the impediment of C-H bond metathesis reactions with **72**. Nonetheless, reaction of **84** with phenylacetylene proceeded much more rapidly than with other alkynes to cleanly furnish $Cp_2\overline{Zr(P(Mes^*)C(H)=CPh)}$ **119** (Eq. 4.1). It is noteworthy that reactions involving unsymmetrical alkynes are completely regioselective, strictly producing complexes in which the phenyl substituent is located α to the metal. These determinations were made based on P-C and P-H coupling constants in the ^{1}H and

$^{13}C\{^1H\}$ NMR spectra, and are consistent with the trend previously observed by Bergman *et al.* for zirconocene oxo, sulfido[11a-c, 15] and imido complexes.[19, 23, 24]

The reversible formation of metallacycles **117** and **118** was illustrated by the addition of trimethylphosphine to either complex, which rapidly resulted in the quantitative conversion to **84** along with the release of alkyne (Fig. 4.1). Similarly, addition of one equivalent of 1-phenylpropyne to **117** resulted in alkyne exchange to give an equilibrium mixture of **117** and **118** (K_{eq} = 1.1 at 25 °C). Comparable to related oxa-[11a-c, 15b] sulfa-[11b, c] and azametallacyclobutenes,[19, 23, 24b, c] these reactions are thought to occur through [2+2] retrocycloadditions to generate a transient [Cp_2Zr=PMes*] intermediate which then reacts with either PMe_3 or alkyne.

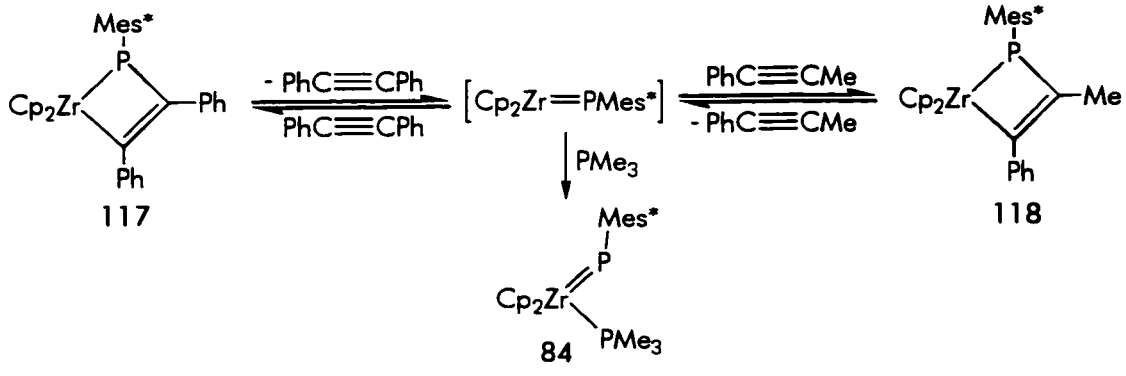

Figure 4.1 Reversibility of formation of metallacycles **117** and **118**.

Attempted exchange reactions of **117** with phenylacetylene did not produce metallacycle **119**, rather C-H bond activation across the Zr-P bond resulted in the formation of the zirconocene alkynyl alkenyl complex $Cp_2Zr(C{\equiv}CPh)(CPh{=}C(Ph)PHMes^*)$ **120**, isolated in 86% yield (Eq. 4.2).

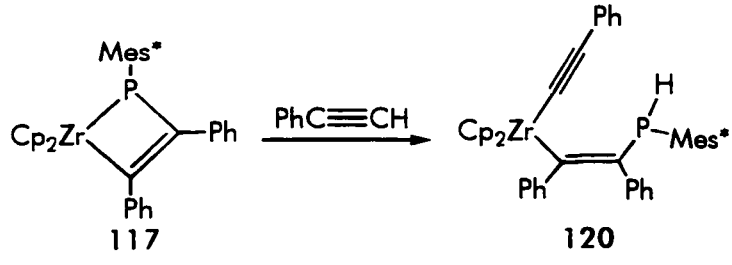

(4.2)

The secondary phosphine moiety in **120** was indicated by the ^{31}P NMR signal at -84.9 ppm with a one-bond P-H coupling constant of 300.9 Hz. Furthermore, signals at 203.4 and 202.9 ppm in the $^{13}C\{^1H\}$ NMR spectrum testified to the presence of two quaternary carbons bound to zirconium. **120** is analogous to $Cp_2Zr(C{\equiv}CPh)(C(Ph){=}C(H)P(SiMe_3)_2)$ **121**, which has recently been prepared by Hey-Hawkins *et al.* via insertion of phenylacetylene into the Zr-P bond of $Cp_2Zr(P(SiMe_3)_2)(Cl)$, followed by reaction with lithium phenylacetylide.[79] It is interesting that the Zr=P multiple bond tolerates the C-H group of the terminal alkyne, while the Zr-P single bond of the metallacycle does not. Presumably, the [2+2] retrocycloaddition of **117** that generates the [Cp_2Zr=PMes*] intermediate is far slower than acidolysis of the Zr-P single bond of **117** by the acetylenic C-H group; thus **120** is the sole product of the reaction.

Efforts to expand the family of phosphametallacycles to include less sterically hindered substituents on phosphorus instead resulted in the formation of a novel diphosphametallacyclopentene. The mesityl substituted analogue of **117** was anticipated to be the product of the reaction of $Cp_2ZrMeCl$ and LiHPMes•2THF in the presence of diphenylacetylene. However, fractional crystallization of the resulting complex mixture of products instead gave **122** in 19% yield. This product exhibited signals in the ^{31}P NMR spectrum at 60.4 and -96.2 ppm with a P-P coupling constant of 349.8 Hz. ^1H and ^{13}C NMR data were consistent with the formulation of **122** as diphosphametallacyclopentene $Cp_2\overline{Zr(P(Mes)P(Mes)C(Ph)=CPh)}$. The structure of **122** was subsequently confirmed by an X-ray crystallographic study (Figure 4.2). The geometry about each phosphorus atom is pyramidal, and steric congestion in the metallacycle is minimized by the *transoid* disposition of the mesityl substituents. The Zr-P bond length of 2.596(9) Å compares well with the shorter Zr-P distance in the cyclic complex (η^5-$C_5H_3(SiMe_3)_2)_2Zr(P(Ph)C_6H_4PPh$-1,2) (2.560(4) Å).[68]

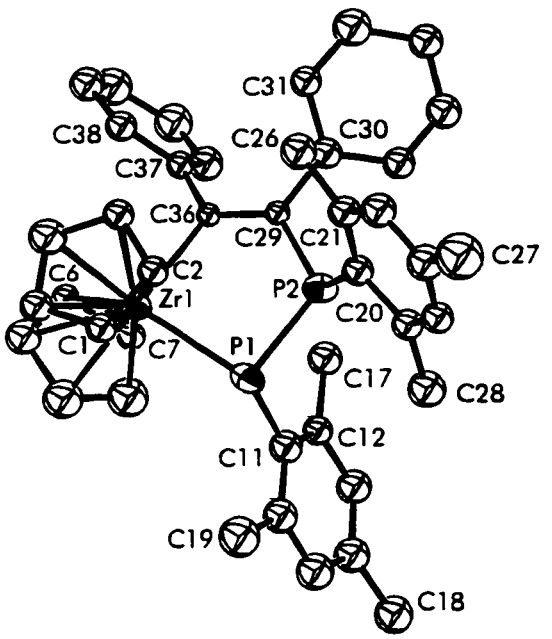

Figure 4.2 ORTEP drawing of **122**; 30% thermal ellipsoids are shown, hydrogen atoms have been omitted for clarity. Selected bond distances and angles: Zr(1)-P(1) 2.596(9) Å; Zr(1)-C(36) 2.31(2) Å; P(1)-P(2) 2.19(1) Å; P(1)-Zr(1)-C(36) 89.0(7)°; Zr(1)-P(1)-P(2) 94.2(4)°; P(1)-P(2)-C(29) 114(1)°.

The mechanism of formation of **122** is not clear. It was established in Chapter Two that the reaction of $Cp_2ZrMeCl$ with LiHPMes•2THF produced a complex mixture of products such as **79**, which was formed by a bimolecular loss of H_2PMes. Although no change in this reaction was observed in the presence of PMe_3, we initially presumed that a highly reactive terminal phosphinidene intermediate [Cp_2Zr=PMes] was generated and trapped by cycloaddition with diphenylacetylene to give the intermediate metallacyclobutene **123**. Further reaction with an equivalent of primary phosphine H_2PMes and elimination of hydrogen would then produce **122** (Figure 4.3). In order to probe this mechanism, a synthetic route to **123** was devised using information gleaned from the foundation studies described in Chapter Two. It was demonstrated that the reaction of $(Cp_2ZrCl)_2(\mu$-PMes) **80** with Li_2PMes provided a source of the reactive *bis*-phosphinidene bridged dimer **82**, which could be split by PMe_3. The analogous reaction employing diphenylacetylene instead of PMe_3 was quite

successful, providing the mesityl substituted analogue of **117**, $Cp_2\overline{Zr(P(Mes)C(Ph)=CPh)}$ **123** in 81% yield. This species was analogous in ^1H and $^{13}C\{^1H\}$ NMR spectra to metallacycles **117**, **118** and **119**. The reaction of **123** with an equivalent of H_2PMes did not furnish **122**. The product of P-H addition across the Zr-P bond was indeed formed, however the regiochemistry of the addition instead yielded the zirconocene alkenyl phosphide $Cp_2Zr(C(Ph)=C(Ph)PMesH)(PMesH)$ **124**. This species appeared in the ^{31}P NMR spectrum at -90.4 and -130.5 ppm with a P-P coupling constant of 75.1 Hz. Both signals exhibited one-bond coupling to proton of 309.8 Hz and 205.4 Hz, respectively. Although **124** was unstable, the formation of **122** was not detected in solutions of either **123** or **124** upon aging for several weeks or heating to 100 °C. These observations thus dismiss the possibility of **123** as an intermediate in **122** formation (Figure 4.3).

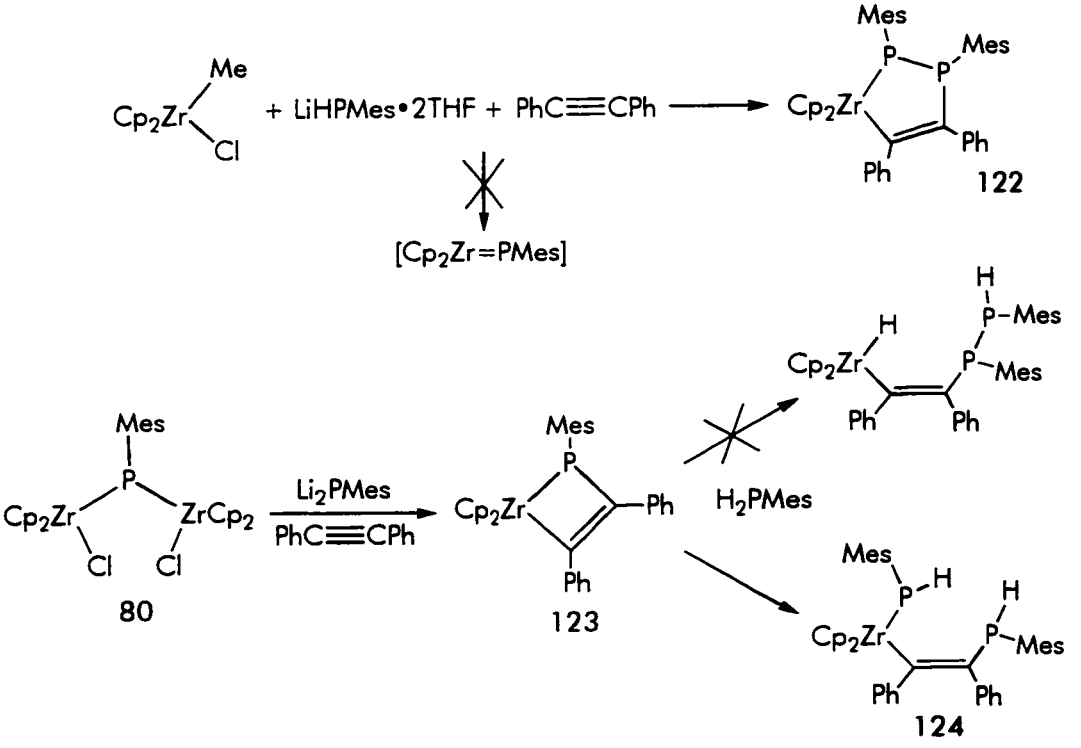

Figure 4.3 Mechanistic investigation of the formation of **122**.

We believe that the most probable mechanism for the formation of **122** involves the generation of an unstable diphosphametallacyclopropane **125** which is trapped

through insertion of alkyne into a Zr-P bond (Eq. 4.3). More sterically demanding cyclopentadienyl ligands have been reported to stablize diphosphametallacyclopropanes.[35c, 80] In addition, insertion of alkyne into the Zr-P bond of an acyclic phosphide to give **124** has been previously observed by Hey-Hawkins *et al.*[79] The proposed mechanism is also comparable to the insertion of alkyne into the Zr-N bond of the η^2-1,2-diphenylhydrazidozirconocene complex $Cp_2Zr(N_2Ph_2)(THF)$ as described by Bergman and coworkers.[81] Efforts to investigate this pathway and improve the yield of **122** will be the subject of future studies.

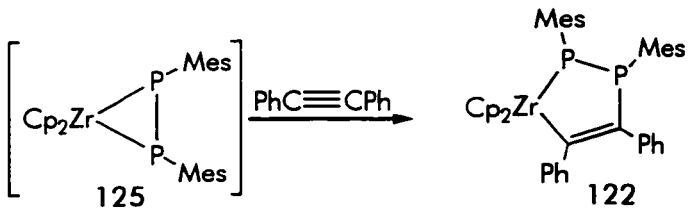

(4.3)

Insertion Reactions of 117

The reaction of *t*-butylisocyanide with **117** proceeded rapidly, giving a bright yellow product **126** which appeared in ^{31}P NMR spectrum at 17.4 ppm. Insertion into the Zr-P bond was evidenced by the two high-field resonances in the $^{13}C\{^1H\}$ NMR spectrum at 223.3 and 198.5 ppm, which indicated the presence of two Zr-C bonds. Preferential insertion into the Zr-P bond contrasts with reactions of related aza-[25] and oxametallacyclobutenes[11d] in which insertions occur exclusively at the Zr-C bond, but is compatible with the highly reactive nature of the Zr-P bond. The spectroscopic data were thus consistent with the formulation of **126** as $Cp_2\overline{Zr(C(=N\text{-}t\text{-}Bu)P(Mes^*)C(Ph)=CPh)}$. The hapticity of the imino fragment was determined by an X-ray crystallographic study, which clearly showed η^2 coordination of the iminoacyl group to the zirconium centre. The Zr(1)-C(43), Zr(1)-N(1) and C(43)-N(1) bond distances are very similar to those of the acyclic iminoacyl species $Cp_2Zr(\eta^2\text{-}C(=NMe)CHPh_2)(Me)$,[82] however the cyclic nature of **126** enforces the "N-outside" coordination mode of the imino group. This coordination mode is

disfavoured in open-chain metallocene acyl and iminoacyl complexes,[83] but has been previously observed in cyclic titanocene iminoacyls.[84] The pyramidal geometry about phosphorus in **126** was apparent from sum of the angles about P(1) of 332.4°. The inequivalence of the cyclopentadienyl rings indicated by this parameter of the solid state structure was not reflected in the ^{1}H and $^{13}C\{^{1}H\}$ NMR spectra, which furthermore were temperature invariant.

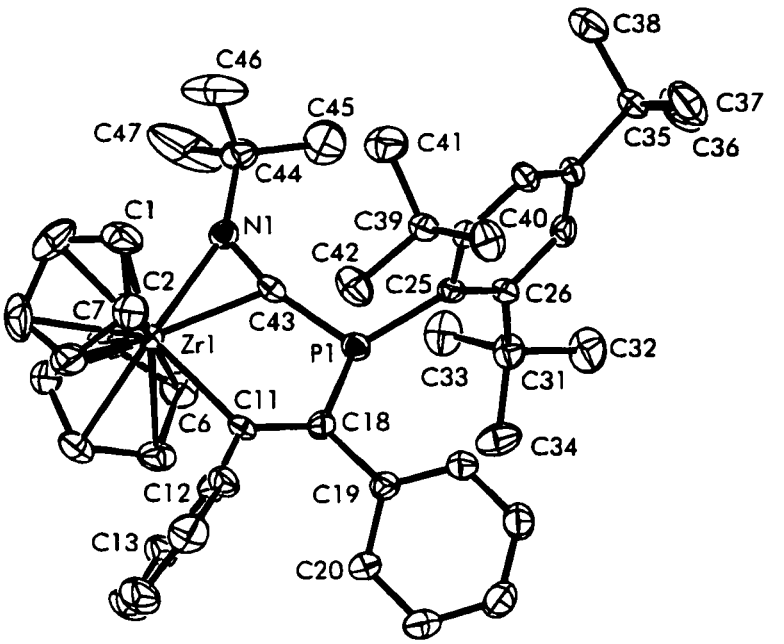

Figure 4.4 ORTEP drawing of **126**; 30% thermal ellipsoids are shown, hydrogen atoms have been omitted for clarity. Selected bond distances and angles: Zr(1)-N(1) 2.221(6) Å; Zr(2)-C(43) 2.217(7) Å; Zr(1)-C(11) 2.389(8) Å; N(1)-C(43) 1.274(9) Å; C(11)-Zr(1)-C(43) 73.0(3)°; C(11)-Zr(1)-N(1) 106.0(2)°; N(1)-Zr(1)-C(43) 33.3(2)°; C(43)-P(1)-C(18) 98.3(4)°.

Ketone and nitrile insertions also occurred into the Zr-P bond of **117**. For example, insertion of acetone rapidly produced the phosphaoxametallacyclohexene $Cp_2\overline{Zr(OCMe_2P(Mes^*)C(Ph)=CPh)}$ **127** in 51% yield. Likewise, reactions of **117** with cyclohexanone or benzonitrile afforded the similar six-membered metallacycles $Cp_2\overline{Zr(O(c\text{-}C_6H_{11})P(Mes^*)C(Ph)=CPh)}$ **128** and $Cp_2\overline{Zr(N=C(Ph)P(Mes^*)C(Ph)=CPh)}$ **129** in 58% and 46% yield, respectively (Fig. 4.5). X-ray crystallographic studies of **127** and

128 confirmed the formulations of the phosphaoxametallacyclohexenes (Fig. 4.6 and 4.7, respectively).

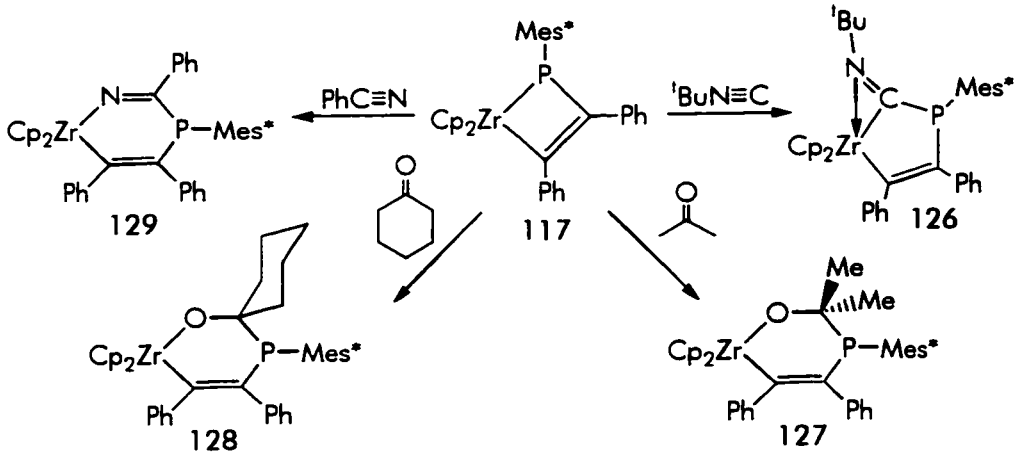

Figure 4.5 Insertion reactions of **117**.

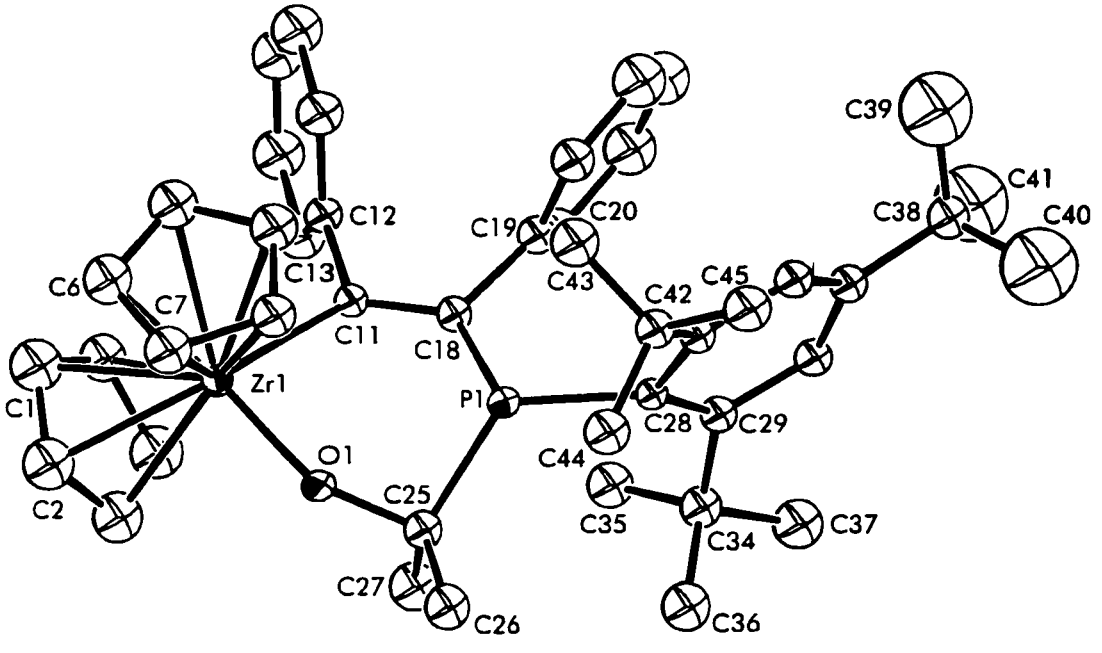

Figure 4.6 ORTEP drawing of **127**; 30% thermal ellipsoids are shown, hydrogen atoms have been omitted for clarity. Selected bond distances and angles: Zr(1)-O(1) 1.934(9) Å; Zr(1)-C(11) 2.30(1) Å; P(1)-C(25) 1.97(1) Å; O(1)-Zr(1)-C(11) 87.1(5)°.

In each of the closely related structures the geometry at phosphorus is pyramidal and the supermesityl substituent adopts an equatorial position relative to the ring. Unlike isocyanide insertion product **126**, the inequivalence of the cyclopentadienyl rings and methyl groups of **127** indicated by the solid state structure was consistent with the ^{1}H NMR spectrum at -80 °C. The fluxionality of this complex was indicated by the single broad resonances observed in the room temperature ^{1}H and ^{13}C NMR spectra ($\Delta G_c^{\ddagger}$ = 13.4 kcal/mol). Variable temperature NMR studies of **128** and **129** showed that they exhibited similar dynamic behaviour corresponding to $\Delta G_c^{\ddagger}$ = 14.1 and 13.0 kcal/mol respectively.

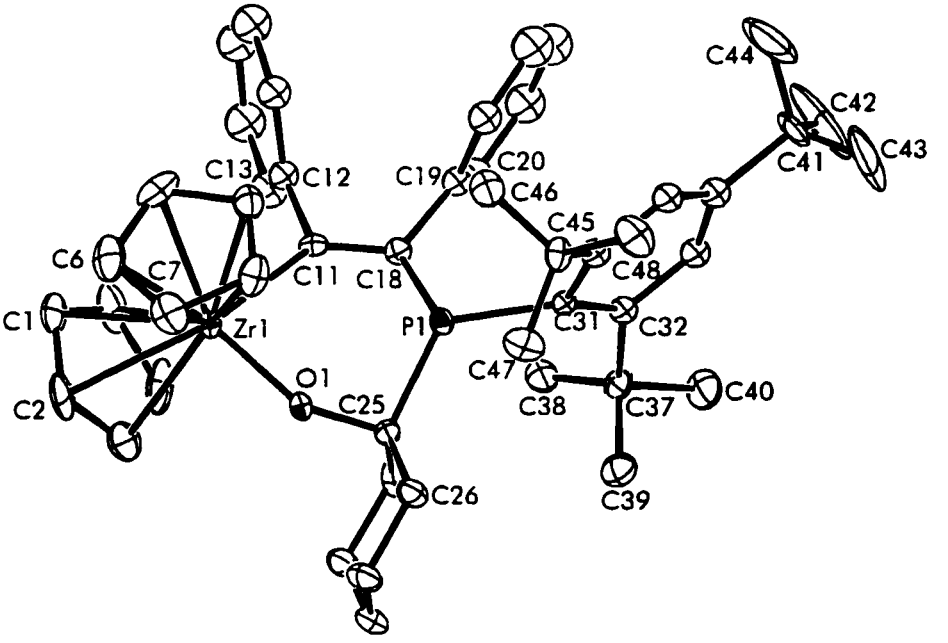

Figure 4.7 ORTEP drawing of **128**; 30% thermal ellipsoids are shown, hydrogen atoms have been omitted for clarity. Selected bond distances and angles: Zr(1)-O(1) 1.919(5) Å; Zr(1)-C(11) 2.336(7) Å; P(1)-C(25) 1.957(8) Å; O(1)-Zr(1)-C(11) 85.8(2)°.

By virtue of reactivity studies, a process involving a [4+2] retrocycloaddition of metallacycles **127** - **129** was ascertained. Addition of one equivalent of benzaldehyde to **127** resulted in the liberation of free acetone and the formation of metallacycle $Cp_2\overline{Zr(OCHPhP(Mes^*)C(Ph)=CPh)}$ **130**. **130** was also formed via corresponding

reactions with either **128** or **129**; as an alternative this species could be synthesized directly through the reaction of benzaldehyde with **117** to afford **130** in 61% yield.

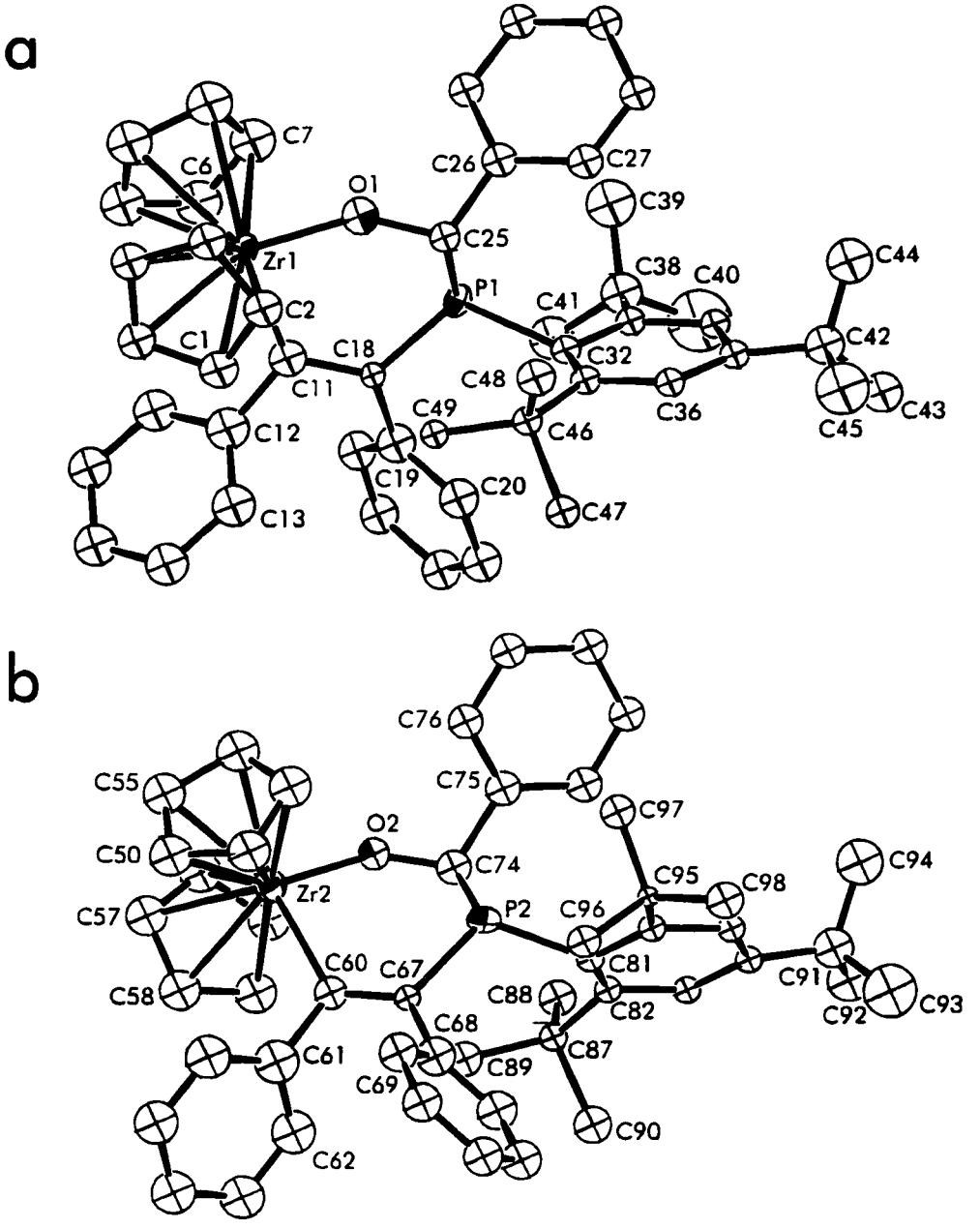

Figure 4.8 ORTEP drawing of the two molecules of **130** in the asymmetric unit, 30% thermal ellipsoids are shown, hydrogen atoms have been omitted for clarity. Selected bond distances and angles: (a) Zr(1)-O(1) 1.97(3) Å; Zr(1)-C(11) 2.25(4) Å; P(1)-C(25) 1.94(4) Å; O(1)-Zr(1)-C(11) 90(1)°. (b) Zr(2)-O(2) 1.93(2) Å; Zr(2)-C(60) 2.31(4) Å; P(2)-C(74) 1.87(4) Å; O(2)-Zr(2)-C(60) 86(1)°.

The observation of one ^{31}P NMR resonance for **130**, as well as ^{1}H and $^{13}C\{^{1}H\}$ NMR spectra corresponding to only one species, indicated that the insertion reaction was diastereoselective. An X-ray crystallographic study of **130** confirmed the selective formation of the RR/SS pair of enantiomers, in which the supermesityl group on phosphorus and the ketonic phenyl group both adopt equatorial positions and thus are *trans* with respect to the metallacyclic ring (Fig. 4.8). In a similar way, reactions of **117** or **127 - 129** with one equivalent of styrene oxide resulted in the formation of phosphaoxametallacycloheptene $Cp_2\overline{Zr(OCH_2CHPhP(Mes^*)C(Ph)=CPh)}$ **131** in 68% yield (from **117**). X-ray crystallography again confirmed that the RR/SS enantiomeric pair was selectively formed (Fig. 4.9). In contrast to **127 - 129**, neither **130** nor **131** are fluxional species; the solution ^{1}H and ^{13}C NMR data are temperature invariant and in accord with the solid state structures.

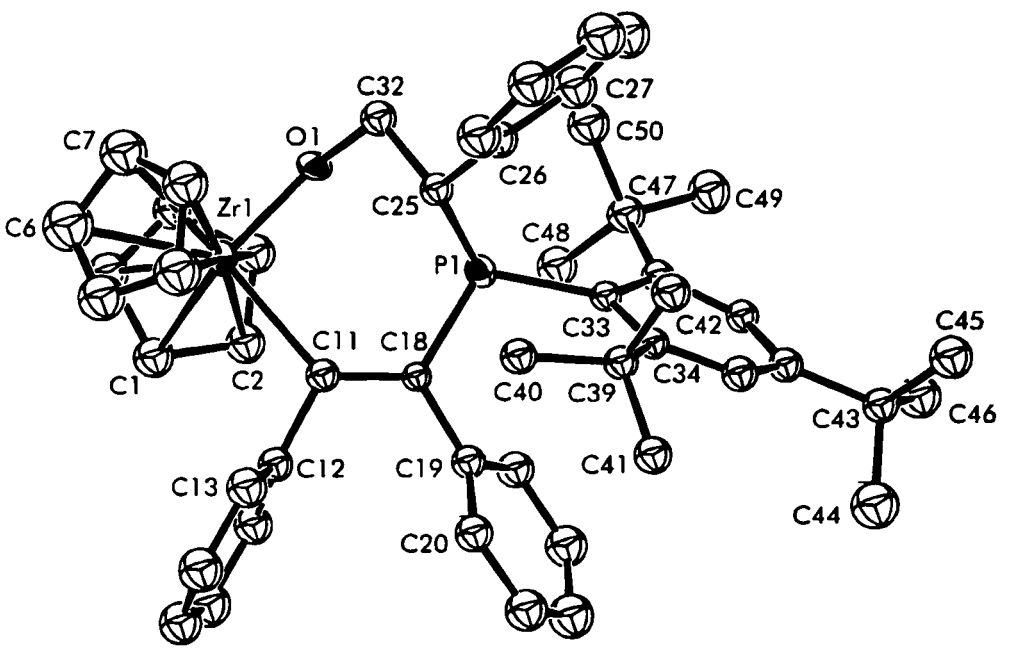

Figure 4.9 ORTEP drawing of **131**; 30% thermal ellipsoids are shown, hydrogen atoms have been omitted for clarity. Selected bond distances and angles: Zr(1)-O(1) 1.92(1) Å; Zr(1)-C(11) 2.36(1) Å; P(1)-C(25) 1.91(1) Å; O(1)-Zr(1)-C(11) 96.2(4)°.

Kinetic studies of the reactions of **127** with either benzaldehyde or styrene oxide showed that the rates of formation of metallacycles **130** and **131** were first order in the concentration of **127** but independent of changes in the concentration of either benzaldehyde or styrene oxide.[85] This indicated a rate limiting loss of acetone from **127** through a [4+2] retrocycloaddition, comparable to organic retro-Diels-Alder reactions, which generated zirconocene alkylidene intermediate **132**. A subsequent [4+2] cycloaddition with benzaldehyde lead to the formation of **130**, while the ring opening of styrene oxide resulted in the production of **131** (Fig. 4.10). Both reactions were irreversible; addition of excess acetone to solutions of either **130** or **131** did not produce metallacycle **127**. The reactive nature of **127** may be attributed to steric congestion in the six-membered ring. Close contacts between both methyl groups and supermesityl *t*-butyl fragments (five H...H distances ranging from 2.098 Å to 2.234 Å) are observed in the solid state structure. Replacement of one of the offending methyl groups with a hydrogen atom (as in metallacycle **130**) stabilizes the complex and [4+2] retrocycloadditions are not observed.

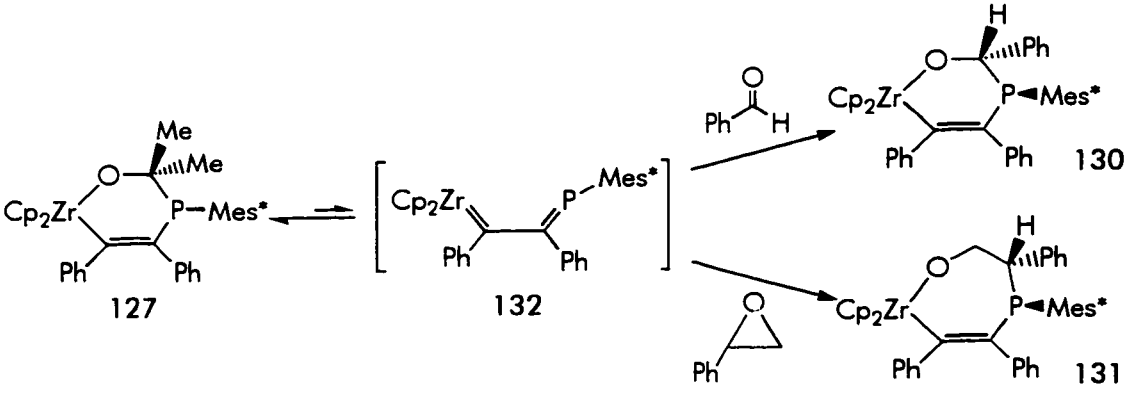

Figure 4.10 [4+2] Retrocycloadditions of **127**.

Related [4+2] retrocycloadditions have been reported for azaoxametallacyclohexenes[25] and oxatitanacyclohexenes.[86] In these cases, preferential insertion of the ketone into the metal-vinyl bond results in retrocycloadditions that

furnish $(Cp_2M=O)_n$ along with either α,β-unsaturated imines or conjugated dienes. Because the exclusive insertion of ketone into the Zr-P bond of **117** precludes this reaction path, the retrocycloaddition yields acetone and the alkylidene intermediate **132**. Attempts to trap this intermediate with excess PMe_3, pyridine, or by [4+2] cycloaddition with 1-phenylpropyne were unsuccessful. Nonetheless, the related work of Doxsee *et al.*[26] on vinylimido complexes of titanocene (Eq. 1.19 in Chapter One) and the trapping the imido-phosphaalkene complex $(Cp_2Zr=NC(Ph)=PMes^*)(PMe_3)$ **107b** as described in Chapter Three give credence to the elusive alkylidene-phosphaalkene intermediate.

Sterically Induced Epimerization at Phosphorus

A feature common to metallacyclobutenes **117 - 119** and **123**, metallacyclopentenes **122** and **126**, and metallacyclohexenes **127 - 129** is the discrepancy between the spectroscopic data and the expected pyramidal geometry at phosphorus. This geometry imposes inequivalent environments on the two cyclopentadienyl rings; however, each of these complexes exhibit only one resonance attributable to these ligands in the ^1H and $^{13}C\{^1H\}$ NMR spectra. This indicates that the metallacycles are either planar or rapidly undergoing inversion at phosphorus. These alternatives could not be distinguished for **117** or **118**, as cooling to -80 °C merely resulted in the observation of line broadening. However, a pyramidal configuration has been confirmed crystallographically for **122**, **126** and **127 - 129**.

While the kinetic studies described in the previous section provide mechanistic insight into the reactivity of **127 - 129**, the rate limiting loss of acetone also indicates the lack of a rapid equilibrium between **127** and zirconocene alkylidene intermediate **132**. The variable temperature NMR studies of **127 - 129** yielded values of $\Delta G_c^{\ddagger}$ consistent with a reduced barrier to inversion at phosphorus. The [2+2] retrocycloadditions exhibited by phosphametallacyclobutenes **117 - 119** and **123** are comparable to the above [4+2] retrocycloadditions, as preliminary kinetic investigations of the reaction between **117** and PMe_3 also revealed a rate limiting loss of alkyne. These notions for **117 - 119**,

123 and **127 - 129** are supported by the ^{1}H and $^{13}C\{^{1}H\}$ NMR spectra as the chemical shifts and coupling constants to phosphorus in each case are not indicative of fragmentation of the metallacycles.

Rationalization of the NMR spectra of metallacyclopentenes **122** and **126** also excluded any implication of metallacycle fragmentation. Neither complex underwent dissociative exchange with alkyne or reaction with PMe_3. As mentioned in the previous section, the NMR spectra of **126** were temperature invariant; however, the ^{1}H NMR spectrum of **122** showed a marked temperature dependence over a range of 80 °C to -80 °C. As the temperature was lowered the broad resonance due to the cyclopentadienyl rings split and eventually sharpened into two lines ($\Delta G_c^{\ddagger}$ = 13.8 kcal mol^{-1}). While this value is within the range expected for metal-assisted inversion at phosphorus, the averaging of the cyclopentadienyl resonances implies that the process is occurring at *both* phosphorus centres.

The feature common to the family of four- five- and six-membered phosphametallacycles is a great deal of steric congestion, and it is this quality that causes abnormally low phosphorus inversion barriers. Preliminary molecular orbital calculations[87] are consistent with this postulate, as there is no suggestion of either delocalization of the phosphorus lone pair into the π orbital of the alkenyl moiety or any dative interaction with the metal centre. The steric effects are manifested in two ways: the reduced inversion barriers at phosphorus and the aforementioned [4+2] retrocycloadditions of **126 - 129**. Phosphaoxametallacyclohexene **130** and phosphaoxametallacycloheptene **131** are immune to these effects as their solution NMR spectra match the solid state structures and they do not undergo [4+2] retrocycloadditions. This may be attributed to reduced steric constraints due to the presence of a hydrogen substituent on the metallacyclic carbon atom α to phosphorus. Increasing the steric demands of this substituent results in the destabilization of the metallacycle and dynamic behaviour is observed, as in **126 - 129**. Support for these

ideas is given by further increases of the steric demands in the six-membered metallacycle. For example, reaction of **117** with 2-butanone resulted in the formation of both diastereomers of the fluxional and highly unstable metallacycle $Cp_2\overline{Zr(OCMeEtP(Mes^*)C(Ph)=CPh)}$.

4.4 Conclusion

In summary, the first examples of phosphametallacyclobutenes exhibit intriguing chemistry. These complexes undergo [2+2] retrocycloadditions and also readily insert unsaturated polar organic molecules into the Zr-P bond. Such insertions, along with reactions tailored to accommodate smaller substituents on phosphorus, have allowed for the preparation of a family of four-, five- and six-membered metallacycles. Our results demonstrate that steric factors exert considerable influence over the entire group of complexes. These traits are made apparent via reduced inversion barriers at phosphorus and [4+2] retrocycloadditions. In contrast, when aldehyde is inserted into phosphametallacyclobutene **117** the product is not fluxional. Furthermore, the insertion proceeds with a high degree of P/C diastereoselectivity, which augurs well for future applications of these metallacycles in enantioselective syntheses. The present studies of steric influences on the epimerization at phosphorus will be critical to the development of this area of research.

Chapter Five
Metallacycle Transfer Reactions: Synthetic Routes to Heterocycles

5.1 Introduction

A number of methods have been developed for the application of Group 4 metallacycles to the synthesis of organic and heterocyclic compounds. One technique is removal of the metal fragment via hydrolysis of the metallacycle.[88] For example, acidolysis of heteroatom-containing zirconacycles has been reported to yield ketones.[11c, d, 19, 26b] As discussed in Section 1.6, Bergman *et al.* have shown that protonolysis of azametallacyclobutenes by primary amines yields enamines and $Cp_2Zr(NHR)_2$.[24b, c]

A general synthetic route to an extensive variety of heterocycles involves metallacycle transfer from zirconocene to main group halides. Since Nugent and Fagan's initial report in 1988,[89] further research efforts have extended the scope of this synthetic protocol. For example, Doxsee *et al.* have applied titanacyclobutene $Cp_2\overline{Ti(CH_2C(Ph)=CPh)}$ to the preparation of 1,2-dihydrophosphetes, via reactions with alkyl- and aryldichlorophosphines.[90] In addition, myriad carbon-based zirconacycles have been exploited in the preparations of a wide variety of group 13 - 16 heterocycles.[88,91] However, the only example of the reaction of a main group dihalide with a heteroatom-containing zirconacycle involves the preparation of an isothiazole from an azazirconacycle such as **132** and sulfur monochloride (Eq. 5.1).[91]

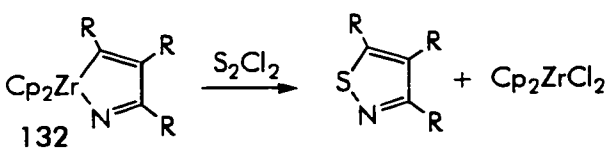

(5.1)

The present studies of phosphorus-containing metallacycles have been extended to include protonolysis and metallacycle transfer reactions. Phosphametallacyclobutene **117** and diphosphametallacyclopentene **122** react smoothly with main group dihalides under mild conditions. These observations are not surprising in view of the established

reactivity of the Zr-P bond. In order to further exploit this characteristic, we have also explored metallacycle transfer reactions with the known triphosphanato zirconocene metallacycle $Cp_2Zr(PPh)_3$ **133**.[42]

5.2 Experimental

General Data All preparations, ^1H, $^{13}C\{^1H\}$, ^{31}P and $^{31}P\{^1H\}$ NMR spectroscopy, mass spectrometry and combustion analyses were carried out under similar conditions as described in Section 2.2. $Cp_2Zr(PPh)_3$ **133** was prepared by literature methods.[42]

Synthesis of (CH(Ph)=C(Ph)PHMes* 134, P(Ph)P(Mes*)C(Ph)=CPh 135 and PH(C_6H_2-(2-$CH_2C(CH_3)_2$)-4,6-t-Bu_2)B(Ph)CPh=CPh 136

Compounds **134 - 136** were prepared through similar routes, thus only one representative procedure is described. To a benzene solution of **117** (135 mg, 0.2 mmol) was added phenol (38 mg, 0.4 mmol). The reaction mixture stood 8 h, resulting in the formation of a colourless solution. After filtration, the solvent was removed in vacuo and the product dissolved in pentane. Colourless crystals formed over 12 h at room temperature and were isolated by filtration. **134**: Yield: 62 mg (68%). ^1H NMR (25 °C, C_6D_6): δ 7.70 (br, 2H, Ar-*H*), 7.36-6.75 (m, 10H, Ph-*H*), 5.80 (dd, $|J_{P\text{-}H}|$ = 230.7 Hz, $|^4J_{H\text{-}H}|$ = 2.3 Hz, 1H, P-*H*), 5.34 (dd, $|^3J_{P\text{-}H}|$ = 4.9 Hz, $|^4J_{H\text{-}H}|$ = 2.3 Hz, 1H, C-*H*), 1.83 (br s, 9H, *o*-^{t}Bu), 1.53 (br s, 9H, *o*-^{t}Bu), 1.35 (s, 9H, *p*-^{t}Bu). $^{13}C\{^1H\}$ NMR (25 °C, C_6D_6): δ 157.9 (br s, quat), 157.6 (br s, quat), 155.6 (br s, quat), 150.9 (s, quat), 143.6 (d, $|J|$ = 21.9 Hz, quat), 141.2 (d, $|J|$ = 20.8 Hz, quat), 137.6 (s, quat), 133.1 (d, $|J|$ = 8.2 Hz, arom. *C*-H), 132.1 (s, arom. *C*-H), 130.6 (s, arom. *C*-H), 128.4 (d, $|J|$ = 6.4 Hz, arom. *C*-H), 128.0 (s, arom. *C*-H), 127.4 (s, arom. *C*-H), 126.6 (s, arom. *C*-H), 122.9 (br s, arom. *C*-H), 122.0 (br s, arom. C-H), 38.7 (br s, *o*-$C(CH_3)_3$), 38.1 (s, *o*-$C(CH_3)_3$), 35.0 (s, *p*-$C(CH_3)_3$), 33.3 (br s, *o*-$C(CH_3)_3$), 31.2 (s, *p*-$C(CH_3)_3$). ^{31}P NMR (25 °C, C_6D_6): δ -48.3 (d, $|J_{P\text{-}H}|$ = 231.4 Hz). Anal. Calcd for $C_{32}H_{41}P$: C: 84.17; H: 9.05; Found: C: 84.41; H: 8.84.

135: Yield: 60 mg (53%). ^{1}H NMR (25 °C, C_6D_6): δ 7.59 (m, 4H, Ph-*H*), 7.34 (s, 2H, Ph-*H*), 7.18 (m, 2H, Ph-*H*), 6.86 (m, 9H, Ph-*H*), 1.58 (s, 18H, *o*-^{t}Bu), 1.22 (s, 9H, *p*-^{t}Bu). ^{13}C{^{1}H} NMR (25 °C, C_6D_6): δ 159.4 (d, $|J|$ = 13.1 Hz, quat), 151.2 (s, quat), 142.2 (m, quat), 136.6 (m, quat), 135.9 (m, quat), 135.2 (s, quat), 134.8 (d, $|J|$ = 5.6 Hz, arom. *C*-H), 134.6 (d, $|J|$ = 4.9 Hz, arom. *C*-H), 131.1 (s, arom. *C*-H), 122.0 (d, $|J|$ = 5.2 Hz, arom. *C*-H), 39.1 (s, *o*-$C(CH_3)_3$), 34.6 (s, *p*-$C(CH_3)_3$), 33.5 (*AB* d, $|J_{AB}|$ = 5.5 Hz, *o*-$C(CH_3)_3$), 31.1 (s, *p*-$C(CH_3)_3$). ^{31}P NMR (25 °C, C_6D_6): δ -23.1, -27.4 (*AB* q, $|J_{AB}|$ = 151.9 Hz). Anal. Calcd for $C_{38}H_{44}P_2$: C: 81.11; H: 7.88; Found: C: 81.33; H: 8.15.

136: Yield: 51 mg (47%). ^{1}H NMR (25 °C, C_6D_6): δ 8.03 (br d, $|J|$ = 7.5 Hz, 2H, Ph-*H*), 7.85 (br d, $|J|$ = 3.7 Hz, 1H, Ph-*H*), 7.58-7.44 (m, 5.5H, Ph-*H* and P-*H*), 7.05-6.86 (m, 8H, Ph-*H*), 6.35 (d, $|J|$ = 2.2 Hz, 0.5 H, P-*H*), 2.08 (br, 2H, CH_2), 1.76 (s, 3H, CH_3), 1.68 (s, 3H, CH_3), 1.24 (s, 9H, ^{t}Bu), 1.06 (s, 9H, ^{t}Bu). ^{13}C{^{1}H} NMR (25 °C, C_6D_6): δ 160.2 (d, $|J|$ = 14.6, quat), 154.8 (s, quat), 153.7 (s, quat), 139.2 (d, $|J|$ = 51.5 Hz, quat), 137.8 (s, quat), 133.2 (d, $|J|$ = 8.3 Hz, arom. C-H), 131.2 (d, $|J|$ = 46.1 Hz, quat), 130.2 (s, arom. *C*-H), 128.8 (s, arom. *C*-H), 128.5 (s, arom. *C*-H), 128.3 (d, $|J|$ = 3.6 Hz, arom. *C*-H), 128.1 (s, arom. *C*-H), 127.9 (d, $|J|$ = 2.2 Hz, arom. *C*-H), 127.2 (s, arom. *C*-H), 126.1 (d, $|J|$ = 3.5 Hz, arom. *C*-H), 123.8 (d, $|J|$ = 10.4 Hz, arom. *C*-H), 122.1 (d, $|J|$ = 6.4 Hz, arom. *C*-H), 117.6 (d, $|J|$ = 21.8 Hz, quat), 42.0 (d, $|J|$ = 10.1 Hz, quat), 38.7 (s, Me), 37.1 (s, quat), 35.2 (s, quat), 34.7 (v br s, CH_2), 33.7 (s, Me), 33.3 (s, ^{t}Bu), 31.0 (s, ^{t}Bu). ^{31}P NMR (25 °C, C_6D_6): δ -35.3 (dd, $|^{1}J_{P\text{-}H}|$ = 371.4 Hz, $|J|$ = 31.9 Hz). Anal. Calcd for $C_{38}H_{44}BP$: C: 84.13; H: 8.17; Found: C: 84.37; H: 7.97.

Synthesis of P(Ph)P(Mes)P(Mes)C(Ph)=CPh 138

To a benzene solution of **122** (140 mg, 0.2 mmol) was added phenyldichlorophosphine (27.1 μL, 0.2 mmol). The reaction mixture stood 4 h, resulting in the formation of a pale yellow solution. After filtration, the solvent was removed in vacuo and the product dissolved in hexane. Colourless crystals formed over 12 h at room temperature and

were isolated by filtration. Yield: 54 mg (46%). ^{1}H NMR (25 °C, C_6D_6): δ 7.65 (m, 2H, Ph-*H*), 7.48 (m, 2H, Ph-*H*), 7.06-6.51 (m, 15H, Ph-*H*), 2.90 (s, 6H, *o*-C*H*$_3$), 2.77 (br s, 3H, C*H*$_3$), 2.29 (br s, 3H, C*H*$_3$), 2.08 (s, 3H, C*H*$_3$), 1.95 (s, 3H, C*H*$_3$). ^{13}C{^{1}H} NMR (25 °C, C_6D_6): δ 150.3 (dd, $|J|$ = 25.5Hz, $|J|$ = 4.5 Hz, quat), 146.3 (m, quat), 145.6 (br d, $|J|$ = 13.5 Hz, quat), 145.1 (s, quat), 144.5 (m, quat), 140.7 (d, $|J|$ = 19.5 Hz, quat), 140.2 (s, quat), 139.9 (s, quat), 139.6 (d, $|J|$ = 12.8 Hz, quat), 139.3 (br s, quat), 132.2 (m, arom. C-H), 130.3 (s, arom. C-H), 130.2 (br s, arom. C-H), 130.0 (s, arom. C-H), 129.4 (br d, $|J|$ = 6.8 Hz, arom. C-H), 129.1 (s, arom. C-H), 128.3 (d, $|J|$ = 4.5 Hz, arom. C-H), 128.2 (s, arom. C-H), 126.8 (d, $|J|$ = 12.8 Hz, arom. C-H), 24.0 (m, CH_3), 20.8 (s, CH_3). ^{31}P NMR (25 °C, C_6D_6): δ 33.7 (d, $|^1J_{P\text{-}P}|$ = 252.0 Hz), 15.6 (d, $|^1J_{P\text{-}P}|$ = 230.8 Hz), -58.2 (dd, $|^1J_{P\text{-}P}|$ = 247.2 Hz, $|^1J_{P\text{-}P}|$ = 237.3 Hz. Anal. Calcd for $C_{38}H_{37}P_3$: C: 77.80; H: 6.36; Found: C: 78.08; H: 6.58.

Synthesis of (PPh)$_4$ 140 and (*t*-Bu)$_2$Sn(PPh)$_3$ 141

Compounds **140** and **141** were prepared through similar routes, thus only one representative procedure is described. To a benzene solution of **133** (109 mg, 0.2 mmol) was added phenyldichlorophosphine (27.1 μL, 0.2 mmol). The reaction mixture stood 1 h, resulting in the formation of a colourless solution. After filtration, the solvent was removed in vacuo and the product dissolved in hexane. Colourless crystals formed over a 3 day period at room temperature and were isolated by filtration. **140**: Yield: 71 mg (82%). ^{31}P NMR (25 °C, C_6D_6): δ -48.0 (s). ^{1}H NMR and ^{13}C{^{1}H} NMR data were consistent with that reported in the literature.[92]

141: Yield: 51 mg (46%). ^{1}H NMR (25 °C, C_6D_6): δ 7.10-6.91 (m, 15H, Ph-*H*), 1.42 ($|J_{P\text{-}Sn}|$ = 78.6 Hz, $|J_{P\text{-}Sn}|$ = 73.1 Hz, 9H, ^{t}Bu), 0.89 ($|J_{P\text{-}Sn}|$ = 80.9 Hz, $|J_{P\text{-}Sn}|$ = 77.8 Hz, 9H, ^{t}Bu). ^{13}C{^{1}H} NMR (25 °C, C_6D_6): δ 137.6 (m, quat), 131.7 (m, arom. C-H), 130.9 (m, arom. C-H), 128.3 (d, $|J|$ = 18.5 Hz, arom. C-H), 128.1 (s, arom. C-H), 127.6 (s, arom. C-H), 126.3 (s, arom. C-H), 42.7 (s, $C(CH_3)_3$), 31.3 (s, $C(CH_3)_3$). ^{31}P NMR (25 °C, C_6D_6): δ -51.3 (t,

$|{}^{1}J_{P\text{-}P}|$ = 139.9 Hz), -70.5 (d, $|{}^{1}J_{P\text{-}P}|$ = 140.6 Hz, $|{}^{1}J_{P\text{-}Sn}|$ = 573.9 Hz). Anal. Calcd for $C_{26}H_{33}P_3Sn$: C: 56.05; H: 5.97; Found: C: 55.88; H: 5.84.

X-Ray Structure Determinations of 134 - 136, 138, 140 and 141

The P-H hydrogen atoms of the two molecules of **134** in the asymmetric unit and of **136** were located in a difference Fourier map, and their contributions included but not refined in subsequent least squares calculations. The final values of R, R_w and the maximum Δ/σ on any of the parameters in the final cycle of refinement is given in Tables 5.1 and 5.2. ORTEP drawings of **134 - 136, 138, 140** and **141** are shown in Figures 5.1 - 5.6, respectively, with 30% thermal ellipsoids. Hydrogen atoms have been omitted for clarity. Selected bond distances and angles are listed in the captions for Figures 5.1 - 5.6. Other structural parameters are given in Tables A4.1-A4.18 in Appendix Four.

Table 5.1: Crystallographic Parameters for 134, 135 and 136

	134	135	136
Formula	$C_{32}H_{41}P$	$C_{38}H_{44}P_2$	$C_{38}H_{44}BP$
Formula weight	456.64	562.71	542.55
Cryst Colour, Form	colourless blocks	yellow blocks	yellow blocks
a(Å)	16.568(7)	26.327(7)	17.00(1)
b(Å)	16.885(4)	10.211(7)	13.496(4)
c(Å)	20.736(3)	26.918(7)	29.56(1)
α(deg)			
β(deg)	98.46(2)	106.37(2)	102.13(4)
γ(deg)			
Crystal System	monoclinic	monoclinic	monoclinic
Space group	$P2_1/c$	C2/c	C2/c
Vol(Å^3)	5738(3)	6826(5)	6630(5)
D_{calcd} (gcm^{-3})	1.06	1.10	1.09
Z	8	8	8
Abs coeff, μ, cm^{-1}	1.12	1.50	1.06
Temp (°C)	24	24	24
Scan speed, °/min	32 ($\theta/2\theta$) (1-3 scans)	8 ($\theta/2\theta$) (1-3 scans)	8 ($\theta/2\theta$) (1-3 scans)
Scan range (deg)	1.0 above $K\alpha_1$, 1.0 below $K\alpha_2$	1.0 above $K\alpha_1$, 1.0 below $K\alpha_2$	1.0 above $K\alpha_1$, 1.0 below $K\alpha_2$
Bkgd/scan ratio	0.5	0.5	0.5
Data collected	10487	6377	6101
2θ range (deg)	4.5-50.0	4.5-50.0	4.5-50.0
Index range	$\pm h,k,l$	$\pm h,k,l$	$\pm h,k,l$
Data $F_o^2 > 3\sigma(F_o^2)$	2152	1044	1114
Variables	276	171	166
Transmission factors	0.675-1.072	0.655-1.106	0.598-1.117
R (%)[a]	9.7	10.4	9.5
Rw (%) [a]	7.4	8.4	7.5
Largest Δ/σ	0.07	0.01	0.00
Goodness of fit	2.43	2.28	2.32

[a] $R = \Sigma | |F_o| - |F_c| | / \Sigma |F_o|$, $Rw = [\Sigma(|F_o| - |F_c|)^2 / \Sigma |F_o|^2]^{0.5}$

Table 5.2: Crystallographic Parameters for 138, 140 and 141

	138	140	141
Formula	$C_{38}H_{37}P_3$	$C_{24}H_{20}P_4$	$C_{26}H_{33}P_3Sn$
Formula weight	586.63	432.06	557.16
Cryst Colour, Form	colourless blocks	colourless blocks	pale yellow blocks
a(Å)	11.468(2)	11.757(4)	30.583(9)
b(Å)	14.627(2)	12.612(7)	8.482(3)
c(Å)	10.374(2)	7.558(3)	21.566(5)
α(deg)	98.21(1)		
β(deg)	109.52(1)		
γ(deg)	81.23(1)		
Crystal System	triclinic	orthorhombic	orthorhombic
Space group	$P\bar{1}$	$P2_12_12$	$Pca2_1$
Vol(Å^3)	1613.2(5)	1120.8(7)	5594(7)
D_{calcd} (gcm^{-3})	1.21	1.12	1.32
Z	2	8	4
Abs coeff, μ, cm^{-1}	2.09	0.70	10.95
Temp (°C)	24	24	24
Scan speed, °/min	32 ($\theta/2\theta$) (1-3 scans)	16 ($\theta/2\theta$) (1-3 scans)	16 ($\theta/2\theta$) (1-3 scans)
Scan range (deg)	1.0 above $K\alpha_1$, 1.0 below $K\alpha_2$	1.0 above $K\alpha_1$, 1.0 below $K\alpha_2$	1.0 above $K\alpha_1$, 1.0 below $K\alpha_2$
Bkgd/scan ratio	0.5	0.5	0.5
Data collected	5689	1174	5556
2θ range (deg)	4.5-50.0	4.5-50.0	4.5-50.0
Index range	$\pm h, \pm k, l$	h,k,l	h,k,l
Data $F_o^2 > 3\sigma(F_o^2)$	2668	590	2717
Variables	370	67	280
Transmission factors	0.894-1.076	0.887-1.105	0.787-1.224
R (%)[a]	5.6	6.0	8.0
Rw (%) [a]	4.7	4.4	7.2
Largest Δ/σ	0.00	0.00	0.00
Goodness of fit	1.66	1.54	2.21

[a] $R = \Sigma | |F_o| - |F_c| | / \Sigma |F_o|$, $Rw = [\Sigma(|F_o| - |F_c|)^2 / \Sigma |F_o|^2]^{0.5}$

5.3 Results and Discussion

Reactions of phosphametallacyclobutene 117

Metallacycle **117** has been found to readily undergo both protonolysis and transfer to a main group dihalide. Reaction of **117** with two equivalents of phenol proceeded to give a colourless solution which exhibited a ^{31}P NMR signal at -48.3 ppm ($|J_{P\text{-}H}|$ = 231.4 Hz), indicative of a secondary phosphine.

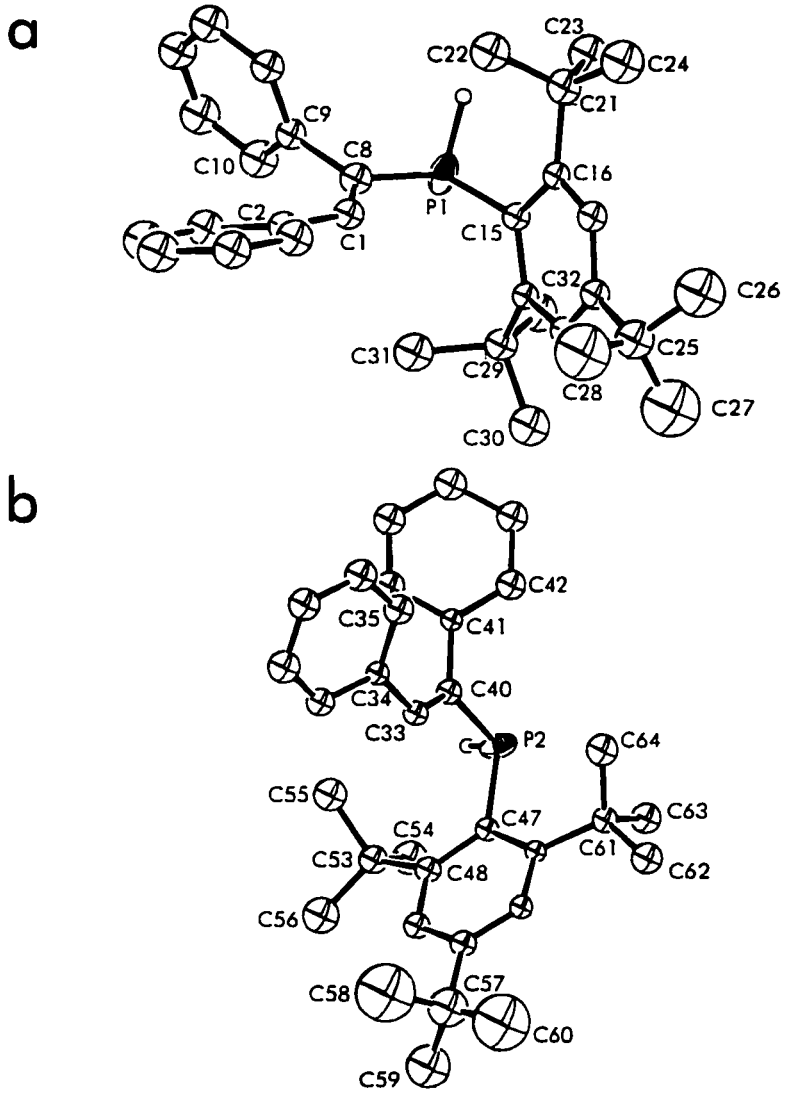

Figure 5.1 ORTEP drawing of the two molecules of **134** in the asymmetric unit, 30% thermal ellipsoids are shown, hydrogen atoms have been omitted for clarity. Selected bond distances and angles: P(1)-C(8) 1.83(1) Å; P(1)-C(15) 1.84(1) Å; C(8)-P(1)-C(15) 102.5(7)°. (b) P(2)-C(40) 1.84(1) Å; P(2)-C(47) 1.83(1) Å; C(40)-P(2)-C(47) 103.2(7)°.

The ^{1}H NMR spectrum revealed the formation of $Cp_2Zr(OPh)_2$[93] as well as product **134**. The signal at 5.34 ppm which coupled both to the adjacent phosphorus atom and the phosphorus-bound proton was attributed to the alkenyl C-H. The $^{13}C\{^1H\}$ NMR spectra supported the formulation of **134** as secondary phosphine (CH(Ph)=C(Ph)PHMes* (Eq. 5.2). An X-ray crystallographic study confirmed the connectivity of this compound (Fig. 5.1).

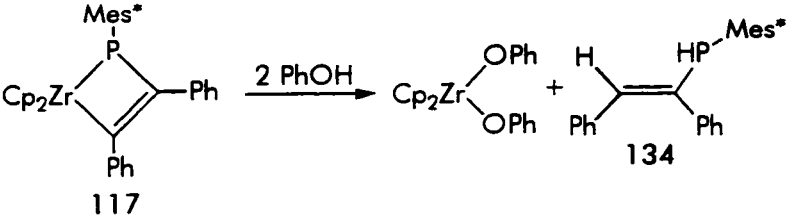

117 134 (5.2)

Metallacycle transfer reactions involving phenyldichlorophosphine have been used in the past with titanacyclobutenes and zirconacyclopentadienes to synthesize 1,2-dihydrophosphetes[90] and phospholes,[91] respectively. Phosphametallacyclobutene **117** has been found to undergo an analogous reaction which allows for the facile introduction of two heteroatoms into the cyclic product. **117** reacted with one equivalent of phenyldichlorophosphine to yield a yellow crystalline product in 65% yield along with Cp_2ZrCl_2. The ^{31}P NMR spectrum of the organic product consisted of an AB quartet, consistent with the formulation of product **135** as an unsymmetrically substituted 1,2-diphosphetene ring P(Ph)P(Mes*)C(Ph)=CPh (Eq. 5.3).

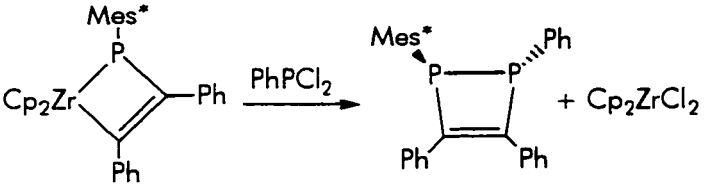

117 135 (5.3)

The ^{1}H and $^{13}C\{^1H\}$ NMR data were consistent with this assignment, and the structure was confirmed via an X-ray crystallographic study. The substituents on the two phosphorus atoms in **135** are of a *transoid* disposition with respect to the four-membered ring. The C=C bond length of 1.37(2) Å and P(1)-C(8) and P(2)-C(1) bond lengths of

1.79(2) and 1.76(2) Å are all typical, thus illustrating the lack of aromaticity. Steric congestion in **135** is apparent in the distortion about the C=C bond. The Ph-C=C angles of 128(2)° and 127(2)° and the P-C=C angles of 104(1)° and 102(1)° all attest to this crowding. The structural features of **135** correlate very well with those of 1,2,3,4-tetraphenyl-1,2-diphosphetene.[94]

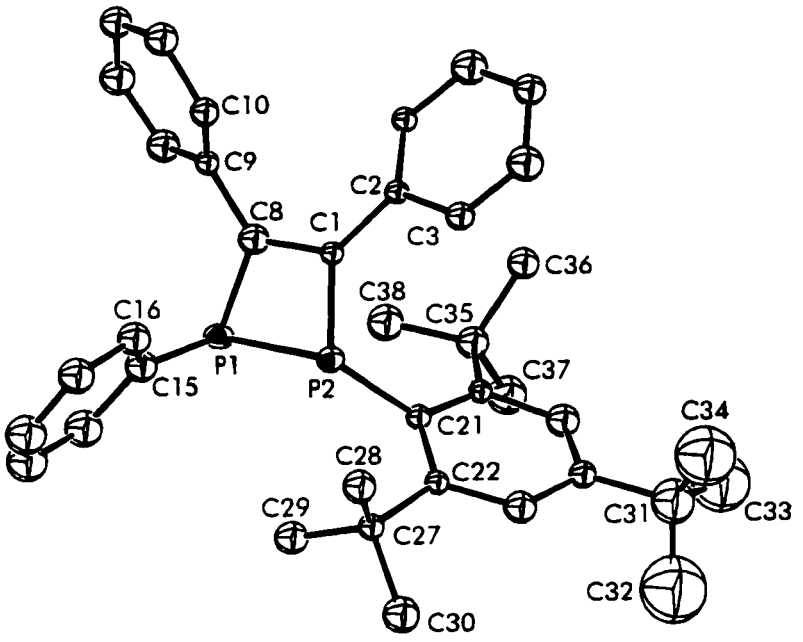

Figure 5.2 ORTEP drawing of **135**; 30% thermal ellipsoids are shown, hydrogen atoms have been omitted for clarity. Selected bond distances and angles: P(1)-P(2) 2.253(9) Å; P(1)-C(8) 1.79(2) Å; P(2)-C(1) 1.76(2) Å; P(2)-P(1)-C(8) 73.8(8)°; P(1)-P(2)-C(1) 76.1(8)°.

1,2-Diphosphetenes were discovered in 1964 by Mahler.[95] Since that time several organic synthetic routes to these species have been developed,[96] the most satisfactory being reported by Mathey *et al.*[94] The ring contraction of 1,2,3-triphospholenes occurs via reaction with lithium to remove (PR), followed by ring closure with phosgene to yield 1,2-diphosphetenes in fair yields. Unsymmetrical alkynes may be incorporated in the parent 1,2,3-triphospholene, thus the subsequent 1,2-diphosphetene may possess an unsymmetrical substitution pattern with respect to the ring carbon atoms. However, the lack of synthetic routes to 1,2,3-triphospholenes with differing substituents on

phosphorus prohibits the introduction of these substitution patterns in the 1,2-diphosphetenes. In contrast, phosphametallacyclobutenes are amenable to versatility in each ring substituent.

The analogous reaction of **117** with phenylboron dichloride also proceeded to give Cp_2ZrCl_2 and a yellow crystalline product. The ^{31}P NMR spectrum consisted of a P-H coupled doublet of doublets at -35.3 ppm ($|{}^1J_{P\text{-}H}|$ = 371.4 Hz, $|J|$ = 31.9 Hz), while ^1H and $^{13}C\{^1H\}$ NMR spectra both indicated only two *t*-butyl groups remained intact on the supermesityl substituent. The remaining *t*-butyl group had evidently undergone C-H activation, as two inequivalent methyl groups and a methylene fragment were also suggested. Compound **136** was thus formulated as $\overline{PH(C_6H_2\text{-}(2\text{-}CH_2C(CH_3)_2)\text{-}4,6\text{-}t\text{-}Bu_2)B(Ph)CPh{=}CPh}$, which was subsequently confirmed through a crystallographic study (Fig. 5.3).

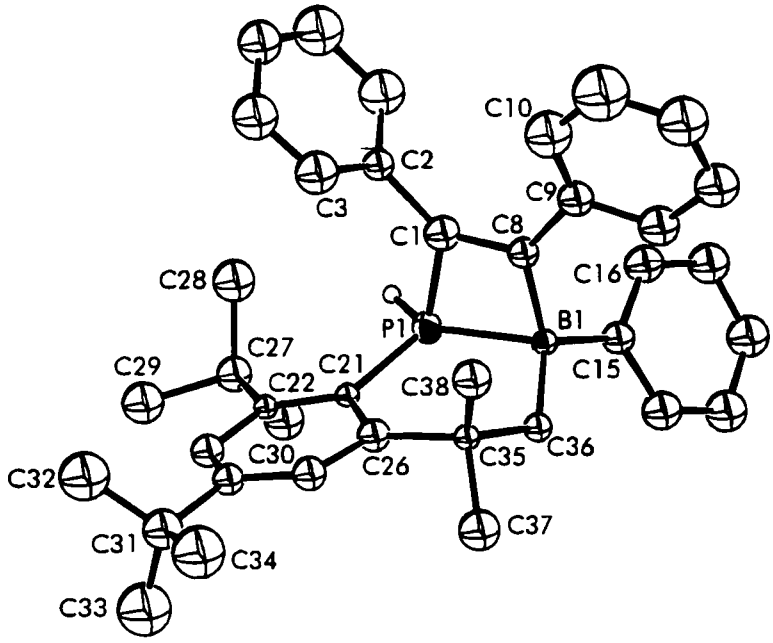

Figure 5.3 ORTEP drawing of **136**; 30% thermal ellipsoids are shown, hydrogen atoms have been omitted for clarity. Selected bond distances and angles: P(1)-B(1) 1.99(2) Å; P(1)-C(1) 1.80(2) Å; B(1)-C(8) 1.62(2) Å; B(1)-C(36) 1.65(2) Å; C(1)-P(1)-B(1) 78.8(8)°; C(21)-P(1)-B(1) 117.0(7)°; P(1)-B(1)-C(8) 79(1)°; P(1)-B(1)-C(36) 102(1)°.

The structure of **136** revealed that C-H activation of one of the *ortho-t*-Bu groups had indeed occurred. The structure consists of a five- and a four-membered ring, fused via a P(1)-B(1) dative bond. The P(1)-B(1) bond length of 1.99(2) Å is comparable to that of adducts such as H_3PBH_3 and Me_3PBH_3 (ca. 1.93 Å).[97] The location of the P-H hydrogen establishes the pseudo-tetrahedral geometry at this site. The geometry about boron is also best described as a distorted tetrahedron.

A number of heterocycles containing boron, phosphorus and carbon atoms in the ring have been synthesized through salt and phosphine elimination reactions; however, these species all contain two or more phosphorus and/or boron atoms in the ring.[98] The formation of **136** is likely to proceed through metallacycle transfer to boron, resulting in the formation of an intermediate analogous to **135** and one equivalent of Cp_2ZrCl_2 as the by-product. Subsequent C-H activation of the *ortho-t*-butyl group effects the ring expansion (Eq. 5.4).

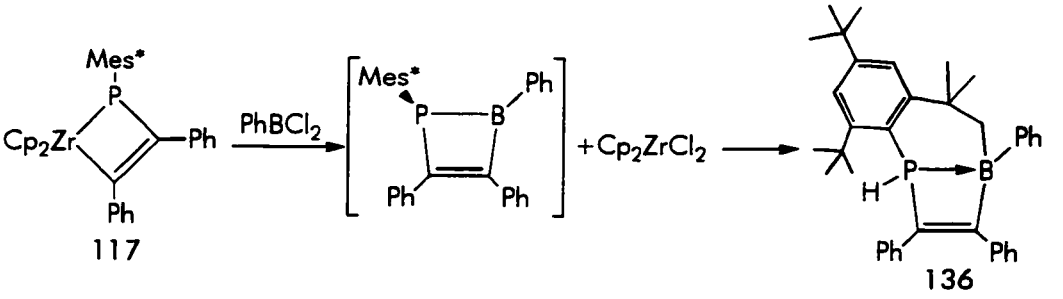

117 136 **(5.4)**

A similar process has been observed in the attempted synthesis of Br_2BPMes_2, in which C-H activation of one of the *ortho*-methyl groups of a mesityl substituent led to the formation of heterocycle **137**.[99] The formation of **136** and **137** illustrates that sterically demanding substituents are not always innocuous.

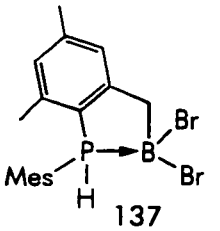

137

Metallacycle transfer from diphosphametallacyclopentene 122

The versatility of phosphametallacycles can also be employed in the synthesis of an unsymmetrical 1,2,3-triphospholene. The reaction of diphosphametallacyclopentene **122** with phenyldichlorophosphine yielded Cp_2ZrCl_2 and **138** in 46% yield (Eq. 5.5). **138** exhibited P-P coupled signals in the ^{31}P NMR spectrum at 33.7, 15.6 and -58.2 ppm, the last being attributable to the central phosphorus atom of the ring. The P-P coupling constants were compatible with a P(Mes)-P(Mes)-P(Ph) fragment.

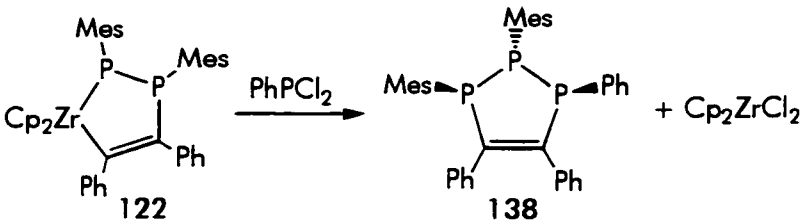

(5.5)

P(Ph)P(Mes)P(Mes)C(Ph)=CPh **138** was crystallographically characterized, which is apparently the first crystallographic study of an uncomplexed triphospholene.

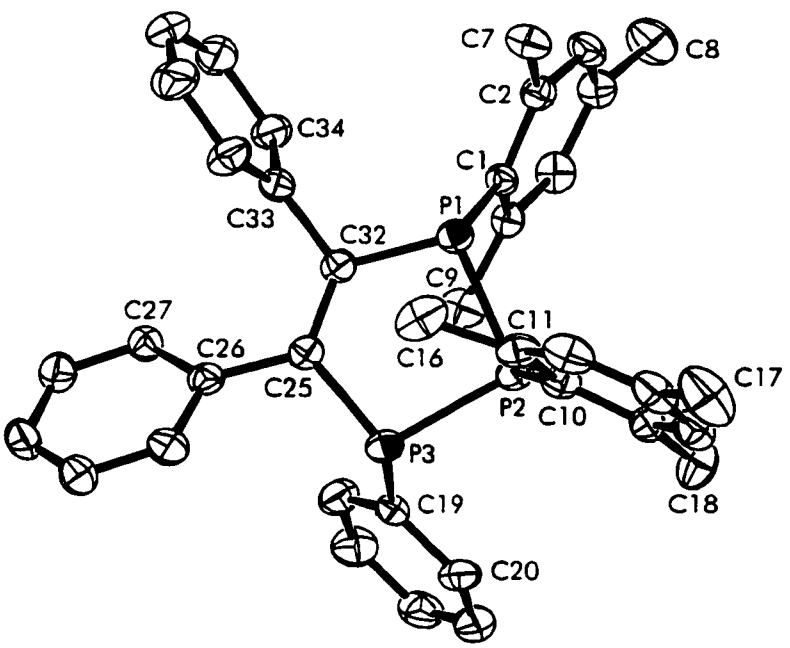

Figure 5.4 ORTEP drawing of **138**; 30% thermal ellipsoids are shown, hydrogen atoms have been omitted for clarity. Selected bond distances and angles: P(1)-P(2) 2.200(2) Å; P(2)-P(3) 2.207(3) Å; P(1)-C(32) 1.818(7) Å; P(3)-C(25) 1.838(6) Å; P(2)-P(1)-C(32) 99.0(2)°; P(2)-P(3)-C(25) 99.4(2)°.

The structural parameters of **138** are comparable to those of the related 1,2,3-triphenyl-1,2,3-triphosphaindane **139**.[100] The mesityl group on P(2) is *trans* to both the mesityl group on P(1) and the phenyl group on P(3). The non-planarity of the metallacycle is indicated by the P(1)-P(2)-P(3)-C(25) and P(3)-P(2)-P(1)-C(32) torsion angles of 11.8(2)° and -12.8(2)°, respectively. The P-P bond lengths of 2.200(2) Å and 2.207(3) Å are analogous to those of **139**.

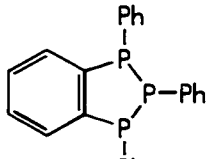

139

A number of triphospholenes have been reported in the literature.[94, 96, 101] These compounds are generally prepared either by reaction of *cis*-1,2-dichloroalkenes with $(PR)_3$ dianions or by reaction of cyclopolyphosphines with alkynes. These procedures are limited with respect to the introduction of differing substituents on the phosphorus atoms. The use of diphosphametallacyclopentene **122** is less restricted, allowing for variation in the third PR group.

Metallacycle transfer from zirconocene triphosphanato complex 133

The facile metallacycle transfer reactions of **117** and **122** can be partly attributed to the reactive nature of the Zr-P bond. Due to this characteristic, we reasoned that the known triphosphanato metallacycle $Cp_2Zr(PPh)_3$ **133**[42, 102] should also readily undergo metallacycle transfer. Such reactions were indeed observed to provide routes to main group phosphacycles (Eq. 5.6).

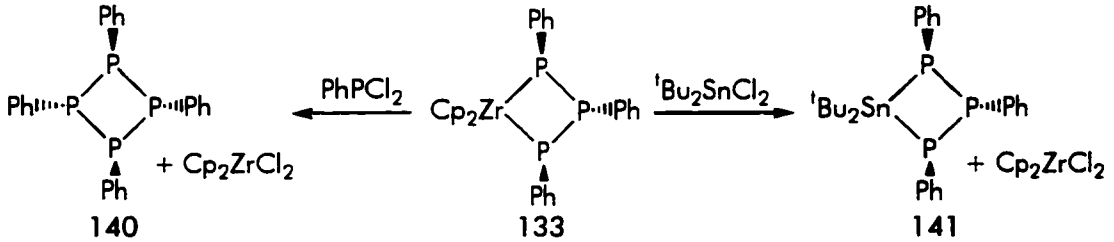

140 **133** **141** **(5.6)**

For example, the reaction of **133** with phenyldichlorophosphine rapidly produced Cp_2ZrCl_2 and the known phosphacycle $P(Ph)_4$ **140**. **140** has been previously synthesized via the reaction of $K_2(PPh)_3$ or $(Me_3Si)_2(PPh)_3$ with phenyldichlorophosphine by Baudler *et al.*[92] In the present studies, the structural characterization of **140** has also been performed. Compound **140** crystallizes in the space group $P2_12_12$, and sits on a crystallographic twofold axis. The so-called "all-*trans*" form indicated by the NMR data is thus confirmed by this crystal structure.

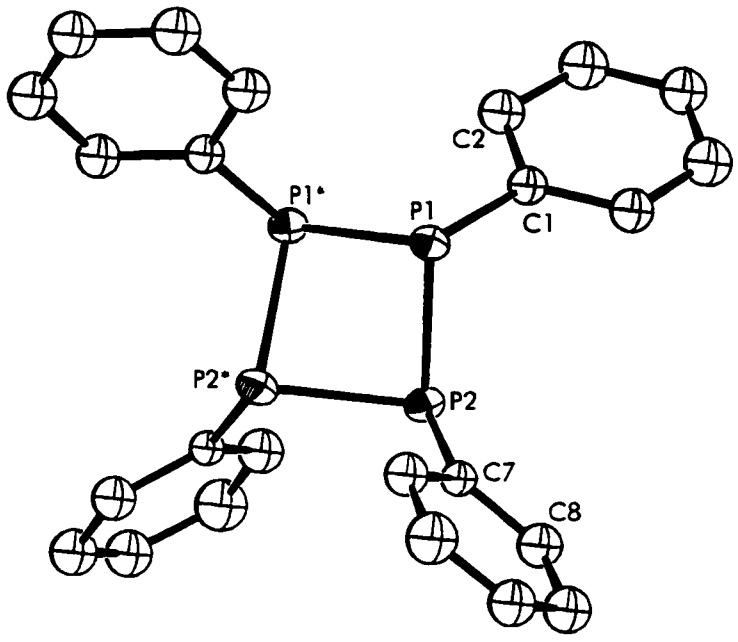

Figure 5.5 ORTEP drawing of **140**; 30% thermal ellipsoids are shown, hydrogen atoms have been omitted for clarity. Selected bond distances and angles: P(1)-P(1)* 2.218(6) Å; P(1)-P(2) 2.240(4) Å; P(2)-P(2)* 2.232(6) Å; P(1)*-P(1)-P(2) 84.6(1)°; P(1)-P(2)-P(2)* 84.2(1)°.

The reaction of **133** with one equivalent of di-*t*-butyltin dichloride yielded compound **141**, which exhibited a ^{31}P NMR spectrum consisting of a triplet at -51.3 ppm and a doublet at -70.5 ppm; the signals were coupled to each other ($|J_{P\text{-}P}|$ = 140 Hz) and the latter exhibited tin satellites. The NMR data supported the formulation of **141** as $(t\text{-Bu})_2Sn(PPh)_3$, which was confirmed by a crystallographic study. The Sn-P distances of **141** (ca. 2.54 Å) compare well to those of $(t\text{-Bu}_2SnPMes^*)_2$ **104**.

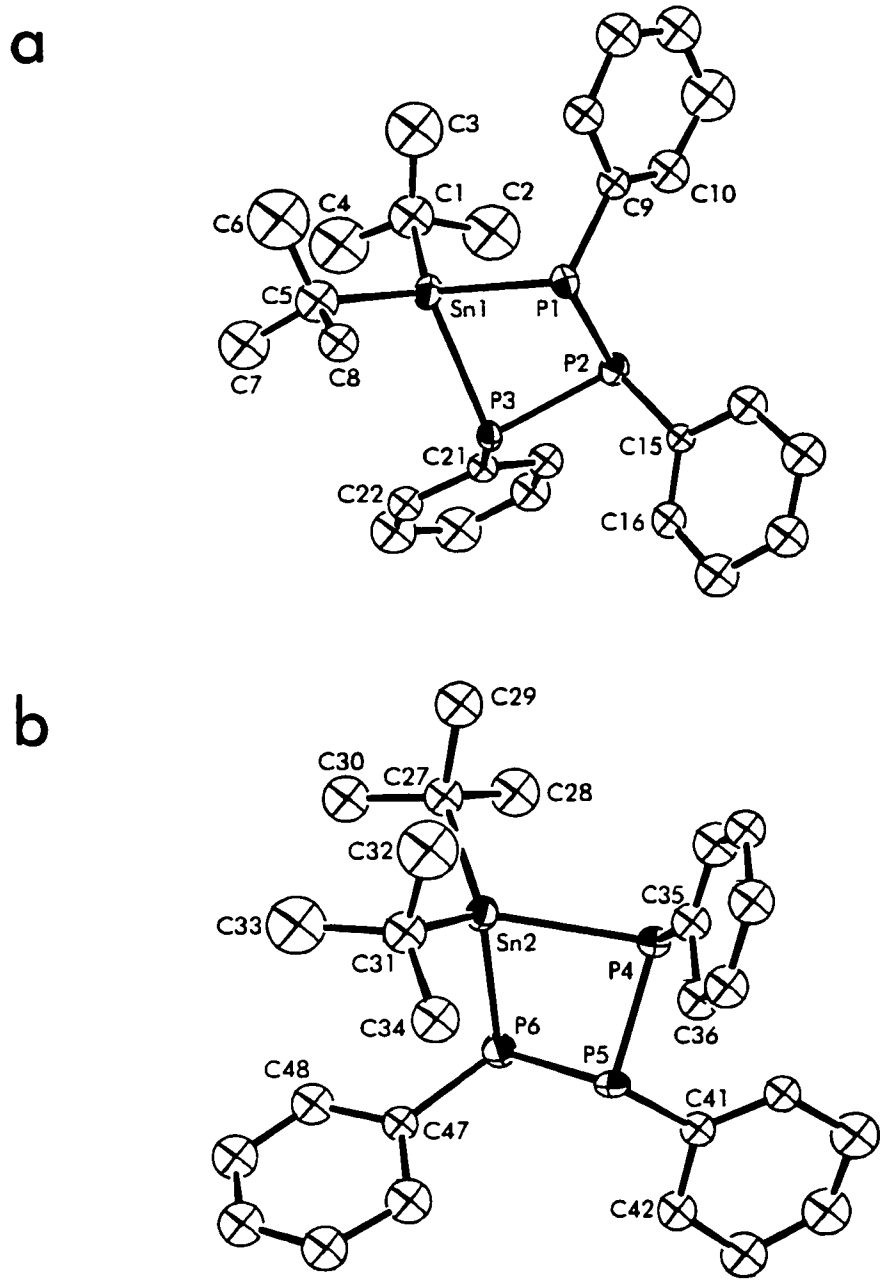

Figure 5.6 ORTEP drawing of the two molecules of **141** in the asymmetric unit, 30% thermal ellipsoids are shown, hydrogen atoms have been omitted for clarity. Selected bond distances and angles: (a) Sn(1)-P(1) 2.538(8) Å; Sn(1)-P(3) 2.549(7) Å; Sn(1)-P(1)-P(2) 83.3(3)°; Sn(1)-P(3)-P(2) 83.1(3)°; P(1)-P(2)-P(3) 92.2(4)°. (b) Sn(2)-P(4) 2.533(8) Å; Sn(2)-P(6) 2.538(8) Å; Sn(2)-P(4)-P(5) 83.0(3)°; Sn(2)-P(6)-P(5) 82.4(3)°; P(4)-P(5)-P(6) 92.4(4)°.

Similar to **140**, steric congestion in **141** is minimized by an "all-*trans*" arrangement of the phenyl substituents. The structure of **141** is consistent with that proposed for

$Et_2Sn(P^tBu)_3$, which was one of a number of products derived from the reaction of K(^{t}Bu)P-P(^{t}Bu)K with Et_2SnCl_2.[59b] Although tin-phosphorus heterocycles have been synthesized in the past,[59] both **104** and **141** are rare examples of the structural characterization of these species.

5.4 Conclusion

In conclusion, the phosphametallacycles studied herein readily undergo metallacycle transfer reactions with main group dihalides. Along with Equation 5.1, these reactions are rare examples of metallacycle transfer from heteroatom-containing metallacycles. The reactive nature of the Zr-P bond is again highlighted by the reactions of phosphametallacyclobutene **117**, diphosphametallacyclopentene **122** and triphosphanato complex **133**. These complexes offer several advantages as potential synthons for novel main group phosphacycles, such as the possibility of substitution patterns that are not available by conventional syntheses. The reactions that have been explored here have demonstrated these points.

The studies described in Chapter Four have provided the foundation for the use of phosphametallacyclobutenes and the as yet unique diphosphametallacyclopentene as precursors to main group phosphacycles. Further development of synthetic routes to these species, along with exploration of their phosphametallacycle transfer reactions, will be necessary to advance this fledgling area of research. In contrast, numerous synthetic routes to precursors of the form $Cp_2Zr(PR)_3$ have been established.[42, 102] These studies, combined with the present work, have laid the groundwork for the application of $Cp_2Zr(PR)_3$ to the preparation of a host of main group phosphacycles.

Chapter Six
Summary

The studies described herein have provided vital information about zirconium phosphorus chemistry. The first area of focus has been on the stabilization and reactivity of terminal phosphinidene complexes, and these efforts have engendered a second major avenue of research concerned with the chemistry of phosphametallacycles.

The first synthetic goal of this project was the preparation of a terminal phosphinidene complex of zirconium. Several fundamental reactions illustrated the feasibility of this objective. Trapping a [Cp_2Zr=PR] intermediate with ketone or nitrile was barred by the reactive nature of the Zr-P single bond, since insertions rapidly occur at this site. The stabilization of the Zr=P multiple bond required an extremely sterically demanding substituent on phosphorus. When less bulky substituents were used, the Cp_2Zr(PHR)Me intermediate underwent a bimolecular loss of primary phosphine. Alternative synthetic routes resulted in the dimerization of [Cp_2Zr=PR] and subsequent C-H bond activation of the cyclopentadienyl ring. The use of the supermesityl substituent on phosphorus obviated both dimerizations and bimolecular reactions of Cp_2Zr(PHMes*)Me **72**, and intramolecular loss of methane generated [Cp_2Zr=PMes*]. Trapping with PMe_3 furnished the first stable terminal phosphinidene complex of zirconium (Cp_2Zr=PMes*)(PMe_3) **84**.

Reactivity studies of **84** proved to be extremely fruitful. Complex **84** participated in a number of metathetical reactions with organic reagents, as well as some of their lower congeners. The phosphinidene moiety of **84** could be exchanged for an oxo, sulfido or two chloride groups, resulting in the formation of an assortment of organophosphorus derivatives and the corresponding zirconocene oxide, sulfide or dichloride. Similar reactions of **84** with C-N multiple bonds effected phosphinidene transfer to carbon. 1,2-Addition reactions of polar E-H bonds across the Zr-P double

bond of **84** is a facile route to complexes of the form $Cp_2Zr(PHMes^*)(ER)$ and $Cp_2Zr(PHMes^*)(EHR)$. The metal-mediated inversion of the pyramidal phosphide ligands was established by variable temperature NMR studies. These investigations also indicated that Zr-E π-interactions are generally weak, yet they influence the ^{31}P NMR chemical shift as well as the energetics of inversion at the phosphide ligand.

Investigations of [2+2] cycloaddition reactions of **84** or $[Cp_2Zr{=}PMes^*]$ with alkynes led to the second major area of research. These reactions furnished the first examples of phosphametallacyclobutenes, while a novel diphosphametallacyclopentene resulted from reactions incorporating the mesityl substituent on phosphorus. Insertions of unsaturated polar organic molecules occurred exclusively at the Zr-P bond of phosphametallacyclobutene $Cp_2Zr(P(Mes^*)C(Ph){=}CPh)$ **117**, and thus have extended the family of phosphametallacycles to encompass four-, five- and six-membered rings. Variable temperature NMR and crystallographic studies of these complexes have revealed the influential role that sterics play in phosphametallacycles. Steric congestion provokes reduced inversion barriers at phosphorus as well as [4+2] retrocycloadditions. Reduction of the sterics of specific substituents resulted in stable, non-fluxional metallacycles. Furthermore, the high degree of P/C diastereoselectivity in these cases augurs well for future applications of these metallacycles in enantioselective syntheses.

While the above studies have established fundamental properties of phosphametallacycles, these species are also appealing from a metal-mediated synthetic standpoint. Phosphametallacycles readily underwent metallacycle transfer reactions with main group dihalides, to furnish heterocycles containing (PR), $(PR)_2$ and $(PR)_3$ units. Advantages offered by these complexes as synthons for main group phosphacycles include the viability of substitution patterns that are not available by conventional syntheses.

In conclusion, this research has established the chemistry of both zirconium phosphinidene complexes and phosphazirconacycles. The reactive nature of both the

Zr-P single bond and the Zr=P multiple bond is a consistent theme throughout these studies. This attribute has dominated the reactivity of these complexes, and distinguishes this chemistry from that of imido, oxo and sulfido derivatives. The fundamental studies described herein lay the foundation for further progress in both the understanding and application of these unique complexes.

References

1. Fischer, E. O.; Maasböl, A. *Angew. Chem., Int. Ed. Eng.* **1964**, *3*, 580.
2. Schrock, R. R. *J. Organomet. Chem.* **1986**, *300*, 249.
3. Nugent, W. A.; Mayer, J. M. *Metal-Ligand Multiple Bonds*; John Wiley & Sons: New York, NY, 1988, and references cited therein.
4. Labinger, J. A. in *Comprehensive Organometallic Chemistry Volume* 2 Wilkinson, G.; Stone, F. G. A.; Abel, E. W. Eds., Pergamon Press: New York, 1982.
5. (a) Tebbe, F. N.; Harlow, R. L. *J. Am. Chem. Soc.* **1980**, *102*, 6151. (b) McKinney, R. J.; Tulip, T. H.; Thorn, D. L.; Coolbaugh, T. S.; Tebbe, F. N. *J. Am. Chem. Soc.* **1981**, *103*, 5584.
6. Tebbe, F. N.; Parshall, G. W.; Reddy, G. S. *J. Am. Chem. Soc.* **1978**, *100*, 3611.
7. Wittig, G. *J. Organomet. Chem.* **1975**, *100*, 279.
8. Howard, T. R.; Lee, J. B.; Grubbs, R. H. *J. Am. Chem. Soc.* **1980**, *102*, 6878.
9. Wood, C. D.; McLain, S. J.; Schrock, R. R. *J. Am. Chem. Soc.* **1979**, *101*, 3210.
10. Cowley, A. H.; Barron, A. R. *Acc. Chem. Res.* **1988**, *21*, 81.
11. (a) Carney, M. J.; Walsh, P. J.; Hollander, F. J.; Bergman, R. G. *J. Am. Chem. Soc.* **1989**, *111*, 8751. (b) Carney, M. J.; Walsh, P. J.; Bergman, R. G. *J. Am. Chem. Soc.* **1990**, *112*, 6426. (c) Carney, M. J.; Walsh, P. J.; Hollander, F. J.; Bergman, R. G. *Organometallics* **1992**, *11*, 761. (d) Vaughan, G. A.; Hillhouse, G. L.; Rheingold, A. L. *J. Am. Chem. Soc.* **1990**, *112*, 7994.
12. (a) Goedkin, V. L.; Ladd, J. A. *J. Chem. Soc., Chem. Commun.* **1982**, 142. (b) Yang, C. H.; Ladd, J. A.; Goedkin, V. L. *J. Coord. Chem.* **1988**, *19*, 235. (c) Goedkin, V. L.; Weiss, M. C. *Inorg. Synth.* **1980**, *20*, 115. (d) Bodner, A.; Jeske, P.; Weyhermuller, T.; Wieghardt, K.; Dubler, E.; Schmalle, H.; Nuber, B. *Inorg. Chem.* **1992**, *31*, 3737.
13. Jacoby, D.; Floriani, C.; Chiesi-Villa, A.; Rizzoli, C. *J. Am. Chem. Soc.* **1993**, *115*, 7025.

14. (a) Housmekerides, C. E.; Pilato, R. S.; Geoffroy, G. L.; Rheingold, A. L. *J. Chem. Soc., Chem. Commun.* **1991**, 563. (b) Housmekerides, C. E.; Ramage, D. L.; Kretz, C. M.; Shontz, J. T.; Pilato, R. S.; Geoffroy, G. L.; Rheingold, A. L.; Haggerty, B. S. *Inorg. Chem.* **1992**, *31*, 4453.

15. (a) Smith III, M. R.; Matsunaga, P. T.; Andersen, R. S. *J. Am. Chem. Soc.* **1993**, *115*, 7049. (b) Polse, J. L.; Andersen, R. A.; Bergman, R. G. *J. Am. Chem. Soc.* **1995**, *117*, 5393.

16. Ketzelnigg, W. *Angew. Chem., Int. Ed. Engl.* **1984**, *23*, 272.

17. Christou, V.; Arnold, J. *J. Am. Chem. Soc.* **1992**, *114*, 6240.

18. (a) Howard, W. A.; Waters, M.; Parkin, G. *J. Am. Chem. Soc.* **1993**, *115*, 4917. (b) Howard, W. A.; Parkin, G. *Organometallics* **1993**, *12*, 2362. (c) Howard, W. A.; Parkin, G. *J. Am. Chem. Soc.* **1994**, *116*, 606.

19. Walsh, P. J.; Hollander, F. J.; Bergman, R. G. *J. Am. Chem. Soc.* **1988**, *110*, 8729.

20. (a) Cummins, C. C.; Baxter, S. M.; Wolczanski, P. T. *J. Am. Chem. Soc.* **1988**, *110*, 8731. (b) Schaller, C. P.; Bonanno, J. B.; Wolczanski, P. T. *J. Am. Chem. Soc.* **1994**, *116*, 4133.

21. Roesky, H. W.; Voeler, H.; Witt, M.; Noltmeyer, M. *Angew. Chem., Int. Ed. Engl.* **1990**, *29*, 669.

22. (a) Cummins, C. C.; Schaller, C. P.; Van Duyne, G. D.; Wolczanski, P. T.; Chan, A. W. E.; Hoffmann, R. *J. Am. Chem. Soc.* **1991**, *113*, 2985. (b) Bennett, J. L.; Wolczanski, P. T. *J. Am. Chem. Soc.* **1994**, *116*, 2179.

23. Walsh, P. J.; Hollander, F. J.; Bergman, R. G. *Organometallics* **1993**, *12*, 3705.

24. (a) Walsh, P. J.; Carney, M. J.; Bergman, R. G. *J. Am. Chem. Soc.* **1991**, *113*, 6343. (b) Walsh, P. J.; Baranger, A. M.; Bergman, R. G. *J. Am. Chem. Soc.* **1992**, *114*, 1708. (c) Baranger, A. M.; Walsh, P. J.; Bergman, R. G. *J. Am. Chem. Soc.* **1993**, *115*, 2753.

25. Hanna, T. A.; Baranger, A. M.; Walsh, P. J.; Bergman, R. G. *J. Am. Chem. Soc.* **1995**, *117*, 3292.

26. (a) Doxsee, K. M.; Farahi, J. B. *J. Chem. Soc., Chem. Commun.* **1990**, 1452. (b) Doxsee, K. M.; Farahi, J. B.; Hope, H. *J. Am. Chem. Soc.* **1991**, *113*, 8889.

27. (a) Hill, J. E.; Profilet, R. D.; Fanwick, P. E.; Rothwell, I. P. *Angew. Chem., Int. Ed. Engl.* **1990**, *29*, 664. (b) Profilet, R. D.; Zambrano, C. H.; Fanwick, P. E.; Nash, J. J.; Rothwell, I. P. *Inorg. Chem.* **1990**, *29*, 4362. (c) Hill, J. E.; Fanwick, P. E.; Rothwell, I. P. *Inorg. Chem.* **1991**, *30*, 1143. (d) Duchateau, R.; Williams, A. J.; Gambarotta, S.; Chiang, M. Y. *Inorg. Chem.* **1991**, *30*, 4863. (e) Bai, Y.; Roesky, H. W.; Noltemeyer, M; Witt, M. *Chem. Ber.* **1992**, *125*, 825. (f) Arney, D. J.; Bruck, M. A.; Huber, S. R.; Wigley, D. E. *Inorg. Chem.* **1992**, *31*, 3749.

28. (a) Mathey, F.; *Angew. Chem., Int. Ed. Engl.* **1987**, *26*, 275. (b) Marinetti, A.; Mathey, F. *Organometallics* **1987**, *6*, 2189.

29. Hitchcock, P. B.; Lappert, M. F.; Leung, W. P. *J. Chem. Soc., Chem. Commun.* **1987**, 1282.

30. Cowley, A. H.; Pellerin, B.; Atwood, J. L.; Bott, S. G. *J. Am. Chem. Soc.* **1990**, *112*, 6734.

31. (a) Cummins, C. C.; Schrock, R. R.; Davis, W. M. *Angew. Chem., Int. Ed. Engl.* **1993**, *32*, 756. (b) Bonanno, J. B.; Wolczanski, P. T.; Lobkovsky, E. B. *J. Am. Chem. Soc.* **1994**, *116*, 11159.

32. Chisholm, M. H.; Folting, K.; Pasterczyk, J. W. *Inorg. Chem.* **1988**, *27*, 3057.

33. Laplaza, C. E.; Davis, W. M.; Cummins, C. C. *Angew. Chem., Int. Ed. Engl.* **1995**, *34*, 2042.

34. Zanetti, N. C.; Schrock, R. R.; Davis, W. M. *Angew. Chem., Int. Ed. Engl.* **1995**, *34*, 2044.

35. (a) Ho, J.; Hou, Z.; Drake, R. J.; Stephan, D. W. *Organometallics* **1993**, *12*, 3145. (b) Ho, J.; Rousseau, R.; Stephan, D. W. *Organometallics* **1994**, *13*, 1918. (b) Ho,

J.; Stephan, D. W. *Inorg. Chem.* **1994**, *33*, 4595. (c) Hou, Z.; Stephan, D. W. *J. Am. Chem. Soc.* **1992**, *114*, 10088.

36. Jordan, R. F. *J. Organomet. Chem.* **1985**, *294*, 321.
37. Cowley, A. H.; Kilduff, J. E.; Newman, T. H.; Pakulski, M. *J. Am. Chem. Soc.* **1982**, *104*, 5820.
38. Hope, H.; Pestana, D. C.; Power, P. P. *Angew. Chem., Int. Ed. Engl.* **1991**, *30*, 691.
39. (a) Cromer, D. T.; Mann, J. B. *Acta Crystallogr. Sect. A: Cryst. Phys. Theor. Gen. Crystallogr.* **1968**, *A24*, 324. (b) *ibid* **1968**, *A24*, 390.
40. Cromer, D. T.; Waber, J. T. *International Tables for X-ray Crystallography*; Knoch Press: Birmingham England, **1974**.
41. Stephan, D. W. *Organometallics* **1990**, *9*, 2718.
42. Hey, E.; Bott, S. G.; Atwood, J. L. *Chem. Ber.* **1988**, *121*, 561.
43. Larsonneur, A. M.; Choukroun, R.; Daran, J. C.; Cuenca, T.; Flores, J. C.; Royo, P. *J. Organomet. Chem.* **1993**, *444*, 83.
44. Arif, A. M.; Cowley, A. H.; Nunn, C. M.; Pakulski, M. *J. Chem. Soc., Chem. Commun.* **1987**, 994.
45. ^{31}P NMR data for Cp_2Zr=PMes*(pyr): 708.4 ppm (s).
46. (a) Hey-Hawkins, E. *Chem. Rev.* **1994**, *94*, 1661. (b) Stephan, D. W.; Nadasdi, T. T. *Coord. Chem. Rev.* **1996**, *147*, 147.
47. Yoshifuji, M.; Toyota, K.; Inamoto, N. *Tetrahedron Lett.* **1985**, *26*, 1727.
48. Etemad-Moghadam, G.; Bellan, J.; Tachon, C.; Koenig, M. *Tetrahedron* **1987**, *43*, 1793.
49. Jouaiti, A.; Geoffroy, M.; Terron, G.; Bernardinelli, G. *J. Am. Chem. Soc.* **1995**, *117*, 2251.
50. Yoshifuji, M.; Toyota, K.; Shibayama, K.; Inamoto, N. *Tetrahedron Lett.* **1984**, *25*, 1809.

51. Appel, R.; Casser, C.; Immenkoppel, M.; Knoch, F. *Angew. Chem., Int. Ed. Eng.* **1984**, *23*, 895.

52. Appel, R.; Immenkoppel, M. *Z. Anorg. Allg. Chem.* **1987**, *553*, 7.

53. Oshikawa, T.; Yamashita, M. *Synthesis*, **1985**, 290.

54. Yoshifuji, M.; Toyota, K.; Inamoto, N. *Chem. Lett.* **1985**, 441.

55. (a) Bottomley, F.; Drummond, D. F.; Egharevba, G. O.; White, P. S. *Organometallics* **1986**, *5*, 1620. (b) Gelmini, L.; Stephan, D. W. *Organometallics* **1987**, *6*, 1515.

56. (a) Goldwaite, H.; Rowsell, D.; Vertal, L. E.; Bowers, M. T.; Cooper, M. A.; Manatt, S. L. *Org. Magn. Reson.* **1983**, *21*, 494. (b) *Phosphorus-31 NMR Spectroscopy in Stereochemical Analysis* Verkade, J. G.; Quin, L. D. Eds., VCH Publishers: Deerfield Beach Fla., 1987.

57. Richter, W. J. *Chem. Ber.* **1983**, *116*, 3293.

58. (a) Ranaivonjatovo, H.; Escudie, J.; Couret, C.; Satge, J. *J. Chem. Soc., Chem. Commun.* **1992**, 1047. (b) Couret, C.; Escudie, J.; Satge, J.; Raharinirina, A.; Andriamizaka, J. D. *J. Am. Chem. Soc.* **1985**, *107*, 8280. (c) Escudie, J.; Couret, C.; Andrianarison, M.; Satge, J. *J. Am. Chem. Soc.* **1987**, *109*, 386. (d) Smit, C. N.; Bickelhaupt, F. *Organometallics* **1987**, *6*, 1156. (e) Cowley, A. H.; Jones, R. A.; Mardones, M. A.; Ruiz, J.; Atwood, J. L.; Bott, S. G. *Angew. Chem., Int. Ed. Engl.* **1990**, *29*, 1150. (f) Hope, H.; Pestana, D. C.; Power, P. P. *Angew. Chem., Int. Ed. Engl.* **1991**, *30*, 691. (g) Waggoner, K. M.; Parkin, S.; Pestana, D. C.; Hope, H.; Power, P. P. *J. Am. Chem. Soc.* **1991**, *113*, 3597. (h) Atwood, J. L.; Cowley, A. H.; Jones, R. A.; Mardones, M. A. *J. Am. Chem. Soc.* **1991**, *113*, 7050. (i) Weber, L. *Chem. Rev.* **1992**, *92*, 1839.

59. (a) Schumann, H.; Benda, H. *Chem. Ber.* **1971**, *104*, 333. (b) Baudler, M.; Suchomel, H. *Z. Anorg. Allg. Chem.* **1983**, *505*, 39.

60. Breen, T. L.; Stephan, D. W. Unpublished results.

61. Davies, A. G.; Smith, P. J. in *Comprehensive Organometallic Chemistry, Volume 2* Wilkinson, G.; Stone, F. G. A.; Abel, E. W. Eds., Pergamon Press: New York, 1982.

62. Nugent, W. A.; Harlow, R. L. *Inorg. Chem.* **1979**, *18*, 2030.

63. Hey-Hawkins, E.; Kurz, S. Z. *Naturforsch.* **1995**, *50b*, 239.

64. Hey-Hawkins, E.; Kurz, S. *J. Organomet. Chem.* **1994**, *479*, 125

65. Vann Bynum, R.; Hunter, W. E.; Rogers, R. D.; Atwood, J. L. *Inorg. Chem.* **1980**, *19*, 2368.

66. Baker, R. T.; Whitney, J. F.; Wreford, S. S. *Organometallics* **1983**, *2*, 1049.

67. Roddick, D. M.; Santarsiero, B. D.; Bercaw, J. E. *J. Am. Chem. Soc.* **1985**, *107*, 4670.

68. Bohra, R.; Hitchcock, P. B.; Lappert, M. F.; Leung, W-P. *J. Chem. Soc., Chem. Commun.* **1989**, 728.

69. (a) Crisp, G. T.; Salem, G.; Stephens, F. S.; Wild, S. B. *J. Chem. Soc., Chem. Commun.* **1987**, 600. (b) Crisp, G. T.; Salem, G.; Wild, S. B. *Organometallics* **1989**, *8*, 2360.

70. (a) Buhro, W. E.; Gladysz, J. A. *Inorg. Chem.* **1985**, *24*, 3507. (b) Buhro, W. E.; Zwick, B. D.; Georgiou, S.; Hutchinson, J. P.; Gladysz, J. A. *J. Am. Chem. Soc.* **1988**, *110*, 2427. (c) Zwick, B. D.; Dewey, M. A.; Knight, D. A.; Buhro, W. E.; Arif A. M.; Gladysz, J. A. *Organometallics* **1992**, *11*, 2673.

71. Jorg, K.; Malisch, W.; Reich, W.; Meyer, A.; Schubert, U. *Angew. Chem., Int. Ed. Engl.* **1986**, *25*, 92.

72. Rogers, J. R.; Wagner, T. P. S.; Marynick, D. S. *Inorg. Chem.* **1994**, *33*, 3104.

73. (a) Hillhouse, G. L.; Bercaw, J. E. *Organometallics* **1982**, *1*, 1025. (b) Hillhouse, G. L.; Bulls, A. R.; Santarsiero, B. D.; Bercaw, J. E. *Organometallics* **1988**, *7*, 1309.

74. (a) Chisholm, M. H.; Cotton, F. A.; Frenz, B. A.; Reichert, W. W.; Shive, L. W.; Stults, B. R. *J. Am. Chem. Soc.* **1976**, *98*, 4469. (b) Chisholm, M. H.; Cotton, F. A.; Extine, M.; Stults, B. R. *J. Am. Chem. Soc.* **1976**, *98*, 4477.

75. (a) Huffman, J. C.; Moloy, K. G.; Marsella, J. A.; Caulton, K. G. *J. Am. Chem. Soc.* **1980**, *102*, 3009. (b) Marsella, J. A.; Moloy, K. G.; Caulton, K. G. *J. Organomet. Chem.* **1980**, 201, 389.

76. (a) Macdonell, G. D.; Berlin, K. D.; Baker, J. R.; Ealick, S. E.; van der Helm, D.; Marsi, K. L. *J. Am. Chem. Soc.* **1978**, *100*, 4535. (b) Schmidbaur, H.; Schier, A.; Lauteschlager, S.; Reide, J.; Muller, G. *Organometallics* **1984**, *3*, 1906.

77. Lauher, J.; Hoffmann, R. *J. Am. Chem. Soc.* **1976**, *98*, 1729.

78. (a) Wulff, W. in *Advances in Metal-Organic Chemistry Volume 1* Liebeskind, L. S. Ed., Jai Press Inc.: Greenwich, CT, 1989. (b) Herndon, J. W.; Tumer, S. U.; McMullen, L. A.; Matasi, J. J.; Schnatter, W. F. K. in *Advances in Metal-Organic Chemistry Volume 3* Liebeskind, L. S. Ed., Jai Press Inc.: Greenwich, CT, 1994.

79. (a) Hey-Hawkins, E.; Lindenberg, F. *Chem. Ber.* **1992**, *125*, 1815. (b) Lindenberg, F.; Hey-Hawkins, E. *Z. Anorg. Allg. Chem.* **1995**, *621*, 1531.

80. Kurz, S.; Hey-Hawkins, E. *J. Organomet. Chem.* 1993, *462*, 203.

81. Walsh, P. J.; Hollander, F. J.; Bergman, R. G. *J. Organomet. Chem.* **1992**, *428*, 13.

82. Cardin, D. J.; Lappert, M. F.; Raston, C. L. *Chemistry of Organo-Zirconium and -Hafnium Compounds*; John Wiley & Sons: New York, NY, 1986, pp 221-223.

83. Tatsumi, K.; Nakamura, A.; Hofmann, P.; Stauffert, P.; Hoffmann, R. *J. Am. Chem. Soc.* **1985**, *107*, 4440.

84. Cámpora, J.; Buchwald, S. L. *Organometallics* **1995**, *14*, 2039.

85. While we were able to determine that the rate of reaction did not depend on concentrations of either benzaldehyde or styrene oxide, rate constants have not been included due to unavoidable problems with decomposition.

86. Doxsee, K. M.; Mouser, J. K. M. *Tetrahedron Lett.* **1991**, *32*, 1687.

87. Breen, T. L.; Stephan, D. W. Unpublished results.

88. Buchwald, S. L.; Nielson, R. B. *Chem. Rev.* **1988**, *88*, 1047, and references cited therein.

89. Fagan, P. J.; Nugent, W. A. *J. Am. Chem. Soc.* **1988**, *110*, 2310.

90. Doxsee, K. M.; Shen, G. S.; Knobler, C. B. *J. Am. Chem. Soc.* **1989**, *111*, 9129.

91. Fagan, P. J.; Nugent, W. A.; Calabrese, J. C. *J. Am. Chem. Soc.* **1994**, *116*, 1880, and references cited therein.

92. Baudler, M.; Reuschenbach, G. *Z. Anorg. Allg. Chem.* **1980**, *464*, 9.

93. $Cp_2Zr(OPh)_2$ was detected in the ^1H NMR spectrum by comparison with an authentic sample. Wailes, P. C.; Coutts, R. S. P.; Weigold, H. *Organometallic Chemistry of Titanium, Zirconium and Hafnium*; Academic Press Inc.: New York, NY, 1974.

94. Charrier, C.; Guilhem, J.; Mathey, F. *J. Org. Chem.* **1981**, *46*, 3.

95. Mahler, W. *J. Am. Chem. Soc.* **1964**, *86*, 2306.

96. Charrier, C.; Maigrot, N.; Mathey, F.; Robert, F.; Jeannin, Y. *Organometallics* **1986**, *5*, 623, and references cited therein.

97. Bryan, P. S.; Kuczkowski, R. L. *Inorg. Chem.* **1972**, *11*, 553.

98. Paine, R. T.; Nöth, H. *Chem. Rev.* **1995**, *95*, 343.

99. Karsch, H. H.; Hanika, G.; Huber, B.; Meindl, K.; König, S.; Krüger, C.; Müller, G. *J. Chem. Soc., Chem. Commun.* **1989**, 373.

100. Daly, J. J. *J. Chem. Soc. (A)* **1966**, 1020.

101. (a) Baudler, M.; Tolle, E. *Z. Naturforsch.* **1978**, *33 b*, 691. (b) Baudler, M.; Tolls, E.; Clef, E.; Koch, D.; Kloth, B. *Z. Anorg. Allg. Chem.* **1979**, *456*, 5.

102. (a) Issleib, K.; Wille, G.; Krech, F. *Angew. Chem., Int. Ed. Engl.* **1972**, *11*, 527. (b) Köpf, H.; Voigtlander, R. *Chem. Ber.* **1981**, *114*, 2731. (c) Benac, B.; Jones, R. A. *Polyhedron* **1989**, *8*, 1774. (c) Ho, J.; Breen, T. L.; Ozarowski, A.; Stephan, D. W. *Organometallics* **1993**, *12*, 3145.

Appendix One
Supplementary Crystallographic Parameters for 73, 79, 81 and 84

Table A1.1: Positional Parameters and B(eq) for 73

Atom	x	y	z	B(eq)	Atom	x	y	z	B(eq)
Zr(1)	-0.08	-0.01684(7)	-0.33	2.96(3)	C(21)	0.337(2)	-0.1999(9)	-0.2702(9)	4.7(4)
P(1)	0.0073(4)	-0.1603(2)	-0.4973(2)	2.8(1)	C(22)	0.406(2)	-0.1439(9)	-0.2922(9)	4.6(4)
O(1)	-0.0307(8)	-0.1095(5)	-0.3684(5)	2.7(3)	C(23)	0.354(1)	-0.1002(8)	-0.3477(9)	4.4(4)
C(1)	-0.016(2)	-0.066(1)	-0.2062(10)	5.7(5)	C(24)	0.233(1)	-0.1110(8)	-0.3798(8)	3.4(3)
C(2)	0.086(2)	-0.0418(10)	-0.227(1)	5.8(5)	C(25)	-0.033(1)	-0.2475(7)	-0.5409(7)	2.2(3)
C(3)	0.080(2)	0.0329(9)	-0.2345(9)	4.4(4)	C(26)	-0.154(1)	-0.2761(7)	-0.5513(7)	2.6(3)
C(4)	-0.033(2)	0.057(1)	-0.2153(10)	5.3(5)	C(27)	-0.170(1)	-0.3501(8)	-0.5613(8)	3.2(3)
C(5)	-0.086(2)	-0.0039(10)	-0.1960(8)	4.5(4)	C(28)	-0.076(1)	-0.3986(8)	-0.5665(8)	2.9(3)
C(6)	-0.026(2)	0.036(1)	-0.453(1)	5.6(5)	C(29)	0.039(1)	-0.3681(8)	-0.5705(8)	2.8(3)
C(7)	-0.149(2)	0.027(1)	-0.4615(10)	5.9(5)	C(30)	0.061(1)	-0.2952(7)	-0.5609(7)	2.2(3)
C(8)	-0.200(2)	0.0737(10)	-0.4167(9)	4.8(4)	C(31)	-0.275(1)	-0.2288(9)	-0.5567(9)	2.5(4)
C(9)	-0.110(2)	0.111(1)	-0.3797(10)	6.2(5)	C(32)	-0.261(2)	-0.1654(8)	-0.6086(9)	4.2(4)
C(10)	0.004(2)	0.0869(10)	-0.403(1)	6.0(5)	C(33)	-0.306(2)	-0.2047(9)	-0.4836(9)	5.1(4)
C(11)	-0.272(2)	-0.0467(9)	-0.3239(9)	5.7(5)	C(34)	-0.385(2)	-0.272(1)	-0.5923(10)	4.5(5)
C(12)	0.029(1)	-0.1724(7)	-0.3903(7)	2.6(3)	C(35)	-0.094(1)	-0.4818(9)	-0.5727(8)	3.3(3)
C(13)	-0.029(1)	-0.2413(9)	-0.3673(8)	2.5(3)	C(36)	-0.216(1)	-0.5038(10)	-0.5537(9)	5.5(4)
C(14)	-0.126(2)	-0.2394(9)	-0.3267(10)	4.2(4)	C(37)	-0.081(1)	-0.5053(9)	-0.6486(8)	4.7(4)
C(15)	-0.177(2)	-0.304(1)	-0.3014(10)	4.6(5)	C(38)	0.003(2)	-0.521(1)	-0.5198(9)	4.9(4)
C(16)	-0.128(2)	-0.369(1)	-0.321(1)	5.4(6)	C(39)	0.187(2)	-0.2636(9)	-0.5786(9)	3.4(4)
C(17)	-0.033(2)	-0.372(1)	-0.361(1)	4.1(5)	C(40)	0.256(2)	-0.3245(9)	-0.6154(9)	4.5(4)
C(18)	0.014(2)	-0.309(1)	-0.3844(10)	4.3(5)	C(41)	0.271(1)	-0.2406(8)	-0.5110(8)	3.8(4)
C(19)	0.164(1)	-0.1671(7)	-0.3583(8)	2.7(3)	C(42)	0.163(1)	-0.2021(8)	-0.6331(8)	4.1(4)
C(20)	0.218(1)	-0.2106(8)	-0.3041(8)	4.0(4)					

Table A1.2: Selected Bond Distances (Å) for 73

Atom	Atom	Distance	Atom	Atom	Distance
Zr(1)	O(1)	1.926(9)	P(1)	C(12)	1.99(1)
Zr(1)	C(11)	2.27(2)	P(1)	C(25)	1.83(1)
O(1)	C(12)	1.42(2)	C(12)	C(13)	1.51(2)
C(12)	C(19)	1.54(2)			

Table A1.3: Selected Bond Angles (°) for 73

Atom	Atom	Atom	Angle	Atom	Atom	Atom	Angle
O(1)	Zr(1)	C(11)	95.9(5)	Zr(1)	O(1)	C(12)	167.7(9)
C(12)	P(1)	C(25)	109.7(6)	O(1)	C(12)	C(13)	112(1)
P(1)	C(12)	O(1)	101.3(9)	P(1)	C(12)	C(13)	112(1)
P(1)	C(12)	C(19)	111.4(9)	O(1)	C(12)	C(19)	107(1)
C(13)	C(12)	C(19)	111(1)				

Table A1.4: Positional Parameters and B(eq) for 79

Atom	x	y	z	B(eq)	Atom	x	y	z	B(eq)
Zr(1)	0.25774(6)	0.1334(1)	0.40537(5)	2.68(3)	C(15)	0.3151(8)	0.481(2)	0.6922(7)	5.5(4)
Zr(2)	0.39963(6)	0.3293(1)	0.63707(5)	3.12(3)	C(16)	0.4406(7)	0.585(1)	0.5837(7)	4.6(4)
P(1)	0.2840(2)	0.2335(4)	0.5339(1)	3.31(8)	C(17)	0.5002(8)	0.540(2)	0.6436(7)	5.3(4)
C(1)	0.1249(6)	0.198(2)	0.3908(7)	4.2(3)	C(18)	0.5270(6)	0.380(2)	0.6294(6)	4.7(4)
C(2)	0.1379(6)	0.030(2)	0.4150(6)	4.2(4)	C(19)	0.4841(6)	0.325(2)	0.5630(6)	4.1(3)
C(3)	0.1519(7)	-0.070(2)	0.3635(6)	4.5(3)	C(20)	0.4327(6)	0.456(2)	0.5353(6)	4.1(3)
C(4)	0.1487(6)	0.037(2)	0.3069(6)	4.0(3)	C(21)	0.1999(6)	0.274(1)	0.5569(5)	2.7(3)
C(5)	0.1315(6)	0.201(2)	0.3233(7)	4.8(4)	C(22)	0.1699(7)	0.151(1)	0.5894(5)	3.6(3)
C(6)	0.3309(7)	-0.139(2)	0.4274(7)	4.7(4)	C(23)	0.1080(7)	0.181(2)	0.6071(6)	4.7(4)
C(7)	0.3802(6)	-0.010(2)	0.4615(6)	4.2(3)	C(24)	0.0732(6)	0.342(2)	0.5956(5)	4.7(4)
C(8)	0.3912(6)	0.101(1)	0.4096(7)	4.2(3)	C(25)	0.1022(6)	0.465(2)	0.5624(5)	3.9(3)
C(9)	0.3488(8)	0.037(2)	0.3432(6)	4.6(4)	C(26)	0.1626(6)	0.436(1)	0.5421(5)	2.9(3)
C(10)	0.3130(7)	-0.106(2)	0.3549(6)	4.7(4)	C(27)	0.2051(8)	-0.026(2)	0.6092(6)	5.5(4)
C(11)	0.3168(9)	0.316(2)	0.7139(7)	6.3(5)	C(28)	0.0065(7)	0.380(2)	0.6169(6)	6.8(4)
C(12)	0.387(1)	0.282(2)	0.7564(7)	6.2(5)	C(29)	0.1921(6)	0.575(1)	0.5070(5)	3.5(3)
C(13)	0.4288(7)	0.435(3)	0.7586(7)	6.0(4)	C(30)	0.4505(6)	0.058(1)	0.6683(5)	3.3(2)
C(14)	0.3826(10)	0.555(2)	0.7182(7)	5.3(4)	C(31)	0.2728(4)	0.405(1)	0.3532(4)	1.0(2)

Table A1.5: Selected Bond Distances (Å) for 79

Atom	Atom	Distance	Atom	Atom	Distance
Zr(1)	P(1)	2.606(3)	Zr(2)	C(30)	2.33(1)
Zr(1)	C(31)	2.411(8)	P(1)	C(21)	1.84(1)
Zr(2)	P(1)	2.646(3)			

Table A1.6: Selected Bond Angles (°) for 79

Atom	Atom	Atom	Angle	Atom	Atom	Atom	Angle
P(1)	Zr(1)	C(31)	99.4(2)	Zr(1)	P(1)	C(21)	112.6(3)
P(1)	Zr(2)	C(30)	98.1(2)	Zr(2)	P(1)	C(21)	110.3(3)
Zr(1)	P(1)	Zr(2)	136.6(1)				

Table A1.7: Positional Parameters and B(eq) for 81

Atom	x	y	z	B(eq)	Atom	x	y	z	B(eq)
Zr(1)	0.4048(2)	0.6317(1)	-0.0005(2)	3.27(6)	C(18)	0.608(2)	0.604(1)	-0.261(2)	4.4(8)
Zr(2)	0.5655(2)	0.7093(1)	-0.1888(2)	3.20(6)	C(19)	0.674(2)	0.608(1)	-0.186(2)	3.5(7)
P(1)	0.4517(5)	0.7468(3)	-0.0500(5)	3.5(2)	C(20)	0.632(2)	0.613(1)	-0.099(2)	3.9(8)
P(2)	0.4214(5)	0.7116(4)	-0.3420(5)	4.2(2)	C(21)	0.456(2)	0.821(1)	0.020(2)	3.5(6)
C(1)	0.540(2)	0.639(2)	0.135(2)	7(1)	C(22)	0.368(2)	0.860(1)	0.016(2)	5.0(6)
C(2)	0.463(2)	0.673(1)	0.171(2)	5.4(9)	C(23)	0.379(2)	0.925(1)	0.061(2)	5.4(7)
C(3)	0.384(2)	0.626(2)	0.184(2)	5.7(9)	C(24)	0.465(2)	0.942(1)	0.108(2)	5.1(7)
C(4)	0.420(2)	0.562(1)	0.156(2)	5.2(9)	C(25)	0.546(2)	0.905(1)	0.122(2)	5.4(7)
C(5)	0.522(3)	0.570(1)	0.124(2)	5.2(9)	C(26)	0.541(2)	0.840(1)	0.078(2)	5.8(8)
C(6)	0.227(2)	0.654(1)	-0.059(3)	4.9(8)	C(27)	0.276(2)	0.838(1)	-0.035(2)	6.3(8)
C(7)	0.221(2)	0.606(2)	0.012(2)	4.7(8)	C(28)	0.466(2)	1.011(2)	0.145(2)	7.7(9)
C(8)	0.261(2)	0.551(1)	-0.033(3)	5.0(9)	C(29)	0.634(2)	0.802(1)	0.103(2)	6.5(8)
C(9)	0.293(2)	0.567(2)	-0.127(2)	5.2(9)	C(30)	0.426(2)	0.783(1)	-0.424(2)	3.1(5)
C(10)	0.272(2)	0.630(2)	-0.151(2)	5.3(9)	C(31)	0.386(2)	0.837(1)	-0.392(2)	3.8(6)
C(11)	0.734(2)	0.747(2)	-0.240(3)	7(1)	C(32)	0.391(2)	0.895(1)	-0.451(2)	5.1(7)
C(12)	0.730(3)	0.768(2)	-0.144(3)	5(1)	C(33)	0.433(2)	0.890(1)	-0.549(2)	4.4(6)
C(13)	0.654(3)	0.812(2)	-0.147(3)	6(1)	C(34)	0.469(2)	0.834(1)	-0.582(2)	5.3(7)
C(14)	0.610(2)	0.821(1)	-0.248(3)	4.0(8)	C(35)	0.466(2)	0.781(1)	-0.521(2)	4.2(6)
C(15)	0.656(2)	0.778(2)	-0.306(2)	6(1)	C(36)	0.336(2)	0.844(1)	-0.294(2)	4.9(7)
C(16)	0.522(2)	0.6052(10)	-0.113(2)	2.8(6)	C(37)	0.439(2)	0.955(2)	-0.603(2)	8.3(9)
C(17)	0.511(2)	0.5977(10)	-0.215(2)	2.9(6)	C(38)	0.505(2)	0.719(1)	-0.565(2)	5.7(7)

Table A1.8: Selected Bond Distances (Å) for 81

Atom	Atom	Distance	Atom	Atom	Distance
Zr(1)	P(1)	2.586(7)	Zr(2)	P(2)	2.718(7)
Zr(1)	C(16)	2.29(2)	P(1)	C(21)	1.81(2)
Zr(2)	P(1)	2.576(7)			

Table A1.9: Selected Bond Angles (°) for 81

Atom	Atom	Atom	Angle	Atom	Atom	Atom	Angle
P(1)	Zr(1)	C(16)	82.9(6)	Zr(2)	P(1)	C(21)	128.8(8)
P(1)	Zr(2)	P(2)	96.5(2)	Zr(2)	P(2)	C(30)	114.3(7)
Zr(1)	P(1)	Zr(2)	93.3(2)	Zr(1)	C(16)	Zr(2)	103.6(8)
Zr(1)	P(1)	C(21)	132.2(8)				

Table A1.10: Positional Parameters and B(eq) for 84

Atom	x	y	z	B(eq)	Atom	x	y	z	B(eq)
Zr(1)	0.75042(9)	0.0357(2)	0.44554(6)	2.75(3)	C(16)	0.888(1)	0.514(2)	0.6565(10)	8.3(7)
P(1)	0.8393(3)	0.0706(4)	0.5568(2)	3.1(1)	C(17)	0.963(1)	0.301(2)	0.649(1)	9.5(8)
P(2)	0.8350(3)	0.2206(5)	0.3835(2)	4.2(1)	C(18)	0.889(2)	0.421(2)	0.553(1)	11.7(9)
C(1)	0.7815(8)	0.165(1)	0.6083(5)	1.9(3)	C(20)	0.809(1)	0.205(2)	0.2973(8)	8.0(6)
C(2)	0.7193(9)	0.100(1)	0.6390(6)	2.4(3)	C(21)	0.959(1)	0.213(2)	0.4047(10)	8.3(7)
C(3)	0.6493(9)	0.177(1)	0.6551(6)	2.9(4)	C(22)	0.813(1)	0.402(2)	0.3876(8)	7.4(6)
C(4)	0.6442(9)	0.316(1)	0.6493(6)	2.8(4)	C(31)	0.825(1)	-0.194(2)	0.4724(7)	4.2(3)
C(5)	0.7189(10)	0.380(1)	0.6358(6)	2.7(3)	C(32)	0.743(1)	-0.214(2)	0.4303(7)	4.2(3)
C(6)	0.7898(9)	0.309(1)	0.6187(6)	3.0(4)	C(33)	0.749(1)	-0.166(2)	0.3711(7)	4.4(4)
C(7)	0.7238(9)	-0.055(1)	0.6586(6)	3.2(4)	C(34)	0.832(1)	-0.105(2)	0.3768(8)	5.0(4)
C(8)	0.824(1)	-0.094(2)	0.6855(7)	4.7(4)	C(35)	0.8827(10)	-0.124(1)	0.4415(7)	4.1(3)
C(9)	0.681(1)	-0.150(1)	0.6025(6)	4.6(4)	C(41)	0.5831(9)	0.008(1)	0.4410(7)	4.2(3)
C(10)	0.672(1)	-0.084(1)	0.7097(7)	4.7(4)	C(42)	0.6150(10)	0.112(1)	0.4846(7)	3.9(3)
C(12)	0.588(1)	0.522(2)	0.6981(8)	6.6(5)	C(43)	0.641(1)	0.222(2)	0.4560(8)	5.5(4)
C(13)	0.494(1)	0.318(2)	0.6849(8)	6.0(5)	C(44)	0.622(1)	0.191(2)	0.3901(8)	5.1(4)
C(14)	0.511(1)	0.443(2)	0.5905(9)	8.7(7)	C(45)	0.5898(9)	0.062(2)	0.3825(7)	4.3(3)
C(15)	0.879(1)	0.388(2)	0.6171(8)	5.0(5)					

Table A1.11: Selected Bond Distances (Å) for 84

Atom	Atom	Distance	Atom	Atom	Distance
Zr(1)	P(1)	2.505(4)	Zr(1)	P(2)	2.741(5)
P(1)	C(1)	1.82(1)	P(2)	C(20)	1.83(2)
P(2)	C(21)	1.81(2)	P(2)	C(22)	1.82(2)

Table A1.12: Selected Bond Angles (°) for 84

Atom	Atom	Atom	Angle	Atom	Atom	Atom	Angle
P(1)	Zr(1)	P(2)	100.4(1)	Zr(1)	P(1)	C(1)	116.1(4)
Zr(1)	P(2)	C(20)	115.9(7)	Zr(1)	P(2)	C(21)	114.2(7)
Zr(1)	P(2)	C(22)	121.1(7)	C(20)	P(2)	C(21)	102.8(10)
C(20)	P(2)	C(22)	97.6(8)	C(21)	P(2)	C(22)	102.5(9)

Appendix Two
Supplementary Crystallographic Parameters for 104,107b, 108, and 112

Table A2.1: Positional Parameters and B(eq) for 104

Atom	x	y	z	B(eq)	Atom	x	y	z	B(eq)
Sn(1)	0.34974(5)	0.17630(2)	0.39978(5)	2.80(3)	C(25)	0.3026(9)	0.2171(5)	0.688(1)	5.9(6)
Sn(2)	0.36640(5)	0.33301(3)	0.38953(6)	3.17(3)	C(26)	0.3626(8)	0.1058(5)	0.639(1)	6.1(6)
P(1)	0.5067(3)	0.2376(1)	0.4232(4)	8.8(2)	C(27)	0.0758(6)	0.3007(3)	0.2821(7)	2.5(3)
P(2)	0.2056(2)	0.2763(1)	0.3964(2)	2.9(1)	C(28)	0.0563(6)	0.2818(3)	0.1432(7)	2.7(4)
C(1)	0.6436(6)	0.1950(3)	0.3708(8)	2.9(4)	C(29)	-0.0190(6)	0.3196(4)	0.0675(7)	3.1(4)
C(2)	0.7110(7)	0.1597(4)	0.4615(8)	3.4(4)	C(30)	-0.0810(7)	0.3736(4)	0.1215(8)	3.2(4)
C(3)	0.7827(7)	0.1087(4)	0.4112(8)	3.7(4)	C(31)	-0.0746(7)	0.3843(3)	0.2553(8)	3.4(4)
C(4)	0.7975(7)	0.0914(4)	0.2814(8)	3.5(4)	C(32)	-0.0045(6)	0.3487(3)	0.3385(7)	2.8(4)
C(5)	0.7486(7)	0.1332(4)	0.2015(8)	3.7(4)	C(33)	0.1049(7)	0.2195(4)	0.0696(7)	3.2(4)
C(6)	0.6762(6)	0.1856(4)	0.2435(8)	3.3(4)	C(34)	0.0885(7)	0.1716(4)	0.1427(8)	4.3(4)
C(7)	0.7215(8)	0.1753(5)	0.6127(8)	4.5(5)	C(35)	0.2312(8)	0.2158(4)	0.0550(8)	4.2(5)
C(8)	0.632(1)	0.1535(5)	0.663(1)	7.7(8)	C(36)	0.0404(8)	0.2055(4)	-0.0680(8)	5.9(5)
C(9)	0.725(1)	0.2389(6)	0.664(1)	12(1)	C(37)	-0.1553(8)	0.4176(4)	0.0370(9)	4.6(5)
C(10)	0.834(1)	0.1421(8)	0.680(1)	13(1)	C(38)	-0.129(1)	0.4038(6)	-0.101(1)	13(1)
C(11)	0.8705(8)	0.0316(4)	0.229(1)	4.7(5)	C(39)	-0.138(1)	0.4801(5)	0.094(1)	10.1(9)
C(12)	0.847(2)	-0.0162(6)	0.284(2)	23(2)	C(40)	-0.277(1)	0.4163(7)	0.037(2)	14(1)
C(13)	0.991(1)	0.0356(6)	0.256(2)	15(1)	C(41)	-0.0228(7)	0.3642(4)	0.4861(7)	3.4(4)
C(14)	0.843(2)	0.0150(8)	0.087(2)	24(2)	C(42)	-0.1391(8)	0.4038(5)	0.5028(8)	5.7(6)
C(15)	0.6421(8)	0.2318(4)	0.1500(9)	4.1(5)	C(43)	0.0668(9)	0.3992(4)	0.5693(9)	5.8(6)
C(16)	0.527(1)	0.2245(5)	0.070(1)	8.0(7)	C(44)	-0.0237(8)	0.3078(4)	0.5381(9)	5.3(6)
C(17)	0.6404(9)	0.2953(5)	0.226(1)	6.4(6)	C(45)	0.3265(7)	0.3942(4)	0.242(1)	4.2(5)
C(18)	0.731(1)	0.2244(5)	0.057(1)	7.1(7)	C(46)	0.310(1)	0.3615(4)	0.100(1)	6.4(6)
C(19)	0.3905(7)	0.0851(4)	0.2755(9)	4.1(4)	C(47)	0.2127(9)	0.4319(4)	0.269(1)	5.9(6)
C(20)	0.410(1)	0.0875(4)	0.140(1)	6.2(6)	C(48)	0.4187(9)	0.4333(4)	0.257(1)	6.3(6)
C(21)	0.3004(8)	0.0459(4)	0.271(1)	5.8(5)	C(49)	0.4220(8)	0.3902(4)	0.5813(9)	4.6(5)
C(22)	0.5034(8)	0.0577(4)	0.3490(9)	4.8(5)	C(50)	0.3521(9)	0.4533(4)	0.603(1)	6.2(6)
C(23)	0.2961(8)	0.1608(4)	0.5840(9)	4.2(5)	C(51)	0.4102(8)	0.3601(4)	0.692(1)	5.8(6)
C(24)	0.1714(8)	0.1527(4)	0.546(1)	5.6(6)	C(52)	0.5454(8)	0.3940(4)	0.586(1)	5.8(6)

Table A2.2: Selected Bond Distances (Å) for 104

Atom	Atom	Distance	Atom	Atom	Distance
Sn(1)	P(1)	2.524(3)	Sn(1)	P(2)	2.614(2)
Sn(2)	P(1)	2.556(3)	Sn(2)	P(2)	2.557(2)
Sn(1)	C(19)	2.257(8)	Sn(1)	C(23)	2.262(8)
Sn(2)	C(45)	2.240(9)	Sn(2)	C(49)	2.253(8)
P(1)	C(1)	1.862(8)	P(2)	C(27)	1.876(7)

Table A2.3: Selected Bond Angles (°) for 104

Atom	Atom	Atom	Angle	Atom	Atom	Atom	Angle
P(1)	Sn(1)	P(2)	87.30(9)	P(1)	Sn(2)	P(2)	87.87(9)
Sn(1)	P(1)	Sn(2)	93.0(1)	Sn(1)	P(2)	Sn(2)	90.92(7)
P(1)	Sn(1)	C(19)	111.8(2)	P(1)	Sn(1)	C(23)	118.1(3)
P(2)	Sn(1)	C(19)	140.3(2)	P(2)	Sn(1)	C(23)	92.7(2)
C(19)	Sn(1)	C(23)	106.6(3)	P(1)	Sn(2)	C(45)	136.3(2)
P(1)	Sn(2)	C(49)	97.2(3)	P(2)	Sn(2)	C(45)	114.4(2)
P(2)	Sn(2)	C(49)	114.2(3)	C(45)	Sn(2)	C(49)	105.7(3)
Sn(1)	P(1)	C(1)	115.2(3)	Sn(2)	P(1)	C(1)	139.8(3)
Sn(1)	P(2)	C(27)	133.7(2)	Sn(2)	P(2)	C(27)	110.6(2)

Table A2.4: Positional Parameters and B(eq) for 107b

Atom	x	y	z	B(eq)	Atom	x	y	z	B(eq)
Zr(1)	0.6164(3)	0.2456(3)	0.1908(2)	3.5(1)	C(18)	0.846(1)	0.324(2)	0.0422(8)	4.1
P(1)	0.7314(8)	0.2825(7	-0.0225(5)	5.6(7)	C(19)	0.845(1)	0.409(1)	0.071(1)	4.1
P(2)	0.4116(9)	0.1912(8	0.1623(6)	5.1(6)	C(20)	0.911(2)	0.428(1)	0.132(1)	4.1
N(1)	0.626(2)	0.254(2)	0.094(1)	2.3(5)	C(21)	0.977(2)	0.362(2)	0.1641(9)	4.1
C(1)	0.616(1)	0.084(1)	0.229(1)	5.6	C(22)	0.978(1)	0.277(1)	0.135(1)	4.1
C(2)	0.654(2)	0.131(2)	0.289(1)	5.6	C(23)	0.913(2)	0.257(1)	0.074(1)	4.1
C(3)	0.750(2)	0.169(1)	0.280(1)	5.6	C(24)	0.795(1)	0.492(1)	0.026(1)	5.6
C(4)	0.772(2)	0.146(2)	0.215(1)	5.6	C(25)	0.841(2)	0.581(2)	0.058(1)	5.6
C(5)	0.688(2)	0.093(2)	0.183(1)	5.6	C(26)	0.823(2)	0.482(2)	-0.047(1)	5.6
C(6)	0.507(1)	0.372(2)	0.239(1)	6.1	C(27)	0.675(1)	0.493(2)	0.022(1)	5.6
C(7)	0.553(2)	0.409(1)	0.186(1)	6.1	C(28)	1.043(1)	0.381(1)	0.237(1)	8.3
C(8)	0.662(2)	0.411(2)	0.206(1)	6.1	C(29)	1.001(2)	0.463(2)	0.273(2)	8.3
C(9)	0.683(2)	0.374(2)	0.272(1)	6.1	C(30)	1.045(2)	0.298(1)	0.284(2)	8.3
C(10)	0.588(2)	0.350(1)	0.292(1)	6.1	C(31)	1.154(2)	0.401(2)	0.222(1)	8.3
C(11)	0.633(2)	0.253(3)	0.030(1)	2.7(6)	C(32)	0.939(2)	0.160(1)	0.039(1)	7.2
C(12)	0.537(2)	0.216(2)	-0.017(1)	6.4	C(33)	0.944(2)	0.183(2)	-0.037(1)	7.2
C(13)	0.522(2)	0.125(2)	-0.031(1)	6.4	C(34)	1.045(2)	0.122(2)	0.072(1)	7.2
C(14)	0.430(2)	0.094(1)	-0.070(1)	6.4	C(35)	0.852(2)	0.091(2)	0.043(1)	7.2
C(15)	0.353(1)	0.156(2)	-0.096(1)	6.4	C(36)	0.332(2)	0.272(2)	0.110(2)	5(1)
C(16)	0.367(2)	0.247(2)	-0.083(1)	6.4	C(37)	0.383(3)	0.084(3)	0.114(2)	9(1)
C(17)	0.459(2)	0.278(1)	-0.043(1)	6.4	C(38)	0.349(3)	0.170(3)	0.232(2)	9(1)

Table A2.5: Selected Bond Distances (Å) for 107b

Atom	Atom	Distance	Atom	Atom	Distance
Zr(1)	P(2)	2.74(1)	Zr(1)	N(1)	1.93(2)
P(1)	C(11)	1.81(3)	P(1)	C(18)	1.91(2)
P(2)	C(37)	1.86(4	P(2)	C(38)	1.72(5)
N(1)	C(11)	1.29(3)			

Table A2.6: Selected Bond Angles (°) for 107b

Atom	Atom	Atom	Angle	Atom	Atom	Atom	Angle
P(2)	Zr(1)	N(1)	91.2(7)	C(11)	P(1)	C(18)	103(1)
Zr(1)	P(2)	C(36)	111(1)	Zr(1)	P(2)	C(37)	117(1)
Zr(1)	P(2)	C(38)	116(1)	C(36)	P(2)	C(37)	103(1)
C(36)	P(2)	C(38)	106(1)	C(37)	P(2)	C(38)	99(2)
Zr(1)	N(1)	C(11)	175(3)	P(1)	C(11)	N(1)	135(2)
P(1)	C(11)	C(12)	107(1)	N(1)	C(11)	C(12)	116(2)

Table A2.7: Positional Parameters and B(eq) for 108

Atom	x	y	z	B(eq)	Atom	x	y	z	B(eq)
Zr(1)	0.15	0.0486(2)	0.09	3.1(1)	C(20)	0.025(2)	-0.205(2)	0.254(1)	4.2(7)
P(1)	0.0249(6)	-0.2425(6)	0.0465(4)	3.9(4)	C(21)	-0.012(2)	-0.123(3)	0.288(2)	4.8(9)
N(1)	0.153(1)	-0.078(1)	0.0280(9)	2.4(5)	C(22)	-0.068(2)	-0.054(3)	0.238(1)	5.2(7)
N(2)	0.081(1)	-0.072(2)	0.1121(9)	2.8(5)	C(23)	-0.010(2)	-0.021(2)	0.189(1)	3.6(6)
C(1)	0.264(1)	0.132(2)	0.188(1)	7.1	C(24)	0.037(1)	-0.307(1)	-0.0306(7)	3.2
C(2)	0.304(2)	0.154(1)	0.136(1)	7.1	C(25)	-0.014(1)	-0.272(1)	-0.0933(9)	3.2
C(3)	0.341(1)	0.067(2)	0.1175(9)	7.1	C(26)	0.009(1)	-0.307(1)	-0.1492(6)	3.2
C(4)	0.324(2)	-0.010(1)	0.157(1)	7.1	C(27)	0.083(1)	-0.377(1)	-0.1424(7)	3.2
C(5)	0.277(2)	0.030(2)	0.201(1)	7.1	C(28)	0.134(1)	-0.411(1)	-0.0798(9)	3.2
C(6)	0.094(1)	0.226(1)	0.069(1)	4.8	C(29)	0.111(1)	-0.377(1)	-0.0239(7)	3.2
C(7)	0.100(1)	0.194(2)	0.008(1)	4.8	C(30)	-0.118(2)	-0.212(2)	-0.111(1)	3.7(6)
C(8)	0.031(1)	0.119(1)	-0.0149(8)	4.8	C(31)	-0.096(2)	-0.108(2)	-0.088(1)	5.8(8)
C(9)	-0.019(1)	0.106(1)	0.032(1)	4.8	C(32)	-0.180(3)	-0.262(3)	-0.072(2)	8(1)
C(10)	0.020(1)	0.172(2)	0.0845(8)	4.8	C(33)	-0.174(2)	-0.215(2)	-0.182(1)	5.3(8)
C(11)	0.189(2)	-0.120(2)	-0.024(1)	3.0(6)	C(34)	0.115(2)	-0.408(2)	-0.206(1)	4.4(7)
C(12)	0.172(2)	-0.046(2)	-0.081(1)	5.4(7)	C(35)	0.060(2)	-0.347(2)	-0.266(2)	6.2(8)
C(13)	0.208(2)	-0.088(2)	-0.139(2)	6.8(9)	C(36)	0.084(2)	-0.515(3)	-0.218(2)	8(1)
C(14)	0.319(3)	-0.107(3)	-0.108(2)	6(1)	C(37)	0.220(2)	-0.399(2)	-0.195(1)	4.9(7)
C(15)	0.339(2)	-0.182(2)	-0.053(2)	6.2(9)	C(38)	0.165(2)	-0.435(2)	0.042(1)	4.1(7)
C(16)	0.296(3)	-0.144(3)	0.000(2)	6(1)	C(39)	0.217(2)	-0.525(2)	0.028(1)	5.1(8)
C(17)	0.087(2)	-0.130(2)	0.057(1)	2.0(5)	C(40)	0.082(2)	-0.480(2)	0.068(2)	5.8(8)
C(18)	0.026(2)	-0.106(2)	0.158(1)	2.7(6)	C(41)	0.237(2)	-0.372(3)	0.093(2)	6.7(9)
C(19)	0.085(2)	-0.176(3)	0.207(2)	5.9(8)					

Table A2.8: Selected Bond Distances (Å) for 108

Atom	Atom	Distance	Atom	Atom	Distance
Zr(1)	N(1)	2.11(2)	Zr(1)	N(2)	2.08(2)
P(1)	C(17)	1.74(3)	P(1)	C(24)	1.90(2)
N(1)	C(11)	1.46(4)	N(1)	C(17)	1.44(3)
N(2)	C(17)	1.43(3)	N(2)	C(18)	1.48(4)

Table A2.9: Selected Bond Angles (°) for 108

Atom	Atom	Atom	Angle	Atom	Atom	Atom	Angle
N(1)	Zr(1)	N(2)	66.3(8)	C(17)	P(1)	C(24)	109(1)
Zr(1)	N(1)	C(11)	144(1)	Zr(1)	N(1)	C(17)	92(1)
C(11)	N(1)	C(17)	123(1)	Zr(1)	N(2)	C(17)	94(1)
Zr(1)	N(2)	C(18)	144(1)	C(17)	N(2)	C(18)	121(2)
Zr(1)	C(17)	P(1)	167(1)	Zr(1)	C(17)	N(1)	54(1)
Zr(1)	C(17)	N(2)	52(1)	P(1)	C(17)	N(1)	137(1)
P(1)	C(17)	N(2)	116(1)	N(1)	C(17)	N(2)	105(1)

Table A2.10: Positional Parameters and B(eq) for 112

Atom	x	y	z	B(eq)	Atom	x	y	z	B(eq)
Zr(1)	0.2268(1)	0.41926(6)	0.78211(9)	3.17(3)	C(17)	0.597(1)	0.4052(6)	0.6230(9)	3.4(4)
P(1)	0.5123(3)	0.4338(1)	0.7974(2)	3.34(9)	C(18)	0.436(1)	0.4233(7)	0.5882(8)	5.2(4)
N(1)	0.1426(10)	0.4620(5)	0.6625(7)	3.5(3)	C(19)	0.691(2)	0.4626(7)	0.6539(10)	6.2(5)
C(1)	0.146(2)	0.5237(7)	0.8308(9)	5.0(4)	C(20)	0.638(1)	0.3828(7)	0.5413(9)	5.7(5)
C(2)	0.075(1)	0.4754(7)	0.8621(9)	4.7(3)	C(21)	0.755(2)	0.1778(6)	0.706(1)	4.4(4)
C(3)	0.179(1)	0.4420(6)	0.9247(9)	4.6(3)	C(22)	0.786(3)	0.1805(9)	0.619(2)	17(1)
C(4)	0.312(2)	0.4693(7)	0.9303(10)	5.4(4)	C(23)	0.886(2)	0.1539(10)	0.767(2)	16.3(9)
C(5)	0.294(2)	0.5187(7)	0.8701(10)	5.2(4)	C(24)	0.638(2)	0.1337(9)	0.699(2)	15(1)
C(6)	0.066(1)	0.3321(7)	0.7005(9)	5.0(4)	C(25)	0.718(1)	0.3285(6)	0.9398(8)	3.3(3)
C(7)	0.205(2)	0.3172(7)	0.6935(9)	4.9(3)	C(26)	0.818(1)	0.3865(7)	0.9643(8)	4.7(4)
C(8)	0.285(1)	0.3020(6)	0.7765(9)	4.4(3)	C(27)	0.587(1)	0.3335(6)	0.9771(9)	4.7(4)
C(9)	0.202(2)	0.3097(7)	0.8342(9)	4.8(3)	C(28)	0.811(2)	0.2728(7)	0.9935(9)	5.7(5)
C(10)	0.066(1)	0.3278(7)	0.7831(9)	5.0(4)	C(29)	0.124(1)	0.5240(6)	0.6339(9)	3.5(4)
C(11)	0.616(1)	0.3635(6)	0.7785(8)	2.9(3)	C(30)	-0.009(1)	0.5477(7)	0.5800(9)	4.2(4)
C(12)	0.625(1)	0.3526(6)	0.6930(8)	3.0(3)	C(31)	-0.027(2)	0.6096(8)	0.554(1)	5.1(5)
C(13)	0.668(1)	0.2922(6)	0.6715(8)	3.4(4)	C(32)	0.082(2)	0.6521(7)	0.582(1)	6.0(5)
C(14)	0.714(1)	0.2442(6)	0.7314(10)	3.3(4)	C(33)	0.213(2)	0.6315(7)	0.635(1)	5.8(5)
C(15)	0.722(1)	0.2586(6)	0.8159(9)	3.3(3)	C(34)	0.235(1)	0.5709(7)	0.6594(9)	4.7(4)
C(16)	0.681(1)	0.3169(6)	0.8423(7)	2.5(3)					

Table A2.11: Selected Bond Distances (Å) for 112

Atom	Atom	Distance	Atom	Atom	Distance
Zr(1)	P(1)	2.707(4)	Zr(1)	N(1)	2.086(10)
P(1)	C(11)	1.86(1)	N(1)	C(29)	1.38(2)
P(1)	H(46)	1.19	N(1)	H(45)	1.05

Table A2.12: Selected Bond Angles (°) for 112

Atom	Atom	Atom	Angle	Atom	Atom	Atom	Angle
P(1)	Zr(1)	N(1)	99.0(3)	Zr(1)	P(1)	C(11)	118.3(4)
Zr(1)	N(1)	C(29)	134.5(8)	Zr(1)	P(1)	H(46)	98.0
C(11)	P(1)	H(46)	107.1	Zr(1)	N(1)	H(45)	124.5
C(29)	N(1)	H(45)	100.9				

Appendix Three
Supplementary Crystallographic Parameters for 122, 126, 127, 128, 130 and 131.

Table A3.1: Positional Parameters and B(eq) for 122

Atom	x	y	z	B(eq)	Atom	x	y	z	B(eq)
Zr(1)	0.8996(2)	0.2216(3)	0.6419(1)	3.79(8)	C(21)	1.010(2)	0.287(3)	0.877(1)	4.4(7)
P(1)	1.0398(5)	0.1395(8)	0.6870(4)	4.8(3)	C(22)	1.025(2)	0.233(3)	0.936(1)	5.3(8)
P(2)	1.0622(5)	0.3157(9)	0.7464(4)	4.8(3)	C(23)	1.093(2)	0.158(3)	0.952(1)	5.9(8)
C(1)	0.849(2)	0.029(3)	0.706(1)	3.9(7)	C(24)	1.146(2)	0.133(3)	0.908(1)	4.5(8)
C(2)	0.866(2)	0.134(3)	0.751(1)	4.1(7)	C(25)	1.137(2)	0.182(3)	0.847(1)	4.3(8)
C(3)	0.810(2)	0.235(3)	0.734(1)	4.1(7)	C(26)	0.938(2)	0.373(3)	0.865(1)	5.8(8)
C(4)	0.761(2)	0.192(3)	0.681(1)	5.8(8)	C(27)	1.104(2)	0.100(4)	1.021(2)	10(1)
C(5)	0.784(2)	0.065(3)	0.664(1)	4.5(8)	C(28)	1.201(2)	0.149(3)	0.801(1)	6.2(8)
C(6)	0.857(2)	0.329(2)	0.535(1)	2.9(7)	C(29)	0.990(2)	0.447(3)	0.728(1)	2.6(6)
C(7)	0.944(2)	0.322(3)	0.539(1)	3.4(7)	C(30)	1.007(2)	0.576(3)	0.760(1)	4.2(7)
C(8)	0.965(2)	0.190(4)	0.541(1)	7.2(9)	C(31)	0.947(2)	0.663(3)	0.780(1)	4.2(8)
C(9)	0.897(2)	0.113(3)	0.538(1)	6.8(9)	C(32)	0.966(2)	0.785(4)	0.807(1)	6.4(8)
C(10)	0.829(2)	0.198(3)	0.535(1)	5.5(8)	C(33)	1.047(2)	0.822(3)	0.821(1)	5.1(8)
C(11)	1.130(2)	0.131(3)	0.636(1)	4.9(8)	C(34)	1.104(2)	0.738(3)	0.800(1)	5.4(8)
C(12)	1.167(2)	0.244(3)	0.611(1)	3.7(7)	C(35)	1.085(2)	0.618(3)	0.774(1)	4.5(8)
C(13)	1.240(2)	0.221(3)	0.582(1)	5.1(7)	C(36)	0.929(2)	0.431(2)	0.683(1)	2.4(6)
C(14)	1.269(2)	0.089(3)	0.577(1)	5.3(8)	C(37)	0.886(2)	0.546(3)	0.652(1)	3.3(7)
C(15)	1.229(2)	-0.020(3)	0.596(1)	6.1(9)	C(38)	0.805(2)	0.557(3)	0.649(1)	4.1(8)
C(16)	1.156(2)	0.000(3)	0.626(1)	5.3(8)	C(39)	0.763(2)	0.659(3)	0.614(1)	5.1(8)
C(17)	1.142(2)	0.388(3)	0.618(1)	5.0(8)	C(40)	0.804(2)	0.741(3)	0.580(1)	6.4(8)
C(18)	1.350(2)	0.072(3)	0.545(1)	6.3(9)	C(41)	0.886(2)	0.739(3)	0.582(1)	6.7(9)
C(19)	1.113(2)	-0.122(3)	0.644(1)	7.5(9)	C(42)	0.928(2)	0.638(3)	0.618(1)	5.2(8)
C(20)	1.066(2)	0.260(3)	0.830(1)	4.1(7)					

Table A3.2: Selected Bond Distances (Å) for 122

Atom	Atom	Distance	Atom	Atom	Distance
Zr	P(1)	2.596(9)	Zr	C(36)	2.31(2)
P(1)	P(2)	2.19(1)	P(1)	C(11)	1.90(3)
P(2)	C(20)	1.86(3)	P(2)	C(29)	1.81(3)
C(29)	C(30)	1.48(4)	C(29)	C(36)	1.35(3)
C(36)	C(37)	1.48(4)			

Table A3.3: Selected Bond Angles (°) for 122

Atom	Atom	Atom	Angle	Atom	Atom	Atom	Angle
P(1)	Zr	C(36)	89.0(6)	Zr	P(1)	P(2)	94.2(4)
Zr	P(1)	C(11)	121.7(9)	P(2)	P(1)	C(11)	104(1)
P(1)	P(2)	C(20)	107.5(9)	P(1)	P(2)	C(29)	111.8(9)
C(20)	P(2)	C(29)	114(1)	P(2)	C(29)	C(30)	115(1)
P(2)	C(29)	C(36)	121(1)	C(30)	C(29)	C(36)	122(2)
Zr	C(36)	C(29)	120(1)	Zr	C(36)	C(29)	120(1)
C(29)	C(36)	C(37)	122(2)				

Table A3.4: Positional Parameters and B(eq) for 126

Atom	x	y	z	B(eq)	Atom	x	y	z	B(eq)
Zr(1)	0.43036(8)	0.18557(4)	0.94022(9)	2.73(2)	C(23)	0.8560(9)	0.2526(5)	1.6563(10)	4.9(3)
P(1)	0.7086(2)	0.26562(10)	1.1685(2)	2.83(5)	C(24)	0.7809(8)	0.2595(4)	1.5158(9)	4.0(2)
N(1)	0.5137(6)	0.2745(3)	0.8845(7)	3.0(2)	C(25)	0.7836(7)	0.3462(4)	1.2375(8)	2.6(2)
C(1)	0.2474(9)	0.2584(5)	0.904(1)	5.5(3)	C(26)	0.9104(8)	0.3560(4)	1.2425(8)	2.8(2)
C(2)	0.2576(8)	0.2225(5)	1.019(1)	4.7(3)	C(27)	0.9606(7)	0.4192(4)	1.2436(8)	3.3(2)
C(3)	0.2218(9)	0.1612(5)	0.980(1)	5.1(3)	C(28)	0.8926(8)	0.4718(4)	1.2439(8)	2.9(2)
C(4)	0.1886(9)	0.1550(6)	0.834(1)	6.4(3)	C(29)	0.7760(8)	0.4607(4)	1.2524(8)	3.2(2)
C(5)	0.2093(9)	0.2177(7)	0.785(1)	6.3(3)	C(30)	0.7174(7)	0.4001(4)	1.2487(8)	2.8(2)
C(6)	0.6187(9)	0.1364(4)	0.905(1)	4.6(3)	C(31)	1.0050(8)	0.3058(4)	1.2489(9)	3.8(2)
C(7)	0.514(1)	0.1341(5)	0.770(1)	4.7(3)	C(32)	1.1446(9)	0.3323(5)	1.300(1)	6.3(3)
C(8)	0.4135(10)	0.0936(5)	0.7730(10)	4.8(3)	C(33)	0.9763(9)	0.2760(5)	1.101(1)	5.5(3)
C(9)	0.4498(10)	0.0697(4)	0.909(1)	4.5(3)	C(34)	1.0028(9)	0.2509(5)	1.354(1)	5.4(3)
C(10)	0.5742(10)	0.0945(4)	0.9907(9)	4.3(3)	C(35)	0.9471(8)	0.5403(4)	1.2383(9)	3.6(2)
C(11)	0.5275(7)	0.1802(3)	1.1912(8)	2.7(2)	C(36)	1.080(1)	0.5426(5)	1.233(1)	7.7(4)
C(12)	0.4636(7)	0.1387(4)	1.2662(8)	2.9(2)	C(37)	0.951(1)	0.5787(5)	1.362(1)	7.6(4)
C(13)	0.4532(8)	0.0715(4)	1.2505(9)	3.8(2)	C(38)	0.859(1)	0.5701(5)	1.103(1)	6.8(3)
C(14)	0.386(1)	0.0344(4)	1.316(1)	5.4(3)	C(39)	0.5862(8)	0.4034(4)	1.2673(9)	3.1(2)
C(15)	0.322(1)	0.0612(5)	1.390(1)	5.9(3)	C(40)	0.6110(9)	0.4356(4)	1.411(1)	5.1(3)
C(16)	0.3297(9)	0.1274(6)	1.405(1)	5.4(3)	C(41)	0.4948(9)	0.4415(5)	1.148(1)	5.7(3)
C(17)	0.4017(8)	0.1648(4)	1.3440(9)	3.9(2)	C(42)	0.5090(8)	0.3402(4)	1.265(1)	4.8(3)
C(18)	0.6371(7)	0.2148(4)	1.2707(8)	2.9(2)	C(43)	0.5772(7)	0.2662(3)	1.0150(8)	2.6(2)
C(19)	0.7170(7)	0.2081(4)	1.4260(8)	3.0(2)	C(44)	0.5335(9)	0.3245(5)	0.7865(9)	4.3(3)
C(20)	0.7324(9)	0.1476(4)	1.4839(10)	4.9(3)	C(45)	0.652(1)	0.3661(7)	0.858(1)	11.7(5)
C(21)	0.8040(10)	0.1401(5)	1.630(1)	6.0(3)	C(46)	0.423(1)	0.3657(6)	0.742(2)	10.0(5)
C(22)	0.8683(9)	0.1940(5)	1.7143(10)	5.3(3)	C(47)	0.528(2)	0.2905(6)	0.656(1)	13.8(6)

Table A3.5: Selected Bond Distances (Å) for 126

Atom	Atom	Distance	Atom	Atom	Distance
Zr(1)	N(1)	2.221(6)	Zr(1)	C(11)	2.389(8)
Zr(1)	C(43)	2.217(7)	P(1)	C(18)	1.856(8)
P(1)	C(25)	1.864(8)	P(1)	C(43)	1.707(8)
N(1)	C(43)	1.274(9)	N(1)	C(44)	1.523(10)
C(11)	C(12)	1.493(10)	C(11)	C(18)	1.361(10)
C(18)	C(19)	1.515(10)			

Table A3.6: Selected Bond Angles (°) for 126

Atom	Atom	Atom	Angle	Atom	Atom	Atom	Angle
N(1)	Zr(1)	C(11)	106.0(2)	N(1)	Zr(1)	C(43)	33.3(2)
C(11)	Zr(1)	C(43)	73.0(3)	C(18)	P(1)	C(25)	120.4(3)
C(18)	P(1)	C(43)	98.3(4)	C(25)	P(1)	C(43)	113.7(3)
Zr(1)	N(1)	C(43)	73.2(4)	Zr(1)	N(1)	C(44)	156.0(5)
C(43)	N(1)	C(44)	130.4(7)	Zr(1)	C(11)	C(18)	123.2(5)
C(12)	C(11)	C(18)	117.8(7)	P(1)	C(18)	C(11)	114.7(6)
P(1)	C(18)	C(19)	117.0(5)	C(11)	C(18)	C(19)	127.4(7)
Zr(1)	C(43)	P(1)	123.0(4)	Zr(1)	C(43)	N(1)	73.5(5)
P(1)	C(43)	N(1)	157.5(6)				

Table A3.7: Positional Parameters and B(eq) for 127

Atom	x	y	z	B(eq)	Atom	x	y	z	B(eq)
Zr(1)	0.0640(1)	0.8337(1)	0.1937(1)	2.95(3)	C(22)	0.581(1)	0.814(1)	0.120(2)	6.2(4)
P(1)	0.2991(3)	0.7267(2)	0.3398(3)	2.53(9)	C(23)	0.577(1)	0.858(1)	0.235(2)	6.3(4)
O(1)	0.0923(6)	0.7337(5)	0.2747(8)	3.4(2)	C(24)	0.482(1)	0.8407(9)	0.259(1)	4.2(3)
C(1)	-0.104(1)	0.876(1)	0.023(2)	6.3(4)	C(25)	0.150(1)	0.6597(9)	0.289(1)	3.1(3)
C(2)	-0.141(1)	0.818(1)	0.084(2)	6.2(4)	C(26)	0.144(1)	0.6312(9)	0.410(1)	4.7(3)
C(3)	-0.122(1)	0.736(1)	0.040(2)	6.1(4)	C(27)	0.090(1)	0.5857(10)	0.162(1)	5.0(4)
C(4)	-0.064(1)	0.736(1)	-0.044(2)	6.0(4)	C(28)	0.4282(9)	0.6759(8)	0.383(1)	2.4(3)
C(5)	-0.056(1)	0.826(1)	-0.055(2)	5.3(4)	C(29)	0.456(1)	0.6051(8)	0.301(1)	3.0(3)
C(6)	0.052(1)	0.991(1)	0.311(2)	5.7(4)	C(30)	0.565(1)	0.6092(9)	0.322(1)	3.1(3)
C(7)	0.075(1)	0.942(1)	0.406(2)	5.3(4)	C(31)	0.651(1)	0.6742(9)	0.419(1)	3.1(3)
C(8)	0.183(1)	0.9253(9)	0.435(1)	4.2(3)	C(32)	0.625(1)	0.7305(8)	0.511(1)	2.9(3)
C(9)	0.223(1)	0.9618(10)	0.356(1)	4.7(4)	C(33)	0.5177(10)	0.7325(8)	0.502(1)	2.7(3)
C(10)	0.143(1)	1.003(1)	0.280(1)	5.1(4)	C(34)	0.373(1)	0.5187(9)	0.204(1)	4.1(3)
C(11)	0.2017(10)	0.8049(8)	0.120(1)	2.6(3)	C(35)	0.293(1)	0.5381(10)	0.076(1)	4.7(3)
C(12)	0.2134(10)	0.8446(8)	0.012(1)	2.8(3)	C(36)	0.315(1)	0.480(1)	0.282(2)	5.2(4)
C(13)	0.162(1)	0.7975(10)	-0.126(1)	4.7(4)	C(37)	0.431(1)	0.447(1)	0.156(1)	5.4(4)
C(14)	0.178(1)	0.836(1)	-0.226(2)	5.6(4)	C(38)	0.771(1)	0.6773(10)	0.429(1)	4.1(3)
C(15)	0.240(1)	0.918(1)	-0.190(2)	5.4(4)	C(39)	0.832(2)	0.774(2)	0.477(2)	12.4(8)

C(16)	0.290(1)	0.965(1)	-0.058(2)	5.4(4)	C(40)	0.831(2)	0.630(2)	0.528(2)	12.8(8)
C(17)	0.274(1)	0.9269(9)	0.042(1)	4.1(3)	C(41)	0.778(2)	0.640(2)	0.301(2)	12.5(8)
C(18)	0.2866(10)	0.7669(8)	0.185(1)	2.8(3)	C(42)	0.507(1)	0.7942(9)	0.624(1)	3.5(3)
C(19)	0.396(1)	0.7771(9)	0.166(1)	3.0(3)	C(43)	0.491(1)	0.889(1)	0.607(1)	5.3(4)
C(20)	0.398(1)	0.7322(9)	0.044(1)	4.3(3)	C(44)	0.413(1)	0.7536(10)	0.656(1)	4.8(3)
C(21)	0.499(1)	0.752(1)	0.026(2)	6.1(4)	C(45)	0.611(1)	0.8039(10)	0.751(1)	4.8(4)

Table A3.8: Selected Bond Distances (Å) for 127

Atom	Atom	Distance	Atom	Atom	Distance
Zr(1)	O(1)	1.916(9)	Zr(1)	C(11)	2.30(1)
P(1)	C(18)	1.89(2)	P(1)	C(25)	1.96(1)
P(1)	C(28)	1.88(1)	O(1)	C(25)	1.44(2)
C(11)	C(12)	1.51(2)	C(11)	C(18)	1.35(2)
C(18)	C(19)	1.55(2)	C(25)	C(26)	1.50(2)
C(25)	C(27)	1.52(2)			

Table A3.9: Selected Bond Angles (°) for 127

Atom	Atom	Atom	Angle	Atom	Atom	Atom	Angle
O(1)	Zr(1)	C(11)	87.2(5)	C(18)	P(1)	C(25)	103.7(6)
C(18)	P(1)	C(28)	105.0(7)	C(25)	P(1)	C(28)	124.7(6)
Zr(1)	O(1)	C(25)	147.3(10)	Zr(1)	C(11)	C(12)	120.7(9)
Zr(1)	C(11)	C(18)	122(1)	Zr(1)	C(11)	C(18)	122(1)
P(1)	C(18)	C(11)	123(1)	P(1)	C(18)	C(19)	113.1(9)
C(11)	C(18)	C(19)	121(1)	P(1)	C(25)	O(1)	97.9(8)
P(1)	C(25)	C(26)	110.5(8)	P(1)	C(25)	C(27)	122(1)
O(1)	C(25)	C(26)	108(1)	O(1)	C(25)	C(27)	105(1)
C(26)	C(25)	C(27)	110(1)				

Table A3.10: Positional Parameters and B(eq) for 128

Atom	x	y	z	B(eq)	Atom	x	y	z	B(eq)
Zr(1)	0.56590(7)	0.83299(7)	0.20227(10)	2.25(2)	C(24)	0.9598(7)	0.8308(6)	0.2301(9)	3.4(2)
P(1)	0.7988(2)	0.7309(2)	0.3449(2)	1.97(6)	C(25)	0.6616(6)	0.6633(6)	0.3128(8)	2.2(2)
O(1)	0.6003(4)	0.7332(4)	0.2844(6)	2.6(2)	C(26)	0.6696(7)	0.6445(6)	0.4461(9)	3.1(2)
C(1)	0.4044(7)	0.8784(7)	0.026(1)	4.1(3)	C(27)	0.5626(7)	0.6030(7)	0.437(1)	4.0(3)
C(2)	0.3672(7)	0.8308(9)	0.100(1)	4.8(3)	C(28)	0.5102(7)	0.5178(7)	0.321(1)	4.2(3)
C(3)	0.3786(8)	0.7397(9)	0.069(1)	5.1(3)	C(29)	0.4978(7)	0.5371(6)	0.1887(10)	3.5(3)
C(4)	0.4267(9)	0.7295(8)	-0.020(1)	5.5(3)	C(30)	0.6044(7)	0.5768(7)	0.1945(9)	3.1(2)
C(5)	0.4402(8)	0.8162(9)	-0.0481(9)	4.8(3)	C(31)	0.9256(6)	0.6800(5)	0.3880(8)	1.8(2)
C(6)	0.5587(8)	0.9975(7)	0.319(1)	4.8(3)	C(32)	0.9501(6)	0.6054(6)	0.3086(8)	2.3(2)
C(7)	0.5906(8)	0.9491(7)	0.4196(10)	4.1(3)	C(33)	1.0537(7)	0.6110(6)	0.3196(9)	2.7(2)

C(8)	0.6929(8)	0.9333(7)	0.4404(9)	3.8(3)	C(34)	1.1352(7)	0.6821(6)	0.4095(9)	2.8(2)
C(9)	0.7218(7)	0.9648(7)	0.3498(10)	3.5(3)	C(35)	1.1136(7)	0.7436(6)	0.5012(8)	2.7(2)
C(10)	0.6387(9)	1.0064(6)	0.2731(10)	4.3(3)	C(36)	1.0143(7)	0.7440(6)	0.5013(8)	2.5(2)
C(11)	0.6917(6)	0.7984(5)	0.1182(8)	1.8(2)	C(37)	0.8717(7)	0.5139(6)	0.2220(9)	2.9(2)
C(12)	0.6915(7)	0.8340(6)	0.0029(9)	2.7(2)	C(38)	0.7847(7)	0.5232(6)	0.0924(10)	3.5(2)
C(13)	0.6373(8)	0.7811(7)	-0.134(1)	4.4(2)	C(39)	0.8302(8)	0.4762(6)	0.316(1)	4.1(3)
C(14)	0.6429(8)	0.8144(7)	-0.239(1)	5.1(3)	C(40)	0.9272(8)	0.4367(6)	0.177(1)	4.9(3)
C(15)	0.7018(8)	0.8979(8)	-0.211(1)	4.9(3)	C(41)	1.2476(7)	0.6851(7)	0.413(1)	4.0(3)
C(16)	0.7573(8)	0.9518(7)	-0.082(1)	4.8(2)	C(42)	1.2469(10)	0.627(1)	0.287(2)	13.2(6)
C(17)	0.7490(7)	0.9175(7)	0.0218(9)	3.5(2)	C(43)	1.316(1)	0.656(2)	0.533(2)	16.9(9)
C(18)	0.7754(6)	0.7603(6)	0.1840(8)	2.3(2)	C(44)	1.296(1)	0.780(1)	0.424(2)	11.5(6)
C(19)	0.8691(7)	0.7651(6)	0.1468(9)	2.6(2)	C(45)	1.0109(7)	0.8128(6)	0.6223(8)	2.6(2)
C(20)	0.8611(7)	0.7115(6)	0.0230(9)	3.7(2)	C(46)	0.9946(7)	0.9081(6)	0.6004(9)	3.8(3)
C(21)	0.9478(9)	0.7243(7)	-0.014(1)	4.9(3)	C(47)	0.9252(7)	0.7759(7)	0.6649(9)	3.7(3)
C(22)	1.0329(9)	0.7881(8)	0.070(1)	5.5(3)	C(48)	1.1151(7)	0.8248(7)	0.7485(10)	4.4(3)
C(23)	1.0437(9)	0.8445(8)	0.192(1)	5.4(3)					

Table A3.11: Selected Bond Distances (Å) for 128

Atom	Atom	Distance	Atom	Atom	Distance
Zr(1)	O(1)	1.918(5)	Zr(1)	C(11)	2.337(8)
Zr(1)	C(11)	2.337(8)	P(1)	C(25)	1.957(8)
P(1)	C(31)	1.907(8)	O(1)	C(25)	1.418(9)
C(11)	C(12)	1.49(1)	C(11)	C(18)	1.35(1)
C(18)	C(19)	1.52(1)	C(25)	C(26)	1.54(1)
C(25)	C(30)	1.54(1)			

Table A3.12: Selected Bond Angles (°) for 128

Atom	Atom	Atom	Angle	Atom	Atom	Atom	Angle
O(1)	Zr(1)	C(11)	85.7(2)	C(18)	P(1)	C(25)	104.4(4)
C(18)	P(1)	C(31)	104.5(3)	C(25)	P(1)	C(31)	123.9(4)
Zr(1)	O(1)	C(25)	150.2(5)	Zr(1)	C(11)	C(12)	119.2(5)
Zr(1)	C(11)	C(18)	121.9(6)	C(12)	C(11)	C(18)	118.0(7)
P(1)	C(18)	C(11)	123.2(6)	P(1)	C(18)	C(19)	116.3(6)
C(11)	C(18)	C(19)	118.4(7)	P(1)	C(25)	O(1)	98.5(5)
P(1)	C(25)	C(26)	108.4(6)	P(1)	C(25)	C(30)	121.8(6)
O(1)	C(25)	C(26)	109.5(6)	O(1)	C(25)	C(30)	107.0(6)
C(26)	C(25)	C(30)	110.7(7)				

Table A3.13: Positional Parameters and B(eq) for 130

Atom	x	y	z	B(eq)	Atom	x	y	z	B(eq)
Zr(1)	0.09	0.3305(2)	0.58	3.4(1)	C(47)	-0.083(1)	0.415(2)	0.777(2)	3.6(9)
Zr(2)	0.1775(2)	0.9154(3)	0.7614(4)	4.3(1)	C(48)	-0.013(1)	0.478(3)	0.806(2)	4(1)
P(1)	0.0357(4)	0.2290(6)	0.7436(7)	2.9(3)	C(49)	-0.027(1)	0.393(2)	0.689(2)	2.7(9)
P(2)	0.2369(4)	0.7287(7)	0.6930(6)	3.1(3)	C(50)	0.1344(10)	0.993(1)	0.650(2)	6.69
O(1)	0.0917(8)	0.334(2)	0.694(2)	5.1(7)	C(51)	0.1467(8)	0.921(2)	0.613(1)	6.69
O(2)	0.1868(8)	0.803(2)	0.791(1)	4.1(7)	C(52)	0.1262(10)	0.855(1)	0.647(2)	6.69
C(1)	0.0344(6)	0.433(2)	0.521(2)	4.87	C(53)	0.1012(8)	0.887(2)	0.704(2)	6.69
C(2)	0.0590(9)	0.472(2)	0.585(1)	4.87	C(54)	0.1062(9)	0.972(2)	0.705(2)	6.69
C(3)	0.0998(7)	0.482(1)	0.562(2)	4.87	C(55)	0.204(1)	0.931(1)	0.910(2)	6.3
C(4)	0.1003(7)	0.450(2)	0.484(2)	4.87	C(56)	0.1648(8)	0.972(2)	0.894(2)	6.3
C(5)	0.0599(9)	0.420(1)	0.459(1)	4.87	C(57)	0.1710(9)	1.040(2)	0.846(2)	6.3
C(6)	0.1198(8)	0.191(2)	0.543(2)	6.85	C(58)	0.2136(10)	1.042(2)	0.832(2)	6.3
C(7)	0.144(1)	0.216(2)	0.614(2)	6.85	C(59)	0.2337(7)	0.975(2)	0.871(2)	6.3
C(8)	0.1680(8)	0.283(2)	0.596(2)	6.85	C(60)	0.239(1)	0.906(3)	0.700(2)	4(1)
C(9)	0.1593(9)	0.300(2)	0.514(2)	6.85	C(61)	0.259(1)	0.987(1)	0.674(2)	7.3
C(10)	0.1295(10)	0.243(2)	0.481(1)	6.85	C(62)	0.299(1)	1.001(2)	0.713(2)	7.3
C(11)	0.031(1)	0.256(2)	0.570(2)	4(1)	C(63)	0.3191(7)	1.076(2)	0.703(2)	7.3
C(12)	0.0035(10)	0.245(2)	0.491(1)	6.12	C(64)	0.299(1)	1.136(1)	0.654(2)	7.3
C(13)	-0.0349(10)	0.285(1)	0.473(2)	6.12	C(65)	0.259(1)	1.122(2)	0.615(1)	7.3
C(14)	-0.0545(7)	0.284(1)	0.394(2)	6.12	C(66)	0.2388(7)	1.047(2)	0.625(2)	7.3
C(15)	-0.0358(9)	0.242(2)	0.334(1)	6.12	C(67)	0.257(1)	0.834(2)	0.674(2)	2.5(9)
C(16)	0.0026(9)	0.201(1)	0.353(2)	6.12	C(68)	0.2879(9)	0.833(2)	0.613(2)	5.93
C(17)	0.0222(7)	0.203(1)	0.431(2)	6.12	C(69)	0.2729(7)	0.866(2)	0.539(2)	5.93
C(18)	0.011(1)	0.233(2)	0.640(2)	2.3(9)	C(70)	0.2983(9)	0.866(1)	0.476(1)	5.93
C(19)	-0.0267(7)	0.168(2)	0.632(2)	5.38	C(71)	0.3387(9)	0.832(2)	0.487(1)	5.93
C(20)	-0.0625(10)	0.185(1)	0.670(1)	5.38	C(72)	0.3537(7)	0.798(1)	0.561(2)	5.93
C(21)	-0.0967(7)	0.132(2)	0.663(2)	5.38	C(73)	0.3283(10)	0.799(2)	0.624(1)	5.93
C(22)	-0.0951(7)	0.060(1)	0.618(2)	5.38	C(74)	0.211(1)	0.733(3)	0.787(2)	4(1)
C(23)	-0.0593(9)	0.042(1)	0.580(1)	5.38	C(75)	0.1837(8)	0.653(1)	0.792(1)	4.67
C(24)	-0.0251(7)	0.096(2)	0.586(1)	5.38	C(76)	0.1410(9)	0.659(1)	0.764(1)	4.67
C(25)	0.069(1)	0.326(2)	0.763(2)	3.3(9)	C(77)	0.1156(6)	0.589(2)	0.760(1)	4.67
C(26)	0.1000(7)	0.310(1)	0.838(1)	4.09	C(78)	0.1330(8)	0.513(1)	0.785(1)	4.67
C(27)	0.0875(6)	0.327(1)	0.914(2)	4.09	C(79)	0.1757(9)	0.508(1)	0.813(1)	4.67
C(28)	0.1144(8)	0.309(1)	0.983(1)	4.09	C(80)	0.2010(6)	0.577(2)	0.817(1)	4.67
C(29)	0.1538(7)	0.273(1)	0.976(1)	4.09	C(81)	0.2811(7)	0.648(1)	0.721(2)	2.77
C(30)	0.1663(6)	0.257(1)	0.900(2)	4.09	C(82)	0.3048(7)	0.645(1)	0.795(1)	2.77
C(31)	0.1394(8)	0.275(1)	0.831(1)	4.09	C(83)	0.3241(6)	0.572(2)	0.822(1)	2.77
C(32)	-0.0035(7)	0.249(2)	0.823(1)	2.89	C(84)	0.3195(7)	0.502(1)	0.774(2)	2.77
C(33)	0.0017(7)	0.191(1)	0.885(2)	2.89	C(85)	0.2958(8)	0.505(1)	0.699(1)	2.77
C(34)	-0.0107(8)	0.211(1)	0.961(1)	2.89	C(86)	0.2766(7)	0.578(2)	0.672(1)	2.77
C(35)	-0.0284(8)	0.287(2)	0.974(1)	2.89	C(87)	0.320(1)	0.715(2)	0.856(2)	2.9(9)
C(36)	-0.0336(7)	0.344(1)	0.911(2)	2.89	C(88)	0.308(1)	0.694(2)	0.947(2)	4(1)
C(37)	-0.0212(7)	0.325(1)	0.836(1)	2.89	C(89)	0.310(1)	0.805(2)	0.836(2)	4(1)

C(38)	0.017(2)	0.103(3)	0.880(3)	5(1)	C(90)	0.372(1)	0.716(2)	0.868(2)	5(1)
C(39)	0.063(2)	0.092(3)	0.901(3)	8(1)	C(91)	0.334(1)	0.417(3)	0.802(3)	6(1)
C(40)	-0.007(2)	0.040(4)	0.933(4)	14(2)	C(92)	0.359(1)	0.416(3)	0.887(3)	7(1)
C(41)	0.004(1)	0.057(3)	0.798(3)	6(1)	C(93)	0.364(2)	0.383(4)	0.747(3)	11(1)
C(42)	-0.036(1)	0.309(3)	1.060(2)	5(1)	C(94)	0.298(2)	0.355(3)	0.808(3)	8(1)
C(43)	-0.067(1)	0.249(3)	1.089(2)	5(1)	C(95)	0.255(1)	0.569(2)	0.587(2)	1.6(8)
C(44)	0.003(1)	0.305(3)	1.112(3)	7(1)	C(96)	0.259(1)	0.647(2)	0.529(2)	4(1)
C(45)	-0.060(2)	0.388(3)	1.067(3)	9(1)	C(97)	0.207(1)	0.560(2)	0.586(2)	4(1)
C(46)	-0.033(1)	0.398(2)	0.776(2)	2.9(9)	C(98)	0.270(1)	0.499(3)	0.535(2)	5(1)

Table A3.14: Selected Bond Distances (Å) for 130

Atom	Atom	Distance	Atom	Atom	Distance
Zr(1)	O(1)	1.95(3)	Zr(1)	C(11)	2.25(4)
Zr(2)	O(2)	1.91(3)	Zr(2)	C(60)	2.31(4)
P(1)	C(18)	1.83(3)	P(1)	C(25)	1.92(4)
P(1)	C(32)	1.93(2)	P(2)	C(67)	1.87(4)
P(2)	C(74)	1.85(4)	P(2)	C(81)	1.94(2)
O(1)	C(25)	1.42(4)	O(2)	C(74)	1.38(5)
C(11)	C(18)	1.44(5)	C(11)	C(12)	1.51(5)
C(18)	C(19)	1.59(4)	C(25)	C(26)	1.53(4)
C(60)	C(67)	1.40(6)	C(60)	C(61)	1.54(5)
C(67)	C(68)	1.47(4)	C(74)	C(75)	1.58(5)

Table A3.15: Selected Bond Angles (°) for 130

Atom	Atom	Atom	Angle	Atom	Atom	Atom	Angle
O(1)	Zr(1)	C(11)	90(1)	O(2)	Zr(2)	C(60)	86(1)
C(18)	P(1)	C(25)	108(1)	C(18)	P(1)	C(32)	112(1)
C(25)	P(1)	C(32)	97(1)	C(67)	P(2)	C(74)	107(1)
C(67)	P(2)	C(81)	114(1)	C(74)	P(2)	C(81)	101(1)
Zr(1)	O(1)	C(25)	147(2)	Zr(2)	O(2)	C(74)	148(2)
Zr(1)	C(11)	C(18)	122(2)	Zr(1)	C(11)	C(12)	121(2)
C(18)	C(11)	C(12)	114(3)	P(1)	C(18)	C(11)	126(2)
P(1)	C(18)	C(19)	107(2)	C(11)	C(18)	C(19)	119(2)
P(1)	C(25)	O(1)	104(2)	P(1)	C(25)	C(26)	107(2)
O(1)	C(25)	C(26)	110(2)	Zr(2)	C(60)	C(67)	126(2)
Zr(2)	C(60)	C(61)	117(2)	C(67)	C(60)	C(61)	115(3)
P(2)	C(67)	C(60)	124(2)	P(2)	C(67)	C(68)	111(2)
C(60)	C(67)	C(68)	123(3)	P(2)	C(74)	O(2)	111(2)
P(2)	C(74)	C(75)	107(2)	O(2)	C(74)	C(75)	111(2)

Table A3.16: Positional Parameters and B(eq) for 131

Atom	x	y	z	B(eq)	Atom	x	y	z	B(eq)
Zr(1)	0.1570(2)	0.68547(4)	0.8046(1)	3.14(3)	C(25)	0.075(1)	0.6018(4)	0.713(1)	3.3(3)
P(1)	-0.0487(4)	0.6235(1)	0.5720(4)	3.2(1)	C(26)	0.085(2)	0.5653(4)	0.726(1)	4.1(4)
O(1)	0.2173(9)	0.6498(2)	0.7201(8)	3.4(3)	C(27)	0.106(2)	0.5453(5)	0.630(2)	5.7(4)
C(1)	0.097(2)	0.7445(4)	0.734(1)	4.9(4)	C(28)	0.126(2)	0.5115(5)	0.650(2)	6.6(5)
C(2)	0.055(2)	0.7251(4)	0.623(1)	4.9(4)	C(29)	0.125(2)	0.4993(5)	0.762(2)	6.8(5)
C(3)	0.175(2)	0.7130(4)	0.599(1)	4.9(4)	C(30)	0.104(2)	0.5163(5)	0.860(2)	6.3(5)
C(4)	0.291(2)	0.7228(4)	0.698(1)	4.6(4)	C(31)	0.085(2)	0.5503(4)	0.838(2)	5.7(4)
C(5)	0.247(2)	0.7425(4)	0.778(1)	4.9(4)	C(32)	0.224(2)	0.6152(4)	0.722(1)	3.7(3)
C(6)	0.298(2)	0.7024(5)	1.024(2)	7.9(6)	C(33)	-0.176(1)	0.5952(3)	0.467(1)	2.8(3)
C(7)	0.353(2)	0.6732(5)	1.000(2)	6.5(5)	C(34)	-0.289(1)	0.5766(3)	0.491(1)	2.9(3)
C(8)	0.254(2)	0.6507(5)	1.002(2)	6.5(5)	C(35)	-0.391(2)	0.5635(4)	0.389(1)	4.0(4)
C(9)	0.137(2)	0.6639(5)	1.016(2)	7.1(5)	C(36)	-0.396(2)	0.5680(4)	0.265(1)	3.6(3)
C(10)	0.167(2)	0.6969(5)	1.032(2)	6.6(5)	C(37)	-0.285(1)	0.5844(3)	0.242(1)	3.2(3)
C(11)	-0.083(1)	0.6721(3)	0.741(1)	3.3(3)	C(38)	-0.170(1)	0.5969(3)	0.336(1)	3.3(3)
C(12)	-0.175(1)	0.6946(4)	0.792(1)	3.6(3)	C(39)	-0.313(2)	0.5663(4)	0.622(1)	3.6(3)
C(13)	-0.204(2)	0.6869(4)	0.907(1)	5.1(4)	C(40)	-0.235(2)	0.5844(4)	0.743(1)	3.9(3)
C(14)	-0.286(2)	0.7081(5)	0.960(2)	6.1(5)	C(41)	-0.469(2)	0.5669(4)	0.616(1)	4.4(4)
C(15)	-0.329(2)	0.7368(4)	0.901(2)	5.7(4)	C(42)	-0.266(2)	0.5306(4)	0.642(1)	4.5(4)
C(16)	-0.307(2)	0.7449(5)	0.790(2)	6.3(5)	C(43)	-0.518(2)	0.5548(4)	0.158(1)	3.7(3)
C(17)	-0.228(2)	0.7247(4)	0.736(1)	4.6(4)	C(44)	-0.656(2)	0.5675(4)	0.178(2)	6.9(5)
C(18)	-0.151(1)	0.6517(3)	0.643(1)	2.5(3)	C(45)	-0.516(2)	0.5165(4)	0.165(1)	5.7(4)
C(19)	-0.301(1)	0.6572(4)	0.568(1)	3.4(3)	C(46)	-0.514(2)	0.5647(4)	0.024(2)	5.6(4)
C(20)	-0.415(2)	0.6552(4)	0.616(1)	4.3(4)	C(47)	-0.046(2)	0.6117(4)	0.288(1)	4.2(4)
C(21)	-0.553(2)	0.6599(4)	0.539(2)	5.4(4)	C(48)	-0.055(2)	0.6497(4)	0.283(1)	5.0(4)
C(22)	-0.578(2)	0.6669(4)	0.415(2)	6.2(5)	C(49)	-0.063(2)	0.6010(4)	0.148(2)	5.9(5)
C(23)	-0.466(2)	0.6696(4)	0.363(2)	5.4(4)	C(50)	0.096(2)	0.5994(4)	0.363(1)	5.2(4)
C(24)	-0.328(2)	0.6649(4)	0.438(1)	4.0(4)					

Table A3.17: Selected Bond Distances (Å) for 131

Atom	Atom	Distance	Atom	Atom	Distance
Zr(1)	O(1)	1.918(9)	Zr(1)	C(11)	2.36(1)
P(1)	C(18)	1.85(1)	P(1)	C(25)	1.91(1)
P(1)	C(33)	1.86(1)	O(1)	C(32)	1.43(2)
C(11)	C(12)	1.51(2)	C(11)	C(18)	1.38(2)
C(18)	C(19)	1.50(2)	C(25)	C(26)	1.51(2)
C(25)	C(32)	1.56(2)			

Table A3.18: Selected Bond Angles (°) for 131

Atom	Atom	Atom	Angle	Atom	Atom	Atom	Angle
O(1)	Zr(1)	C(11)	96.2(4)	C(18)	P(1)	C(25)	105.0(6)
C(18)	P(1)	C(33)	106.9(6)	C(25)	P(1)	C(33)	112.4(6)
Zr(1)	O(1)	C(32)	140.9(8)	Zr(1)	C(11)	C(12)	114.4(9)
Zr(1)	C(11)	C(18)	127.2(10)	C(12)	C(11)	C(18)	116(1)
P(1)	C(18)	C(11)	119(1)	P(1)	C(18)	C(19)	116.2(9)
C(11)	C(18)	C(19)	121(1)	P(1)	C(25)	C(26)	123(1)
P(1)	C(25)	C(32)	105.6(9)	C(26)	C(25)	C(32)	108(1)
O(1)	C(32)	C(25)	108(1)				

Appendix Four
Supplementary Crystallographic Parameters for 134, 135, 136, 138, 140 and 141.

Table A4.1: Positional Parameters and B(eq) for 134

Atom	x	y	z	B(eq)	Atom	x	y	z	B(eq)
P(1)	0.9796(3)	0.0120(3)	0.7028(2)	4.9(1)	C(32)	0.9195(10)	-0.0846(10)	0.5643(8)	6.1(5)
P(2)	1.5113(3)	-0.3954(3)	0.2898(2)	4.6(1)	C(33)	1.6315(8)	-0.3903(8)	0.4013(7)	3.1(3)
C(1)	1.1074(9)	-0.0567(9)	0.7894(7)	3.8(4)	C(34)	1.6825(8)	-0.3616(9)	0.4622(7)	2.9(3)
C(2)	1.1550(9)	-0.0931(9)	0.8456(7)	3.7(4)	C(35)	1.7000(9)	-0.2818(10)	0.4748(7)	4.4(4)
C(3)	1.1197(10)	-0.1310(10)	0.8965(8)	5.5(4)	C(36)	1.7458(10)	-0.2600(10)	0.5318(8)	5.2(4)
C(4)	1.171(1)	-0.165(1)	0.9510(8)	6.7(5)	C(37)	1.7755(10)	-0.316(1)	0.5751(8)	5.2(4)
C(5)	1.253(1)	-0.163(1)	0.9539(9)	6.8(5)	C(38)	1.7623(10)	-0.394(1)	0.5640(8)	5.4(4)
C(6)	1.2873(10)	-0.127(1)	0.9063(9)	5.9(5)	C(39)	1.7154(9)	-0.4175(9)	0.5069(7)	3.9(4)
C(7)	1.239(1)	-0.0929(10)	0.8519(8)	5.5(4)	C(40)	1.5658(9)	-0.3562(9)	0.3670(7)	3.3(4)
C(8)	1.0342(9)	-0.0253(9)	0.7801(7)	4.1(4)	C(41)	1.5289(8)	-0.2809(8)	0.3861(7)	2.4(3)
C(9)	0.9825(9)	-0.0148(9)	0.8346(7)	3.7(4)	C(42)	1.5200(9)	-0.2157(10)	0.3479(7)	4.4(4)
C(10)	0.911(1)	-0.058(1)	0.8334(8)	5.8(5)	C(43)	1.4868(9)	-0.1450(10)	0.3673(8)	4.8(4)
C(11)	0.864(1)	-0.044(1)	0.8842(9)	6.3(5)	C(44)	1.4617(9)	-0.1413(10)	0.4282(9)	5.3(4)
C(12)	0.889(1)	0.009(1)	0.9310(8)	5.7(4)	C(45)	1.4710(9)	-0.207(1)	0.4678(7)	5.0(4)
C(13)	0.956(1)	0.054(1)	0.9324(8)	5.8(5)	C(46)	1.5021(9)	-0.2760(9)	0.4469(7)	4.4(4)
C(14)	1.0048(9)	0.0409(9)	0.8826(8)	4.4(4)	C(47)	1.5676(8)	-0.4864(9)	0.2774(6)	2.8(3)
C(15)	1.0584(8)	0.0082(9)	0.6490(6)	3.1(3)	C(48)	1.5534(8)	-0.5591(9)	0.3077(7)	3.3(3)
C(16)	1.1175(9)	0.0699(9)	0.6464(7)	3.2(3)	C(49)	1.6079(9)	-0.6211(9)	0.3061(7)	3.4(4)
C(17)	1.1857(9)	0.0521(9)	0.6182(7)	3.9(4)	C(50)	1.6752(9)	-0.6131(9)	0.2743(7)	3.4(4)
C(18)	1.1982(9)	-0.0203(10)	0.5898(7)	3.8(4)	C(51)	1.6867(8)	-0.5453(9)	0.2424(6)	2.8(3)
C(19)	1.1367(9)	-0.0745(8)	0.5875(6)	3.1(3)	C(52)	1.6333(8)	-0.4817(8)	0.2412(6)	2.3(3)
C(20)	1.0651(8)	-0.0636(9)	0.6139(6)	3.0(3)	C(53)	1.4768(9)	-0.5803(9)	0.3411(7)	4.1(4)
C(21)	1.1116(10)	0.157(1)	0.6719(8)	5.1(4)	C(54)	1.399(1)	-0.5669(10)	0.2929(8)	6.0(5)
C(22)	1.1277(10)	0.159(1)	0.7460(8)	6.3(5)	C(55)	1.4753(9)	-0.5309(9)	0.4049(7)	5.6(4)
C(23)	1.028(1)	0.193(1)	0.6453(8)	6.6(5)	C(56)	1.477(1)	-0.666(1)	0.3629(8)	6.8(5)
C(24)	1.172(1)	0.212(1)	0.6485(8)	7.9(6)	C(57)	1.738(1)	-0.685(1)	0.275(1)	8.0(6)
C(25)	1.278(1)	-0.041(1)	0.5602(9)	6.5(5)	C(58)	1.777(2)	-0.696(2)	0.343(1)	18(1)
C(26)	1.312(1)	0.035(1)	0.5358(10)	10.3(7)	C(59)	1.694(1)	-0.761(1)	0.2576(9)	9.7(7)
C(27)	1.260(1)	-0.093(2)	0.503(1)	14.0(9)	C(60)	1.800(2)	-0.670(2)	0.237(1)	17(1)
C(28)	1.337(2)	-0.071(2)	0.610(1)	14.1(9)	C(61)	1.6510(8)	-0.4107(9)	0.1966(7)	3.5(4)
C(29)	0.9962(9)	-0.1262(9)	0.5987(8)	4.3(4)	C(62)	1.7223(9)	-0.4262(9)	0.1599(7)	5.0(4)
C(30)	1.018(1)	-0.191(1)	0.5515(8)	6.8(5)	C(63)	1.5761(9)	-0.3945(9)	0.1441(7)	4.8(4)
C(31)	0.9804(10)	-0.1719(10)	0.6590(8)	6.2(5)	C(64)	1.6775(9)	-0.3348(10)	0.2344(7)	5.5(5)

Table A4.2: Selected Bond Distances (Å) for 134

Atom	Atom	Distance	Atom	Atom	Distance
P(1)	C(8)	1.83(1)	P(1)	C(15)	1.84(1)
P(2)	C(40)	1.84(1)	P(2)	C(47)	1.83(1)
C(1)	C(2)	1.45(2)	C(1)	C(8)	1.31(2)
C(8)	C(9)	1.53(2)	C(33)	C(34)	1.49(2)
C(33)	C(40)	1.34(2)	C(33)	C(40)	1.34(2)
P(1)	H(81)	1.45	P(2)	H(82)	1.27

Table A4.3: Selected Bond Angles (°) for 134

Atom	Atom	Atom	Angle	Atom	Atom	Atom	Angle
C(8)	P(1)	C(15)	102.5(7)	C(40)	P(2)	C(47)	103.2(7)
C(2)	C(1)	C(8)	132(1)	P(1)	C(8)	C(1)	126(1)
P(1)	C(8)	C(9)	110(1)	C(1)	C(8)	C(9)	123(1)
C(34)	C(33)	C(40)	128(1)	P(2)	C(40)	C(33)	124(1)
P(2)	C(40)	C(41)	111(1)	C(33)	C(40)	C(41)	124(1)
C(8)	P(1)	H(81)	95.5	C(15)	P(1)	H(81)	94.9
C(40)	P(2)	H(82)	107.1	C(47)	P(2)	H(82)	107.6

Table A4.4: Positional Parameters and B(eq) for 135

Atom	x	y	z	B(eq)	Atom	x	y	z	B(eq)
P(1)	0.2731(3)	0.5183(7)	0.4245(3)	3.8(2)	C(19)	0.406(1)	0.281(3)	0.448(1)	7.3(8)
P(2)	0.2004(3)	0.4050(7)	0.3754(3)	3.5(2)	C(20)	0.368(1)	0.371(3)	0.4565(10)	6.3(7)
C(1)	0.1923(8)	0.560(2)	0.3450(8)	2.3(5)	C(21)	0.1469(8)	0.349(2)	0.4004(8)	2.7(5)
C(2)	0.1444(8)	0.617(2)	0.3016(8)	2.4(5)	C(22)	0.1383(8)	0.208(2)	0.3922(8)	2.6(5)
C(3)	0.1037(9)	0.528(2)	0.2725(8)	3.5(6)	C(23)	0.087(1)	0.159(2)	0.3855(9)	4.8(6)
C(4)	0.058(1)	0.578(3)	0.236(1)	5.9(7)	C(24)	0.0451(9)	0.237(2)	0.3875(8)	3.4(6)
C(5)	0.0509(9)	0.710(2)	0.2266(9)	4.4(6)	C(25)	0.0555(10)	0.367(3)	0.4025(9)	4.8(7)
C(6)	0.0886(10)	0.794(3)	0.2536(10)	5.6(7)	C(26)	0.1062(8)	0.425(2)	0.4097(7)	2.3(5)
C(7)	0.1349(8)	0.749(2)	0.2936(8)	2.8(5)	C(27)	0.1837(8)	0.106(2)	0.3906(8)	3.3(5)
C(8)	0.2425(9)	0.614(2)	0.3668(9)	4.2(6)	C(28)	0.1871(9)	0.092(2)	0.3372(9)	5.3(7)
C(9)	0.2681(8)	0.723(2)	0.3458(9)	2.7(5)	C(29)	0.2379(9)	0.145(2)	0.4327(9)	5.0(7)
C(10)	0.2648(8)	0.732(2)	0.2928(9)	3.9(6)	C(30)	0.1697(9)	-0.030(2)	0.4104(10)	6.1(7)
C(11)	0.2890(10)	0.843(3)	0.2768(9)	5.2(7)	C(31)	-0.014(1)	0.172(4)	0.372(1)	9(1)
C(12)	0.3189(9)	0.933(2)	0.313(1)	4.5(6)	C(32)	-0.007(2)	0.050(5)	0.403(2)	22(1)
C(13)	0.3232(10)	0.914(3)	0.366(1)	5.5(7)	C(33)	-0.045(2)	0.258(4)	0.396(2)	16(1)
C(14)	0.2982(9)	0.811(3)	0.3814(9)	4.9(7)	C(34)	-0.040(2)	0.176(4)	0.319(2)	17(1)
C(15)	0.3262(10)	0.424(2)	0.412(1)	4.5(6)	C(35)	0.1095(10)	0.564(2)	0.4350(9)	4.5(6)
C(16)	0.3272(10)	0.391(3)	0.3622(9)	4.8(6)	C(36)	0.0718(9)	0.660(2)	0.3971(9)	4.5(6)
C(17)	0.366(1)	0.300(3)	0.3564(10)	5.7(7)	C(37)	0.0928(10)	0.552(2)	0.485(1)	6.7(8)
C(18)	0.403(1)	0.249(3)	0.398(1)	7.3(8)	C(38)	0.1654(10)	0.621(2)	0.4532(9)	5.8(7)

Table A4.5: Selected Bond Distances (Å) for 135

Atom	Atom	Distance	Atom	Atom	Distance
P(1)	P(2)	2.253(9)	P(1)	C(8)	1.79(2)
P(1)	C(15)	1.82(2)	P(2)	C(1)	1.76(2)
P(2)	C(21)	1.84(2)	C(1)	C(2)	1.52(2)
C(1)	C(8)	1.37(2)	C(8)	C(9)	1.50(3)

Table A4.6: Selected Bond Angles (°) for 135

Atom	Atom	Atom	Angle	Atom	Atom	Atom	Angle
P(2)	P(1)	C(8)	73.8(8)	P(2)	P(1)	C(15)	100.0(9)
C(8)	P(1)	C(15)	106(1)	P(1)	P(2)	C(1)	76.1(8)
P(1)	P(2)	C(21)	123.3(7)	C(1)	P(2)	C(21)	117(1)
P(2)	C(1)	C(2)	129(1)	P(2)	C(1)	C(8)	102(1)
C(2)	C(1)	C(8)	127(2)	P(1)	C(8)	C(1)	104(1)
P(1)	C(8)	C(9)	127(1)	C(1)	C(8)	C(9)	128(2)

Table A4.7: Positional Parameters and B(eq) for 136

Atom	x	y	z	B(eq)	Atom	x	y	z	B(eq)
B(1)	0.316(1)	0.164(1)	0.3631(7)	2.0(4)	C(19)	0.225(1)	0.387(1)	0.2838(7)	5.5(5)
P(1)	0.2496(3)	0.0443(4)	0.3680(2)	3.4(1)	C(20)	0.267(1)	0.301(1)	0.3010(7)	4.7(5)
C(1)	0.2921(10)	0.069(1)	0.4279(6)	4.0(4)	C(21)	0.2840(9)	-0.071(1)	0.3486(5)	1.9(4)
C(2)	0.279(1)	0.011(1)	0.4690(6)	3.2(4)	C(22)	0.2408(9)	-0.160(1)	0.3410(5)	1.9(4)
C(3)	0.320(1)	-0.075(2)	0.4811(7)	6.2(6)	C(23)	0.280(1)	-0.249(1)	0.3334(5)	3.6(4)
C(4)	0.311(1)	-0.135(2)	0.5164(8)	7.2(6)	C(24)	0.361(1)	-0.250(1)	0.3351(5)	3.3(4)
C(5)	0.256(1)	-0.102(2)	0.5431(7)	6.5(6)	C(25)	0.404(1)	-0.162(1)	0.3397(6)	3.9(4)
C(6)	0.214(1)	-0.017(2)	0.5328(8)	8.3(7)	C(26)	0.367(1)	-0.069(1)	0.3440(6)	3.4(4)
C(7)	0.227(1)	0.042(2)	0.4951(8)	6.7(6)	C(27)	0.148(1)	-0.168(1)	0.3402(6)	4.2(5)
C(8)	0.3357(9)	0.149(1)	0.4186(6)	3.2(4)	C(28)	0.128(1)	-0.145(1)	0.3861(7)	6.1(6)
C(9)	0.391(1)	0.208(1)	0.4554(7)	4.1(5)	C(29)	0.118(1)	-0.274(1)	0.3273(6)	5.7(5)
C(10)	0.421(1)	0.179(2)	0.5002(8)	7.5(6)	C(30)	0.102(1)	-0.103(1)	0.2989(6)	5.2(5)
C(11)	0.477(2)	0.235(2)	0.5304(9)	10.7(8)	C(31)	0.404(1)	-0.350(1)	0.3259(7)	5.5(5)
C(12)	0.508(1)	0.316(2)	0.5132(9)	8.2(7)	C(32)	0.388(1)	-0.429(2)	0.3594(7)	8.1(7)
C(13)	0.486(1)	0.350(1)	0.4700(8)	6.4(6)	C(33)	0.374(1)	-0.379(2)	0.2774(8)	9.2(7)
C(14)	0.429(1)	0.289(1)	0.4402(6)	5.0(5)	C(34)	0.496(1)	-0.336(2)	0.3310(8)	9.4(7)
C(15)	0.2694(10)	0.263(1)	0.3459(6)	3.2(4)	C(35)	0.4234(9)	0.024(1)	0.3459(5)	2.2(4)
C(16)	0.223(1)	0.319(1)	0.3720(6)	4.6(5)	C(36)	0.3805(9)	0.122(1)	0.3332(5)	2.7(4)
C(17)	0.183(1)	0.405(1)	0.3558(7)	5.5(5)	C(37)	0.469(1)	0.009(1)	0.3056(6)	5.5(5)
C(18)	0.185(1)	0.436(1)	0.3124(7)	5.8(5)	C(38)	0.484(1)	0.025(1)	0.3912(6)	4.9(5)

Table A4.8: Selected Bond Distances (Å) for 136

Atom	Atom	Distance	Atom	Atom	Distance
P(1)	C(1)	1.80(2)	P(1)	C(21)	1.80(1)
P(1)	B(1)	1.99(2)	C(1)	C(2)	1.50(2)
C(1)	C(8)	1.37(2)	C(8)	C(9)	1.50(2)
C(8)	B(1)	1.62(2)	C(21)	C(22)	1.40(2)
C(21)	C(26)	1.44(2)	C(26)	C(35)	1.57(2)
C(35)	C(36)	1.52(2)	C(35)	C(37)	1.56(2)
C(35)	C(38)	1.51(2)	C(36)	B(1)	1.65(2)
C(15)	B(1)	1.58(2)	P(1)	H(44)	1.05

Table A4.9: Selected Bond Angles (°) for 136

Atom	Atom	Atom	Angle	Atom	Atom	Atom	Angle
C(1)	P(1)	C(21)	112.5(8)	C(1)	P(1)	B(1)	78.8(8)
C(21)	P(1)	B(1)	117.0(7)	P(1)	C(1)	C(2)	127(1)
P(1)	C(1)	C(8)	94(1)	C(2)	C(1)	C(8)	138(1)
C(1)	C(8)	C(9)	123(1)	C(1)	C(8)	B(1)	107(1)
C(9)	C(8)	B(1)	129(1)	P(1)	C(21)	C(22)	126(1)
P(1)	C(21)	C(26)	113(1)	C(22)	C(21)	C(26)	119(1)
C(21)	C(26)	C(25)	116(1)	C(21)	C(26)	C(35)	128(1)
C(25)	C(26)	C(35)	115(1)	C(26)	C(35)	C(36)	115(1)
C(26)	C(35)	C(37)	105(1)	C(26)	C(35)	C(38)	109(1)
C(36)	C(35)	C(37)	102(1)	C(36)	C(35)	C(38)	114(1)
C(37)	C(35)	C(38)	108(1)	C(35)	C(36)	B(1)	120(1)
P(1)	B(1)	C(8)	79(1)	P(1)	B(1)	C(15)	117(1)
P(1)	B(1)	C(36)	102(1)	C(8)	B(1)	C(15)	114(1)
C(8)	B(1)	C(36)	118(1)	C(15)	B(1)	C(36)	117(1)
C(1)	P(1)	H(44)	126.2	C(21)	P(1)	H(44)	103.2
B(1)	P(1)	H(44)	118.8				

Table A4.10: Positional Parameters and B(eq) for 138

Atom	x	y	z	B(eq)	Atom	x	y	z	B(eq)
P(1)	-0.2603(1)	0.7716(1)	-0.7797(2)	3.40(4)	C(19)	0.0799(5)	0.7007(4)	-0.4388(6)	3.5(1)
P(2)	-0.1986(2)	0.6885(1)	-0.6033(2)	3.61(4)	C(20)	0.0732(5)	0.6632(4)	-0.3252(7)	4.5(2)
P(3)	-0.0069(2)	0.6475(1)	-0.6090(2)	3.66(4)	C(21)	0.1297(6)	0.7009(5)	-0.1935(6)	5.2(2)
C(1)	-0.3178(5)	0.8892(3)	-0.7168(5)	3.0(1)	C(22)	0.1972(6)	0.7748(5)	-0.1720(6)	5.3(2)
C(2)	-0.4354(5)	0.9255(4)	-0.7987(6)	3.4(2)	C(23)	0.2069(6)	0.8120(4)	-0.2804(7)	5.0(2)
C(3)	-0.4942(5)	1.0073(4)	-0.7509(6)	4.1(2)	C(24)	0.1498(6)	0.7750(4)	-0.4139(6)	4.4(2)
C(4)	-0.4388(6)	1.0565(4)	-0.6256(6)	4.0(2)	C(25)	-0.0041(5)	0.7269(3)	-0.7301(5)	3.1(1)
C(5)	-0.3206(6)	1.0216(4)	-0.5503(6)	4.0(2)	C(26)	0.1183(5)	0.7225(4)	-0.7542(5)	3.4(2)
C(6)	-0.2576(5)	0.9395(4)	-0.5917(5)	3.3(1)	C(27)	0.1668(5)	0.8012(4)	-0.7662(6)	3.7(2)
C(7)	-0.5024(5)	0.8800(4)	-0.9398(6)	4.7(2)	C(28)	0.2826(6)	0.7964(5)	-0.7787(6)	4.8(2)

C(8)	-0.5061(6)	1.1428(4)	-0.5754(7)	6.1(2)	C(29)	0.3560(6)	0.7118(5)	-0.7803(6)	5.1(2)
C(9)	-0.1266(6)	0.9103(4)	-0.5045(6)	4.6(2)	C(30)	0.3092(6)	0.6326(5)	-0.7706(7)	5.5(2)
C(10)	-0.2769(5)	0.5821(3)	-0.6724(6)	3.4(2)	C(31)	0.1936(6)	0.6376(4)	-0.7565(6)	4.5(2)
C(11)	-0.2919(6)	0.5344(4)	-0.8050(6)	4.3(2)	C(32)	-0.1095(5)	0.7793(4)	-0.7970(5)	3.2(1)
C(12)	-0.3672(6)	0.4612(4)	-0.8466(7)	5.2(2)	C(33)	-0.1204(5)	0.8327(4)	-0.9142(6)	3.5(2)
C(13)	-0.4172(6)	0.4297(4)	-0.7608(8)	5.1(2)	C(34)	-0.1337(5)	0.9295(4)	-0.9006(6)	4.2(2)
C(14)	-0.3928(6)	0.4718(4)	-0.6275(7)	4.6(2)	C(35)	-0.1475(6)	0.9774(4)	-1.0114(7)	5.3(2)
C(15)	-0.3245(5)	0.5484(4)	-0.5836(6)	3.7(2)	C(36)	-0.1525(6)	0.9311(5)	-1.1358(7)	5.8(2)
C(16)	-0.2279(7)	0.5533(4)	-0.9016(6)	6.1(2)	C(37)	-0.1431(6)	0.8349(5)	-1.1520(6)	5.8(2)
C(17)	-0.4948(6)	0.3477(5)	-0.8104(8)	7.8(2)	C(38)	-0.1268(6)	0.7869(4)	-1.0412(6)	4.8(2)
C(18)	-0.3049(6)	0.5909(4)	-0.4372(7)	5.6(2)					

Table A4.11: Selected Bond Distances (Å) for 138

Atom	Atom	Distance	Atom	Atom	Distance
P(1)	P(2)	2.200(2)	P(1)	C(1)	1.855(5)
P(1)	C(32)	1.818(7)	P(2)	P(3)	2.207(3)
P(2)	C(10)	1.849(6)	P(3)	C(19)	1.840(5)
P(3)	C(25)	1.838(6)	C(25)	C(26)	1.497(9)
C(25)	C(32)	1.357(7)	C(32)	C(33)	1.498(9)

Table A4.12: Selected Bond Angles (°) for 138

Atom	Atom	Atom	Angle	Atom	Atom	Atom	Angle
P(2)	P(1)	C(1)	106.3(2)	P(2)	P(1)	C(32)	99.0(2)
C(1)	P(1)	C(32)	107.3(3)	P(1)	P(2)	P(3)	96.1(1)
P(1)	P(2)	C(10)	103.4(2)	P(3)	P(2)	C(10)	104.3(2)
P(2)	P(3)	C(19)	99.5(2)	P(2)	P(3)	C(25)	99.4(2)
C(19)	P(3)	C(25)	104.7(3)	P(3)	C(25)	C(26)	114.8(4)
P(3)	C(25)	C(32)	120.5(5)	C(26)	C(25)	C(32)	124.6(6)
P(1)	C(32)	C(25)	122.9(5)	P(1)	C(32)	C(33)	112.2(4)
C(25)	C(32)	C(33)	123.6(6)				

Table A4.13: Positional Parameters and B(eq) for 140

Atom	x	y	z	B(eq)	Atom	x	y	z	B(eq)
P(1)	-0.0770(2)	1.0508(2)	1.5986(4)	3.19(7)	C(6)	-0.0902(10)	1.2638(9)	1.510(2)	4.3(3)
P(2)	-0.0296(2)	1.0840(2)	1.8802(4)	3.20(7)	C(7)	-0.1648(8)	1.0762(8)	2.000(1)	2.8(2)
C(1)	-0.0251(9)	1.1721(8)	1.487(1)	3.3(2)	C(8)	-0.1951(9)	1.1610(8)	2.103(2)	4.5(3)
C(2)	0.0634(9)	1.1707(8)	1.366(2)	4.6(3)	C(9)	-0.296(1)	1.1581(10)	2.207(2)	5.0(3)
C(3)	0.089(1)	1.2655(10)	1.272(2)	5.3(3)	C(10)	-0.3600(9)	1.070(1)	2.202(1)	5.1(3)
C(4)	0.027(1)	1.3554(9)	1.297(1)	5.0(3)	C(11)	-0.335(1)	0.9842(10)	2.102(2)	6.3(3)
C(5)	-0.0588(10)	1.3570(9)	1.414(2)	5.3(3)	C(12)	-0.236(1)	0.9880(9)	1.998(1)	4.4(3)

Table A4.14: Selected Bond Distances (Å) for 140

Atom	Atom	Distance	Atom	Atom	Distance
P(1)	P(1)*	2.218(6)	P(1)	P(2)	2.240(4)
P(1)	C(1)	1.85(1)	P(2)	P(2)*	2.232(6)
P(2)	C(7)	1.830(10)			

Table A4.15: Selected Bond Angles (°) for 140

Atom	Atom	Atom	Angle	Atom	Atom	Atom	Angle
P(1)*	P(1)	P(2)	84.6(1)	P(1)*	P(1)	C(1)	102.0(4)
P(2)	P(1)	C(1)	101.4(3)	P(1)	P(2)	P(2)*	84.2(1)
P(1)	P(2)	C(7)	104.0(3)	P(2)*	P(2)	C(7)	102.7(4)

Table A4.16: Positional Parameters and B(eq) for 141

Atom	x	y	z	B(eq)	Atom	x	y	z	B(eq)
Sn(1)	0.47112(6)	0.3872(2)	0.2	3.48(4)	C(23)	0.542(1)	-0.080(4)	0.343(2)	6.7(9)
Sn(2)	0.72289(6)	0.2274(2)	0.4730(1)	3.27(4)	C(24)	0.568(1)	-0.172(4)	0.310(2)	7.0(9)
P(1)	0.5205(2)	0.5697(9)	0.1412(3)	3.4(2)	C(25)	0.583(1)	-0.107(4)	0.257(2)	5.0(7)
P(2)	0.5713(2)	0.3911(9)	0.1642(4)	3.5(2)	C(26)	0.5779(9)	0.045(3)	0.237(1)	3.9(6)
P(3)	0.5440(2)	0.3541(9)	0.2588(3)	2.9(2)	C(27)	0.6753(10)	0.087(3)	0.422(1)	4.2(6)
P(4)	0.7949(2)	0.2628(9)	0.4166(3)	3.3(2)	C(28)	0.701(1)	-0.043(4)	0.386(2)	6.5(9)
P(5)	0.8226(2)	0.2233(9)	0.5100(3)	3.3(2)	C(29)	0.652(1)	0.197(4)	0.370(2)	6.0(8)
P(6)	0.7724(3)	0.0413(9)	0.5328(4)	3.5(2)	C(30)	0.641(1)	0.027(3)	0.462(2)	6.0(8)
C(1)	0.442(1)	0.177(4)	0.159(2)	6.5(9)	C(31)	0.698(1)	0.439(4)	0.522(2)	5.1(7)
C(2)	0.480(2)	0.093(5)	0.129(2)	10(1)	C(32)	0.680(1)	0.547(5)	0.473(3)	10(1)
C(3)	0.413(1)	0.222(5)	0.108(2)	10(1)	C(33)	0.656(1)	0.388(5)	0.562(2)	9(1)
C(4)	0.423(2)	0.071(5)	0.205(3)	11(1)	C(34)	0.735(1)	0.510(4)	0.559(2)	6.3(9)
C(5)	0.429(1)	0.529(4)	0.264(2)	6.1(8)	C(35)	0.801(1)	0.472(4)	0.397(1)	4.2(7)
C(6)	0.385(2)	0.567(6)	0.234(2)	12(1)	C(36)	0.826(1)	0.567(4)	0.438(2)	4.8(7)
C(7)	0.415(1)	0.428(5)	0.319(2)	8(1)	C(37)	0.8309(10)	0.731(4)	0.425(2)	5.3(7)
C(8)	0.449(1)	0.673(4)	0.283(1)	5.0(7)	C(38)	0.814(1)	0.790(4)	0.372(2)	5.7(8)
C(9)	0.5078(10)	0.532(3)	0.060(1)	3.5(6)	C(39)	0.7910(10)	0.693(3)	0.332(1)	4.4(7)
C(10)	0.528(1)	0.435(4)	0.023(2)	6.2(8)	C(40)	0.786(1)	0.538(4)	0.348(2)	5.5(8)
C(11)	0.519(2)	0.412(5)	-0.041(2)	9(1)	C(41)	0.8704(9)	0.099(3)	0.492(1)	3.4(6)
C(12)	0.484(1)	0.497(5)	-0.063(2)	7(1)	C(42)	0.888(1)	0.019(3)	0.542(1)	4.5(7)
C(13)	0.460(1)	0.592(4)	-0.028(2)	6.7(8)	C(43)	0.927(1)	-0.074(4)	0.534(2)	5.8(8)
C(14)	0.472(1)	0.610(3)	0.036(2)	5.2(7)	C(44)	0.945(1)	-0.076(4)	0.477(2)	6.2(8)
C(15)	0.6208(9)	0.509(3)	0.177(1)	2.7(5)	C(45)	0.931(1)	0.014(4)	0.428(2)	6.3(9)
C(16)	0.643(1)	0.518(3)	0.231(1)	4.3(7)	C(46)	0.8908(9)	0.102(3)	0.438(1)	3.7(6)
C(17)	0.680(1)	0.605(4)	0.243(2)	6.2(8)	C(47)	0.7581(9)	0.080(3)	0.615(1)	3.4(6)
C(18)	0.694(1)	0.695(4)	0.192(2)	5.9(8)	C(48)	0.721(1)	0.011(3)	0.638(2)	4.9(7)
C(19)	0.674(1)	0.696(4)	0.137(2)	6.2(8)	C(49)	0.708(1)	0.027(3)	0.700(2)	5.7(7)
C(20)	0.636(1)	0.605(4)	0.130(1)	4.9(7)	C(50)	0.730(1)	0.121(4)	0.736(2)	5.8(8)

C(21)	0.5539(8)	0.143(3)	0.273(1)	2.9(5)	C(51)	0.767(1)	0.197(3)	0.717(2)	5.7(8)
C(22)	0.5356(10)	0.087(3)	0.327(1)	4.0(6)	C(52)	0.784(1)	0.172(4)	0.656(2)	5.8(8)

Table A4.17: Selected Bond Distances (Å) for 141

Atom	Atom	Distance	Atom	Atom	Distance
Sn(1)	P(1)	2.538(8)	Sn(1)	P(3)	2.549(7)
Sn(1)	C(1)	2.21(4)	Sn(1)	C(5)	2.20(4)
Sn(2)	P(4)	2.533(8)	Sn(2)	P(6)	2.538(8)
Sn(2)	C(27)	2.18(3)	Sn(2)	C(31)	2.22(3)
P(1)	P(2)	2.23(1)	P(1)	C(9)	1.83(3)
P(2)	P(3)	2.23(1)	P(2)	C(15)	1.83(3)
P(3)	C(21)	1.84(3)	P(4)	P(5)	2.209(10)
P(4)	C(35)	1.83(3)	P(5)	P(6)	2.23(1)
P(5)	C(41)	1.84(3)	P(6)	C(47)	1.85(3)

Table A4.18: Selected Bond Angles (°) for 141

Atom	Atom	Atom	Angle	Atom	Atom	Atom	Angle
P(1)	Sn(1)	P(3)	78.2(2)	P(1)	Sn(1)	C(1)	120(1)
P(1)	Sn(1)	C(5)	109.3(9)	P(3)	Sn(1)	C(1)	118.0(10)
P(3)	Sn(1)	C(5)	107(1)	C(1)	Sn(1)	C(5)	117(1)
P(4)	Sn(2)	P(6)	78.4(2)	P(4)	Sn(2)	C(27)	113.8(8)
P(4)	Sn(2)	C(31)	115.6(8)	P(6)	Sn(2)	C(27)	108.3(8)
P(6)	Sn(2)	C(31)	117.6(9)	C(27)	Sn(2)	C(31)	117(1)
Sn(1)	P(1)	P(2)	83.3(3)	Sn(1)	P(1)	C(9)	105.8(9)
P(2)	P(1)	C(9)	104.1(10)	P(1)	P(2)	P(3)	92.2(4)
P(1)	P(2)	C(15)	103.9(9)	P(3)	P(2)	C(15)	104.6(9)
Sn(1)	P(3)	P(2)	83.1(3)	Sn(1)	P(3)	C(21)	109.3(9)
P(2)	P(3)	C(21)	103.2(9)	Sn(2)	P(4)	P(5)	83.0(3)
Sn(2)	P(4)	C(35)	108(1)	P(5)	P(4)	C(35)	108(1)
P(4)	P(5)	P(6)	92.4(4)	P(4)	P(5)	C(41)	101.6(9)
P(6)	P(5)	C(41)	101.2(9)	Sn(2)	P(6)	P(5)	82.4(3)
Sn(2)	P(6)	C(47)	103.5(9)	P(5)	P(6)	C(47)	104.5(9)

Curriculum Vitae
Tricia L. Breen

Date of Birth August 5, 1969

Citizenship Canadian

Education

Ph.D (1996) University of Windsor
B.Sc. (1992) University of Windsor (Hons. Chem.)

Scholarships and Awards

- NSERC Postdoctoral Fellowship 1996 (Location of Tenure: Massachusetts Institute of Technology)
- University of Windsor Summer Research Scholarship 1996
- ***79th Canadian Society for Chemistry Conference*** Presentation Award 1996
- University of Windsor Conference Travel Award, ***79th Canadian Society for Chemistry Conference***, St. John's, Newfoundland 1996
- University of Windsor Conference Travel Award, ***International Congress of the Pacific Basin Societies***, Honolulu, Hawaii 1995
- University of Windsor Tuition Scholarship 1995
- NSERC Graduate Scholarship (PGS B) 1994 - 1996
- Ontario Graduate Scholarship (declined) 1994
- University of Windsor Tuition Scholarship 1994
- Accounts of Chemical Research Subscription Award 1994
- ***26th Inorganic Discussion Weekend*** Presentation Award 1993
- NSERC Graduate Scholarship (PGS A) 1992 - 1994
- Society of Chemical Industry Merit Award 1992
- General Chemical Canada Ltd. Scholarship 1991
- NSERC Undergraduate Summer Research Assistantship 1991
- Peter Wyzinski Sr. Memorial Award 1991

Experience

- President of the Graduate Chemistry Society, University of Windsor (1994 - 1995).
- Treasurer of the Graduate Chemistry Society, University of Windsor (1993 - 1994).

- Graduate Student, Department of Chemistry and Biochemistry, University of Windsor (1992 - 1996)
- Teaching Assistant, Department of Chemistry and Biochemistry, University of Windsor (1991 - 1996)
- Research Assistant, Department of Chemistry and Biochemistry, University of Windsor (May 1991 - September 1991)
- Research Assistant, Department of Civil and Environmental Engineering, University of Windsor (May 1990 - April 1991)

Publications

1. T.L. Breen, D.W. Stephan (**1996**) Zr-E π-Bonding in Complexes Derived from E-H Additions to $Cp_2Zr(PC_6H_2$-2,4,6-*t*-$Bu_3)(PMe_3)$ ***Organometallics*** (in press).
2. T.L. Breen, D.W. Stephan (**1996**) Reactivity Studies of Methylzirconocene Phosphide Complexes ***Organometallics*** (in press).
3. T.L. Breen, D.W. Stephan (**1996**) Synthesis and Reactivity of Phosphametallacyclobutenes: Sterically Induced [4+2] Retrocycloadditions ***J. Am. Chem. Soc.*** *118*, 4204-4206.
4. T.L. Breen, D.W. Stephan (**1995**) Phosphinidene Transfer Reactions of the Terminal Phosphinidene Complex: $Cp_2Zr(PC_6H_2$-2,4,6-*t*-$Bu_3)(PMe_3)$ ***J. Am. Chem. Soc.*** *117*, 11914-11921.
5. C.S. Vizniowski, J.R. Green, T.L. Breen, A.V. Dalacu (**1995**) Propargyl Chlorides as Sources for Cobalt Stabilized γ-Carbonyl Cations ***J. Org. Chem.*** *60*, 7496-7502.
6. J. Ho, T.L. Breen, A. Ozarowski, D.W. Stephan (**1994**) Early Metal Mediated P-P Bond Formation in $Cp_2M(PR)_2$ and $Cp_2M(PR)_3$ Complexes ***Inorg. Chem.*** *33,* 865-870.
7. Z. Hou, T.L. Breen, D.W. Stephan (**1993**) The Formation and Reactivity of the Early Metal Phosphides and Phosphinidenes $Cp^*_2Zr{=}PR$, $Cp^*_2Zr(PR)_2$ and $Cp^*_2Zr(PR)_3$ ***Organometallics*** *12*, 3158-3167.
8. T.L. Breen, D.W. Stephan (**1992**) Substitution or Nucleophilic Attack by Phosphines in $ZrCl_4(THF)_2$ ***Inorg. Chem.*** *31*, 4019-4022.

Presentations

1. T.L. Breen*, D.W. Stephan (**1996**) Zirconium Phosphides, Phosphinidenes, and Phosphametallacycles, ***79th Canadian Society for Chemistry Conference***, St. John's, Newfoundland.

2. T.L. Breen*, D.W. Stephan (**1995**) Synthesis and Reactivity of Zirconium Phosphinidenes, ***1995 International Congress of the Pacific Basin Societies***, Honolulu, Hawaii.
3. T.L. Breen*, D.W. Stephan (**1995**) Reactivity Studies of the Terminal Phosphinidene Complex: $Cp_2Zr(PC_6H_2\text{-}2,4,6\text{-}t\text{-}Bu_3)(PMe_3)$, ***28th Inorganic Discussion Weekend,*** London, Ontario.
4. T.L. Breen, D.W. Stephan* (**1995**) Phosphinidene Transfer Reactions of The Terminal Phosphinidene Complex: $Cp_2Zr(PC_6H_2\text{-}2,4,6\text{-}t\text{-}Bu_3)(PMe_3)$, ***International Workgroup on Organometallic Chemistry and Catalysis***, Muenster, Germany.
5. T.L. Breen, D.W. Stephan* (**1995**) Synthesis and Reactivity of Phosphametallacyclobutenes: Sterically Induced [4+2] Retrocycloadditions, ***International Workgroup on Organometallic Chemistry and Catalysis***, Muenster, Germany.
6. T.L. Breen*, D.W. Stephan (**1995**) Synthesis and Reactivity of Zirconium Phosphinidenes, ***78th Canadian Society for Chemistry Conference***, Guelph, Ontario.
7. T.L. Breen*, D.W. Stephan (**1994**) Synthesis and Reactivity Studies of a Terminal Zirconium Phosphinidene, ***27th Inorganic Discussion Weekend***, Hamilton, Ontario.
8. Z. Hou, T.L. Breen*, D.W. Stephan (**1993**) The Reactivity of Zr Phosphides and Phosphinidenes, ***26th Inorganic Discussion Weekend***, Guelph, Ontario.
9. Z. Hou, T.L. Breen, D.W. Stephan* (**1993**) The Reactivity of Zr Phosphides and Phosphinidenes, ***ACS Meeting*** Chicago, Illinois.

IMAGE EVALUATION
TEST TARGET (QA-3)

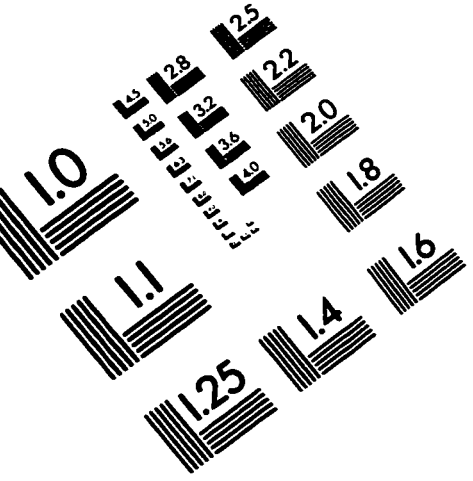

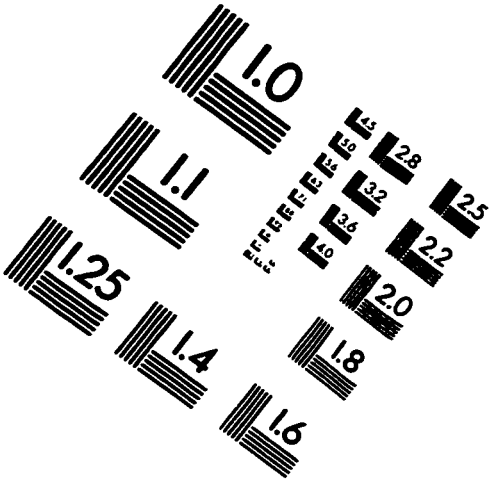

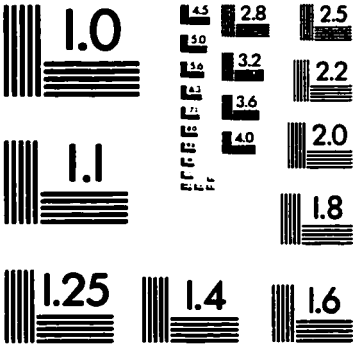

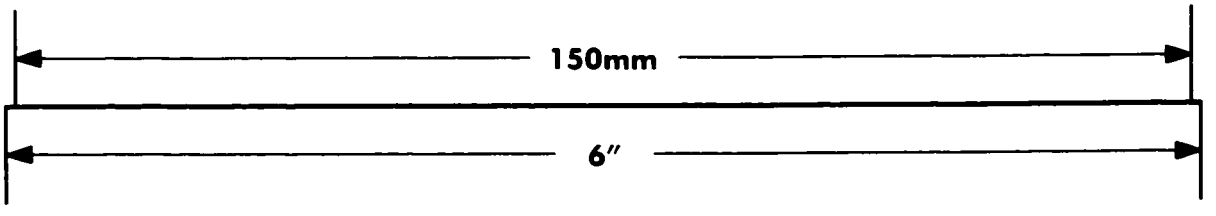

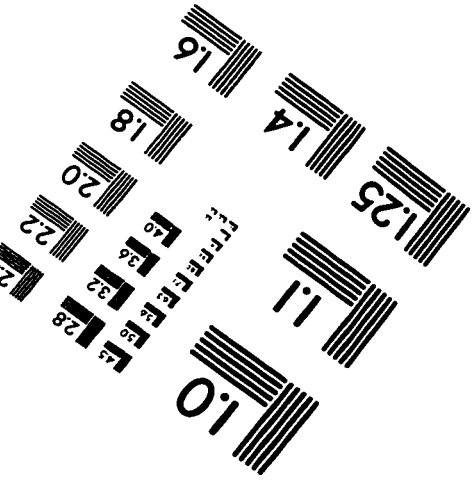

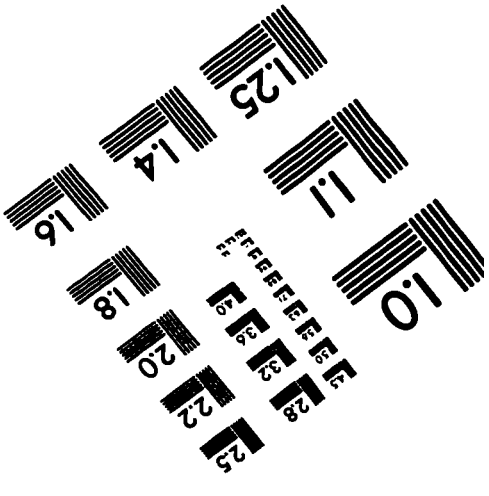

APPLIED IMAGE, Inc
1653 East Main Street
Rochester, NY 14609 USA
Phone: 716/482-0300
Fax: 716/288-5989